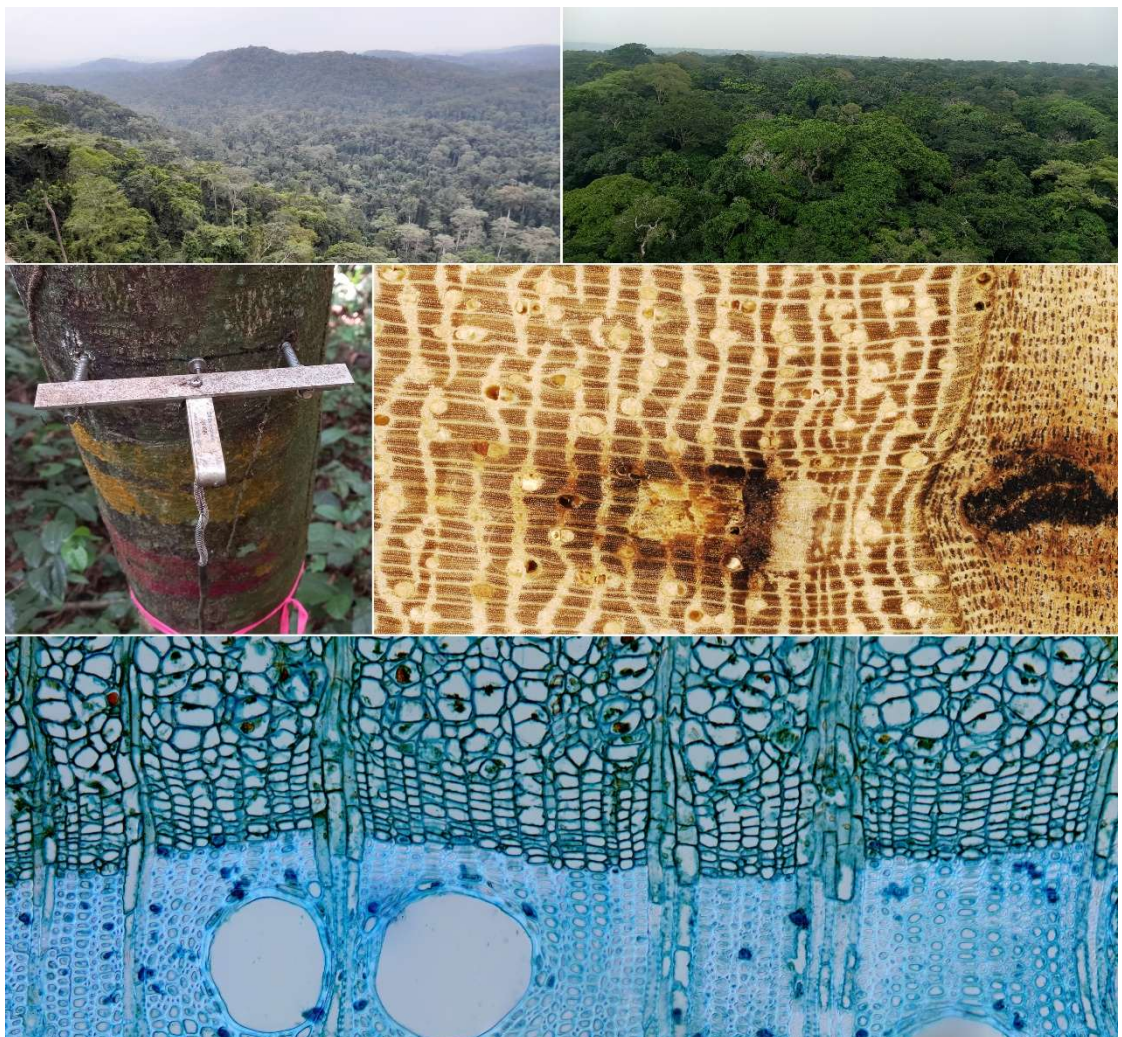


Unraveling the periodicity of secondary growth in the Congo Basin



Basile LUSE BELANGANAYI



Belgium
partner in development

Unraveling the periodicity of secondary growth in the Congo Basin

Basile LUSE BELANGANAYI

Original dissertation submitted for the degree of Doctor of Agronomic Sciences and
Biological Engineering

Thesis Jury:

President: Prof. Philippe LEJEUNE, University of Liège, Belgium

Secretary: Prof. Gauthier LIGOT, University of Liège, Belgium

Members: Prof. Jean-Louis DOUCET, University of Liège, Belgium

Dr. Jiri DOLEŽAL, University of South Bohemia, Czech Republic

Dr. Jonathan BARICHIVIC, Paris-Saclay University, France

Prof. Wannes HUBAU, Ghent University, Belgium

Promoters: Prof. Tom DE MIL, University of Liège

Dr. Hans BEECKMAN, Royal Museum for Central Africa

Calendar year: 2025

Copyright

This work is licensed under a Creative Commons license. You are free to reproduce, modify, distribute, and transmit this work under the following conditions:

- Attribution (BY): You must give appropriate credit to the original author in the manner specified by the author or licensor (but not in any way that suggests they endorse you or your use of the work);
- No Commercial Use (NC): You may not use this work for commercial purposes;
- Share Alike (SA): If you modify, transform, or adapt this work, you may distribute the resulting creation only under the same license as the original. Each time you reuse or distribute this work, you must clearly communicate the license terms under which it is made available.

Any of these conditions may be waived if you obtain permission from the copyright holder. Nothing in this license diminishes or restricts the author's moral rights.

À :

Ma défunte mère Marguerite MUSAU MAKENGA,

Mon père Norbert KANUAPUKI KADIOBHO,

Ma chère épouse Nicole NDOMBA BISOSA et

Ma fille Ornella ASELA LUSE.

Abstract

The Congo Basin forests, as a critical global carbon sink, face increasing threats from climate change, with temperature projections indicating a significant rise above pre-industrial levels by 2027, alongside increased variation in rainfall. Despite their significance, limited studies have focused on understanding the mechanisms of tree growth and the species-specific responses to changing climate conditions.

This thesis investigates the dynamics of secondary growth in two semi-deciduous tropical forests of the Congo Basin: the Luki and Yangambi biosphere reserves. Through three interlinked studies presented as Chapters 2, 3, and 4, the research aims to elucidate the mechanisms underlying secondary growth in this ecologically vital and unique region. To achieve this goal, the study addresses several interrelated research questions: Is there a dormant period in the seasonal tree-growth cycle? If so, what are the timing and duration of dormancy and the growing season? How do climatic factors influence the growth cycle? What anatomical marks does the growth cycle leave on the wood? These questions, spanning multiple chapters, provide a comprehensive understanding of secondary growth dynamics in the Congo Basin.

This thesis comprises five chapters. It begins with an introductory chapter (Chapter 1), which provides a general overview of the Congo Basin and tree growth, with a particular focus on the uncertainties surrounding the seasonality of secondary growth in this region.

Chapter 2 examines diel and seasonal stem growth patterns in 17 trees of 11 dominant canopy and understory species in the Mayombe forest. Highly-resolved measurements of radial stem size variations and associated weather conditions provided insights into secondary growth dynamics. Findings indicate that tree growth primarily occurs from 6 PM to 9 AM, and peaks during the rainy season (October to May). Growth cessation, observed for 1-4 months in some species, typically coincides with the dry season (June to September). A linear mixed-effects model demonstrated a positive relationship between annual radial stem growth and rainfall. These findings suggest that many tree species, including *Terminalia superba*, possess significant resilience to projected increases in temperature and rainfall, though species-specific growth responses vary. It is important to emphasize, however, that when using dendrometers, there remains a possibility of occasionally mistaking swelling caused by turgor pressure for irreversible growth. This highlights the need for more precise methods, such as cambial marking and micro-coring.

Chapter 3 focuses on the formation, distinctness, and periodicity of growth rings in 18 common tree species from two contrasting semi-deciduous rainforests. The presence of growth rings was confirmed across all species using the cambial marking technique, followed by micro- and macroscopic observations. Trees from the site with a well-defined dry season exhibited a higher likelihood of forming periodic growth rings compared to those from a site with less distinct rainfall seasonality. However, the distinctness of growth rings did not show significant variation across the different sites. Trees that exhibited faster growth rates were more likely to form periodic growth rings, potentially due to their greater sensitivity to seasonal environmental fluctuations, which influence the cessation and resumption of cambial activity. This study highlights the importance of understanding cambial dynamics through a more precise method

such as microcore sampling and detailed phenological analysis to capture lateral meristem activity.

Chapter 4 investigates cambial phenology in relation to climatic variables, tree morphological traits, leaf phenology, and reproductive behaviors across two semi-deciduous rainforests with distinct precipitation patterns. Biweekly microcores from 30 trees (10 species) and dendrometer data from 59 trees (20 species) were analyzed to characterize cambial activity and dormancy. Results indicate complex cambial dynamics, with species-specific cycles of activity and dormancy or continuous growth. Trees in the more climate-sensitive Luki site, with a pronounced dry season, may face increased vulnerability due to climate variability. Conversely, trees from the less-seasonal Yangambi site demonstrated resilience to climatic fluctuations but remained sensitive to internal growth dynamics, particularly morphological and reproductive traits.

Chapter 5 offers a comprehensive examination of secondary growth in tropical tree species of the Congo Basin, discussing results from Chapter 2, Chapter 3, and Chapter 4. By synthesizing these distinct but interrelated dimensions, we achieve a clearer understanding of how environmental variables, tree physiology, and growth patterns converge to shape the dynamics of secondary growth in tropical rainforests.

Collectively, this thesis advances our understanding of tree growth and its drivers in the Congo Basin, emphasizing the diversity and resilience of tropical tree species to anticipated climate change. However, further research is needed to elucidate the underlying mechanisms driving cambial dynamics and their long-term implications for forest carbon sequestration and ecosystem functioning in this critical region.

Acknowledgements

This research was made possible thanks to a grant awarded by the Royal Museum for Central Africa (**RMCA**) as part of the PilotMAB and PilotMABplus projects, funded by the Belgian Directorate General for Development Cooperation and Humanitarian Aid (**DGD**) and implemented under The **Raamakkoord/Accord-Cadre (RAAC)** program. I extend my sincere gratitude to these institutions for their support. My gratitude is directed to **Mr. Bart Ouvry**, Director of the RMCA, **Ms. Eva November**, Head of the RAAC program at the RMCA, and **Dr. Wannes Hubau**, Head of the Wood Biology Service and supervisor of the PilotMAB and PilotMABplus projects.

I would like to express my profound gratitude to my two supervisors, **Dr. Hans Beeckman** and **Prof. Tom De Mil**, for their invaluable guidance and support, without which this thesis would not have been possible.

I am deeply indebted to **Nils Bourland**, who, beyond being a mentor, has significantly shaped my scientific career and continued to support me regardless of my shortcomings. I owe him a special thank you. I would also like to extend my gratitude to **Mélissa Rousseau**, his wife and former colleague at the Tervuren laboratory, for her pivotal role in my career.

A special mention goes to **Muriel Van Nuffel**, Coordinator of African Scientists' Mobility Stays at the RMCA, whose warm and maternal care ensured our well-being through organized visits to Belgian institutions and historical sites for all RMCA fellows. Her thoughtful guidance served as much-needed relief from the stress of pursuing a PhD.

I am also grateful to **Annelore Nackaerts** for her indispensable role in facilitating our access to wood samples from the RMCA xylarium and acquiring various fieldwork materials.

I extend my gratitude to the staff and agents of **Nature+ Asbl** for providing a grant that allowed me to acquire additional field equipment, as well as for the subsequent collaboration. I would like to particularly thank **Cecilia Julve Larrubia**, the primary representative of this institution, for her unwavering support.

I would like to express my gratitude to **Dr. Mathilde Leduc Grimaldi** for her dedication in coaching me in communication techniques for the preparation of my doctoral defense. I also extend my thanks to **Thierry Van Pevenage**, Director of the student's residence 'Maison Africaine', for his support during the coaching sessions by providing the venue, as well as for his hospitality and friendship, while I was staying at the 'Maison Africaine'.

I am grateful to **Félix Laurent** and **Brice Yannick Djiofack**, collaborators on the PilotMAB project and colleagues at the RMCA wood laboratory, with whom I shared moments of both hardship and joy—in the field, during training sessions, and within the Wood Biology Service.

I appreciate all colleagues from the Wood Biology laboratories in Tervuren and Yangambi for their continued support and camaraderie. Special thanks go to **Nestor Luambua Kashikija**,

Chadrack Kafuti, Donatien Musepena, Paulin Yangambi, Trésor Bolaya, Odin Akatikale, Joël Lioku, Jean-Pierre Ngongo, Sorel Wasukundi, Alain Kadorho, Francine Liongo, Kévin Liévens, Maaïke De Ridder, Pauline Hicter, Blanca Van Houtte, Ruben de Blaere, Michael Monnoye, Daniel Wallenus, and Sofie Dierickx.

I am deeply grateful to the members of my thesis committee, who served as both evaluators and advisors throughout my doctoral journey. Prof. **Adeline Fayolle**, Prof. **Gauthier Ligot**, and Prof. **Jean-Louis Doucet** have my heartfelt thanks.

I express my appreciation to the authorities of The Regional Post-Graduate Training School on Integrated Management of Tropical Forests and Lands (ERAIFT) and the Institut National pour l'Étude et la Recherche Agronomiques (INERA) for their hospitality during my field stays. Special thanks go to Prof. **Tolérant Lubalega** and Prof. **Bhely Angoboy Ilondea**.

I would like to express my gratitude to **Maximilien Iyokwa** and **Christophe Mbungu Phaka** for their invaluable contributions as forest guides, particularly in micro-core sampling, species identification, and monitoring leaf and reproductive phenology.

My thanks also go to the authorities of the **Université Officielle de Ruwenzori**, my home institution, for their ongoing support. Special acknowledgment goes to Prof. **Mambo Vikandy Silusawa**, who has been a mentor and steadfast supporter throughout my career. I extend my thanks to all my colleagues at the Faculty of Science for their encouragement and collaboration.

Finally, I thank my family and friends for their unwavering support and encouragement. Special thanks go to my father, **Norbert Kanuapuki Kadiobho**, my brothers **Serge Kasili Mubenga**, **René Lumu Shabikangu**, **Nicky Panumvita Mukebayi**, **Michel Kahandja Kanuapuki**, and **Israël Kabuya Kanuapuki**, as well as my sisters **Francine Mubenga Nemaguvhuni**, **Bibi Tshijuka Tshidibi**, **Yolande Lulua Luankabo**, **Florence Biakalua Boni** and **Pacha Odia Kanuapuki**.

I would like to express my heartfelt gratitude to everyone who has contributed in any way to the completion of this thesis. I hope you understand that it is not possible to include every name in these few pages of acknowledgments. Please know that not being mentioned here in no way diminishes the significance of your support and what it truly means to me.

Table of contents

Abstract	vii
Acknowledgements	ix
Table of contents	xi
List of figures	xv
List of tables	xviii
Chapter 1: General introduction.....	1
1.1. The Congo Basin rainforest.....	2
1.1.1. Biodiversity	3
1.1.2. Climate	4
1.1.3. Climate and ecosystem services	5
1.1.4. Economic importance.....	6
1.1.5. Deforestation and environmental threats.....	6
1.1.6. Conservation efforts	6
1.2. Tree growth	6
1.2.1. Tree cell.....	7
1.2.2. Generalities on tree growth	8
1.2.2.1. Meristems as the primary drivers of tree growth	9
1.2.3. Composition and structure of secondary xylem tissue.....	12
1.2.3.1. Parenchyma, collenchyma and sclerenchyma tissues	12
1.2.3.2. Cellular composition of xylem	13
1.2.3.2.1. Tracheids	14
1.2.3.2.2. Fibers	14
1.2.3.2.3. Vessel elements	15
1.2.3.2.4. Parenchyma cells.....	15
1.2.4. Cell wall	16
1.2.4.1. Types of cell wall	16
1.2.4.2. Cell Wall Composition.....	17
1.2.4.3. Cell wall structure	18
1.2.5. Xylogenesis	18
1.2.5.1. Cell division	19
1.2.5.2. Cell enlargement.....	20
1.2.5.3. Cell differentiation	20
1.2.5.4. Secondary wall formation	20
1.2.5.5. Programmed cell death.....	20

1.2.6.	Methods to study secondary growth.....	21
1.2.6.1.	Direct measurement of stem dimension change.....	21
1.2.6.2.	Growth-ring analysis (Dendrochronology)	21
1.2.6.3.	Direct cambium activity monitoring	21
1.2.6.4.	Isotope analysis	22
1.3.	Secondary growth in the Congo basin.....	22
1.4.	The carbon cycle in Congo Basin.....	23
1.5.	Objectives and conceptual framework	24
1.6.	Specificity of this thesis	26
1.7.	Description of study sites and species	27
1.7.1.	Study sites.....	27
1.7.2.	Study tree species	29
Chapter 2: Diel and annual rhythms of tropical stem size changes in the Mayombe forest, Congo Basin		31
Abstract		32
2.1.	Introduction	32
2.2.	Materials and methods.....	34
2.2.1.	Study site	34
2.2.2.	Monitoring set-up and measurements	35
2.2.3.	Data analysis and statistical methods	37
2.3.	Results	42
2.3.1.	General pattern of stem change	42
2.3.2.	Stem changes in relation with environmental variables	43
2.3.3.	Modeling tree's responses to the environmental variables change.....	44
2.4.	Discussion	46
2.4.1.	Diel patterns of stem radial growth	46
2.4.2.	Annual patterns of stem radial growth	46
2.4.3.	Climatic driving stem radial growth.....	47
2.4.4.	Potential limitations of the results	50
2.5.	Conclusion.....	50
Chapter 3: Growth periodicity in semi-deciduous tropical tree species from the Congo Basin		53
Abstract		54
3.1.	Introduction	54
3.2.	Materials and Methods	55
3.2.1.	Study site	55

3.2.2.	Study species	56
3.2.3.	Sample collection	57
3.2.4.	Sample processing and analysis	58
3.2.5.	Auxiliary leaf phenological data	59
3.2.6.	Data analysis.....	59
3.3.	Results	60
3.3.1.	Distinctness of growth ring	60
3.3.2.	Interpretation of the number of growth rings observed.....	60
3.3.3.	Periodicity of growth-ring formation	64
3.4.	Discussion	65
3.4.1.	Distinctness of growth ring	65
3.4.2.	Periodicity of growth-ring formation	66
3.5.	Conclusion.....	68
Chapter 4: Timing of cambial phenology of rainforest trees as indicator of climate sensitivity of the Congo Basin biome.....		71
Abstract		72
4.1.	Introduction	72
4.2.	Materials and Methods	74
4.2.1.	Study sites.....	74
4.2.2.	Monitored trees.....	75
4.2.3.	Sample collection	76
4.2.4.	Sample preparation.....	76
4.2.5.	Anatomical observation of cambial activity.....	77
4.2.6.	Data processing and analysis.....	81
4.3.	Results	81
4.3.1.	Cambial activity patterns.....	81
4.3.2.	Species-specific responses to the predictive variables	86
4.3.3.	Site effects	87
4.4.	Discussion	88
4.4.1.	Cambial activity patterns.....	88
4.4.2.	Scope of environmental variables, morphological traits and reproductive efforts on cambial activity	88
4.4.3.	Site-specific observations.....	90
4.4.4.	Comparing dendrometers measurements and cambial zone analysis	90
4.5.	Conclusion.....	91
Chapter 5: Towards a better understanding of secondary growth in the Congo Basin..		93

5.1.	Key Findings and possible limitations of the results.....	94
5.2.	Strengths, limitations, and issues in applied methodologies	95
5.3.	Responses to the key research questions	96
5.3.1.	Is there a dormant period in the tree growth cycle?	96
5.3.2.	What is the timing and length of both dormancy and growing season?... 97	
5.3.3.	How is the growth cycle influenced by climatic variables?	97
5.3.4.	What anatomical marks does the growth cycle leave on the wood?	98
5.4.	Broader relevance of this research and findings	98
5.4.1.	Complementarity with other research methodologies	98
5.4.2.	Complementarity with others research findings.....	99
5.4.2.1.	Dormancy and Growth Rhythms.....	99
5.4.2.2.	Temperature and rainfall	100
5.4.2.3.	Vapor Pressure Deficit (VPD) and Relative Humidity (RH)	101
5.4.2.4.	Morphological traits	102
5.4.2.5.	Reproductive efforts	102
5.4.2.6.	Leaf phenology	103
5.5.	Prospects for future research	103
	Conclusion.....	105
	References	107
	Appendices	a
	a

List of figures

Figure 1-1. The distribution of tropical rainforests across the countries of the Congo Basin....	3
Figure 1-2. Structure and Composition of a Plant Cell.	8
Figure 1-3. Overview of primary and secondary growth.	10
Figure 1-4. A schematic illustration showing the progression of secondary growth in a dicotyledon stem from primary growth to the formation of the vascular cambium and the onset of secondary growth.	11
Figure 1-5. Cross section of a dicotyledon stem.	12
Figure 1-6. Schematic illustration of wood organization.	16
Figure 1-7. The Congo Basin carbon cycle. Annual flux of Net Primary Production (NPP) and carbon stocks in vegetation ($C_{\text{vegetation}}$) and in soil (C_{soil}), with R_a , R_d , and R_h autotrophic, heterotrophic, and vegetal debris respiration, respectively.	24
Figure 1-8. A conceptual model illustrating the interactions between trees and their environment, highlighting the key processes governing energy utilization and carbon sequestration, which ultimately drive stem growth. The figure also outlines how each chapter contributes to addressing specific research questions related to the secondary growth.....	26
Figure 1-9. Location map of study sites in the Democratic Republic of Congo (indicated by yellow dots), The Luki and Yangambi Man and Biosphere Reserves.	27
Figure 1-10. Climatic diagram of the Luki (A) and Yangambi (B) Biosphere Reserves (1981–2022). Monthly averages of precipitation (bars), average temperature (green), minimum temperature (black), and maximum temperature (red).....	28
Figure 2-1. Location of study trees in the Nkula park, and a photo of a part of the Luki Man and the Biosphere Reserve, showing the hilly landscape. (B) Walter-Lieth Climate Diagram of the Luki Man and the Biosphere reserve from 1981 to 2021. The blue line indicates rainfall curve, the red line indicates the temperature curve, the dry season is shown in dashed red. The blue stripes indicate the humid period, and the blue area shows the wet period. Temperatures in black (19.5°C and 27.9°C), on the left axis, represent the average minimum temperature of the coldest month and the average maximum temperature of the warmest month, respectively. The annual average temperature and annual rainfall are shown in the upper right corner of the diagram.	35
Figure 2-2. The stem radius variation, divided into three distinct phases of shrinkage (brown dots), swelling (orange and green dots) and stem radius growth (green dots). All points represent dendrometer recordings in $\mu\text{m}/\text{h}$	38
Figure 2-3. Diel stem change of 17 tropical trees belonging to 11 species. The dataset, shown in figure, consists of hourly increment rates, quantified as the radial increase in μm per hour according to the ZG principle. (A) Boxplots display the median (horizontal line inside the box), 25th and 75th percentiles (horizontal bases of the box) of the pooled data for all tree individuals. The vertical lines attached to the box represent the minimum and maximum values, the red dot represents mean values, and black dots indicate outliers. (B) The lines show the average hourly increment rates for each tree species. (C) and (D) Diel shrinkage rate in relation to VPD and time for all trees individual. The dataset consists of the relative contribution of hourly TWD to the total annual TWD, representing the average hourly shrinkage rate in the rainy season (C) and the dry season (D). It is colored-coded and ranges from green (low shrinkage), through orange (moderate shrinkage) to red (high shrinkage). The black line indicates the average VPD for hours with shrinkage.....	40

- Figure 2-4. Annual stem radial growth dynamics. (A) Cumulative annual growth. The data set consists of cumulative diel increment rates, quantified as the diel contribution to the total annual growth (in percent). Each curve represents a given tree individual or averaged data for *F. elastica* and *T. superba*, which data spans multiple years. The time is in days of the phenological year (DOPHY), with the first day of the phenological year on October 1 and the last day on September 30. The two vertical dashed lines represent the theoretical beginning and end of the dry season, respectively, on May 15 and September 15. (B and C) Annual variation of monthly growth rate of study species trees. (B) The lines show the median monthly growth rate for each species, quantified as the radial increase in micrometers per month. (C) Boxplots show the median monthly growth rate (horizontal line inside the box), 25 and 75 percentiles (horizontal bases of the box) of the pooled data for all tree individuals. Red dots represent mean values, while black dots are outliers. 42
- Figure 2-5. Biweekly-resolved, radial annual GR in the measured space of temperature and rainfall across all individual trees. GR was quantified as the relative annual contribution to the total annual growth for each tree and ranged from dark purple (no growth, 0%), over yellow (marginal growth, $\geq 8\%$). 45
- Figure 3-1. Location of study sites in the Democratic Republic of Congo (a). Walter- Lieth Climate Diagram of Luki (b) and Yangambi (c) UNESCO Man and Biosphere Reserve from 1981 to 2021. Data were obtained from <https://power.larc.nasa.gov/data-access-viewer/>. The blue line indicates the precipitation curve, the red line indicates the temperature curve, and the dry season is shown in dashed red. The blue stripes indicate the humid period, and the blue area shows the wet period. Temperatures in black, on the left axis, represent the average minimum temperature of the coldest month and the average maximum temperature of the warmest month, respectively. The annual average temperature and annual precipitation are shown in the upper right corner of the diagram. 56
- Figure 3-2. Incident light images of transverse sections showing tree ring boundaries (green triangles): (a) *B. welwitschii*, (b) *C. procera*, (c) *C. mildbraedii*, (d) *C. africanum*, (e) *C. griseiflora*, (f) *E. suaveolens*, (g) *G. punctata*, (h) *G. suaveolens*, (i) *L. thompsonii*, (j) *P. macrophylla*, (k) *P. oxyphylla*, (l) *P. macrocarpus*, (m) *P. angolensis*, (n) *S. kamerunensis*, (o) *S. tetrandra*, (p) *T. gilgiana*, (q) *T. prieuricana*, (r) *T. madagascariense*. 61
- Figure 3-3. Total monthly rainfall and daily variation of monthly temperature during the study years (2014, 2015, and 2016). (a) Luki and (b) Yangambi. The red and green dots on the timeline mark the marking and collection dates, respectively. Data were obtained from <https://power.larc.nasa.gov/data-access-viewer/>. 62
- Figure 3-4. Position of pinning mark on the transverse plane of the stem. (a) Marking inside the last ring, ring n ; (b) marking at the lower limit of the last ring, ring n ; (c) marking inside the penultimate ring, ring $n - 1$; (d) marking at the lower limit of the penultimate ring, ring $n - 1$; (e) marking inside the ring preceding the penultimate ring, ring $n - 2$; (f) marking at the lower limit of the ring preceding the penultimate ring, ring $n - 2$; (g) marking inside the $n - 3$ ring; (h) marking at the lower limit of the $n - 3$ ring. 63
- Figure 3-5. Images of wood samples showing the limits of growth rings (green triangles) and the new wood layers containing the scar (red triangle) resulting from cambial marking: (a) *P. macrocarpus*, (b) *C. procera*, (c) *B. welwitschii*, (d) *P. oxyphylla*, (e) *C. griseiflora*, (f) *T. madagascariense*, (g) *P. angolensis*, (h) *S. kamerunensis*, (i) *P. oxyphylla*, (j) *C. mildbraedii*, (k) *G. suaveolens*, (l) *P. oxyphylla*, and (m) *C. africanum*. 64
- Figure 4-1. Climatic diagrams of the study sites from the Democratic Republic of Congo: (A) for the Luki biosphere reserve, (B) for the Yangambi biosphere reserve. Monthly averages of

precipitation (bars) and temperatures (green: average, black: minimum, red: maximum) from 2013–2022. Data were obtained from <https://power.larc.nasa.gov/data-access-viewer/>. 75

Figure 4-2. Cross sections of stems from four of ten study species showing different intensity of cambial activity. A large number of cells in the enlarging phase near the cambium indicates a highly ((A) and (B)) to moderately (C) productive stage. In contrast, the presence of only a few xylem cells undergoing secondary wall formation and lignification suggests that the cambium stopped producing new cells some time ago (D). (A) *P. balsamifera* in visible light (Luki, May 9, 2022), (B) *F. elastica* in UV light (Luki, July 18, 2022), (C) *T. madagascariense* in UV light (Yangambi, October 15, 2022), (D) *L. thompsonii* in visible light (Yangambi, October 1, 2022). (A) and (B) Periods of strong cambial activity. (C) Period of moderate cambial activity and (D) Period of low cambial activity. (A) and (D). Phl = Phloem, Ca = Cambial zone, Ez = Enlarging zone, Tz = thickening zone, Mz = Mature xylem cells. Scale bars = 100 μm 78

Figure 4-3. Illustration of cambial dormancy in eight of the ten species studied. What persists is a cambial zone composed of a few layers of cells, between the phloem and the xylem. (A) *F. elastica* (Luki, July 4, 2022); (B) *G. giganteum* (Luki, May 23, 2022), (C) *O. gore* (Luki, May 23, 2022); (D) *P. oleosa* (Yangambi, June 6, 2023); (E) *P. macrocarpus* (Yangambi, October 10, 2022); (F) *S. subcordatum* (Yangambi, May 20, 2023); (G) *S. zenkeri* (Yangambi, May 6, 2023), the boundary of the newly formed ring is visible, distinguished by two flattened cell layers with thick secondary walls (Green triangle); (H) *T. madagascariense* (Yangambi, March 11, 2023). 80

Figure 4-4. Overview of Cambial Activity for Study Species, exhibiting the number of trees with cambial activity event for each species. Vertical dashed lines indicate the beginning and end of each month. Vertical red lines represent the onset and end of the dry season in Luki, as well as the start and end of the period with low monthly rainfall (<150mm) in Yangambi. ... 83

Figure 4-5. Annual variation in the radial number of cells in the developing zone. (A) The box plots display the median (horizontal line within the box), the 25th and 75th percentiles (lower and upper edges of the box), of data grouped by species. The vertical lines extending from the box represent the minimum and maximum values, the red dot indicates the mean value, and the black dots denote outliers. (B) The dots represent raw data, with red dots indicating a dormant cambium and green dots indicating an active cambium. The solid lines represent the fitted LOESS (locally estimated scatterplot smoothing) curve, and the shaded area represents the 95% confidence interval. 84

Figure 4-6. Radial Growth dynamics from dendrometer measurements in Yangambi. (A, B) Boxplots show hourly (A) and monthly (B) radial increment rates (μm), with the median (horizontal line), 25th and 75th percentiles (box edges), minimum and maximum values (whiskers), mean (red dot), and outliers (black dots) for all tree individuals. (C) Cumulative annual growth curves represent the daily contributions to total annual radial growth (μm) for each tree. 85

List of tables

Table 1-1. List of study species.....	30
Table 2-1. Characteristics of 17 trees monitored in Nkula Park.	36
Table 3-1. Leaf functional group, tree species, botanical family, stratum at adult stage (Lubini, 1997), distinctness and description of growth-ring boundaries (obtained from this study), and total number of successfully marked trees per species, in Luki and Yangambi forests.....	58
Table 3-2. Model output of quantifying growth-ring periodicity in response to DBH (initial, at start of observation period), relative mean increment, and site as fixed effects, using a generalized linear mixed-effects model. Tree species are nested within site as a random effect.	65
Table 4-1. Significance of predictor variables on the radial number of cells in the developing zone.	87

Chapter 1: General introduction



Ndiondio, Luki reserve

1.1. The Congo Basin rainforest

The Congo Basin, located in central Africa, is one of the world's most significant ecological and hydrological regions. Renowned for its rich biodiversity, the region is home to the livelihoods of 80 million people (White et al., 2021). Several small groups of the most well-known indigenous tribal groups, often referred to as "Pygmies" inhabited the region for thousands of years (Verdu, 2016). The Congo Basin can be viewed from two main perspectives: the Hydrographical Congo Basin and the Ecological Congo Basin.

The Hydrographical Congo Basin, also referred to as the “Cuvette Centrale” (Crosby et al., 2010), encompasses the entire drainage area of the Congo River, Africa's second-longest river and the world's second largest by discharge (after the Amazon). Spanning approximately 400 million hectares, it includes all regions where water flows into the Congo River and its tributaries. Extending beyond rainforest boundaries, it reaches savannahs and non-forested areas. This basin is shared by eight countries: Democratic Republic of the Congo, Republic of Congo, Central African Republic, Angola, Zambia, Tanzania, Burundi, Rwanda, and Cameroon (Harrison et al., 2016). Gabon is occasionally considered part of the Hydrographical Congo Basin due to minor hydrological overlaps near its eastern regions (Yuh et al., 2024).

The Ecological Congo Basin refers to the tropical rainforest biome and associated ecosystems (Fig. 1 - 1), representing the world's second-largest continuous tropical rainforest, following the Amazonian forests (Mayaux et al., 2013). It plays a crucial role in biodiversity conservation and climate regulation (Hubau et al., 2020). It spans about 240 million hectares (White et al., 2021) across six main countries, namely Democratic Republic of the Congo, Republic of Congo, Central African Republic, Gabon, Equatorial Guinea, and Cameroon (Bele et al., 2015). Northern Angola, including regions like Cabinda and Uíge, is partially included due to its rainforest ecosystems connected to the basin (Huntley, 2019).

Throughout this document, any reference to the Congo Basin pertains to its ecological definition.

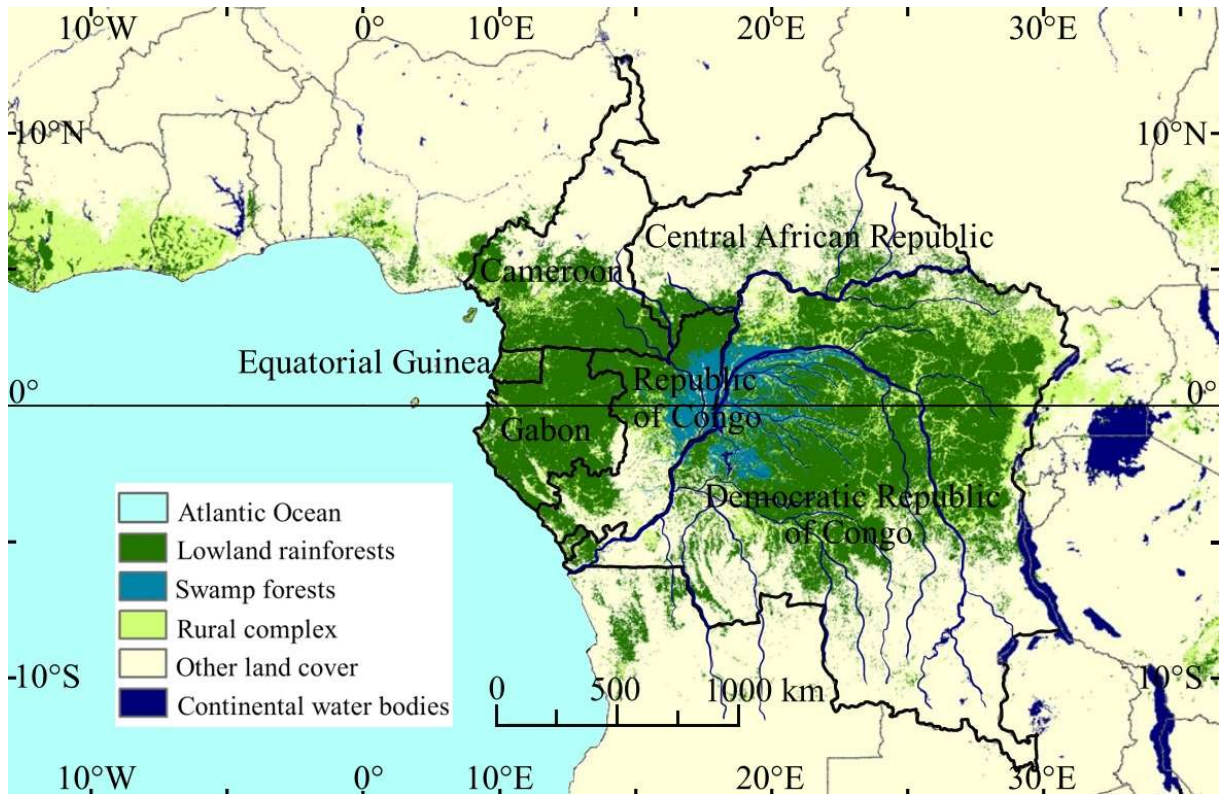


Figure 1-1. The distribution of tropical rainforests across the countries of the Congo Basin.

1.1.1. Biodiversity

The Congo Basin is a dense tropical rainforest, as defined by the Yangambi classification (Aubréville, 1957), this kind of forest is characterized by its complex multi-layered structure, including an emergent canopy (30–50 m or higher), a continuous mid-canopy, and an understory of shade-tolerant plants. It features high species richness with predominantly evergreen species, creating a dense, dark environment with limited light reaching the forest floor. The vegetation is further enriched by the presence of lianas, epiphytes, and climbing plants. The forest floor is relatively open but covered by organic debris. These forests thrive in warm, humid climates with consistent rainfall, relying on efficient nutrient cycling to compensate for nutrient-poor soils.

The Congo Basin is among the most biologically rich ecosystems on the planet, housing more than 1,200 species of fish, 400 species of mammals, 1,000 species of birds, and over 10,000 species of vascular plants, with around 30% being unique to the basin (Harrison et al., 2016; Réjou-Méchain et al., 2021). The composition of vascular plant species in the forest is heterogeneous across regions, though there is considerable overlap between some areas. The forest canopy and mid-canopy feature emblematic species such as *Entandrophragma cylindricum*, *Entandrophragma utile* (Kasongo Yakusu et al., 2018), *Pericopsis elata* (Bourland et al., 2012; Kafuti et al., 2022), *Scorodophloeus zenkeri* (Kearsley et al., 2017), and *Aucoumea klaineana* (Guidosse et al., 2024), while the understory is filled with a diversity of smaller plants, shrubs, and ferns (Hubau et al., 2019). Monodominance, where at least 60% of canopy-level trees belonging to the same species (T. B. Hart et al., 1989), is found in primary rainforests throughout the Congo basin. Many of monodominant species belong to the leguminosae

subfamily detarioideae, *Gilbertiodendron dewevrei* (De (Torti, Coley, Kursar, et al., 2001), *Cynometra alexandri* (T. B. Hart et al., 1989; Luse Belanganayi, 2016), *Julbernardia seretii* (T. B. Hart et al., 1989), *Talbotiella gentii*, and *Tetraberlinia tubmaniana* (Peh et al., 2011).

Iconic animal species like forest elephants (Fay & Agnagna, 1991; Beirne et al., 2021), western lowland gorillas (Fay et al., 1989; Strindberg et al., 2018), bonobos (Nackoney & Terada, 2023), and the elusive okapi (Stanton et al., 2014, 2015) inhabit the region. With the highest primate density in the world, including chimpanzees and numerous monkey species, the Congo Basin is also a critical area for birds, such as the African grey parrot (Fastré et al., 2024). The region is home to a wide range of reptiles and amphibians, including frogs, snakes, and crocodiles. Additionally, its rich insect diversity includes butterflies, beetles, and ants, all playing vital roles in maintaining the ecosystem's health (Harrison et al., 2016; Beekmann et al., 2024).

1.1.2. Climate

The Congo Basin encompasses a wide range of ecosystems with varying tropical climatic conditions. In the northern forests, the region experiences a hot, dry season, while the western forests have a cooler, dry season (De Wasseige et al., 2010). Three main climate zones, classified according to the Köppen-Geiger system, define the region. The northern part of the basin, extending from 2.5°N to the northern border, is characterized by tropical savannah (Aw) and tropical monsoon (Am) climates. Around the equatorial region, between 2.5°N and 3.5°S, the middle zone is dominated by tropical rainforest (Af) and tropical monsoon (Am) climates. Further south, from 3.5°S to the southern border, the region is primarily characterized by a tropical savannah (Aw) climate (Mabrouk et al., 2022). The rainfall and temperature patterns across the basin are highly variable (De Wasseige et al., 2010). However, the climate in the Congo Basin is primarily influenced by rainfall, with only a minor contribution from temperature variations. The region does not experience distinct thermal seasons, as temperatures remain relatively consistent throughout the year with a low annual range. However, the higher altitudes along the eastern and southern edges of the basin exhibit the greatest annual temperature variation, reaching up to 4°C (Munzimi et al., 2015; Cook et al., 2024). Over the past four decades, the Congo Basin peatlands have recorded an average annual temperature of 25.5°C, which is slightly higher than temperatures measured over open water areas but comparable to those observed in savannah regions (Eba'a Atyi et al., 2022).

The Congo Basin experiences diverse precipitation patterns shaped by its equatorial location and complex climate dynamics. The dominant form of precipitation is convective rainfall, driven by intense surface heating and moisture convergence, which frequently generates thunderstorms. The highest mean annual rainfall (~2,000 mm) is concentrated in the central region of the Congo River Basin near the equator, gradually decreasing to less than 1,000 mm towards the northern and southern edges (Mabrouk et al., 2022).

The spatiotemporal distribution of monthly rainfall in the Congo Basin is influenced by the north–south migration of the Intertropical Convergence Zone (ITCZ). Rainfall is most widespread (50–300 mm) in March, April, October, and November, while the smallest areas (0–200 mm) are observed from June to August. The rainfall belt moves northward from February to July and shifts southward from August to January. Regions with the highest monthly rainfall (>200 mm) vary seasonally: the south and southeast experience peak rainfall

in December and January, the north and northwest from August to October, and the west and central areas in April and November. Conversely, minimum rainfall (<50 mm) occurs from May to October in the south and southeast and from November to January in the north and northwest. Notably, the southeastern region receives the most rainfall (>250 mm) from December to February but experiences almost no rainfall (0 mm) from June to August (Mabrouk et al., 2022).

The World Meteorological Organization (WMO) recently reported that global near-surface temperatures are highly likely to surpass pre-industrial levels by 1.5°C for at least one year between 2023 and 2027. Additionally, projections indicate wetter-than-average conditions across large parts of Asia and Central Africa during this period (WMO, 2023). Recent studies further support this trend. Kasongo Yakusu et al., (2023) report a shift toward a drier dry season and a more intense wet season since the early 2000s. The ongoing warming, along with increased seasonality and rainfall intensity, is already significantly impacting crop yields in Yangambi. Additionally, Cook et al., (2024). project that surface temperatures in the Congo Basin will rise by 4.0–5.4 K by the end of the century, with variations depending on region and season. These temperature changes are strongly influenced by feedback mechanisms, including increased atmospheric water vapor and cloud dynamics, which amplify radiative forcing.

1.1.3. Climate and ecosystem services

The Congo Basin rainforest is often referred to as the "lungs of Africa" due to its critical role in carbon sequestration. The entire basin absorbs approximately 1.5 billion metric tons of carbon dioxide annually, making it one of the most significant carbon sinks on the planet (UNEP, 2023). The Congo Basin forests contain a high level of carbon. It is estimated that they hold between 25 and 30 billion tons of carbon in their vegetation (Hoare, 2007), and an additional 30.6 billion tons of carbon in their peatlands (Dargie et al., 2017). Currently, these forests store more carbon per hectare than Amazonian forests, primarily due to their distinct structural characteristics. Although tree density per hectare is lower in the Congo Basin, the region has a higher proportion of large-diameter trees, and trees of similar diameter tend to be taller. As a result, The average carbon or biomass per hectare is higher in Congo Basin forests compared to Amazonian forests (Sullivan et al., 2017). In addition, unlike the Congo Basin forests, Amazonian forests have experienced a decline in atmospheric carbon uptake capacity over the past 30 years, primarily due to increased tree mortality linked to climate change (Brienen et al., 2015; Hubau et al., 2020).

The Congo Basin rainforests provide approximately 30% of Africa's freshwater resources, supporting millions of people who rely on these ecosystems for their livelihoods and daily needs (De Wasseige et al., 2010; White et al., 2021). These forests play a crucial role in both regional and global water cycles, generating 75% to 95% of their own rainfall (De Wasseige et al., 2010). This moisture not only sustains the Congo River system but also influences weather patterns across the African continent, extending as far as the Sahel and the Ethiopian highlands. As a result, these forests provide vital water resources that support an additional 300 million rural Africans (White et al., 2021). Furthermore, the forest's dense canopy helps regulate temperatures, reducing extreme heat and contributing to the stability of its microclimates (De Frenne et al., 2019).

1.1.4. Economic importance

The Congo Basin is a critical economic resource for central African countries. Timber extraction is a significant industry, with valuable woods such as okoumé (*Aucoumea klaineana*), sapelli (*Entandrophragma cylindricum*), ayous (*Triplochiton scleroxylon*), iroko (*Milicia excelsa*), sipo (*Entandrophragma utile*), padouk (*Pterocarpus soyauxii*), and moabi (*Baillonella toxisperma*) being the main species harvested in the beginning of the 21st century (Pérez et al., 2005).

1.1.5. Deforestation and environmental threats

The forest ecosystems of the Congo Basin remain relatively well preserved compared to other tropical regions, such as Amazonia and Southeast Asia, where deforestation rates are significantly higher (Hubau et al., 2020). However, there are growing indications that the Congo Basin may be approaching a turning point, facing increased risks of deforestation and forest degradation. Historically, low deforestation rates have been attributed to factors such as poor infrastructure, low population densities, and political instability, which have provided a form of passive protection for the forests (Megevand et al., 2013). Despite this, the Congo Basin is now under increasing pressure from both internal and external forces, including illegal logging, poor governance, high levels of corruption, mineral extraction, road development, wood energy exploitation, and the expansion of shifting cultivation for subsistence (Bauters et al., 2021; Piabuo et al., 2021). These factors, combined with population growth, threaten to significantly intensify deforestation. As a result, the region could shift from its current "high forest/low deforestation" status to one marked by accelerated deforestation in the coming decades (Megevand et al., 2013). Additionally, rising temperatures (Anderegg et al., 2015) and shifting rainfall patterns (Trenberth, 2011) are altering the rainforest's structure, leading to changes in species distribution and an increased frequency of wildfires (Fauset et al., 2012).

1.1.6. Conservation efforts

Efforts to protect the Congo Basin rainforest and its biodiversity are ongoing. Several national parks (Imarhiagbe et al., 2022), such as Virunga National Park and Odzala-Kokoua National Park, have been established to conserve wildlife and ecosystems. In addition, UNESCO World Heritage Sites, including Salonga National Park in the Democratic Republic of Congo (DRC), serve as crucial protected areas (Egbe, 2022). The countries of the Congo Basin actively participate in the REDD+ program (Reducing Emissions from Deforestation and Forest Degradation), which should offer financial incentives for conservation and sustainable forest management (Somorin et al., 2012). International conservation organizations like the World Wildlife Fund (WWF), Rainforest Foundation, and Conservation International collaborate with governments and local communities to promote the sustainable use of resources and protect endangered species. Increasingly, indigenous communities and local populations are becoming involved in these conservation initiatives, using their traditional knowledge to manage the forest in a sustainable manner (Eba'a Atyi et al., 2022).

1.2. Tree growth

A tree is a specific type of plant, defined as an organism that performs photosynthesis, and is distinguished by its woody, lignified trunk, branches, and typically significant height. Trees are perennial plants, meaning they live for more than two years, and they play a crucial role in

ecosystems by sequestering carbon and providing habitats for various other living organisms. Growth is a vital function of trees, allowing their trunks and branches to increase in length (primary growth) and in diameter (secondary growth) over time (Campbell & Reece, 2012).

To gain a clearer understanding of the dynamics of growth in tree wood, it is important to first grasp its fundamental composition and structure. This section offers a general overview of wood biology without getting too deep into plant physiology, laying the groundwork for a more detailed exploration of the process of xylogenesis.

1.2.1. Tree cell

Cells represent the smallest components of living organisms that perform all essential biological functions, serving as the fundamental structural and functional units of life. This concept is a core principle of cell theory, which highlights that all living organisms, no matter how simple or complex, are made up of cells. These cells are responsible for carrying out vital functions such as energy capture, nutrient absorption, waste elimination, and reproduction. Single-celled organisms perform all necessary functions within one cell, while multicellular organisms depend on the specialization and coordination of many different cell types to sustain life (Evert, 2006; Campbell & Reece, 2012).

Plants, as living organisms, are made up of cells (Fig. 1 – 2), which vary greatly in size, shape, and function. Some cells have microscopic size, while others can reach sizes of millimeters or even centimeters, as seen in certain plant fibers. While some cells carry out multiple functions, others are highly specialized for specific tasks. Despite this remarkable diversity, cells share striking similarities in their physical structure and biochemical properties, highlighting a common organizational framework across diverse forms of life (Evert, 2006; Crang et al., 2018).

Tree cells, like other plant cells, consist of the **cell wall** and the **protoplasm**. The protoplasm includes both the cytoplasm and the **nucleus**. The **cell wall** is mainly composed of cellulose, hemicellulose, and lignin, giving the cell its strength and structure. Inside, the cytoplasm is a gel-like substance that houses the organelles, which perform essential functions like energy production, protein synthesis, and nutrient storage (Evert, 2006; Taiz & Zeiger, 2010; Crang et al., 2018). Key organelles include:

- **Chloroplast:** Organelle responsible for **photosynthesis**.
- **Mitochondria:** The powerhouse of the cell, where energy (ATP) is produced.
- **Endoplasmic Reticulum (ER):** Involved in protein and lipid synthesis.
- **Golgi Apparatus:** Processes and packages proteins and lipids for transport.
- **Vacuole:** A large, central organelle in tree cells that stores nutrients, waste products, and helps maintain cell turgor (pressure), crucial for supporting the plant's structure.
- **Plasmodesmata:** Channels between adjacent cells, allowing for communication and transport of materials.

The nucleus controls cell activities and contains genetic material (DNA). Together, cell components support growth, transport of water and nutrients, and overall tree function (Evert, 2006; Taiz & Zeiger, 2010; Crang et al., 2018).

The cytoplasm of every living cell is surrounded by a **plasma membrane which** is a selectively permeable barrier that surrounds its cytoplasm. The plasma membrane is composed primarily of a phospholipid bilayer with embedded proteins. It plays a crucial role in regulating the transport of substances in and out of the cell, ensuring cellular homeostasis. Additionally, it facilitates communication between cells through various signaling molecules. **Plasmodesmata**, small membrane-lined channels, are extensions of the plasma membrane that traverse the cell wall to connect the cytoplasm of neighboring plant cells. These structures allow the plasma membranes of adjacent cells to remain continuous, enabling the direct exchange of ions, small molecules, and even macromolecules between cells. This connection ensures coordination in cellular activities (Evert, 2006).

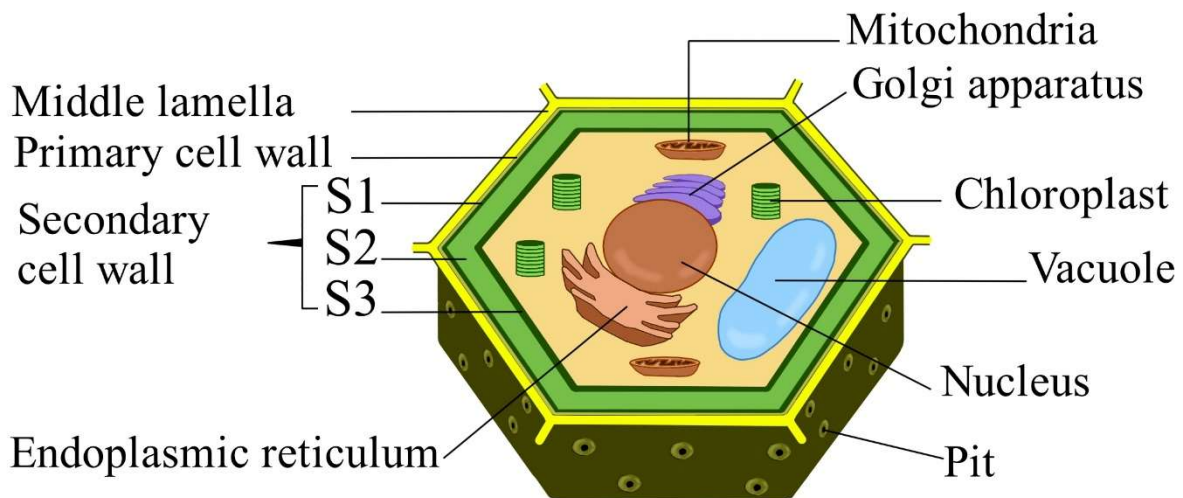


Figure 1-2. Structure and Composition of a Plant Cell.

1.2.2. Generalities on tree growth

Carbon sequestration in trees is a complex sequence of chemical and physiological processes that begins with photosynthesis (J. W. Hart, 2012) and culminates in the deposition of lignin in the cell walls of woody tissues (Verbančič et al., 2018). This series of processes not only drives tree growth but also plays a crucial role in mitigating climate change by capturing carbon dioxide from the atmosphere (Crang et al., 2018). As highlighted earlier, the Congo Basin, one of the world's largest carbon sinks, sequesters vast amounts of CO₂, making it indispensable to global carbon regulation. Tree growth is one of the mechanisms contributing to the carbon sinks of the Congo Basin (Nkem et al., 2008). Given the ecological and climatic significance of this region, it is imperative to understand the growth dynamics of its trees. By studying the processes underlying tree growth, we can gain valuable insights into the factors that influence carbon storage and forest productivity.

In the following sections, we will provide a general overview of tree growth, with particular attention to the processes involved in both primary and secondary growth. This will be followed by a more detailed examination of secondary growth, which has emerged as the primary driver of carbon sequestration in trees.

1.2.2.1. Meristems as the primary drivers of tree growth

At any point, plants have embryonic, growing, and mature organs. Except during dormancy, most plants grow continuously. This phenomenon is known as infinite or indeterminate growth. Indefinite growth is possible because plants constantly produce undifferentiated tissues called **meristems**, which divide under favorable conditions to produce new cells that can enlarge. There are two types of meristems: **apical meristems** and **lateral meristems** (Campbell & Reece, 2012; Crang et al., 2018).

Apical meristems, located at the tips of roots and stems, as well as in the axillary buds of shoots, provide the cells necessary for growth in length. This type of elongation is called primary growth, allowing roots to extend into the soil and stems to increase their exposure to light. The terminal buds carry out the lengthwise growth of each tree axis by extending its free end, creating a new axis portion of length l (Fig. 1- 3). The segment of the stem formed during an uninterrupted period of elongation is referred to as the **primary growth unit (GU)** (Hallé et al., 1968; Hallé & Oldeman, 1970).

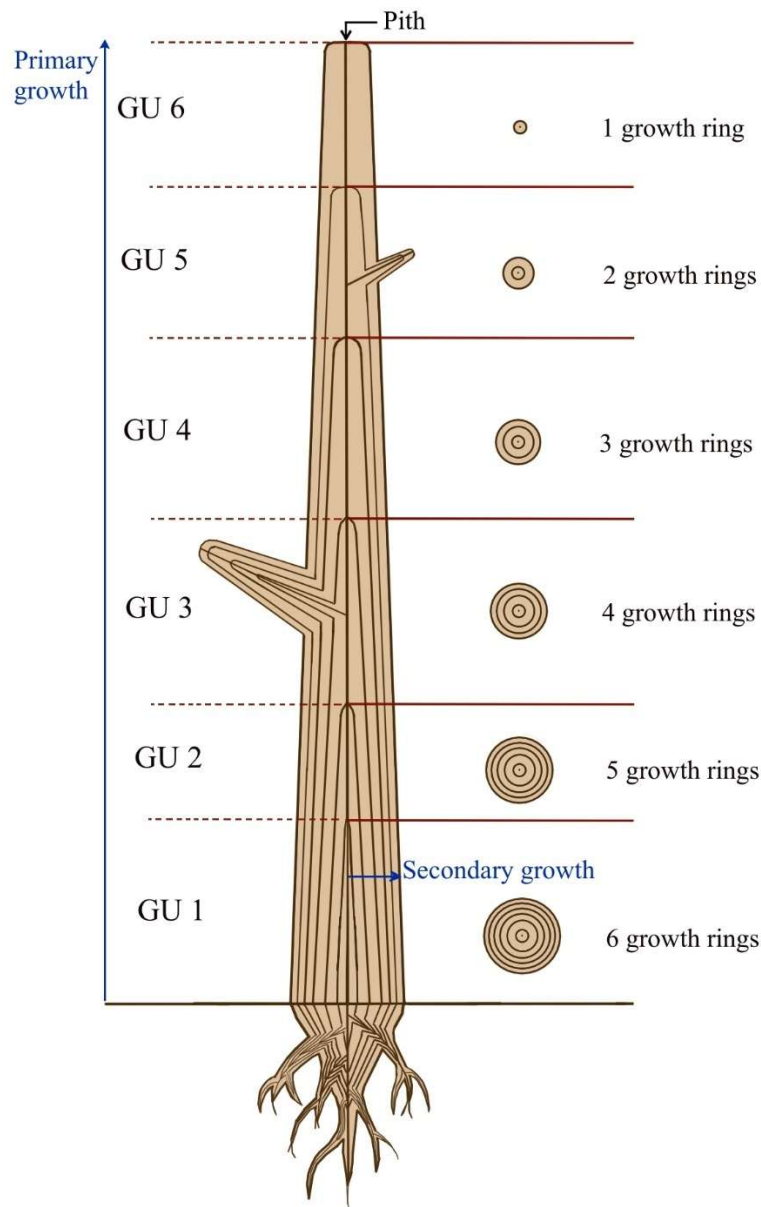


Figure 1-3. Overview of primary and secondary growth.

In woody plants, the parts of stems and roots where growth in length has ceased begin to increase in circumference. This thickening, known as secondary growth, occurs due to the activity of **lateral meristems**, specifically the **vascular cambium** (from the Latin *cambiare*, meaning "to change") and the **cork cambium** or the **phellogen** (from the Greek *phellos*, meaning "cork"). These cylindrical structures of dividing cells extend along the roots and stems. The vascular cambium generates additional layers of conductive tissue, known as secondary xylem (wood) and secondary **phloem**. The phellogen replaces the epidermis with the thicker tissue (Fig. 1 – 4) (Campbell & Reece, 2012; Crang et al., 2018).

The phloem, the inner bark part, is a vascular tissue responsible for transporting organic nutrients, particularly the products of photosynthesis, such as sugars, from the leaves (where they are produced) to other parts of the plant, including the roots, stems, and growing tissues.

The phloem is essential for distributing energy to maintain plant growth, development, and storage (Taiz & Zeiger, 2010).

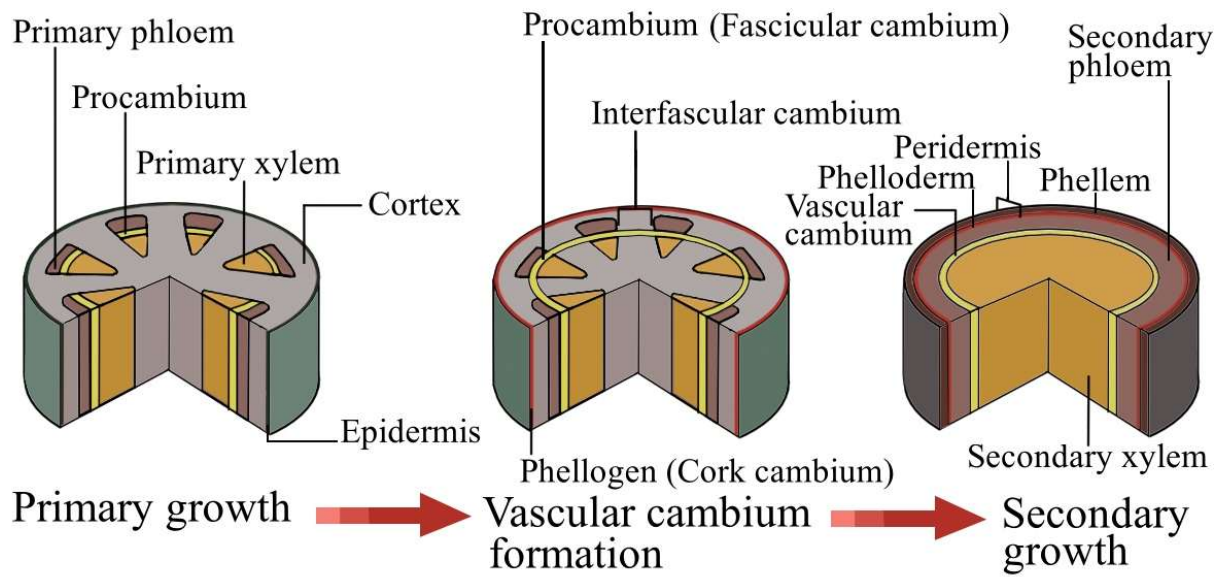


Figure 1-4. A schematic illustration showing the progression of secondary growth in a dicotyledon stem from primary growth to the formation of the vascular cambium and the onset of secondary growth.

The peridermis, or more commonly referred to simply as the periderm or suber, is the outer part of the tree's bark that plays a crucial role in protecting the plant from environmental stresses, such as physical damage, pathogens, and water loss. The periderm is made up of three main components (Glimn-Lacy & Kaufman, 2006) (Fig. 1 – 5) :

1. **Phellogen (Cork Cambium):** This is a layer of meristematic cells that divides to produce the other two layers of the periderm. It is the origin of the periderm and is responsible for the growth of the cork tissue.
2. **Phellem (Cork):** The outer layer produced by the phellogen, made up of dead cells filled with a substance called suberin, which is waterproof. The phellem serves as the primary protective barrier against physical damage, pathogens, and water loss.
3. **Phelloderm:** The inner layer produced by the phellogen, which consists of living cells. The phelloderm is often thin and can assist in nutrient storage and transport, though its exact role can vary depending on the plant species.

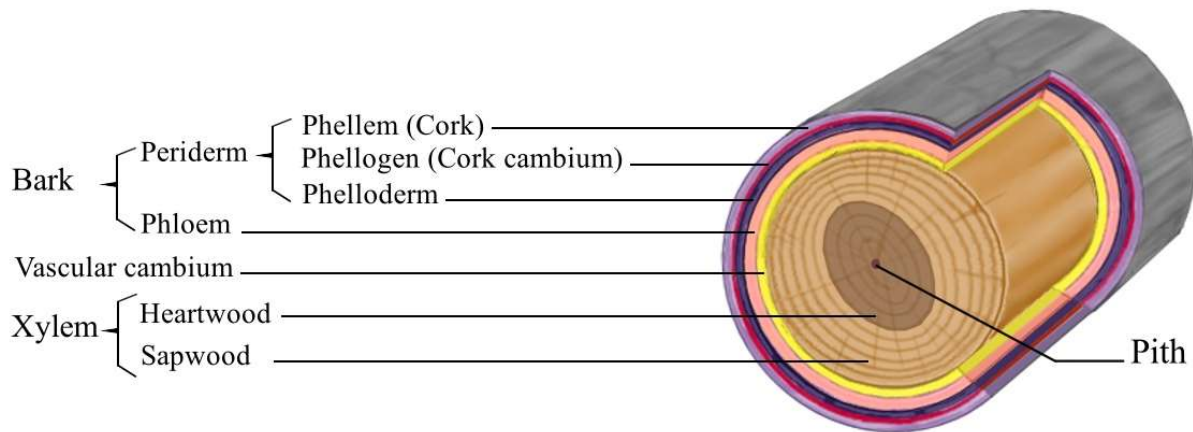


Figure 1-5. Cross section of a dicotyledon stem.

Meristem cells divide frequently to produce new cells. Some of these new cells remain in the meristems as a source for further cell production. Traditionally called initial cells, they are increasingly referred to as stem cells. Another portion of the new cells specialize and become integrated into the tissues and organs of the growing plant (Campbell & Reece, 2012).

The central core of the stem or trunk, often composed of soft parenchyma cells, is known as the pith. It is typically present in younger plant stems, where it is involved in nutrient storage and transport. As the tree matures, the pith becomes less significant and eventually disappears in older trees (Rittner & McCabe, 2004).

1.2.3. Composition and structure of secondary xylem tissue

1.2.3.1. Parenchyma, collenchyma and sclerenchyma tissues

Like all plants tissues, woody cells are primarily classified into parenchyma, collenchyma, and sclerenchyma, each serving distinct structural and functional roles (Crang et al., 2018).

Parenchyma cells have thin primary cell walls, remain alive at maturity, and are the most common type of plant cells. They are primarily responsible for storage, photosynthesis, and wound repair in wood tissues. In xylem, parenchyma cells are found in rays and axial and serve to store starch and aid in water transport (Evert, 2006).

Collenchyma cells have unevenly thickened primary walls that provide flexibility. Unlike sclerenchyma, they lack lignin, allowing them to offer flexible support. In some cases, secondary deposition may occur, leading to a gradient in development (Leroux, 2012). They are found mainly in young growing tissues and in herbaceous parts (such as leaves) of angiosperms. In xylem, they are less abundant but can be found in areas that require flexibility. Collenchyma cells provide mechanical and structural support while allowing for growth. Of the three fundamental plant tissues, collenchyma accounts for only about 1% (Crang et al., 2018).

Sclerenchyma cells have thickened secondary walls rich in lignin, which gives them rigidity. These cells are typically dead at maturity and provide essential mechanical support and strength to the plant. The primary sclerenchyma cells include fibers, tracheids, and vessel elements found throughout the xylem, as well as sclereids located mainly in the phloem, all of which contribute significantly to the hardness and structural integrity of tree stem (Crang et al., 2018).

1.2.3.2. Cellular composition of xylem

Xylem tissue is composed of various types of cells that differ in structure and function (Evert, 2006; Crang et al., 2018). As in all plant tissues, there is a layer of 0.5 to 1.5 μm thick between adjacent wood cells, known as the middle lamella (Plomion et al., 2001). It serves as a kind of cement that holds neighboring cells together, providing structural stability and helping tissues maintain their shape and integrity. The middle lamella is primarily composed of pectins, a group of polysaccharides that are sticky and gel-like, making it highly effective at binding cells (Tan et al., 2013; Anderson, 2016). During the process of lignification, which occurs in the secondary cell wall formation of certain tissues like xylem, the middle lamella can become impregnated with lignin, contributing to the rigidity and strength of tissues like wood (Taiz & Zeiger, 2010).

The primary wood cell types include tracheids, fibers, vessel elements, and parenchyma cells, all of which are supported by a cell wall made of cellulose, hemicellulose, and lignin (Lack & Evans, 2001; Taiz & Zeiger, 2010) (Fig. 1 – 6). Tracheids and parenchyma cells are present in both gymnosperms and angiosperms (flowering plants). Fibers are absent in most gymnosperms. Vessels are generally absent in gymnosperms. Gymnosperms, such as conifers, rely on tracheids for both water conduction and structural support (Hacke et al., 2005; Sperry et al., 2006). In some exceptional cases, a few gymnosperms, like members of the Gnetales order (*Gnetum* and *Ephedra*, and *Welwitschia*), have evolved to possess vessel elements. The presence of vessels in these groups is considered a convergent evolution, meaning it evolved independently of the vessels in angiosperms (Carlquist, 2012).

The internal cavity or space within a plant cell is called lumen, particularly in xylem cells such as tracheids, vessel elements, and fibers. In the context of xylem cells, the lumen is the hollow region through which water and nutrients move (Sperry et al., 2006). Cells that perform a conductive function possess specialized structures in their cell walls known as pits. The pit membrane, composed of cellulose, regulates water flow and prevents the entry of air embolisms (air bubbles), which could interfere with water transport (Lack & Evans, 2001). There are three main types of pits: simple pits, bordered pits, and half-bordered pits. Simple pits have a straightforward design. They consist of a pit membrane surrounded by a relatively thin and unthickened cell wall. The pit aperture is simple and not surrounded by any additional thickening. These are common in parenchyma cells, fibers, and sometimes in vessel elements. Bordered pits have a more complex design. They consist of a pit membrane surrounded by a thickened border of secondary cell wall material. The pit chamber is larger, and the aperture is more defined, often appearing as a smaller opening within the larger pit chamber. Bordered pits are primarily found in tracheids and vessel elements (Crang et al., 2018).

In the vessel elements, there are areas at the ends of the cell body where the cell walls are either partially or completely dissolved, creating openings known as perforation plates. These allow for the unrestricted flow of water from one cell element to another. Perforation plates may be simple or compound (Lack & Evans, 2001; Campbell & Reece, 2012; Crang et al., 2018). Here are the main types of perforation plates:

- **Simple perforation plates.** Simple perforation plates consist of a single large opening, without any bars or divisions. Commonly found in species with high water-transport efficiency (Oskolski & Jansen, 2009).
- **Scalariform perforation plates.** Featuring multiple elongated, parallel slits, resembling a ladder. Often found in primitive angiosperms and in regions of the plant with lower water transport demands (Christman & Sperry, 2010; T. Xu et al., 2022).
- **Reticulate perforation plates.** With network-like arrangement of openings, similar to a mesh or net. Found in some species but is relatively less common than simple or scalariform plates (Luo et al., 2019).
- **Foraminiform perforation plates.** Featuring multiple small, round openings that resemble pores. Very rare, they are considered to be a specialized type of perforation plate (Wróblewska, 2015).
- **Ephedroid perforation plates.** Ephedroid perforation plates show a combination of features that are intermediate between primitive and advanced types of perforation plates. They are often partially dissolved, with a mix of narrow, slit-like openings and more perforated areas (Crang et al., 2018). They refer to a specialized type of perforation plate found in the xylem vessel elements of certain members of the Gnetales order (Jiang et al., 2013).

Specialized structures known as spiral thickenings are found in the secondary walls of some xylem cells, such as tracheids and vessel elements. These consist of helical or spiral bands of thickened cell wall material, typically made of cellulose and lignin, which provide structural reinforcement while allowing the cell walls to remain flexible. Spiral thickenings are particularly common in younger or newly formed xylem elements, where they help maintain water transport under challenging conditions by reducing the likelihood of cell collapse during water stress (Lack & Evans, 2001).

1.2.3.2.1. Tracheids

Tracheids (Fig. 1 – 6) are elongated, slender cells with thickened walls and tapered ends, lacking perforations. They have bordered pits that allow water to pass between adjacent cells. Aligned side by side and oriented parallel to the tree's axis, tracheids primarily function in both water transport and structural support. They facilitate the movement of water and dissolved nutrients from the roots to other parts of the plant, particularly in gymnosperms and certain angiosperms (Glimn-Lacy & Kaufman, 2006).

1.2.3.2.2. Fibers

Fibers (Fig. 1 – 6) are long-walled narrow cells with smaller lumens and fewer bordered pits than tracheids, because they are not involved in active water conduction. Fibers are often dead at maturity and unlike tracheids, they do not have plate perforations. Typically, thicker-walled than tracheids, fibers are mainly supporting cells that reinforce the xylem of angiosperms, giving elasticity, flexibility, tensile strength, and mechanical support to plant structure (Rittner & McCabe, 2004). There are two types of fibers found in the xylem tissue of angiosperms: fiber-tracheids and libriform fibers (Li et al., 2024). Fiber-tracheids are intermediate cells between tracheids and fibers. They are elongated cells with thicker cell walls than typical

tracheids, but they still retain some ability for water conduction. Fiber-tracheids contain bordered pits, similar to tracheids, which allow for limited water movement between adjacent cells. However, these pits are generally fewer and smaller, and less efficient in water transport than those in tracheids. The primary function of fiber-tracheids is mechanical support, but they also play a minor role in water conduction. They are more common in primitive angiosperms or plants that need structural reinforcement while maintaining some conduction capacity (Crang et al., 2018).

Libriform fibers are highly specialized fibers that are even more adapted for mechanical support than fiber-tracheids. They are long, narrow cells with thick lignified walls and a small lumen. Unlike fiber-tracheids, libriform fibers have simple pits or no pits at all, making them highly specialized for support but not for conduction. Libriform fibers are primarily responsible for structural reinforcement. They have very little, if any, role in water transport. This specialization for mechanical strength is particularly important in hardwood species, where the plant relies on other cells, such as vessel elements and tracheids, for water movement (Hacke et al., 2015; Crang et al., 2018).

1.2.3.2.3. Vessel elements

Vessel elements (Fig. 1 – 6) are wide, short cells with thick lignified walls and perforation plates at their end, enabling axial water transport. They are aligned end-to-end and forming tubes that allow for more efficient water transport in angiosperms. They generally have a larger lumen than tracheids, which facilitates quicker water flow. Additionally, vessel elements possess pits on their side walls that enable lateral water movement between neighboring cells, though the primary water flow occurs axially through the perforations (Rudall, 2007).

1.2.3.2.4. Parenchyma cells

Parenchyma (Fig. 1 – 6) is a versatile and fundamental plant tissue type, present in nearly all parts of a plant. It plays a wide range of roles, from photosynthesis to storage and repair, and is one of the least specialized yet most crucial tissues in plants (Lack & Evans, 2001; Leroux, 2012).

Within the xylem, parenchyma cells are thin-walled cells and polyhedral shape, generally smaller and less elongated than tracheids and fibers. These cells are responsible for storage (e.g., of starch) and repair of damaged xylem tissue. They can also assist in the lateral transport of water and nutrients. Parenchyma cells may have simple pits that allow for communication with other xylem cells, but they are not directly involved in water transport like tracheids and vessel elements (Evert, 2006; Crang et al., 2018). In contrast to tracheids, most parenchyma cells retain their nuclei and cytoplasm until they die during the process of heartwood formation (Evert, 2006).

There are different types of parenchyma in xylem (Evert, 2006; Crang et al., 2018):

- **Axial parenchyma:** These cells are arranged vertically in the xylem and are responsible for the storage of nutrients and carbohydrates. They run parallel to the xylem vessels and tracheids. When viewed in cross section, the axial parenchyma exhibits various arrangements in relation to the vessels and across the growth rings. The specifics of

these arrangements are classified and described by the International Association of Wood Anatomists (IAWA) (IAWA Committee, 1989).

- **Radial parenchyma:** These cells are arranged radially, extending from the pith toward the bark, and form the xylem rays. They help in the lateral transport of water and nutrients across the plant stem, connecting the inner xylem to the outer living tissues. They also play a key role in wound repair and storage.
- **Chlorenchyma:** though less common in xylem, some specialized parenchyma cells may retain chloroplasts and are involved in photosynthesis when present in living tissues near the xylem.

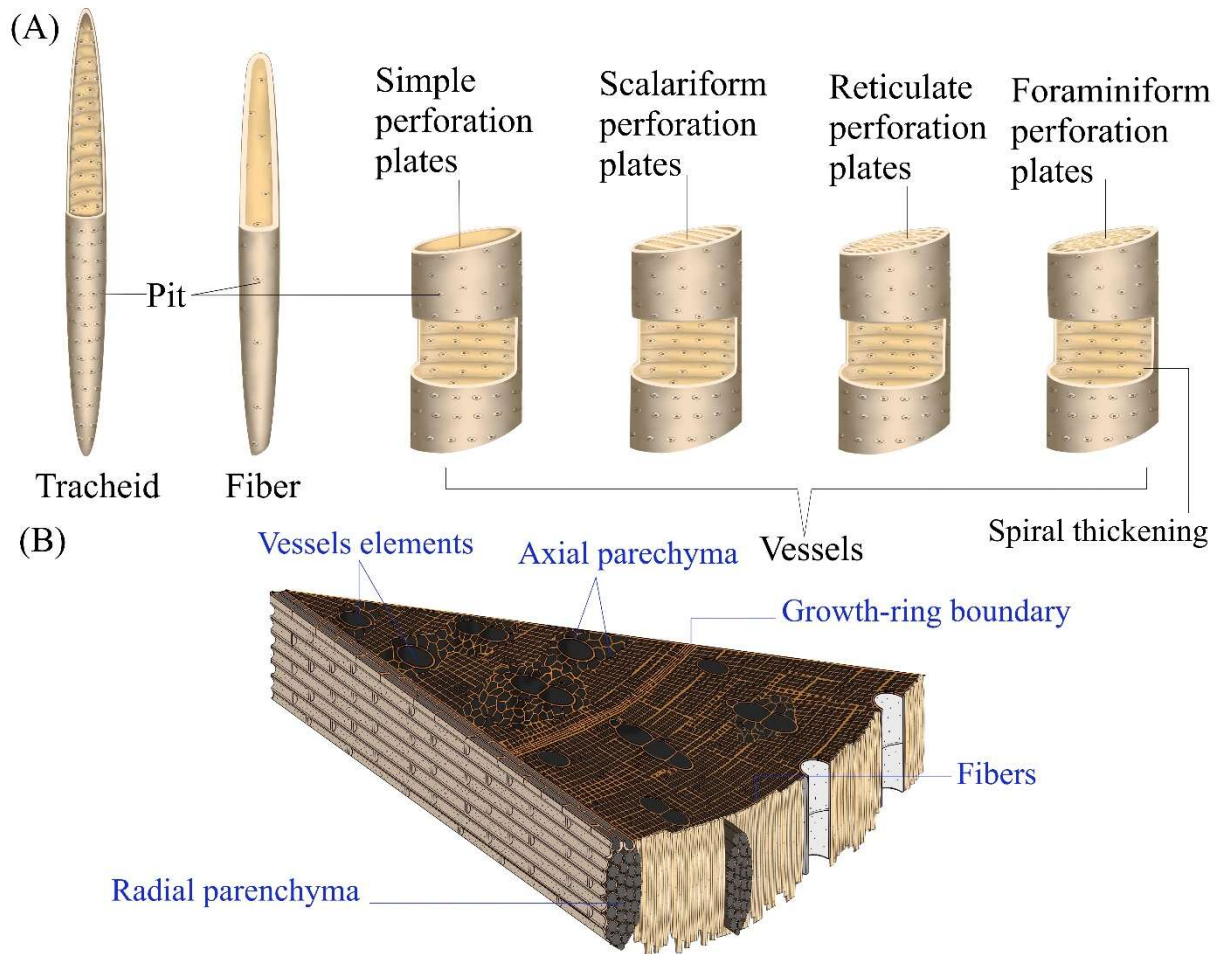


Figure 1-6. Schematic illustration of wood organization.

1.2.4. Cell wall

The cell wall is a distinctive feature of higher plant cells, providing crucial structural support. Plant cells experience significant internal pressures due to water absorption, which would cause rupture without the cell wall (Crang et al., 2018). Plant cell walls, particularly in forest trees, represent one of the most significant carbon sinks within the terrestrial ecosystem (Li et al., 2024).

1.2.4.1. Types of cell wall

There are two main types of cell walls. Primary cell wall surround living plant cells and consists of a flexible matrix of cellulose, cross-linking glycans, and structural proteins. This wall

contains enzymes that can modify its structure by loosening or strengthening the matrix as needed. The primary wall plays a key role in providing physical support during periods of growth and in herbaceous tissues. The secondary cell wall is a more rigid and structured layer that forms inside the primary cell wall once the plant cell has stopped growing. The secondary cell wall is significantly strengthened by the deposition of lignin, making it rigid and well-suited for tissues that require substantial strength and support, such as tracheary elements (tracheids and vessels elements) and fibers. These cells typically die once they mature. (Crang et al., 2018).

1.2.4.2. Cell Wall Composition

In wood, the cell wall is primarily composed of cellulose, hemicellulose, pectin, lignin, proteins, water and other polysaccharides.

Cellulose. Cellulose is the most abundant polysaccharide in the plant cell wall. It forms the primary structure of the cell wall and provides the wall with structural strength and flexibility. It consists of long chains of glucose molecules linked by β -1,4-glycosidic bonds, which form microfibrils. These microfibrils are responsible for cell wall rigidity and tensile strength, which allow the plant cell to resist pressure. There is more cellulose in the secondary wall than in the primary wall (Duchesne & Larson, 1989; Delmer & Amor, 1995; Caffall & Mohnen, 2009).

Hemicellulose. Hemicellulose is a group of polysaccharides that are shorter and branched compared to cellulose. It is made of various sugar monomers like xylose, mannose, and glucose. Hemicellulose binds to the surface of cellulose microfibrils, helping to hold them together, providing stability to the cell wall. There is lower amounts of hemicellulose in the secondary wall than in the primary wall (Duchesne & Larson, 1989; Pauly et al., 2013). The predominant hemicellulose in gymnosperm wood is galactoglucomannan, while in angiosperm wood, it is xylan (Timell, 1967).

Pectin. Pectins are polysaccharides rich in galacturonic acid and are found predominantly in the middle lamella and primary cell wall. Pectins play a crucial role in cell adhesion and provide the cell wall with its ability to resist compression. They also contribute to the flexibility and porosity of the wall, especially in young cells (Mohnen, 2008; Harholt et al., 2010).

Lignin. Lignin is an organic polymer found primarily in the secondary cell walls of woody-plant tissues. Lignin adds rigidity and waterproofing to the cell wall, making it more resistant to decay and mechanical damage. It also helps in conducting water in vascular plants by strengthening the xylem (Ralph et al., 2004; Liu et al., 2018).

Proteins. The wood cell wall contains several types of proteins, including structural proteins like extensins that provide additional support and enzymes involved in wall remodeling. These proteins help regulate the growth and expansion of the cell wall, as well as contribute to its overall structure. Proteins are present in small quantities in the secondary wall, mainly involved in wall remodeling and repair processes (Jamet et al., 2006; Jamet & Dunand, 2020).

Water. The cell wall contains a significant amount of water, which maintains its elasticity and helps in the diffusion of nutrients (Cresswell et al., 2021; Fredriksson et al., 2023).

Other Polysaccharides. There are also smaller amounts of other polysaccharides, such as glycoproteins and arabinogalactan proteins, that contribute to cell wall functions (Abedi et al., 2020; Leszczuk et al., 2023).

1.2.4.3. Cell wall structure

The cell wall forms from the middle lamella and develops inward, first with the primary wall, followed by the secondary wall (Fig. 1 – 2). The primary wall allows for cell growth and flexibility, while the secondary wall, which is deposited later, provides additional strength and rigidity (Timell, 1967; Taiz & Zeiger, 2010). The primary cell wall is a network of cellulose microfibrils loosely organized, along with hemicelluloses and peptide chains, all embedded in a high hydrated matrix of pectins. This structure provides flexibility and strength, enabling the cell to grow and maintain its shape (Timell, 1967; Duchesne & Larson, 1989; Taiz & Zeiger, 2010). The primary cell wall thickness varies between 0.1 and 1 μm (Chebli et al., 2021).

The secondary cell wall is made up of the same basic elements as the primary wall, but with the addition of lignin, which provides increased rigidity and strength. It contains a higher proportion of cellulose, with its microfibrils arranged in a helical pattern across multiple sub-layers. The direction of the helix alternates from one sub-layer to the next, providing enhanced structural strength and rigidity. In most tracheary elements and fibers, the secondary wall consists of three layers: S1, S2 and S3 (Timell, 1967; Duchesne & Larson, 1989; Evert, 2006).

The S1 layer is the outermost layer of the secondary cell wall, located just beneath the primary cell wall. It is the thinnest of the S layers, measuring just 0.1 to 0.35 μm thick and accounting for only 5% to 10% of the total cell wall thickness (Plomion et al., 2001). The cellulose microfibrils in the S1 layer are arranged at a relatively shallow angle to the cell axis and are organized in a crossed helical pattern. This layer provides initial structural strength and stability (Timell, 1967; H. Xu et al., 2022).

The S2 layer is the thickest and most important layer of the secondary cell wall. It accounts for most of the cell wall's thickness and strength. Its thickness varies between 1 and 10 μm (Plomion et al., 2001). The cellulose microfibrils in this layer are arranged almost parallel to the cell axis, providing high tensile strength. The S2 layer contributes most of the mechanical strength and rigidity of the cell wall. It plays a crucial role in the transport of water in vascular tissues (Timell, 1967; Salmén, 2018).

The S3 layer is the innermost and relatively thin layer of the secondary cell wall, being only 0.5 to 1.10 μm (Plomion et al., 2001). It is located just outside the cell membrane. The cellulose microfibrils in the S3 layer are oriented at a steeper angle compared to the S2 layer, closer to the arrangement in the S1 layer. They are oriented almost parallel to the cell elongation axis and form a flat helix. Although thinner than the S2 layer, the S3 layer adds additional support and regulates the interaction between the secondary wall and the cell membrane (Timell, 1967; Zarra et al., 2020).

1.2.5. Xylogenesis

Xylogenesis is the process by which xylem, the vascular tissue responsible for water and nutrient transport in plants, is formed. This process is critical for the growth and development of woody plants, as it contributes to the formation of wood and the overall structure of the plant.

Xylogenesis is a complex and highly regulated process that relies essentially on the activity of the vascular cambium (Funada et al., 2016) and is influenced by environmental factors such as temperature, water availability, and seasonal changes. In many plants, xylogenesis occurs primarily during the growing season, when conditions are favorable for growth (Catesson, 1994; Savidge, 1996).

As described in Section 1.2.2, the cambial zone is a meristematic region responsible for producing secondary xylem towards the inside of the stem and phloem towards the outside, resulting in the thickening of stems and roots. The cambium is composed of two types of initials cells (cambial initials): elongated fusiform initials and smaller, cuboidal ray initials. Fusiform initials give rise to longitudinally aligned cells including vessels, tracheids and fibers, while ray initials give rise to transversely aligned cells, primarily ray parenchyma cells (Bailey, 1920; Evert, 2006; Funada et al., 2016).

Xylogenesis primarily involves periclinal divisions of cambial cells, which add new cells to the radial file, perpendicular to the stem axis. However, anticlinal divisions, which occur parallel to the stem axis, are also observed. Anticlinal divisions do not directly form wood, but they help increase the number of initials cambial cells, ensuring that the cambium can maintain sufficient surface area to support ongoing periclinal divisions (Bannan, 1950; Barlow et al., 2002).

In temperate regions, the cambial zone exhibits seasonal activity. During the growing season (spring and summer), the cambium is highly active, producing large amounts of xylem and phloem. In winter, the cambium becomes dormant, and cell division ceases. This cyclical activity leads to the formation of annual growth rings in woody plants (Riding & Little, 1984; D. Wang et al., 2021). Overall, the total duration of xylogenesis can vary from around 4 to 6 months for temperate species, depending on the latitude and environmental conditions (Güney et al., 2015). In tropical regions, cambial phenology likely exhibits a wide range of complex patterns due to the diverse environmental conditions present in these ecosystems. Despite the ecological importance of tropical forests, little is known about the detailed timing and factors influencing cambial dynamics in these regions, particularly compared to temperate forests (FAO & ITTO, 2011; Pumijumnong et al., 2023).

Xylogenesis involves several stages including cell division, cell expansion, cell differentiation, secondary wall formation and cell death (Plomion et al., 2001; Verbančič et al., 2018; Balzano et al., 2021).

1.2.5.1. Cell division

During this stage, the meristematic mother cell undergoes several mitosis phases, including cell growth, DNA synthesis, nuclear division, and cytoplasmic separation, ultimately resulting in the formation of two daughter cells (Lachaud et al., 1999; Crang et al., 2018). This process repeats actively, producing a greater number of new cells on the xylem side, towards the inside of the plant, than on the phloem side, towards the outside (De Micco et al., 2020). The cell division phase can last several days, ranging between 10 and 50 days, depending on factors like tree species, developmental stages, and environmental conditions (Larson, 1994).

1.2.5.2. Cell enlargement

After the initial cell division, the newly formed xylem cells undergo expansion. This stage involves the elongation and enlargement of the cells, which will later become part of the plant's conductive system (Lachaud et al., 1999; Rathgeber et al., 2016). Cell expansion is a turgor-driven process that requires sufficient water availability, along with free sugars and amino acids. These resources are essential to maintain the turgor pressure needed for protoplast enlargement, which in turn exerts stress on the cell walls, leading to both reversible and irreversible deformations (Ortega, 2017).

For many species, cell enlargement lasts about 10 – 14 days, but this can vary with conditions like water supply (J. Vieira et al., 2014; Cuny et al., 2015; Güney et al., 2015).

1.2.5.3. Cell differentiation

During their differentiation, xylem cells undergo significant morphological and physiological transformations, shaping them according to their future functions. As the cells expand, they begin to differentiate into specialized types of phloem cells or of xylem cells (tracheids, vessel elements, and fibers) (Rathgeber et al., 2016).

1.2.5.4. Secondary wall formation

As the developing cell reaches its final size, a new layer forms inside the primary cell wall: the secondary cell wall, which is the most critical for providing the cell with mechanical strength and the water transport efficiency. As the different layers of the secondary wall forms successively from outer to inner, lignin is incorporated into the matrix (Liu et al., 2018). The duration of secondary wall thickening can last for up to 30–50 days depending on the species and environmental factors (Cuny et al., 2015; Güney et al., 2015).

1.2.5.5. Programmed cell death

In the final stage of xylogenesis, the secondary cell walls of xylem cells become fully lignified, then the concerning cells undergo programmed death, resulting in hollow, tube-like structures that are highly efficient at conducting water and minerals from the roots to the rest of the plant. As with lignification, the programmed cell death process begins earlier and is more rapid in vessels than in tracheids and fibers (Courtois-Moreau et al., 2009; Schuetz et al., 2013). The depletion of oxygen and the enrichment of carbon dioxide within the newly formed xylem lead to the death of parenchyma cells, which initiates the process of heartwood formation. This transition occurs as respiration becomes limited, causing metabolic activity to cease in the parenchyma cells, eventually resulting in the deposition of extractives that protect the heartwood and contribute to its structural integrity (Kampe & Magel, 2013). Unlike xylem, phloem tissue is periodically renewed, with the frequency of renewal varying among species and depending on climatic conditions. Non-lignified phloem cells, such as sieve elements and companion cells, age and degrade over time, leading to a loss of functionality. Additionally, the radial growth of xylem compresses older phloem tissues, contributing to their degradation and disappearance. Consequently, the vascular cambium generates new phloem to maintain the essential transport of photosynthates and signaling molecules throughout the plant (Ray & Savage, 2021).

1.2.6. Methods to study secondary growth

Assessing tree secondary growth typically involves a combination of direct measurements, dendrochronological techniques, and modern technologies. Here are the more commonly used methods:

1.2.6.1. Direct measurement of stem dimension change

This method utilizes dendrometers to measure variations in either the tree's girth or radius at almost any time scale.

Dendrometer bands are mechanical devices consisting of a flexible metal band that measure changes in its tree girth over time. These bands expand or contract as the tree grows or shrinks, allowing researchers to manually track growth patterns (Cardoso et al., 2012; Gliniars et al., 2013).

Point dendrometers are electronic and use sensors to continuously measure changes in stem radius. They automatically record data, in real-time. These electronic versions provide more precise and frequent measurements than traditional band dendrometers, making them useful for capturing high-resolution growth data at various time scales (Steppe et al., 2015; Zweifel, 2016).

1.2.6.2. Growth-ring analysis (Dendrochronology)

Tree ring analysis is one of the most traditional and widely used methods for assessing secondary growth. Using tree cores or cross-sectional discs, researchers examine the width and structure of growth rings to reconstruct a tree's growth history on an inter-annual scale. This technique is particularly effective in temperate and boreal climates, where tree rings form regularly due to distinct seasonal variations. However, it is increasingly being applied in tropical regions as well (Groenendijk et al., 2014; Pompa-García & Camarero, 2020). In tropical regions, where trees often lack clear annual growth rings due to minimal seasonality, cambial marking is widely used as a preliminary step before growth ring analysis. This technique aids in the study of secondary growth in these challenging environments, which are more complex to analyze compared to temperate forests. The cambial zone of trees is periodically wounded—biweekly, monthly, or yearly—using a pin, and samples are collected from the same location at a later date. This approach allows researchers to obtain wood samples with two precisely known cambial positions, enabling them to analyze ring-boundary formation and accurately track the timing of xylogenesis and its relationship to environmental factors (Seo et al., 2007; De Mil et al., 2017).

1.2.6.3. Direct cambium activity monitoring

This method, known as microcoring, involves removing small samples of cambial tissue at regular intervals, typically every one to two weeks, to monitor cambial activity. By analyzing fine sections of these wood samples, researchers can directly observe cambial cell production and wood formation (xylogenesis). This approach provides detailed insights into the timing, rate, and dynamics of secondary growth, allowing for a precise understanding of how trees produce wood and respond to environmental conditions (Rossi, Anfodillo, et al., 2006; Rossi, Deslauriers, et al., 2006).

1.2.6.4. Isotope analysis

Isotope analysis is a valuable tool for studying secondary growth by examining the ratios of stable isotopes, such as hydrogen ($^1\text{H}/^2\text{H}$), carbon ($^{12}\text{C}/^{13}\text{C}$), oxygen ($^{16}\text{O}/^{18}\text{O}$) (Leavitt, 2010; Huang et al., 2023) or nitrogen ($^{14}\text{N}/^{15}\text{N}$) (Savard & Siegwolf, 2022), as well as radioactive isotopes like carbon-14 (^{14}C) (Hajdas et al., 2021), in tree rings. Stable isotopes provide detailed insights into past environmental conditions and physiological processes within the tree, such as water-use efficiency, stomatal conductance, and photosynthetic activity. Variations in isotope ratios reflect changes in factors like temperature, precipitation, and atmospheric CO_2 concentration, making stable isotope analysis an effective method for linking secondary growth to historical climate patterns and tree responses to environmental stressors (Cernusak et al., 2013; Giraldo et al., 2022). In contrast, radioactive isotopes, such as ^{14}C , are particularly useful for dating tree rings through radiocarbon dating, offering precise chronological frameworks for growth analysis. The ^{14}C "bomb pulse" from mid-20th-century nuclear testing provides a distinct marker for dating tree growth within this period, which can be invaluable in dendrochronology and ecological studies. Combining stable and radioactive isotope techniques allows for a comprehensive understanding of both physiological responses and temporal patterns in secondary growth (Quarta et al., 2005).

1.3. Secondary growth in the Congo basin

As detailed earlier, secondary growth refers to the increase in thickness of stems and roots in woody plants, driven by the activity of the vascular cambium and cork cambium, with a greater contribution from the vascular cambium. This process is essential for carbon sequestration, as it enables trees to store more carbon in their expanding biomass (Evert, 2006; Campbell & Reece, 2012; Crang et al., 2018).

Secondary growth is influenced by genetic and environmental factors such as temperature, water availability, and seasonal changes. In many plants, it occurs primarily when conditions are favorable (Catesson, 1994; Savidge, 1996; Fatichi et al., 2019). Conversely, trees archive environmental information in their wood as they grow (Babst et al., 2014). Under unfavorable conditions—such as prolonged dry seasons (Worbes, 1999), flooding in floodplain forests (Schöngart et al., 2002), or salinity fluctuations in mangrove forests (M. Q. Chowdhury et al., 2008)—the cambium halts its activity, resuming only when conditions improve. This interruption is marked by the formation of a growth ring in the wood (Brienen et al., 2016).

Many studies in tropical forests have challenged the long-standing belief that tropical tree species do not form growth rings (Mariaux, 1967, 1969; López et al., 2012). Increasing evidence now shows that annual growth rings are present in a growing number of tropical tree species (Worbes, 2002, 2011; Zuidema et al., 2012). Despite these significant advancements, the forests of the Congo Basin remain underrepresented in studies focused on tree ring formation (Couralet et al., 2013). It is particularly unclear how long the growing season lasts, whether there is a dormancy period and when exactly cambial activity peaks (Borchert, 1999; Morel et al., 2015; De Mil et al., 2017). This lack of representation is a major gap in our understanding, particularly given the Congo Basin's ecological importance and the role its forests play in global carbon storage and biodiversity. Expanding research on growth rings in this region could provide

valuable insights into tree growth dynamics, forest age, and responses to environmental changes, offering a more comprehensive understanding of tropical forest ecosystems.

1.4. The carbon cycle in Congo Basin

The Congo Basin, encompassing the world's second-largest tropical rainforest, plays a pivotal role in the global carbon cycle, due to its vast forests, peatlands and aquatic system (Hastie et al., 2021). Key metrics are essential for understanding the carbon dynamics of the Congo Basin. The total amount of carbon dioxide (CO₂) fixed by vegetation in an ecosystem through photosynthesis is referred to as Gross Primary Production (GPP). A portion of this carbon is respired by the plants themselves (autotrophic respiration R_a), with the remaining portion defined as Net Primary Production (NPP). Finally, after accounting for heterotrophic respiration (R_h), the net amount of carbon is termed Net Ecosystem Production (NEP) (Malhi et al., 2011).

$$NPP = GPP - R_a$$

$$NEP = NPP - R_h = GPP - R_a - R_h$$

While specific GPP values for the Congo Basin are not readily available, global GPP estimates range from approximately 116.4 to 133.94 petagrams of carbon per year (Pg C yr⁻¹), with tropical forests contributing significantly to this total (S. Wang et al., 2024). For the Congo Basin, terrestrial NPP has been estimated at approximately 5.8 Pg C yr⁻¹, with a carbon stock of around 50 Pg C in aboveground biomass and about 100 Pg C in the soil (Hastie et al., 2021). Recent discoveries of extensive peatland systems in the Congo Basin revealed they contain an estimated 30.6 Pg of carbon, equivalent to three years of global fossil fuel emissions (Dargie et al., 2017) (Figure 1-7).

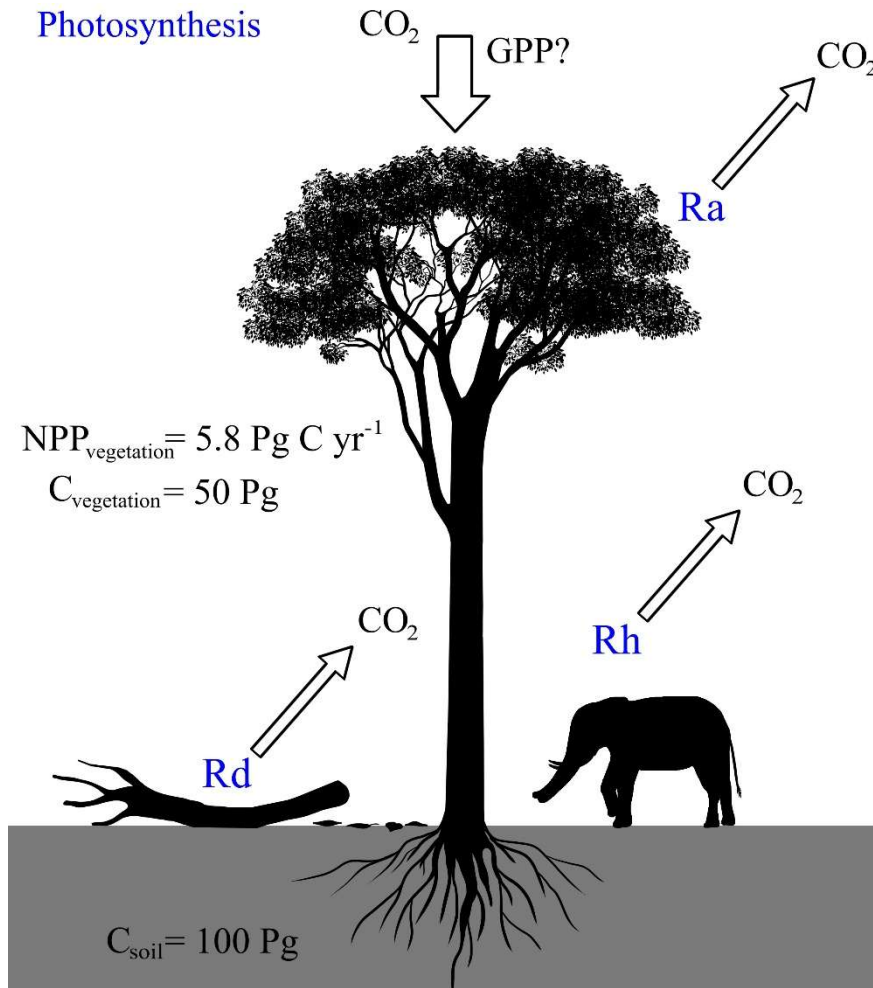


Figure 1-7. The Congo Basin carbon cycle. Annual flux of Net Primary Production (NPP) and carbon stocks in vegetation ($\text{C}_{\text{vegetation}}$) and in soil (C_{soil}), with Ra , Rd , and Rh autotrophic, heterotrophic, and vegetal debris respiration, respectively.

1.5. Objectives and conceptual framework

As previously mentioned, the Congo Basin plays a crucial role in global ecosystem services, including the annual net uptake of atmospheric CO_2 , which directly contributes to mitigating climate change. While this carbon sink has remained stable over recent decades (Hubau et al., 2020), the underlying processes governing carbon sequestration by trees in the region remain insufficiently understood. A clearer understanding is essential to predict how the Congo Basin will respond to future climate change and its associated impacts. Key uncertainties include the duration of the growing season, the existence of a dormancy period in the carbon storage process, and the drivers of tree growth. This study aims to elucidate the mechanisms of secondary growth in this ecologically vital and unique region. To achieve this, the research addresses several interrelated questions, spanning multiple chapters:

- Is there a dormant period in the seasonal tree-growth cycle? (Chapters 2, 3, 4)
- If so, what is the timing and the length of both dormancy and growing season? (Chapters 2 and 4)
- How is the growth cycle influenced by climatic variables? (Chapters 2, 4)
- What anatomical marks does the growth cycle leave on the wood? (chapter 3)

To answer these questions, we employed three distinct approaches, each of which forms the foundation of the three key chapters of this thesis, except for the General introduction (**Chapter 1**) and **Chapter 5** which synthesizes the main findings, and the General conclusion:

- 1) Direct measurement of stem radius change: This was achieved using automatic dendrometers to track changes in radial axis of stems (Drew & Downes, 2009; Luse Belanganayi, Angoboy Ilondea, et al., 2024) (**Chapter 2**). This chapter is published under the reference:

Luse Belanganayi, B., Ilondea, B. A., Phaka, C. M., Laurent, F., Djiofack, B. Y., Kafuti, C., Peters, R. L., Bourland, N., Beeckman, H., & De Mil, T. (2024). Diel and annual rhythms of tropical stem size changes in the Mayombe forest, Congo Basin. *Frontiers in Forests and Global Change*, 7. <https://doi.org/10.3389/ffgc.2024.1185225>

- 2) Analysis of wood formed between two exactly dated marks: We decoded information from cross-sectional planes of wood between two time points, using an artificial wound in the cambial zone as a reference (De Mil et al., 2017) (**Chapter 3**). This chapter is published under the reference:

Luse Belanganayi, B., Delvaux, C., Kearsley, E., Liévens, K., Rousseau, M., Mbungu Phaka, C., Djiofack, B. Y., Laurent, F., Bourland, N., Hubau, W., De Mil, T., & Beeckman, H. (2024). Growth periodicity in semi-deciduous tropical tree species from the Congo Basin. *Plant-Environment Interactions*, 5(3), e10144. <https://doi.org/10.1002/pei3.10144>

- 3) Analysis of the cambial zone in samples taken in short time intervals and examination of the cambial state within a growing cycle: Thin sections of micro-cores were collected and analyzed to study the cambial zone in greater detail (Rossi, Deslauriers, et al., 2006; Noyer et al., 2023) (**Chapter 4**). This chapter is under review in *Global Ecology and Conservation* under the reference:

Luse Belanganayi B., Mbungu Phaka C., Djiofack B. Y., Laurent F., Liévens K., Luambua N. K., Bolaya T., Bourland N., Hubau W., Beeckman H., & De Mil T. (2024). Timing of Cambial Phenology of Rainforest Trees as Indicator of Climate Sensitivity of the Congo Basin Biome (SSRN Scholarly Paper No. 5076845). Social Science Research Network. <https://doi.org/10.2139/ssrn.5076845>

- 4) General synthesis on better understanding of secondary growth in the Congo Basin. **Chapter 5**: Towards a better understanding of secondary growth in the Congo Basin, synthesizes the main findings, emphasizing the connections between the different approaches used in the study, and concludes. It also outlines the prospects for future research and highlights potential avenues for further exploration.

The three main chapters of this thesis (Chapters 2, 3, and 4) explore distinct methodological approaches, yet all contribute to understanding a single phenomenon: secondary growth. Figure 1-8 illustrates the relationship between secondary growth and environmental conditions, highlighting its dependence on plant metabolism, with photosynthesis as a key driver. Additionally, the figure demonstrates how each chapter addresses specific research questions related to this process.

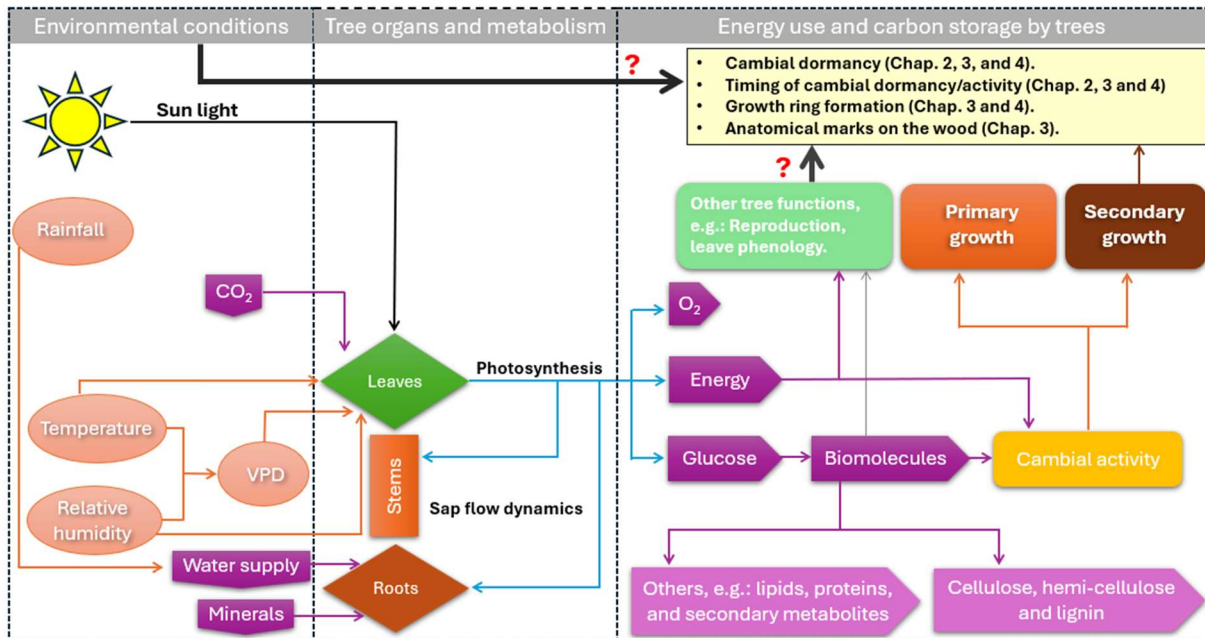


Figure 1-8. A conceptual model illustrating the interactions between trees and their environment, highlighting the key processes governing energy utilization and carbon sequestration, which ultimately drive stem growth. The figure also outlines how each chapter contributes to addressing specific research questions related to the secondary growth.

1.6. Specificity of this thesis

Recent advances in forest monitoring techniques, such as repeated forest inventories, flux tower measurements (Baldocchi et al., 2001; Helbig et al., 2021), and terrestrial and aerial LiDAR scanning (Orwig et al., 2018), have significantly improved our understanding of carbon dynamics and tree growth patterns. However, each of these methods has limitations. While repeated inventories track long-term biomass accumulation, they lack the temporal resolution needed to capture intra-annual growth variations (Johnson et al., 2023). Flux towers provide insights into net carbon fluxes at the ecosystem level but do not distinguish between the contributions of different tree species or physiological processes (Ferster et al., 2015). LiDAR scanning offers high-resolution structural data but does not capture cambial activity or the mechanisms underlying secondary growth (Albert et al., 2019).

This study complements these approaches by providing fine-scale, high-temporal-resolution data on secondary growth dynamics, addressing key uncertainties in growth periodicity, dormancy, and climate sensitivity. By integrating detailed anatomical and dendrometric measurements, this research helps bridge the gap between large-scale monitoring techniques and the physiological mechanisms driving tree growth in the Congo Basin.

The uniqueness of this study lies in its being the first to investigate secondary growth in the Congo Basin using three distinct yet complementary methodological approaches simultaneously. These approaches are applied across a temporal resolution that spans from daily to annual scales, providing a comprehensive and multifaceted understanding of growth dynamics.

1.7. Description of study sites and species

1.7.1. Study sites

The research conducted for this thesis was carried out in the semi-deciduous rainforests within the Luki (33 000 ha) and Yangambi (235 000 ha) UNESCO Biosphere Reserves in the Democratic Republic of Congo (Fig.1 – 9). The two sites, although located in different regions of the Congo Basin, i.e. Luki in the West and Yangambi in Northeast, share many common tree species. However, they are characterized by distinct climates: Luki has an Aw climate, while Yangambi has an Af climate, according to the Köppen classification as updated by Kotték et al. (2006).



Figure 1-9. Location map of study sites in the Democratic Republic of Congo (indicated by yellow dots), The Luki and Yangambi Man and Biosphere Reserves.

From 1981 to 2021, the average annual rainfall was 1,296 mm in Luki and 1,652 mm in Yangambi, while the average annual temperatures were 25.0°C (ranging from 19.5°C to 27.9°C) and 25.4°C (ranging from 22.4°C to 29.9°C), respectively (based on data from <https://power.larc.nasa.gov/data-access-viewer/>). In Luki, the dry season (period with monthly

rainfall below 50 mm) extends from June to September, whereas in Yangambi, there is no distinct dry season, although there is a reduction in rainfall to about 60 mm per month between December and February (Fig. 1 – 10).

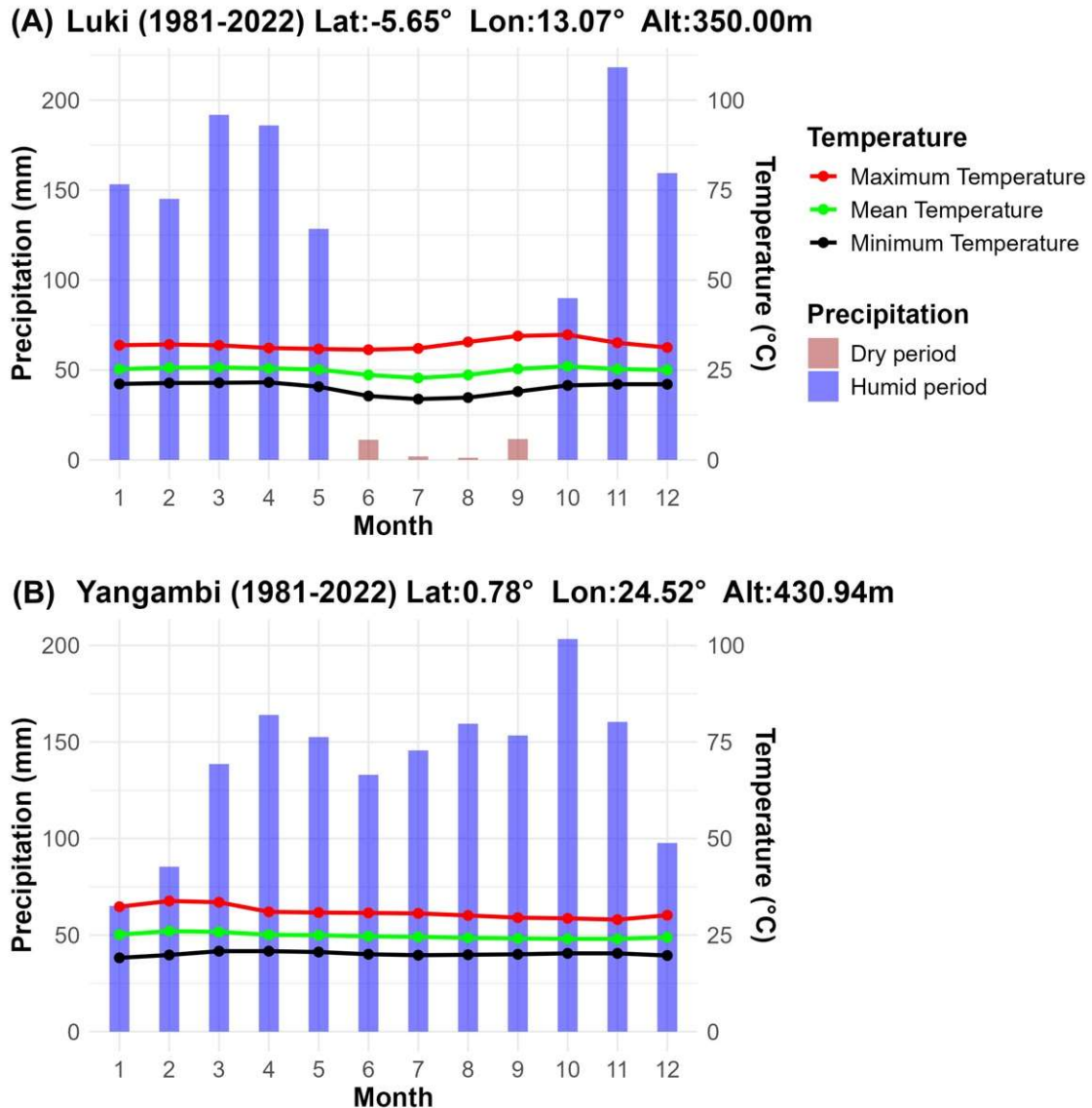


Figure 1-10. Climatic diagram of the Luki (A) and Yangambi (B) Biosphere Reserves (1981–2022). Monthly averages of precipitation (bars), average temperature (green), minimum temperature (black), and maximum temperature (red).

The Luki Biosphere Reserve, part of the Mayombe forest and located 120 km from the Atlantic coast, features a hilly landscape with elevations ranging from 150 to 500 meters (Monteiro, 1962). These conditions contribute to a distinctive climate characterized by high humidity during the dry season. This is explained by the fact that during the year, the Benguela Current, originating from the southern Atlantic, extends its influence into the Gulf of Guinea primarily during the upwelling season, typically from June to September, which corresponds to the dry season in Luki. This current creates a thick, low-level, non-precipitating cloud layer that reduces solar radiation and lowers temperatures, providing conditions that are somewhat favorable for tree growth during the dry season (Sénéchal et al., 1989; Lubini, 1997). The soil in Luki is

heterogeneous but is generally characterized as ferrallitic, acidic, and chemically poor (Couralet et al., 2013). The Reserve is traversed by a dense network of rivers and streams, which exhibit seasonal variations in discharge (Couralet, 2010).

The forest of the Luki Biosphere Reserve is classified as a mesophilous semi-deciduous forest. It occurs in a mosaic landscape, with patches of primary and secondary forests interspersed with savannas, agricultural fields, and settlements (Lubini, 1997; Couralet, 2010). The families Malvaceae, Fabaceae, Ebenaceae, Olacaceae, Rubiaceae, Annonaceae, Myristicaceae, Meliaceae, and Sapotaceae exhibit the highest specific importance index values (Bienu et al., 2023). The forest comprises a mix of evergreen and deciduous species in the upper canopy and predominantly evergreen species in the understory. The most abundant tree species in the canopy are *Prioria balsamifera* and *Terminalia superba*, while in the understory, *Aidia ochroleuca*, *Corynanthe paniculata*, and *Xylopia wilwerthii* are the most prevalent (Couralet, 2010). The diameter distribution of trees is characterized by a predominance of small-diameter individuals, while the vertical distribution is dominated by trees in the lower strata, typically between 10 and 20 meters in height (Bienu et al., 2023).

The Yangambi Biosphere Reserve is located approximately 100 kilometers west of Kisangani, in the lowlands of the central Congo Basin, with an average elevation of 459 meters above sea level (Kearsley et al., 2024). The vegetation in this area is predominantly moist semi-deciduous rainforest, interspersed with patches of moist evergreen rainforest, transitional forest, agricultural fields, fallow land, and swamp forest. The most abundant species include *Scorodophloeus zenkeri*, *Staudtia kamerunensis*, *Petersianthus macrocarpus*, *Panda oleosa*, and *Anonidium mannii* (Kearsley et al., 2017).

1.7.2. Study tree species

This study approached the research sites as integrated ecosystems, functioning as cohesive units rather than as a collection of individual species. While the selected species were among the most abundant at their respective sites—based on previous documentation ((Kearsley et al., 2017; Mokea et al., 2023) for Yangambi and (Lubini, 1997; Couralet, 2010; Bienu et al., 2023) for Luki)—the selection of individual trees for each methodological approach was primarily guided by their proximity. To minimize potential edaphic influences, we deliberately chose trees within the same plot, ensuring a geographically homogeneous study area. Table 1-1 presents a general list of the species studied, while detailed information on tree locations is provided in each chapter, with the most relevant details available in the appendices.

Table 1-1. List of study species.

No	Species	Family	Site	Chapter
1	<i>Anonidium mannii</i> (Oliv.) Engl. & Diels	Annonaceae	Yangambi	4
2	<i>Blighia welwitschii</i> (Hiern) Radlk.	Sapindaceae	Luki & Yangambi	3
3	<i>Carapa procera</i> DC	Meliaceae	Luki & Yangambi	3
4	<i>Celtis mildbraedii</i> Engl.	Cannabaceae	Luki & Yangambi	2 & 3
5	<i>Chrysophyllum africanum</i> A. DC	Sapotaceae	Luki & Yangambi	3
6	<i>Chrysophyllum lacourtianum</i> De wild.	Sapotaceae	Yangambi	4
7	<i>Cola bruneelii</i> De Wild.	Sterculiaceae	Luki	2
8	<i>Cola griseiflora</i> De Wild.	Malvaceae	Luki & Yangambi	3
9	<i>Combretum lokele</i> Liben	Combretaceae	Yangambi	4
10	<i>Corynanthe paniculata</i> Welw.	Rubiaceae	Luki	2
11	<i>Drypetes gossweileri</i> S. Moore	Putranjivaceae	Yangambi	4
12	<i>Erythrophleum suaveolens</i> (Guill. & Perr.) Brenan	Fabaceae Caesalpinioideae	Luki & Yangambi	3
13	<i>Funtumia elastica</i> (P. Preuss) Stapf	Apocynaceae	Luki	2 & 4
14	<i>Ganophyllum giganteum</i> (A. Chev.) Hauman	Sapindaceae	Luki	2 & 4
15	<i>Garcinia punctata</i> Oliver	Clusiaceae	Luki & Yangambi	2
16	<i>Greenwayodendron suaveolens</i> (Engl. & Diels) Verdc	Annonaceae	Luki & Yangambi	2, 3 & 4
17	<i>Hylodendron gabunense</i> Taub.	Fabaceae Detarioideae	Luki	2
18	<i>Isolona dewevrei</i> (De Wild. & T. Durand) Engl. & Diels	Annonaceae	Luki	2
19	<i>Leplaea thompsonii</i> (Sprague & Hutch.) E.J.M. Koenen & J.J.de Wilde	Meliaceae	Luki & Yangambi	3 & 4
20	<i>Microdesmis puberula</i> Hook.f. ex Planch.	Pandaceae	Luki	2
21	<i>Ongokea gore</i> (Hua) Pierre	Olacaceae	Luki	2 & 4
22	<i>Panda oleosa</i> Pierre	Pandaceae	Yangambi	4
23	<i>Pentaclethra macrophylla</i> Benth	Fabaceae Caesalpinioideae	Luki & Yangambi	3
24	<i>Petersianthus macrocarpus</i> (P. Beauv.) Liben	Lecythidaceae	Luki & Yangambi	3 & 4
25	<i>Prioria balsamifera</i> (Vermoesen) Breteler	Fabaceae Detarioideae	Luki	4
26	<i>Prioria oxyphylla</i> (Harms) Breteler	Fabaceae Detarioideae	Luki & Yangambi	3
27	<i>Pycnanthus angolensis</i> (Welw.) Warb.	Myristicaceae	Luki & Yangambi	3
28	<i>Scorodophloeus zenkeri</i> Hams	Fabaceae Detarioideae	Yangambi	4
29	<i>Staudtia kamerunensis</i> Warb	Myristicaceae	Luki & Yangambi	3
30	<i>Strombosiaopsis tetrandra</i> Engler	Olacaceae	Luki & Yangambi	3
31	<i>Synsepalum subcordatum</i> De Wild.	Sapotaceae	Yangambi	4
32	<i>Terminalia superba</i> Engl. & Diels	Combretaceae	Luki	2
33	<i>Trichilia gilgiana</i> Harms	Meliaceae	Luki & Yangambi	3
34	<i>Trichilia prieuriana</i> Juss	Meliaceae	Luki & Yangambi	3
35	<i>Tridesmostemon omphalocarpoides</i> Engl.	Sapotaceae	Yangambi	4
36	<i>Trilepisium madagascariense</i> DC	Moraceae	Luki & Yangambi	3 & 4

Chapter 2: **Diel and annual rhythms of tropical stem size changes in the Mayombe forest, Congo Basin**



Nkula Park, Luki reserve

This study was published under the reference:

Luse Belanganayi, B., Ilondea, B. A., Phaka, C. M., Laurent, F., Djiofack, B. Y., Kafuti, C., Peters, R. L., Bourland, N., Beeckman, H., & De Mil, T. (2024). Diel and annual rhythms of tropical stem size changes in the Mayombe forest, Congo Basin. *Frontiers in Forests and Global Change*, 7. <https://doi.org/10.3389/ffgc.2024.1185225>

Abstract

Introduction: The Congo Basin forests, a crucial global carbon sink, are expected to face increased challenges of climate change by 2027, with an expected temperature rise of 1.5°C above pre-industrial levels, accompanied by increased humidity conditions. However, studies that try to understand their functioning and untangle the species-specific responses about how weather conditions impact secondary growth dynamics are still rare.

Methods: Here we present the results of a study on diel and seasonal stem growth in 17 trees, belonging to 11 most abundant species, both canopy and understory, in the Mayombe forest (Congo Basin) in the Democratic Republic of the Congo (DRC). We measured highly-resolved radial stem size variations and weather conditions, to comprehend the ongoing patterns of secondary growth and examine the potential influence of projected weather conditions on them.

Results: We found that at the diel scale, trees probably grow mainly from 6pm to 9am, and that at the annual scale, they grow mainly during the rainy season, from October to May. Some trees grow year-round, while others stop growing for a period ranging from 1 to 4 months. This growth cessation typically occurs during the dry season from June to September. A linear mixed-effects model revealed that annual radial stem growth is positively related to rainfall.

Discussion: Our results suggest that trees in the study site have a significant potential to cope with the projected 1.5°C increase in global temperature and an additional 50 mm of local rainfall. Trees of the species *T. superba* exhibited improved growth under the projected scenarios, showing continuous year-round growth. For the other tree species, no significant difference in growth was observed between the predicted and observed scenarios. We believe that much remains to be done to better understand the tree growth-climate interaction of the large variety of tree species in the Congo Basin.

Keywords: high-resolution dendrometer, shrinkage-swelling pattern, stem growth rate, secondary growth, Central Africa forests, tropical forests.

2.1. Introduction

Tropical forests host over half of world species richness (Lewis et al., 2015) and contain 55 % of the global terrestrial carbon (Pan et al., 2011). They are particularly rich in other facets of biodiversity, including various patterns of wood anatomy, phenology and tree-growth periodicity (Lowman & Moffett, 1993; Beeckman, 2016; Hubau et al., 2019, 2020). Recent studies have shown that climate change is causing notable shifts in tropical forest ecosystems. Specifically, there is an increase in deciduous canopy species with intermediate light demand and a concurrent decline in evergreen sub-canopy and shade-tolerant species (Fauset et al., 2012). Moreover, higher temperatures (Sullivan et al., 2020), higher Vapor Pressure Deficit (VPD) (Grossiord et al., 2020) and precipitation disturbances, corresponding to dry areas becoming drier and wet areas becoming wetter (Trenberth, 2011), are expected in tropical regions. This would result to a reduction in their carbon storage capacity and possible vegetation dieback (Holm et al., 2017; Hubau et al., 2020). A recent pan-tropical study clarifies that stem growth variability positively responds to rainfall, and that stem growth of tropical trees is reduced (i.e., smaller ring width) in years when the dry season is warmer and drier than normal (Zuidema et al., 2022). This provides further evidence that the global warmer condition might

induce a decline in annual growth (Locosselli et al., 2020, Artaxo et al., 2022). Studying the impact of changing environmental conditions on tree growth and its variability is critical for improving our predictions on the dynamics of forest productivity and their impact on the global carbon cycle (Bonan, 2008; Friedlingstein et al., 2019). It is therefore absolutely necessary to focus current research on understanding their growth dynamics and how they respond to current climate change, and even predict their future responses (Cavaleri et al., 2015; (Albert et al., 2019)).

As inherently self-scaling, tree secondary growth is a widely used proxy for whole tree growth (Bowman et al., 2013). Analyzing secondary growth provides us with the opportunity to understand the direct constraints of environmental variables on tree growth (Friend et al., 2019). To assess tree growth in a detailed way, four approaches exist depending on the timescale: 1) Weekly/biweekly: regular analysis of the cambial zone through periodic sampling (Rossi et al., 2006a, 2006b), 2) Monthly: decoding periodic information in wood due to the rhythmic anatomical marks by the means of artificial wounding of the cambial zone (Seo et al., 2007; De Mil et al., 2017), 3) Inter-annual: dendrochronology and radiocarbon dating (Groenendijk et al., 2014; Pompa-García & Camarero, 2020; Giraldo et al., 2023), 4) all timescales: direct measurement of changes in girth or in stem radial axis using automatic dendrometers (Drew and Downes, 2009; Deslauriers et al., 2011; Steppe et al., 2015).

The Congo Basin forests constitute the second largest continuous area of tropical rainforest in the world, however, they are still underrepresented in studies of species-specific tree growth performance and resilience in the context of global climate change (Couralet et al., 2013). The studies conducted are more focused on wood anatomy (Couralet et al., 2010; Tarelkin et al., 2016, 2019), leaf phenology (Gond et al., 2013; Fétéké et al., 2017; Angoboy Ilondea et al., 2021), and forest dynamics (Morin-Rivat et al., 2017; Forni et al., 2019; Réjou-Méchain et al., 2021). Often, these studies are based on low-frequency measurements from permanent plots. Very few studies have looked at cambial phenology and radial growth at a high temporal resolution (De Mil et al., 2017, 2019). However, cambial activity and xylem enlargement occur on a short time scale (Deslauriers et al., 2008). As result, it is still particularly unclear how long the growing season lasts in Congo basin, and whether there is a dormancy period in carbon storage processes.

Due to various physiological processes in trees, such as sap flow and turgor pressure variation in relation to their hydraulic status, tree stems continuously (i.e. daily) fluctuate between shrinking and swelling (Peters et al., 2021), providing insights on water use and hydric stress as the response of sub-daily environmental conditions (Drew & Downes 2009; Hermann et al., 2016). Despite the use of high temporal resolution dendrometers for several decades (Klepper et al. 1971) to measure stem diameter changes on time scales ranging from minutes to years, it has not been easy to completely separate irreversible stem radial growth from elastic tension-driven and elastic osmotically driven changes in bark water content, on a diel scale, although several approaches have been proposed (Deslauriers et al., 2011; Chan et al, 2016; Zweifel, 2016; Zweifel et al., 2016). Two approaches have provided important insights into this subject. First there is the zero growth (ZG) concept (Zweifel et al. 2016), which is based on high-resolution dendrometer measurements, taken on bark only. That approach assumes that growth

starts when the stem radius exceeds the previous maxima and ends when the stem starts to shrink again (Zweifel et al., 2021). Secondly, there is the Mencuccini approach (Mencuccini et al., 2017), more precise, which is based on the simultaneous use of high-resolution point dendrometer measurements, taken from both xylem and bark, sap flow measurements and theoretical and statistical models. Despite the higher precision of their approach, Mencuccini et al (2017) recognize that although not identical, their approach and that of Zweifel et al (2016) can, under certain conditions, provide similar answers to the question of growth isolation. Thus, the use of ZG theory seems to be the best approximation for isolating growth on a diel basis, when only dendrometer measurements from the bark are available.

According to a new update issued by the World Meteorological Organization (WMO), global near-surface temperatures are very likely to exceed pre-industrial levels by 1.5°C for at least one year between 2023 and 2027 and wetter-than-usual conditions in much of Asia and Central Africa (WMO, 2023). The main objective of this study was to gain insights into the existing dynamics of secondary growth, enabling an understanding of the potential influence of weather conditions, particularly under projected scenarios. Assuming we reach the 1.5°C level in the study area and that the precipitation will increase by 2027, we sought to assess how tree growth could be modified with such projected climate changes. We therefore examined: (1) the swelling-shrinking process on a diel basis; (2) the current pattern of annual stem growth; (3) how will weather conditions impact secondary growth dynamics during the phenological year, under projected conditions?

Here we present the results of the first study of diel and annual stem changes in 17 trees, belonging to 11 most abundant species (both canopy and understory, and evergreen and deciduous) of the Mayombe forest (Congo Basin), based on high-resolved continuous measurements of radial stem variations and weather conditions.

2.2. Materials and methods

2.2.1. Study site

The study was conducted in Nkula Park, situated in the Luki Man and the Biosphere reserve (MAB), which is part of the Mayombe forest in the Congo Basin. The Luki MAB reserve is in the province of Kongo Central at the southwestern part of the Democratic Republic of the Congo (DRC), within latitudes 05°35'S and 05°43'S, and longitudes 13°07'E and 13°15'E (Fig. 2 – 1). It is classified as a tropical semi-evergreen forest of the Guineo-Congolian rainforest domain. It consists of a mixture of evergreen and deciduous species in the upper-stratum and mostly evergreen species in the understory. Its hilly landscape, with altitude ranged from 150 to 500 m above sea level (Monteiro, 1962), consists of moist green valleys and drier tops (Lubini, 1997). The soil is heterogeneous but has been described as generally ferrallitic, acid and chemically poor (Couralet et al., 2013). Climatic data available from Luki Weather Station (5°38'N, 13°7'E) from 1981 to 2021 shows annual averages of temperature and rainfall estimated at 25°C±1.14 and 1298±353 mm respectively. The rainfall regime is marked by a distinct dry period of less than 50 mm of monthly rainfall, from May to September. The average minimum and maximum annual temperatures are 19.5°C and 27.9°C respectively (Fig. 2 – 1). The amplitude of the average daily temperature varies monthly from 6.3 °C to 11.8 °C. It tends

to be lower in wetter months and higher in drier months. However, its variation is more marked during rainy months than during relatively dry months. The Nkula park which is located at 13°04'00"E and -5°38'59"S, is a protected long-term tree monitoring park (since 1948 until present) where the trees are being monitored for tree growth and phenology (Hubau et al. 2019). A Recent study reveals a total of 218 woody species grouped into 41 families in the Luki MAB reserve. The average tree density is estimated at 433 ± 13 trees per hectare. The families Malvaceae, Fabaceae, Ebenaceae, Olacaceae, Rubiaceae, Annonaceae, Myristicaceae, Meliaceae and Sapotaceae have the highest specific importance index values. The diametrical tree distribution is characterized by a predominance of small-diameter trees, and the vertical tree distribution by a predominance of trees in lower strata, between 10 and 20 meters high. These structural features testify to the good natural regeneration capacity of these forests (Bienu et al., 2023).

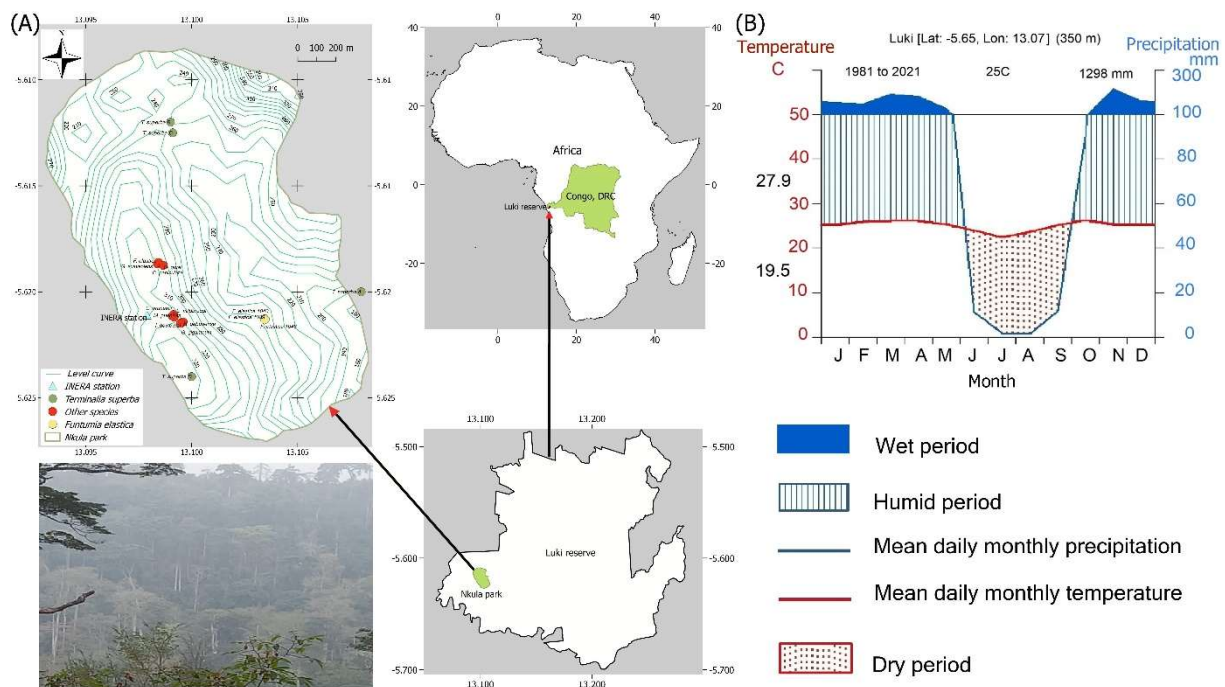


Figure 2-1. Location of study trees in the Nkula park, and a photo of a part of the Luki Man and the Biosphere Reserve, showing the hilly landscape. (B) Walter-Lieth Climate Diagram of the Luki Man and the Biosphere reserve from 1981 to 2021. The blue line indicates rainfall curve, the red line indicates the temperature curve, the dry season is shown in dashed red. The blue stripes indicate the humid period, and the blue area shows the wet period. Temperatures in black (19.5°C and 27.9°C), on the left axis, represent the average minimum temperature of the coldest month and the average maximum temperature of the warmest month, respectively. The annual average temperature and annual rainfall are shown in the upper right corner of the diagram.

2.2.2. Monitoring set-up and measurements

Seventeen healthy trees of eleven species, among the most represented, in the Nkula park forest, without apparent stem deformations or morphological anomalies, and within a dbh range of 11–83 cm, were selected and equipped with a point dendrometer (model DR1, Ecomatik, Munich, resolution 0.2µm, accuracy $\pm 0.1\%$ of reading) at approximately breast height (1.3 m above the

ground). Data from 4 trees (*Terminalia superba*) were taken from a previous study (De Mil et al., 2019) and dendrometers were installed above the buttresses, at 4-5m height, approximately 30 cm above the buttresses (Rondeux, 1999). Tree heights were measured with a Nikon Forestry pro. Metadata of the monitored trees are given in table 2 – 1.

Measurement of stem-radius daily changes were performed during the phenological years 2013-2014, 2014-2015, 2018-2019, and 2021-2022, at the resolution of 30 minutes. We evaluated the growth for the period from October 1 (previous year) to September 30 (current year), which we consider to be the beginning and end of the phenological year, respectively. In the following, we will use the terms "year" or "phenological year" indistinctly when referring to this period. And the term "annual" will always refer to the phenological year. We counted the days in days of the phenological year (DOPHY).

Table 2-1. Characteristics of 17 trees monitored in Nkula Park.

N°	Season of monitoring	Species	Family	Light demand	Leaf phenology	Height (m)	dbh (cm)
1	2013-2014 and 2014-2015	<i>Terminalia superba</i> Engl. & Diels	Combretaceae	H	D	45	69
2	2013-2014 and 2014-2015	<i>Terminalia superba</i> Engl. & Diels	Combretaceae	H	D	35	47
3	2013-2014 and 2014-2015	<i>Terminalia superba</i> Engl. & Diels	Combretaceae	H	D	31	83
4	2013-2014 and 2014-2015	<i>Terminalia superba</i> Engl. & Diels	Combretaceae	H	D	39	65
5	2018-2019	<i>Celtis mildbraedii</i> Engl.	Cannabaceae	ST	E	30	42.8
6	2018-2019	<i>Cola bruneelii</i> De Wild.	Malvaceae	ST	E	13	16.7
7	2018-2019	<i>Corynanthe paniculata</i> Welw.	Rubiaceae	ST	E	20	23.6
8	2018-2019	<i>Funtumia elastica</i> (Preuss) Stapf	Apocynaceae	H	E	24	36.4
9	2018-2019	<i>Ganophyllum giganteum</i> (A.Chev.) Hauman	Sapindaceae	H	E	23	52.1
10	2018-2019	<i>Greenwayodendron suaveolens</i> (Engl. & Diels) Verdc.	Annonaceae	ST	E	26	35.1
11	2018-2019	<i>Hylocodendron gabunense</i> Taub.	Legum. Detarioideae	ST	D	29	46.2
12	2018-2019	<i>Isolona dewevrei</i> (De Wild. & T.Durand) Engl. & Diels	Annonaceae	ST	E	6	13.9
13	2018-2019	<i>Microdesmis puberula</i> Hook.f. ex Planch.	Pandaceae	ST	E	4.5	11
14	2018-2019	<i>Ongokea gore</i> Pierre	Lacaceae	H	E	28	40.1
15	2021-2022	<i>Funtumia elastica</i> (Preuss) Stapf	Apocynaceae	H	E	25	28.5
16	2021-2022	<i>Funtumia elastica</i> (Preuss) Stapf	Apocynaceae	H	E	17	11.4
17	2021-2022	<i>Funtumia elastica</i> (Preuss) Stapf	Apocynaceae	H	E	24	23.7

Information on light demand and leaf phenology is taken from (Lubini, 1997). Light demand: H = heliophilous, ST = shade-tolerant; Leaf habit: D = deciduous, E = evergreen.

During the study period, direct monitoring of air temperature and relative humidity (RH) was performed with a HOBO U23-001 Pro v2 data logger (ONSET, USA), resolution of 30 min, placed at 1.5 m height, under the canopy, in the INERA (*Institut National pour l'Étude et la*

Recherche Agronomiques) weather station site, less than 500m from the tree's location. Rainfall data were obtained from <https://power.larc.nasa.gov/data-access-viewer/>.

The VPD (in kPa) was calculated from the temperature T (in °C) and RH (in %) according to this formula: $VPD = \left(0.61078 * e^{\left(\frac{T}{T+237.3} * 17.2694 \right)} \right) * \left(1 - \frac{RH}{100} \right)$ (Dai et al., 1992; Day, 2000; Grossiord et al., 2020).

2.2.3. Data analysis and statistical methods

All basic analyses and plots were performed using R studio statistical software (RSudio Team, 2022), although we occasionally used XLSTAT (trial version) and 'Past 4.11' (Hammer et al., 2001) to perform some complementary analyses. The package *treenetproc* (Knüsel et al., 2021), in R studio 4.2.1 (RStudio Team, 2022), was used to clean data of outliers, offsets and erroneous jumps, process and display highly resolved time series of dendrometer data. Based on the ZG theory, the package offers functions to extract the day of the year of the onset and the end of the growing season as well as several characteristics of shrinkage and swelling phases.

To describe the diel characteristics of tree stem shrinkage and swelling, we first calculated an hourly increment rate based on the principle of ZG (Zweifel et al., 2016) as in previous studies (Hogan et al., 2019; Etzold et al., 2022; Kaewmano et al., 2022). According to this principle, cumulative growth increases during periods when the stem radius surpasses its previous maximum. During the remaining time, the stems either shrink or expand below this maximum, with the deviation from the maximum referred to as tree water deficit (TWD). Alternatively, the stem radius may exactly meet its previous maximum (Zweifel et al., 2021). TWD values can also be interpreted as temporal shrinkage rates, based on the considered timescale.

The raw recordings from the dendrometer corresponded to the variation in stem radius, in μm , every thirty minutes. Using the R package *treenetproc*, we compiled them over regular 60-minute time intervals, then relativized them so that the initial record, corresponding to time t_0 , was equal to zero. To achieve this, the initial value was subtracted from all records.

On this new data set, if the initial value x_0 , is not exceeded, it is considered to be the value for all subsequent hours. At these hours, the hourly increment rate is zero. Once the dendrometer registers a value x_a , in a given hour h_a , such that $x_a > x_0$, we consider that a radius variation has occurred equal to $x_a - x_0$, corresponding to the increment rate of that hour a . Again, as long as the x_a value is not exceeded, all subsequent hours are considered to have an hourly increment rate equal to zero. The hour h_b , whose record x_b is such that $x_b > x_a$, will be associated with a rate of increase $x_b - x_a$, and so on. In this way, we were able to obtain hourly increment rates over a full phenological year for each tree. The different values x_0 , x_a , x_b , etc., which are such that $x_0 < x_a < x_b$, are defined as swelling peaks (Fig. 2 – 2).

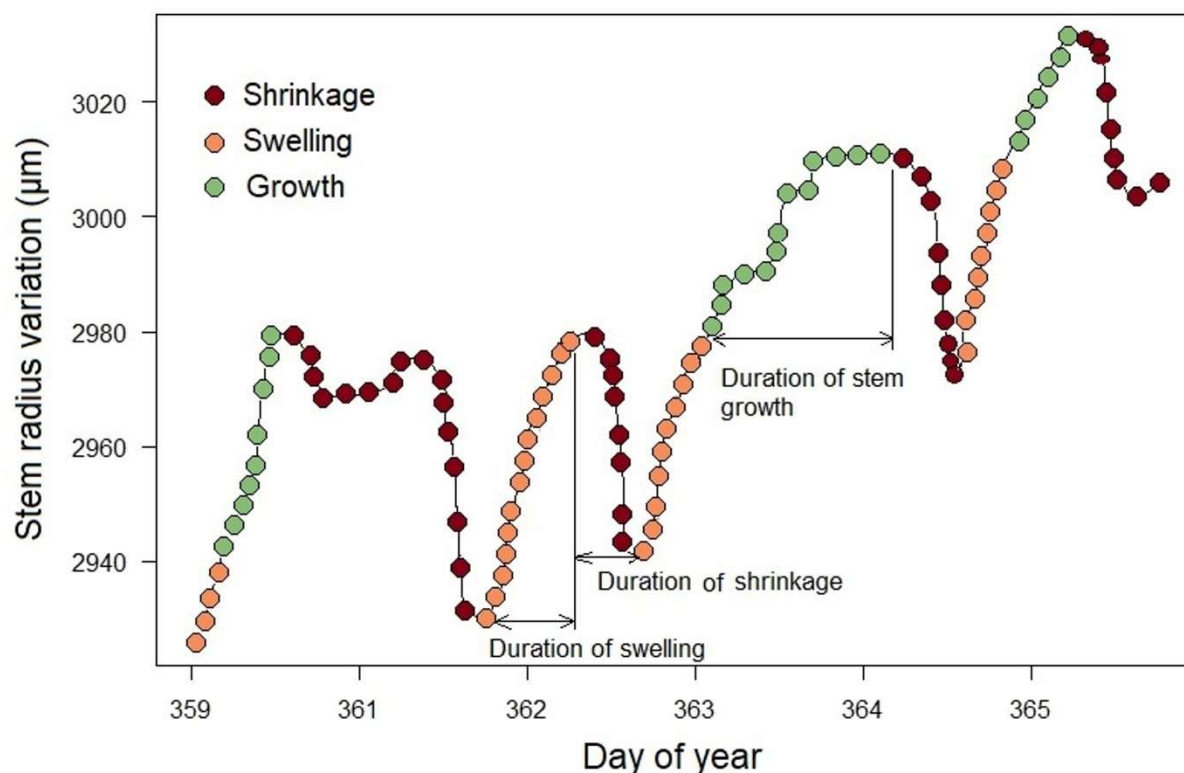


Figure 2-2. The stem radius variation, divided into three distinct phases of shrinkage (brown dots), swelling (orange and green dots) and stem radius growth (green dots). All points represent dendrometer recordings in $\mu\text{m}/\text{h}$.

The increment rate calculated in this way corresponds to the growth rate (GR), in μm , as defined by Zweifel et al. (2021). However, we do not consider that irreversible stem growth occurs undoubtedly at the times when these rates are reached by the stems. We therefore considered the increment rate to be the difference between the highest swelling peak (in μm), reached at the time under consideration, and the previous swelling peak. This is because, at small time scales, such as sub-diurnal and diurnal, it is difficult to separate, from dendrometer over-bark measurements, irreversible growth from swellings due to the water dynamic in the bark (Mencuccini et al., 2017). On the other hand, convinced that the biweekly scale was sufficient to detect irreversible stem growth (D'Orangeville et al., 2022), we calculated biweekly GR based on the ZG principle. The data gathered was then used as a basis for analyzing the response of trees to biweekly environmental variables (mean temperature, mean RH, and sum of rainfall) on an annual scale.

To examine how the radial variation dynamics of tree stems change throughout the day, we analyzed the hourly increment rates of each tree individual plotted against the hours of the day (Fig. 2 – 3). The data were then organized into boxplots to illustrate the distribution (Fig. 2 – 3A) and further averaged to show the overall trend for each tree (Fig. 2 – 3B). The relative hourly shrinkage rate, quantified as the contribution of the average hourly TWD to the total annual TWD, was examined, using the Gaussian RBF kernel model, within the measured space of VPD and diel time for each tree species separately during the rainy season (Fig. 2 – 3C) and the dry season (Fig. 2 – 3D).

To evaluate the potential differences in diurnal and nocturnal levels of environmental variables and their probable influence on the distribution of hourly increment rates during daytime and nighttime periods, we conducted a two-way analysis of variance (two-way ANOVA). This analysis was applied separately to temperature, vapor pressure deficit (VPD), and relative humidity (RH), each categorized into two groups: one comprising data recorded during daytime hours (6 a.m. to 5 p.m.) and the other encompassing data recorded during nighttime hours (6 p.m. to 5 a.m.). Daytime was defined as the period corresponding to the light phase of the day, whereas nighttime referred to the dark phase of the day. Classical clustering was used to compare the onset and end time of growing period, as well as the duration of growth, between different individuals.

To conduct a comparative analysis of diel radial increment rates (Inc_rate) between days characterized by minimal shrinkage and days with more pronounced shrinkage, a linear mixed-effects model (lmer) was fitted using the R package 'lme4' (Bates et al., 2024). The model incorporated DOPHY and VPD_group as fixed effects, while considering tree individual (Tree_ind) as a random effect. The model was formulated as follows:

$$\text{Inc_rate} \sim \text{DOPHY} * \text{VPD_group} + (1|\text{Tree_ind}).$$

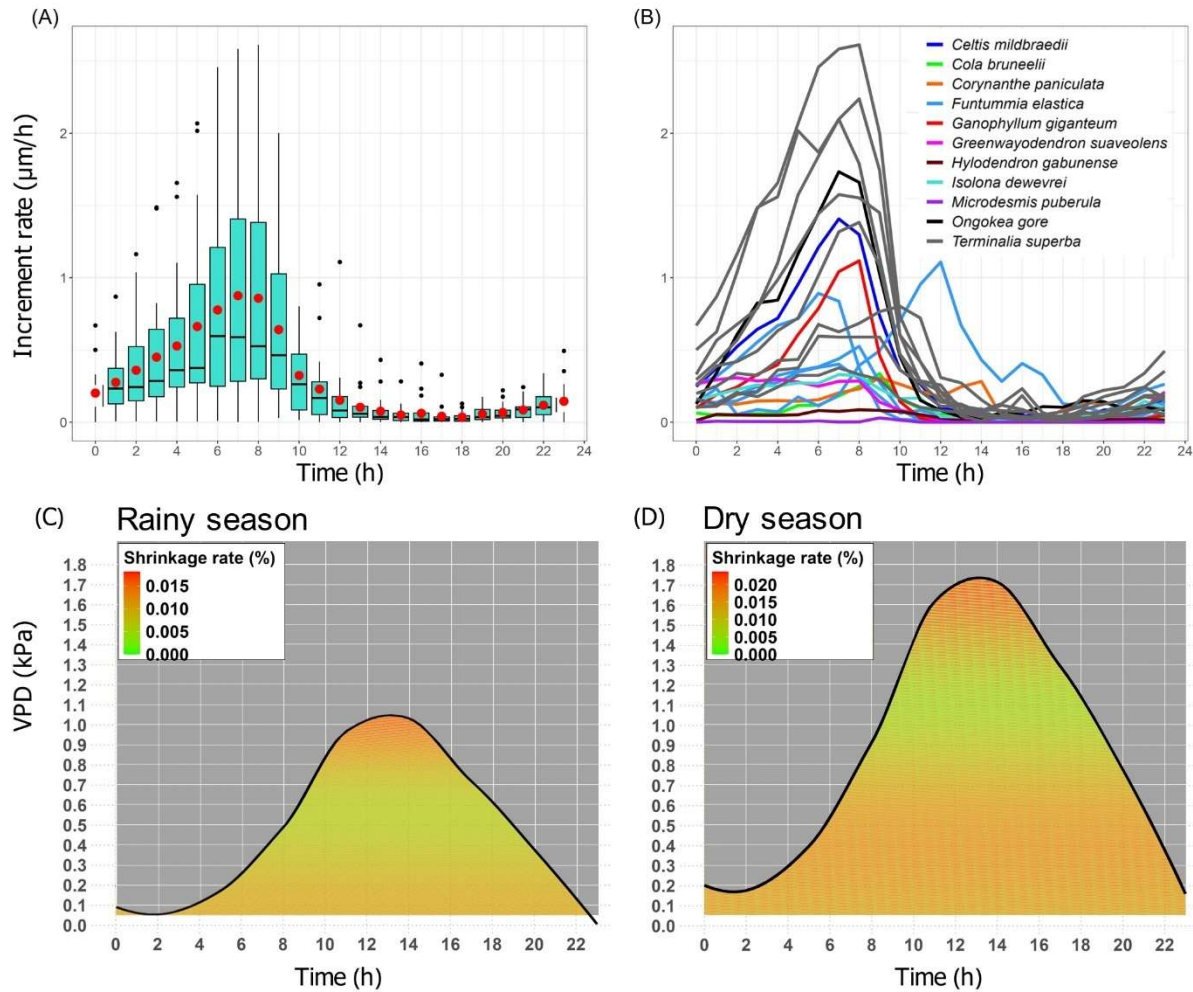


Figure 2-3. Diel stem change of 17 tropical trees belonging to 11 species. The dataset, shown in figure, consists of hourly increment rates, quantified as the radial increase in μm per hour according to the ZG principle. (A) Boxplots display the median (horizontal line inside the box), 25th and 75th percentiles (horizontal bases of the box) of the pooled data for all tree individuals. The vertical lines attached to the box represent the minimum and maximum values, the red dot represents mean values, and black dots indicate outliers. (B) The lines show the average hourly increment rates for each tree species. (C) and (D) Diel shrinkage rate in relation to VPD and time for all trees individual. The dataset consists of the relative contribution of hourly TWD to the total annual TWD, representing the average hourly shrinkage rate in the rainy season (C) and the dry season (D). It is colored-coded and ranges from green (low shrinkage), through orange (moderate shrinkage) to red (high shrinkage). The black line indicates the average VPD for hours with shrinkage.

VPD was categorized into two groups: low VPD (<0.7 kPa) and high VPD (≥ 0.7 kPa). The threshold for defining VPD as low, set at less than 0.7 kPa, was derived from the outcomes of the Gaussian RBF model implemented in this study. This model, which correlated biweekly growth rates with VPD and rainfall, revealed that biweekly growth rates were maximized when VPD values were below 0.7 kPa (Fig. S2 – 1, and table S2 - 1 in appendices).

To assess the variation of GR of individual trees throughout the year, as dependent to their inherent traits and environmental conditions, we fitted a ‘lmer’ using the R ‘lme4’ package. The species and the environmental variables rainfall, RH, temperature, and their derivative VPD were evaluated as fixed effects. The individual tree and the individual tree nested in species were evaluated as random effect, depending on the model structure. The full models evaluated were as follows:

- 1) $GR \sim Temp * Prec + Temp * RH + Tree + (1|Species)$
- 2) $GR \sim Temp * Prec + RH + Tree + (1|Species)$
- 3) $GR \sim Temp * Prec + Tree + (1|Species)$
- 4) $GR \sim Temp * Prec + Tree + (1|Tree|Species)$
- 5) $GR \sim VPD * Prec + Tree + (1|Tree|Species)$
- 6) $GR \sim Temp * RH + Tree + (1|Tree|Species)$

The best model fit was selected by comparing Akaike Information Criterion (AIC; Burnham & Anderson, 2002). Using the “predict” function of the ‘lme4’ package, we examined two possible scenarios of the best model: 1) Temperature increase of 1.5°C and biweekly rainfall increase of 25 mm. 2) Temperature increase of 1.5°C and biweekly rainfall increase of 50 mm. We considered a limit of a 50 mm increase in rainfall over each fortnight (two weeks), as this roughly coincides with a doubling of annual rainfall in the study area. This is a worst-case projection that we imagine occurring in the short term based on WMO forecasts.

Subsequently, we performed a two-way ANOVA test to compare GRs, with Scenario (projected vs. observed) and Species as the two fixed variables.

We used the Gaussian Radial Basis Function (RBF) (Shi and Choi, 2011) of the R package Plotly (Sievert et al., 2024), to plot GR in the measured space of environmental variables.

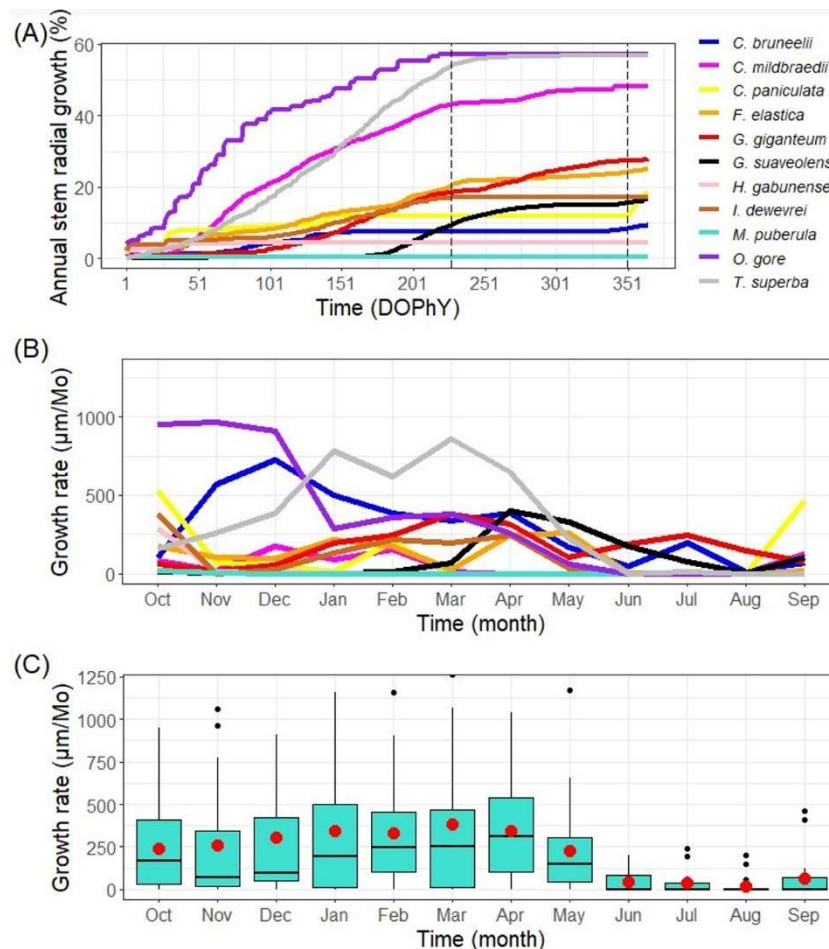


Figure 2-4. Annual stem radial growth dynamics. (A) Cumulative annual growth. The data set consists of cumulative diel increment rates, quantified as the diel contribution to the total annual growth (in percent). Each curve represents a given tree individual or averaged data for *F. elastica* and *T. superba*, which data spans multiple years. The time is in days of the phenological year (DOPHY), with the first day of the phenological year on October 1 and the last day on September 30. The two vertical dashed lines represent the theoretical beginning and end of the dry season, respectively, on May 15 and September 15. (B and C) Annual variation of monthly growth rate of study species trees. (B) The lines show the median monthly growth rate for each species, quantified as the radial increase in micrometers per month. (C) Boxplots show the median monthly growth rate (horizontal line inside the box), 25 and 75 percentiles (horizontal bases of the box) of the pooled data for all tree individuals. Red dots represent mean values, while black dots are outliers.

2.3. Results

2.3.1. General pattern of stem change

On a diel basis, the majority of trees begin to increase their increment rate from 6 pm, as soon as sunset. Increment rates peak between 6 and 9 a.m., then decline sharply until 12 p.m. and remain near zero during the day and afternoon. This is the time of day when the most significant shrinkage occurs. (Fig. 2 – 3).

Annual variability in stem radius is, in general, characterized by rapid growth in the rainy season (which theoretically extends from September 15 to May 15), a sharp decrease in growth for some trees, and a complete cessation of growth for others, during the dry season (Fig. 2 – 4A). We therefore noticed that the majority of trees (fourteen trees) ceased to grow during the dry season, while *F. elastica*, *G. giganteum* and *G. suaveolens* trees remained active throughout the phenological year (Fig. 2 – 4A and 2 – 4B). Mainly, growth begins in October and then fluctuates between October and April, depending on the phenological year and the tree species (Figs. 4A). From April to June, there is a decline, then from June to September, the majority of trees exhibit limited growth, those that do not experience growth cessation showing reduced growth rates (Fig. 2 – 4B). The growth cessation was generally longer and clearer in trees of deciduous species than in those of evergreen species. It means that deciduous species (*T. superba* and *H. gabunense*) tended to stop growing completely during the dry season and resume growth when the rains return, while evergreen species tended to have only a brief interruption or slowing of radial growth during the dry season (Figs. 2 – 4A and 2 – 4B). The timing of growth onset and cessation, as well as the duration of the stem growth period are compared in Fig. S2 – 2, in appendices.

Understory trees grew slower than dominant statue trees: tree height showed a fairly strong significantly positive correlation (Adjusted $R^2 = 0.43$) with annual growth (Fig. S2 – 3, in appendices). In particular, the *M. puberula* tree is too slow growing, with seasonal growth approaching zero (31.24 $\mu\text{m}/\text{year}$). This tree also has an atypical and short growing period of 33 days. Small-diameter trees have a lower annual growth than large-diameter trees. Indeed, tree diameter showed a moderate significant positive correlation (Adjusted $R^2 = 0.17$) with annual growth (Fig. S2 – 4, in appendices).

2.3.2. Stem changes in relation with environmental variables

On a diel basis, stem increment rates were highest at times when VPD was lowest (low temperature and high RH), i.e., from 6pm to 9am. The two-way ANOVA conducted to evaluate potential disparities between diurnal and nocturnal levels of environmental variables revealed statistically significant differences in Temperature, VPD, and RH values across all phenological years. During the nighttime, VPD and temperatures exhibited lower values compared to the daytime, whereas RH displayed higher values during the nighttime than during the daytime (Fig. S2 – 5). When the VPD and temperature starts to get low (at 6pm), trees begin to maximize their radial growth rate, peaking between 6 and 9 am. At around 9 a.m., when the VPD and temperature starts to rise, the increment rate begins to decrease and remains near zero throughout the morning and the afternoon (Figs. 2 – 3A and 2 – 3B).

VPD tends to be higher during the day than at night, regardless of the time of year. However, it has been observed that VPD values are generally higher during the dry season than during the rainy season (black curve in Fig. 2 – 3C and 2 – 3D). The Gaussian RBF kernel model showed that VPD accounts for 23% of diel shrinkage in the dry season and 39% in the rainy season. During the rainy season, periods of low shrinkage (colored areas ranging from green to pale orange, Fig. 2 – 3C) tend to occur for VPD values from 0.2 to 0.7 kPa, with these values most frequently recorded between 9 p.m. and 5 a.m. This suggests that growth tends to predominantly occur during these hours. Conversely, during the dry season, periods of low shrinkage (colored

areas ranging from green to pale orange, Fig. 2 – 3D) occur at higher VPD values, from 0.8 to 1.4 kPa, most often recorded between 8 p.m. and 7 a.m. This implies that growth transpires within a longer time frame compared to the rainy season.

The lmer fitted to analyze daily radial increment rates with DOPhY and VPD, and to compare days characterized by minimal shrinkage and days with more pronounced shrinkage, exhibited a weak explanatory capacity (conditional $R^2 = 0.02$). Within this model, the following observations were noted: The effect of DOPhY was statistically significant and negative (beta = $-7.55\text{e-}04$, 95% CI [$-1.13\text{e-}03$, $-3.78\text{e-}04$], $t(7659) = -3.92$, $p < .001$; Std. beta = -0.07 , 95% CI [-0.11 , -0.04]). The effect of VPD group [Low VPD] was statistically significant and positive (beta = 0.19 , 95% CI [0.08 , 0.31], $t(7659) = 3.23$, $p < .001$; Std. beta = 0.06 , 95% CI [0.09 , 0.19]). The interaction effect of DOPhY and VPD, when VPD group was “Low VPD”, was statistically significant and negative (beta = $-9.82\text{e-}03$, 95% CI [-0.02 , $-1.13\text{e-}03$], $t(7659) = -2.22$, $p = 0.027$; Std. beta = -0.06 , 95% CI [$3.03\text{e-}03$, 0.11]).

The total explanatory power of the model, indicated by the conditional R^2 (0.02), suggests that the model explains about 2% of the variance in the radial increment rate when considering both fixed and random effect, which is low. The standardized beta coefficient for DOPhY indicates a moderate effect on the diel radial increment rate, but insinuating that as the phenological season progresses, the diel radial increment rate decreases. The standardized beta coefficient for VPD group indicates that during periods characterized by low VPD, the radial increment rate is estimated to increase by 0.19%. The interaction between DOPhY and VPD group indicates that the influence of VPD on radial growth rate varies throughout the phenological year. During the initial phase, characterized by low VPD, i.e. rainy season days, there is an increase in growth rates. However, in the subsequent phase, characterized by high VPD, i.e. as dry season days, growth rates tend to decrease.

On an annual basis, the start of growth does not coincide with the return of the rain, which occurs in the second half of September. Instead, it shifts towards October. Similarly, the end of growth does not occur immediately at the beginning of the dry season, in May. Instead, it occurs around June (Fig. 2 – 4). The temperature curve has the same tendency as the rainfall curve (Fig. 2 – 1B). Thus, growth cessation or slowdown occurs during the coldest period of the year. These observations are discussed in detail in the paragraphs that follow.

2.3.3. Modeling tree's responses to the environmental variables change

The lmer to predict GR variation throughout the year including the variables temperature, rainfall, RH, and tree as fixed effects and the variable species as random effect, produced the best fit formulated as follows:

$$\text{GR} \sim \text{Temp} * \text{Prec} + \text{Temp} * \text{RH} + \text{Tree} + (1 | \text{Species})$$

The model's total explanatory power was substantial (conditional $R^2 = 0.32$) and the part related to the fixed effects alone (marginal R^2) was 0.31. A significant positive effect of rainfall (beta = 12.78 , 95% CI [5.47 , 20.09], $t(543) = 3.44$, $p < .001$; Std. beta = 0.21 , 95% CI [0.08 , 0.33]) was found. The interaction between temperature and rainfall was significant and negative (beta = -0.51 , 95% CI [-0.81 , -0.21], $t(543) = -3.37$, $p < .001$; Std. beta = -0.24 , 95% CI [-0.37 , -0.10]).

Temperature and RH showed a non-significant negative effect, while their interaction was non-significant and positive. The effects of different trees varied considerably, emphasizing differences in their growth patterns. Similarly, the random effects for the variable species indicated that the model accounted for variation among tree species.

The results of two-way ANOVA (see appendices) comparing the effects of different temperature-increase scenarios on GR suggest that both tree and scenario variables, along with their interaction, have a statically significant overall effect on GR ($p < 0.05$), without considering species separately. This assumes that the effect of scenario on GR varies across trees. Pairwise comparisons conducted using the emmeans test after the ANOVA, which provide a better understanding of the specific differences between the effects of the scenarios on each tree, reveal that trees of the *T. superba* species would be significantly sensitive to the scenarios predicting a temperature increase of 1.5°C associated with an increase in rainfall. This sensitivity appears as a stabilization throughout the year of the biweekly GR around a value of 197 μm with a standard deviation of 60 μm (Fig. S2 – 6, in appendices). This would imply continuous growth throughout the year. No statistically significant disparity was observed between the effects of the two predicted scenarios and the observed scenario for the rest of the trees in the database.

In the Gaussian RBF model, fitting the observed annual growth pattern, the highest biweekly-resolved annual growth was generally observed at a mean temperature of 21.9 to 25.5°C coupled with rainfall of 80 to 160 mm, corresponding to the greenish to yellow zone in figure 2 – 5. Minimal growth (pale purple to dark areas) is observed in rainfall ranges below 60mm coupled with temperatures below 23°C, and in a few isolated areas corresponding to temperatures above 25°C and rainfall above 80mm. The rest of the temperature-rainfall space is occupied by intermediate GR.

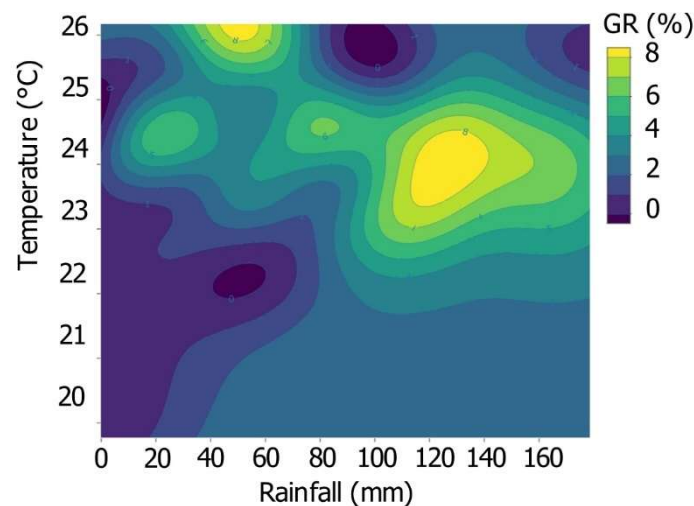


Figure 2-5. Biweekly-resolved, radial annual GR in the measured space of temperature and rainfall across all individual trees. GR was quantified as the relative annual contribution to the total annual growth for each tree and ranged from dark purple (no growth, 0%), over yellow (marginal growth, $\geq 8\%$).

2.4. Discussion

2.4.1. Diel patterns of stem radial growth

We found that trees begin to maximize their increment rate from 6pm (Fig. 2 – 3A), that is to say from sunset, with individual-specific increment rate peaks between 6am and 12am (Figs. 2 – 3B). This period of the day corresponds to the time when trees are assumed to be better supplied with water and therefore likely to provide the best conditions for exceeding the turgor threshold for cell division and expansion (Taiz and Zeiger, 2010; Steppe et al., 2015; Cabon et al., 2020, Zweifel et al., 2021). We are therefore convinced that it is in this time interval that trees grow preferentially on a diel scale. But given the nature of our data, we cannot say with certainty that all the increment rate peaks we observed corresponded to reversible stem growth.

Photosynthesis is the starting point for tree growth. Its primary phase, which requires light, occurs during the daytime. Chlorophyll, the green pigment in leaves, absorbs light energy and converts carbon dioxide from the air and water from the soil into glucose and oxygen. During cellular respiration, the glucose produced during the day is oxidized and broken down into water and carbon dioxide, releasing energy that is used for growth and other cellular functions (J. W. Hart, 2012).

While trees respire continuously, both day and night, the respiration process is more noticeable and can appear to be higher at night. During the daylight period, the oxygen produced by photosynthesis can mask the respiration process because it is being released as a byproduct. At night, the production of glucose and oxygen ceases because there is no light to drive photosynthesis. As a result, respiration becomes the primary metabolic activity and is more pronounced. Trees still require energy for maintenance and growth, which comes from breaking down the glucose produced during the day. This is why growth occurs mainly during nighttime (Eberhard et al., 2008).

2.4.2. Annual patterns of stem radial growth

The timing of radial growth onset as well as the timing of its end and the length of the stem radius growth period, fluctuates between trees. The classical clustering designed to highlight the difference between tree behavior is shown in Figure S2-7 (in appendices). The onset of radial growth occurs mainly from the beginning of October to mid-November, while the end occurs mainly from mid-May to mid-June. This is in accordance with the observation made by Angoboy Ilondea et al. (2021) on *P. balsamifera*. A few trees, however, are exceptions to this rule, some remaining active for the whole of the 2018-2019 phenological year, or most of it (e.g., *C. mildbraedii*, *G. giganteum* and *F. elastica*) and others, mainly found in understory, growing for only a few days of the season (e.g., *M. Puberula*, *H. gabunense*). Taking into account that several disturbances can be observed in a tree due to its presence in the lower strata of a forest (Hladik & Blanc, 1987; De Mil et al., 2017; Hubau et al., 2019), we believe that the abnormal behavior observed on this tree is due to its presence in the understory. This is in accordance with previous studies (Ouédraogo et al., 2013; De Mil et al., 2017; Hubau et al., 2019). The understory is a forest layer with a different energy flow, nutrient cycling, biodiversity and regeneration capacity (Hladik & Blanc, 1987; Gilliam, 2007). It is an environment that can be particularly poor in solar radiation so that the chances of survival can be very reduced for some plants (Hladik & Blanc, 1987; Torti, Coley, & Kursar, 2001).

The few trees that do not stop growing in dry season, are all evergreen, while all individuals of the deciduous species *T. superba* and *H. gabunense* have a clear growth cessation.

We found that large-diameter trees exhibited higher total annual growth compared to small-diameter trees (Fig. S2 – 4, in appendices). However, it's widely recognized that, within one species, that young, small-diameter trees typically have higher cumulative GR than larger trees: when the diameter of a tree is analyzed, ring-width decreases in size over the years of formation (Speer, 2010). When comparing different species with different life history strategies, numerous other factors come into play. In the present study, small-diameter trees belonged to slower-growing understory species, while large-diameter trees were predominantly from faster-growing canopy species, which tend to form relatively wide growth rings.

The observed trend in cumulative annual growth variation with dbh can be attributed to the differences in the ecological strategies of the species. Understory trees, characterized by smaller diameters, generally experience lower growth due to reduced light availability, which affects their photosynthetic rate and subsequently cambium activity (van den Berg et al., 2012). This is especially true for light-demanding species, where individuals in the understory (smaller diameters) are exposed to lower light regimes, resulting in decreased cambium activity and growth (Brienen et al., 2010).

2.4.3. Climatic driving stem radial growth

We found that, on a diel basis, growth preferentially occurs between sunset and early morning. This is a cooler time of day, with little to no sunshine, more humid under the lowest VPD values (Zweifel et al., 2021), while on annual basis, the growth period roughly coincides with the rainy season, the hottest period of the year. This is in accordance with the results of previous studies on tree growth in a seasonal tropical climate (Trouet et al., 2006; Couralet et al., 2010). Basically, plant growth is largely attributed to a conjunction of climatic variables including, mainly, precipitation, temperature, RH, VPD, solar radiation, atmospheric gases (Wagner et al., 2014), etc. Previous experiments have shown that the rate of photosynthesis is critically dependent on variables such as temperature and light intensity (Feeley et al., 2020; Perez & Feeley, 2020). It is well known that the temperature dependence of photosynthesis varies with the growing environment and species. For each environment, there is a temperature range in which photosynthetic enzymes function at their optimal level, resulting in high rates of photosynthesis. At temperatures outside this range, the enzymes that carry out photosynthesis do not function efficiently, which decreases the rate of photosynthesis (Medlyn et al., 2002; Perez & Feeley, 2020). Although trees form new cells using the carbohydrates produced during photosynthesis, it is not primarily the availability of carbohydrates that limits their growth, but the water tension within them. This is mainly due to the humidity of the air, which is higher at nighttime than during the daytime. Even on moist soils, trees grow mainly at night, because the drier daytime air inhibits their growth (Zweifel et al., 2021).

On a diel basis, during the light phase of photosynthesis, which takes place during the daytime, plants need sunlight and CO₂. During the dark phase, which takes place at night, plants have to open their stomata and simultaneously assimilate the glucose synthesized during the light phase. This requires a decrease in temperature and an increase in relative humidity, as high temperature

induces transpiration which reduces water potential and turgor pressure in the cambium, both essential for cambial cell division and expansion (Peters et al., 2021). The observed diel patterns in VPD and its correlation with growth dynamics can be attributed to a combination of environmental and physiological factors. The higher VPD during the day compared to nighttime is a consequence of solar radiation and temperature fluctuations. During daylight hours, solar radiation, and temperatures typically peak, leading to increased evapotranspiration rates and subsequently higher VPD. Conversely, at night, without the influence of direct sunlight, temperatures drop, leading to lower evapotranspiration rates and consequently lower VPD (Grossiord et al., 2020; Peters et al., 2021). The Gaussian RBF kernel model indicates that VPD is a significant factor in both seasons. However, its influence is more pronounced during the rainy season. The disparity in VPD values between the dry and rainy seasons can be primarily attributed to differences in atmospheric moisture content. During the dry season, characterized by reduced rainfall and lower relative humidity, the atmosphere holds less moisture, resulting in higher VPD values. Conversely, during the rainy season, increased rainfall and higher humidity levels contribute to lower VPD values. Periods of low shrinkage occur over a longer nighttime duration during the dry season compared to the rainy season, because the dry season in Luki is characterized by lower temperatures than the rainy season. This results in an extended period of cooler diel temperatures conducive to low evapotranspiration.

We obtained significant findings regarding the correlation between weather conditions and tree growth by examining how temperature, rainfall, RH, and VPD influence radial stem growth throughout the phenological year, while considering the effects of individual trees. The model we fitted accounts for a substantial part of the observed variability in radial growth, underlining the importance of environmental variables and individual trees and species effects on tree growth.

Our results revealed that Rainfall had a significant positive effect on tree growth, suggesting that higher levels of rainfall promote tree growth. This is often observed in tropical forests with a marked dry season as attested in the pre-existing literature (Vieira et al., 2004; Worbes, 1999; Brien et al., 2005; Gliniars et al., 2013). The essential role of rainfall in tree growth explains the time lag between the start of the dry season and the initiation of tree growth, as well as between the end of the dry season and the end of tree growth. However, sensitivity to water stress varies among tree species, depending on their phenological-functional group. While individuals of evergreen species show a certain variability in their sensitivity to drought, individuals of deciduous species appear to be more sensitive to both air and soil drought, as supported by De Souza (et al., 2020). For trees that experience growth cessation, this occurs between June and September, the period when the water potential is lowest (Worbes, 1999). Even trees that are continuously active throughout the whole year experience growth decrease during dry period. However, we found that radial growth starts soon after the beginning of the rainy season and continues until some days or weeks after the beginning of the dry season (Fig. 2 – 4). This is in accordance with previous research (Worbes, 1999; Angoboy Ilondea et al., 2021) and can be explained as follows: Decrease in rainfall during the dry season leads to a decrease in soil water potential (Spanner et al., 2022). As the dry season progresses, the soil water content decreases and so does the water potential (Kursar et al., 1995). Because of this

decrease in water potential, tree growth reduces, depending on the resistance to water deficit of each one. At the most severe part of the dry period, tree water potential reaches a minimum, and trees enter a period of cambial dormancy (Worbes, 1999).

The effect of temperature was statistically non-significant and negative on radial tree growth. This indicates that due to its current low variability in Luki, temperature (Couralet et al., 2010) has no effect on tree growth. However, if it were to increase, it might attenuate the beneficial positive effects of rainfall on tree growth, as demonstrated in several previous studies (Doughty, 2011; Locosselli et al., 2020). This explains why we found a statically significant negative effect of the interaction between temperature and rainfall on radial stem growth. Numerous others studies show that certain tropical tree already responds negatively to temperature (Schippers et al., 2015; Anderson-Teixeira et al., 2022). It therefore appears that tropical forests do not react homogeneously to temperature increase, as their reactions vary considerably based on species, sites and geographical regions (Bauman et al., 2022; T. Chowdhury et al., 2023).

By simulating temperature increases of 1.5°C along with two levels of biweekly rainfall augmentation (25 mm and 50mm), we highlighted the differing sensitivities of tree species to climate change. Trees of the *T. superba* species exhibited notable sensitivity to the projected scenarios, unlike trees of the other species: their annual GR remains close to an average value throughout the year (Fig. S2 – 6, in appendices). It seemed that the rise in rainfall enhanced growth as anticipated, while the rise in temperature continued to show no impact on growth. This implies that if the temperature and rainfall increase forecasted by the WMO were to occur in similar proportions to the scenarios we examined, it could potentially benefit the growth of specific species in Luki, particularly deciduous species. This would allow them to mitigate water stress during the dry season, which had previously hindered their growth.

The study revealed statistically non-significant effects of RH on tree growth. Luki's hilly landscape and proximity to the Atlantic Ocean results in persistent mists yearlong. In the driest months, a dense cloud cover obstructs solar radiation, leading to a decrease in temperature. These conditions compensate partially for rainfall shortage and maintain a RH favorable to tree growth throughout the year (Sénéchal et al., 1989; Lubini, 1997). Consequently, despite relatively low annual rainfall during the three to four months of the dry season (less than 60 mm of rain per month), plants do not suffer severe water stress (Lubini, 1997; Couralet et al., 2013).

The distribution of GR values in the temperature-rainfall space (Fig. 2 – 5) underscores the impact of the dry season (rainfall below 60mm), where low GRs are prevalent, sometimes reaching zero. This clearly indicates that not all trees cease growth during this period. Conversely, it also emphasizes the modest growth observed at temperatures exceeding 25°C, despite adequate rainfall levels. These findings are further supported by the observation that the annual growth curves of some trees peak during the dry season (Figs. 2 – 4) and confirm the inclination of Luki's trees to cope with the projected rise in temperature and rainfall. Paleoecological data from Africa indicate a non-linear and spatially heterogeneous response to climate change, i.e., little change until a certain threshold is crossed, followed by rapid ecosystem change. It appears that the tropical rainforests of West and Central Africa have remained largely resilient over the last 1,000 years in the face of moderate climate change. Their

resilience can be attributed to the diverse and complex natural processes inherent to these ecosystems.

It is, rather, the current increase in human impacts and pressures that would assign them an uncertain and unpredictable potential future (Giresse et al, 2023). There is every reason to believe that if trees were to experience growth disturbances in Luki's forests, deciduous species would be more vulnerable than evergreen species (De Souza et al., 2020).

2.4.4. Potential limitations of the results

There are some limitations to this study. We maximized species covering and the number of replicates per species is low. Logistically, it was not possible to consider several other factors that could enable to better describe the secondary growth dynamics of Congo Basin trees under a changing climate. These include the microclimate of each tree, forest stratum (understory or canopy), soil parameters such as soil moisture, rooting depth, simultaneous measurements of stem radius variation on both xylem and bark, and the monitoring of several individuals for each species. We believe that studies over several phenological year, including a larger number of trees per species and combining precision dendrometer monitoring with analysis of cambial activity and leaf phenology monitoring, are needed to provide a better understanding of secondary growth dynamics in the Congo Basin. Emphasis should be placed on understanding the intraspecific heterogeneity of growth responses to as many environmental variables as possible, to identify species or populations that may be more resistant or vulnerable to changing environmental conditions.

2.5. Conclusion

Our results demonstrate that on a diel basis, tropical trees preferentially grow between sunset and early morning, and on an annual basis, mainly during the rainy season.

The annual growth pattern indicates an overlap of the growing season with the rainy season for most trees. Furthermore, our study highlighted the fact that Luki's unique weather conditions, due to its hilly relief and proximity to the Atlantic Ocean, shelters the trees from severe water stress and high temperatures, particularly during the dry season. We showed that trees in the Luki Man and the Biosphere reserve possess considerable chance to cope with the predicted increase in global temperature and local rainfall.

Data availability statement

The original contributions presented in the study are included in the article/Supplementary material, further inquiries can be directed to the corresponding author.

Author Contributions

BL, HB, NB, and TM designed the study. BL, BA, BD, CM, FL, CK and TM collected the data in the field. BL analyzed the data and wrote the manuscript. TM, HB, and RP reviewed the manuscript.

Funding

This research was carried out thanks to a grant awarded by the Royal Museum for Central Africa within the framework of the PilotMAB project, which is funded by the Belgian Directorate General for Development Cooperation and Humanitarian Aid (DGD). Additional funding was obtained from the non-profit association NATURE PLUS.

Acknowledgements

We are grateful to the management of the Royal Museum for Central Africa, The Regional Post-Graduate Training School on Integrated Management of Tropical Forests and Lands (*ERAIFT*), and the Institut National pour l'Etude et la Recherche Agronomiques - Luki (INERA-Luki).

Conflict of Interest

The authors declare that the research was conducted in the absence of any commercial or financial relationships that could be construed as a potential conflict of interest.

Publisher's note

All claims expressed in this article are solely those of the authors and do not necessarily represent those of their affiliated organizations, or those of the publisher, the editors and the reviewers. Any product that may be evaluated in this article, or claim that may be made by its manufacturer, is not guaranteed or endorsed by the publisher.

Supplementary material

The Supplementary material for this article can be found in the appendices of this document and online at:

Frontiers | Diel and annual rhythms of tropical stem size changes in the Mayombe forest, Congo Basin

Chapter 3: Growth periodicity in semi-deciduous tropical tree species from the Congo Basin



Blighia welwitschii

This study was published under the reference:

Luse Belanganayi, B., Delvaux, C., Kearsley, E., Liévens, K., Rousseau, M., Mbungu Phaka, C., Djiofack, B. Y., Laurent, F., Bourland, N., Hubau, W., De Mil, T., & Beeckman, H. (2024). Growth periodicity in semi-deciduous tropical tree species from the Congo Basin. *Plant-Environment Interactions*, 5(3), e10144. <https://doi.org/10.1002/pei3.10144>

Abstract

In the tropics, more precisely in equatorial dense rainforest, xylogenesis is driven by a little distinct climatological seasonality, and many tropical trees do not show clear growth rings. This makes retrospective analyses and modeling of future tree performance difficult. This research investigates the presence, the distinctness, and the periodicity of growth ring for dominant tree species in two semi-deciduous rainforests, which contrast in terms of precipitation dynamics. Eighteen tree species common to both forests were investigated. We used the cambial marking technique and then verified the presence and periodicity of growth-ring boundaries in the wood produced between pinning and collection by microscopic and macroscopic observation. The study showed that all eighteen species can form visible growth rings in both sites. However, the periodicity of ring formation varied significantly within and between species, and within sites. Trees from the site with clearly defined dry season had a higher likelihood to form periodical growth rings compared to those from the site where rainfall seasonality is less pronounced. The distinctness of the formed rings however did not show a site dependency. Periodical growth-ring formation was more likely in fast-growing trees. Furthermore, improvements can be made by a detailed study of the cambial activity through microcores taken at high temporal resolution, to get insight on the phenology of the lateral meristem.

Keywords: cambial marking, growth-ring distinctness, periodicity of growth-ring formation, secondary growth, tropical forests

3.1. Introduction

Trees archive information on secondary growth dynamics in their xylem (Babst et al., 2014). They form growth rings when they experience cambial dormancy related to adverse conditions (Brienen et al., 2016) including the severity and duration of the dry seasons (Worbes, 1999), flooding in floodplain forests (Schöngart et al., 2002), and salinity fluctuations in mangrove forests (Chowdhury et al., 2008). Analysis of ring patterns on pith-to-bark samples makes it possible to estimate the age of trees, to evaluate past reactions to environmental fluctuations and possibly to reconstruct past climatic conditions (Anchukaitis, 2017). However, temporal morphological markers, such as anatomically distinct growth-ring boundaries, are irregular or difficult to detect in many tropical trees, making retrospective analyses difficult in tropical forests (Tarelkin et al., 2016).

Recent studies conducted in tropical forests have challenged the paradigm that tropical tree species do not form growth rings (López et al., 2012; Mariaux, 2016). Despite the great diversity in appearance and occurrence of growth rings in tropical regions, their annual character has been increasingly identified in more and more tree species (Worbes, 2002, 2011; Zuidema et al., 2012). Despite these recent advances, the forests of the Congo Basin are still under-represented in studies highlighting ring formation by tree species (Couralet et al., 2013). Particularly, it remains unclear whether there is no cambial dormancy, or a single or multiple dormancy period(s) during a growing season.

Given the strong link between carbon sequestration and tree growth (Babst et al., 2014), it is also of key importance to assess the periodicity of secondary growth and understand its drivers,

in order to forecast the feedback of forests to climate change and the carbon dynamics of the atmosphere (Lehnebach et al., 2021).

In the present study, we investigated growth-ring presence, distinctness, and periodicity in eighteen tree species growing under two different climate conditions in the Congo basin (Kottek et al., 2006). As such, wood samples were analyzed in the semi-deciduous rainforests of the Biosphere Reserves of Luki and Yangambi, in the Democratic Republic of Congo to address the research questions: (1) Do a majority of tree species produce annual and anatomically distinct growth rings? (2) Is growth ring regular between individuals of the same tree species, and what could cause irregularity? (3) What is the effect of site on the periodicity of growth ring formation?

Ring boundary can be examined by naked eye or microscopically (Wheeler & Baas, 1998; Brien & Zuidema, 2005; Chowdhury et al., 2016). The periodicity of wood anatomical traits refers to the regularity/frequency of their appearance over time. Growth rings are considered distinct, when an abrupt structural change at the boundaries between them is present, usually including a change in fiber wall thickness and/or fiber radial diameter. The abrupt changes should enable each cell of the ring boundary to be associated exactly with a single growth ring of the two concomitant ones (Tarelkin et al., 2016). Indistinct growth rings are those that are vague and marked by gradual structural changes at their poorly defined or non-visible boundaries (IAWA Committee, 1989). The observation of distinct or indistinct rings implies a wood anatomical assessment. This is most often done at high microscopic resolution on a small fragment along the tree circumference. A distinct or an indistinct border can be a very local phenomenon in a tree stem. Wedging rings, which occur very often in tropical wood, are known to hamper considerably the classical growth-ring analysis. Ring borders can also be of aperiodic nature. Fundamental of growth-ring analysis, certainly in the tropics, is information on their distinctness and their periodicity (Tarelkin et al., 2016).

We hypothesize differences in growth-ring formation between the two sites related to differences in rainfall seasonality and the severity of the dry seasons, and between different species related to inherent growth traits. More specifically, we hypothesize (1) growth rings to be predominantly annual in Luki as opposed to Yangambi where the dry season is less pronounced; (2) deciduous species to produce annual growth rings in both sites; and (3) evergreen species to produce annual growth rings only in Luki where the rainfall seasonality is more pronounced.

3.2. Materials and Methods

3.2.1. Study site

Study sites are located in the semi-deciduous rainforests of the Biosphere Reserves of Luki and Yangambi in the Democratic Republic of Congo (Fig. 3 – 1a). The two sites, whilst in different areas of the Congo Basin, have many tree species in common. The sites are characterized by a different climate: Luki has an Aw climate and Yangambi an Af climate according to the Köppen classification updated by Kottek et al. (2006). The average annual rainfall is 1296 mm in Luki, and 1652 mm in Yangambi, while the average annual temperatures are 25.0 °C (ranging from 19.5 – 27.9 °C) and 25.4 °C (ranging from 22.4 – 29.9 °C) respectively (deduced from data

from <https://power.larc.nasa.gov/data-access-viewer/>). The dry period extends from June to September in Luki (monthly rainfall < 50mm), while there is no clear dry period in Yangambi, except that there is a decrease in rainfall of about 60 mm per month between December and February (Fig. 3 – 1a & 3 – 1c).

3.2.2. Study species

We selected 18 tree species (belonging to 13 families) that occur on both study sites. Three of the species are classified as deciduous, and 15 as evergreen. Species common to both the canopy and understory are included (Table 3 – 1). This classification of leaf phenological and stratum classes was based on literature (Lubini, 1997), and classes are used as such in further analysis.

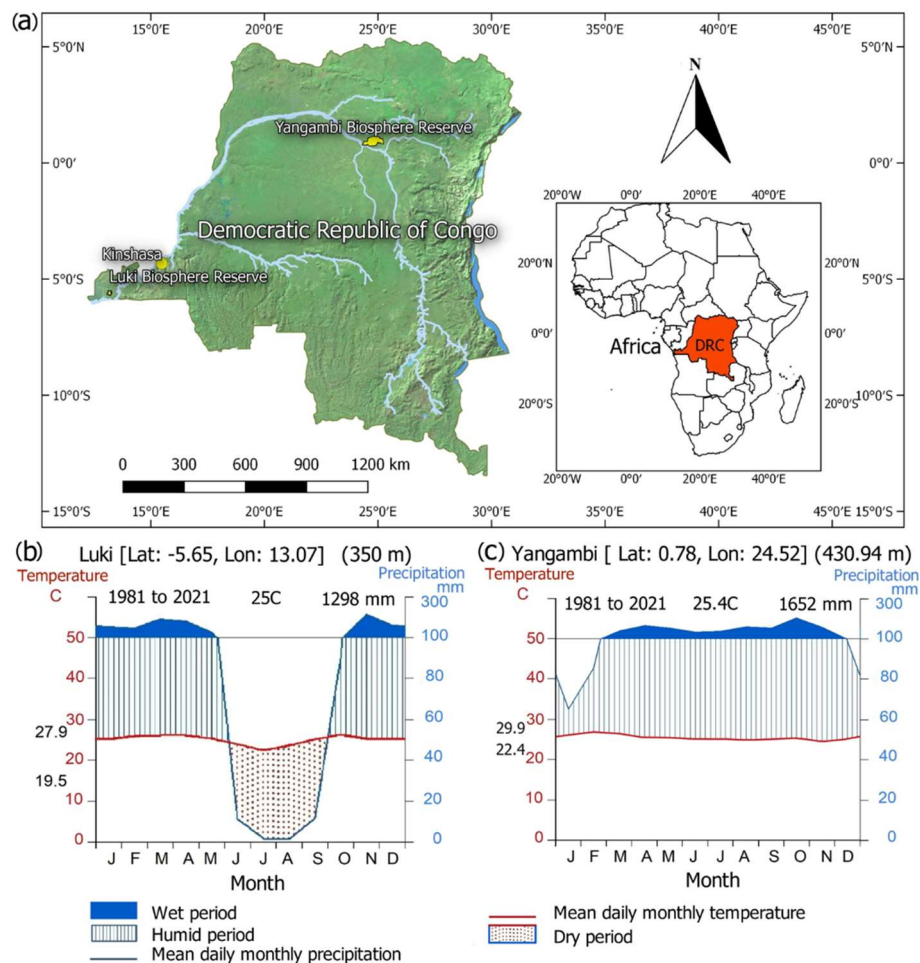


Figure 3-1. Location of study sites in the Democratic Republic of Congo (a). Walter-Lieth Climate Diagram of Luki (b) and Yangambi (c) UNESCO Man and Biosphere Reserve from 1981 to 2021. Data were obtained from <https://power.larc.nasa.gov/data-access-viewer/>. The blue line indicates the precipitation curve, the red line indicates the temperature curve, and the dry season is shown in dashed red. The blue stripes indicate the humid period, and the blue area shows the wet period. Temperatures in black, on the left axis, represent the average minimum temperature of the coldest month and the average maximum temperature of the warmest month, respectively. The annual average temperature and annual precipitation are shown in the upper right corner of the diagram.

3.2.3. Sample collection

Cambial marking was performed on 3 to 20 individuals per species and per site, depending on availability, a total of 317 trees. On each selected tree, the cambial zone was wounded with a pin at 130 cm height, according to the cambium marking technique recommended by Mariaux (2016), from 3 to 7 March 2015 in Luki, and from 4 to 8 August 2014 in Yangambi. For each individual tree, the diameter at breast height (DBH, 130 cm height) was measured with a diameter tape.

The collection of cores with a diameter of 5 cm containing the pinned zone, was done from 29 August to 10 September 2016 in Luki and from 8 to 18 August 2016 in Yangambi. At this time of sample collection, the DBH of each individual tree was remeasured, providing the macroscopic increment during the observation period.

Collected samples were transferred to the wood biology laboratory of the Royal Museum for Central Africa (RMCA) in Tervuren, Belgium, where they were air-dried, given a Tervuren Wood (Tw) collection accession number, and placed in the wood collection (Fig. S3 – 1, in appendices). As such, wood samples were available with two exactly known dates of cambium positions: the time of pinning, revealed by a pin mark, and the time of sampling, revealed by the wood-bark boundary.

Table 3-1. Leaf functional group, tree species, botanical family, stratum at adult stage (Lubini, 1997), distinctness and description of growth-ring boundaries (obtained from this study), and total number of successfully marked trees per species, in Luki and Yangambi forests.

Leaf functional group	Species	Family	Stratum	Distinctness of growth-ring boundaries	Description of growth-ring boundaries	No. Of trees per site	
						Luki	Yangambi
Deciduous	<i>Erythrophleum suaveolens</i> (Guill. & Perr.) Brenan	Fabaceae Caesalpiniaceae	Canopy	Distinct or indistinct	Flattened fibers. Band of marginal parenchyma.	2	2
	<i>Petersianthus macrocarpus</i> (P.Beauv.) Liben	Lecythidaceae	Canopy	Distinct or indistinct	Flattened fibers. Band of marginal parenchyma. Tangential band with little or no apotracheal axial parenchyma.	15	11
	<i>Prioria oxyphylla</i> (Harms) Breteler	Fabaceae Detarioideae	Canopy	Distinct	Flattened fibers. Band of marginal parenchyma.	2	2
Evergreen	<i>Blighia welwitschii</i> (Hiern) Radlk.	Sapindaceae	Canopy	Distinct or indistinct	Flattened fibers.	2	7
	<i>Carapa procera</i> DC	Meliaceae	Understory	Distinct	Band of marginal parenchyma.	4	1
	<i>Celtis mildbraedii</i> Engler	Cannabaceae	Canopy	Distinct or indistinct	Flattened fibers.	12	5
	<i>Chrysophyllum africanum</i> A. DC	Sapotaceae	Canopy	Distinct or indistinct	Flattened fibers.	8	5
	<i>Cola griseiflora</i> De Wild.	Malvaceae	Understory	Distinct or indistinct	Tangential band with little or no apotracheal axial parenchyma.	6	1
	<i>Garcinia punctata</i> Oliver	Clusiaceae	Understory	Distinct or indistinct	Tangential band with little or no apotracheal axial parenchyma.	2	3
	<i>Greenwayodendron suaveolens</i> (Engl. & Diels) Verdc	Annonaceae	Understory	Distinct or indistinct	Flattened fibers.	7	6
	<i>Lepalea thompsonii</i> Sprague & Hutch.	Meliaceae	Canopy	Distinct or indistinct	Flattened fibers.	3	4
	<i>Pentaclethra macrophylla</i> Benth	Fabaceae Caesalpiniaceae	Canopy	Distinct or indistinct	Flattened fibers. Tangential band without vessels or axial parenchyma.	5	1
	<i>Pycnanthus angolensis</i> (Welw.) Warb.	Myristicaceae	Canopy	Distinct or indistinct	Flattened fibers.	7	1
	<i>Staudtia kamerunensis</i> Warb	Myristicaceae	Canopy	Distinct or indistinct	Flattened fibers. Band of marginal parenchyma.	2	5
	<i>Strombosiaopsis tetrandra</i> Engler	Strombosiaceae	Canopy	Distinct or indistinct	Flattened fibers.	6	5
	<i>Trichilia gilgiana</i> Harms	Meliaceae	Understory	Distinct or indistinct	Flattened fibers. Band of marginal parenchyma.	12	1
	<i>Trichilia prieuriana</i> Juss	Meliaceae	Understory	Distinct or indistinct	Flattened fibers. Band of marginal parenchyma.	17	6
	<i>Trilepisium madagascariense</i> DC	Moraceae	Canopy	Distinct or indistinct	Flattened fibers. Band of marginal parenchyma.	13	10
Total						125	76

3.2.4. Sample processing and analysis

All samples were sanded on the pinned cross-sectional plan to highlight the pin mark. Marking was successful on only 201 trees (125 from Luki, 76 from Yangambi, Table 1), and these were used for further analysis. Successful marking means that the insertion of the pin through the cambial zone had left a scar on xylem and caused a production of wound tissue on the wood

formed later, near the pinning point (Seo et al., 2007). Wood anatomical observation and analysis were carried out by three observers, with (1) a SZH10 Olympus stereomicroscope equipped with a UC30 Olympus camera connected to a computer, and (2) an HRX-01 3D Digital Microscope (Fig. S3 – 2, in appendices). This also allowed us to capture high-definition images to examine the presence and distinctness of growth ring boundaries, and to measure the wood produced between pinning and collection. The software Cell Beta and Hirox were used for image capture. We measured the radial growth, outside the reaction zone, to the left and right of the pinning point using the imageJ software (Schneider et al., 2012). The mean value, in millimeters, was taken as the radial increase of the tree (Robert et al., 2011). The position of the pin mark in the xylem as well as the number of growth rings formed after pinning date were determined, and the periodicity (sub-annual, annual or no periodicity) was derived.

In accordance with the terminology of the IAWA, which considers a growth ring distinct when characterized by boundaries defined by an abrupt structural change usually including a change in fiber wall thickness and/or fiber radial diameter (IAWA Committee, 1989), we considered a growth ring distinct when all three observers could associate each cell of the growth ring boundary with exactly one of the two concomitant growth rings (Tarelkin et al., 2016). A growth ring is indistinct when at high magnification, it is not possible to associate a single cell to a particular growth ring. Growth-ring production was considered periodic when the tree produces a constant number of rings per year.

3.2.5. Auxiliary leaf phenological data

In order to verify the general relationship between deciduousness and presence of growth rings, historical long-term phenological observation records from Luki (Couralet et al. 2013; data from 1948 – 1957) and Yangambi (Hufkens & Kearsley, 2023; data from 1937 – 1956) were assessed. These two datasets contain historical ground-based leaf phenological observations of local tropical trees made three or four times each month, at Luki and Yangambi respectively, by the forestry division of the INEAC (Institut National pour l'Étude Agronomique du Congo). The timing at which the canopy contained no (or very few) leaves or was in a state of leaf turnover (partial leaf loss and flushing of new leaves, while retaining significant canopy leaf biomass) was recorded. The average species-level duration of these phenophase events, and presence of (sub-)annual periodicity was determined. Periodicity in the phenological timeseries was determined using a Fourier analysis following the method detailed in Bush et al., (2017). More details on the Fourier analysis as applied to these datasets can be found in Kearsley et al. (2024). Four species under investigation (*Garcinia punctata*, *Cola griseiflora*, *Leplaea thompsonii* and *Strombosiopsis tetrandra*) were not available in the Luki dataset. Genus level assessments were made for *Garcinia* sp., *Cola* sp. and *Leplaea* sp. The genus *Strombosiopsis* was not present in the Luki dataset.

3.2.6. Data analysis

To assess the distinctness and the periodicity of growth ring of individual trees as dependent on their inherent species-specific traits and growing conditions, we fitted a generalized linear mixed-effects model (GLMM) with a binomial link function using the R (R Core Team, 2023) ‘glmmTMB’ package (Brooks et al., 2017). Binomial for the periodicity of growth ring

formation was: no periodicity = 0, annual and sub-annual periodicity = 1, and for growth-ring distinctness: indistinct = 0, distinct = 1.

The fixed effects of individual tree-level parameters DBH and relative mean increment are assessed, as are the effects of species-specific classifications of stratum (understory, canopy) and leaf phenology (evergreen, deciduous), and species-level derived features of average leaf phenophase duration (state of no leaves, state of leaf turnover; duration in weeks) and the periodicity of these phenophase events ((sub)-annual or no annual periodicity). The site (Luki, Yangambi) at which the tree was observed is included as a fixed effect. The tree species nested within site is included as a random effect to account for species-specific effects at site-level. The full GLMM models assessed were:

- 1) periodicity (binary) ~ DBH + Relative mean increment + Stratum + Leaf phenology + Mean leaf phenophase duration + Leaf phenophase periodicity + Site + (1|Site/Species).
- 2) distinctness (binary) ~ DBH + Relative mean increment + Stratum + Leaf phenology + Mean leaf phenophase duration + Leaf phenophase periodicity + Site + (1|Site/Species).

The inclusion of each fixed effect is assessed (i.e., all combinations of fixed effects) and the best model fit was selected by comparing Akaike Information Criterion (AIC; Burnham & Anderson, 2002) and the standard deviation of residuals (residual standard error; $E =$

$$\sqrt{\frac{1}{df} \sum_{i=1}^n (Y_i - \hat{Y}_i)^2}).$$

3.3. Results

3.3.1. Distinctness of growth ring

All trees in this study, whether deciduous or evergreen, could display growth rings, even though not all growth ring boundaries were easily distinguishable, i.e. distinct. Only 2 species (*Carapa procera* (Fig. 3 – 2b) and *Prioria oxyphylla* (Fig. 3 – 2k) always showed distinct rings. The others showed distinct or indistinct rings, varying from one individual to another.

The growth-ring boundaries we found were marked by one or more of the following structural changes (Table 3 – 1): flattened fibers (Fig. 3 – 2a, c, d, f, h, i, l, m, n, p, q, and r), band (narrow or relatively large) of marginal parenchyma (Fig. 3 – 2b, d, g, k, l, n, p, q and r), tangential band with little or no apotracheal axial parenchyma (Fig. 3 – 2e), and tangential band without vessels or axial parenchyma (Fig. 3 – 2j).

The logistic mixed model to predict growth-ring boundary distinctness including features DBH, relative mean increment, stratum and leaf phenology class, dormancy periodicity, average dormancy duration and species nested in site as random did not yield statistically significant results for any of the predictors. The model as a whole did not explain a meaningful portion of the variation in growth-ring boundary distinctness, as indicated by marginal $R^2 = 0.09$. Consequently, none of the investigated variables appear to aid in predicting the distinctness of growth-ring boundaries.

3.3.2. Interpretation of the number of growth rings observed

The interpretation of the number of growth rings observed and their indication of periodic formation differed between Luki and Yangambi, depending on the sample collection period.

The marking in Luki was done within the 2015 wet season (about two months before the start of the dry season) and the collection within the 2016 dry season (Fig. 3 – 3a). As such, the collection was done one and a half seasons after marking. We therefore expect, if growth ring formation is annual, to have two ring boundaries formed, the last one at the wood-bark boundary. In Yangambi, both marking and collection were done during the wet season (August 2014 to August 2016, Fig. 3 – 3b). Considering that collection was done two seasons after marking, we could expect, if the rings are annual, to have two ring boundaries formed, the last one before the wood-bark boundary.

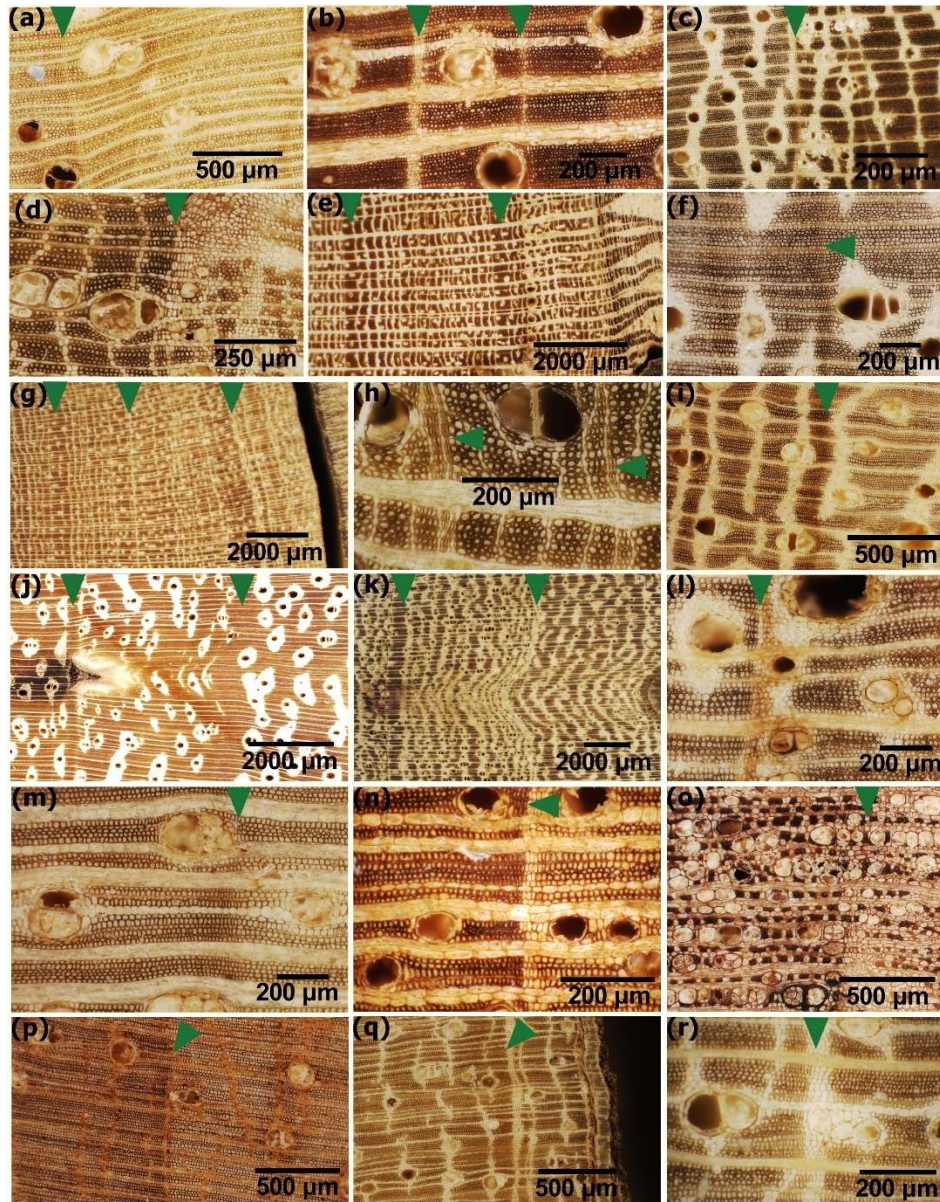


Figure 3-2. Incident light images of transverse sections showing tree ring boundaries (green triangles): (a) *B. welwitschii*, (b) *C. procera*, (c) *C. mildbraedii*, (d) *C. africanum*, (e) *C. griseiflora*, (f) *E. suaveolens*, (g) *G. punctata*, (h) *G. suaveolens*, (i) *L. thompsonii*, (j) *P. macrophylla*, (k) *P. oxyphylla*, (l) *P. macrocarpus*, (m) *P. angolensis*, (n) *S. kamerunensis*, (o) *S. tetrandra*, (p) *T. gilgiana*, (q) *T. prieurieana*, (r) *T. madagascariense*.

The interpretation of the cambial marking in relation to the growth rings observed during the study period varies between Luki and Yangambi. The following cases can be distinguished: (a) Pinning mark inside the only formed ring, ring n (Fig. 3 – 4a): marking was done while the tree was growing, and collection occurred before or at the beginning of the next growing period began. It's very likely that the single ring formed is not annual. (b) Pinning mark at the lower limit of the last and only formed ring, ring n (Fig. 3 – 4b): marking was done at the beginning of a growing period, and collection was done before or at the beginning of the next growing period.

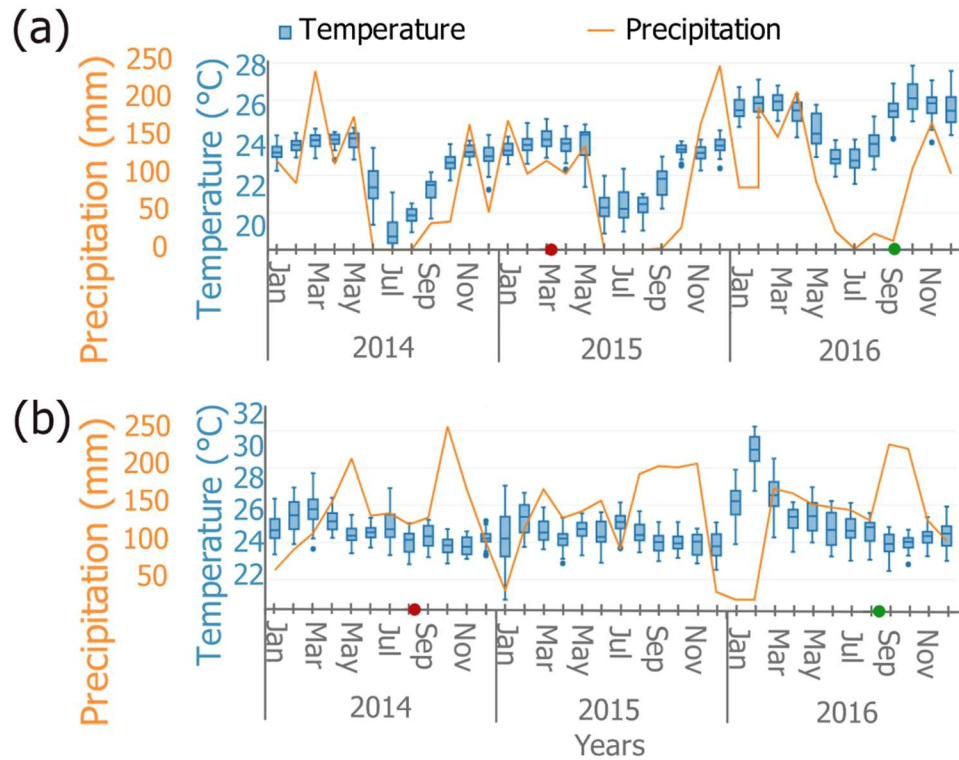


Figure 3-3. Total monthly rainfall and daily variation of monthly temperature during the study years (2014, 2015, and 2016). (a) Luki and (b) Yangambi. The red and green dots on the timeline mark the marking and collection dates, respectively. Data were obtained from <https://power.larc.nasa.gov/data-access-viewer/>.

This case suggests the annual occurrence of ring formation for Luki trees. For Yangambi, there is a high chance that this ring is multiannual. (c) Case like (b) except that the pinning mark is within the penultimate growth ring, the $n-1$ ring (Fig. 3 – 4c). This augurs that the marking was made while the tree was growing. Again, the case highlights the annual occurrence of ring formation for trees in Luki but not for those in Yangambi. (d) Pinning mark at the lower limit of the penultimate ring, ring $n-1$ (Fig. 3 – 4d): marking was done at the beginning of a growing period, and collection was done after the beginning of the next growing period. For Luki, it is possible that the second ring limit was due to lower rainfall in January 2016. For Yangambi, this could suggest that ring formation is annual. (e) Case like (d) except that the pinning mark is inside the ring preceding the penultimate ring, ring $n-2$ (Fig. 3 – 4e). This augurs that the marking was made while the tree was growing. Here again, the case shows the occurrence of a single ring per year for Yangambi trees, but two rings for Luki trees. (f) Pinning mark at the

lower limit of the ring preceding the penultimate ring, ring $n-2$ (Fig. 3 – 4f): marking was done at the beginning of a growing period, and collection was done after the beginning of two supplementary growing periods. This case does not exist for the Luki samples, in Yangambi, it suggests the possibility of several growth rings in some years. (g) Case like (f) except that the pinning mark is located inside the $n-3$ ring (Fig. 3 – 4g). This augurs that the marking was made while the tree was growing. (h) Pinning mark located at the lower limit of the $n-3$ ring: (Fig. 3 – 4h). marking was done at the beginning of a growing period, and collection was done after the beginning of tree supplementary growing periods. This case does not exist in the Luki samples either. For the Yangambi samples, it suggests the possibility of occurrence of two growth rings per year.

These cases of cambial markings in relation to observed growth-ring boundaries were found in the sampled trees at Luki and Yangambi, with a few species-specific examples presented here (Fig. 3 – 5).

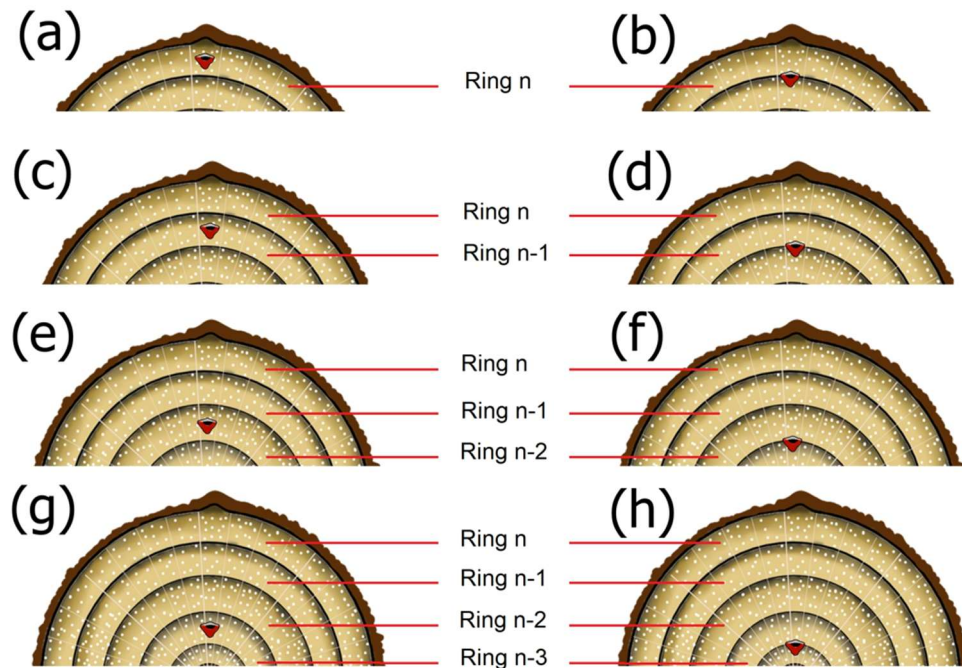


Figure 3-4. Position of pinning mark on the transverse plane of the stem. (a) Marking inside the last ring, ring n ; (b) marking at the lower limit of the last ring, ring n ; (c) marking inside the penultimate ring, ring $n - 1$; (d) marking at the lower limit of the penultimate ring, ring $n - 1$; (e) marking inside the ring preceding the penultimate ring, ring $n - 2$; (f) marking at the lower limit of the ring preceding the penultimate ring, ring $n - 2$; (g) marking inside the $n - 3$ ring; (h) marking at the lower limit of the $n - 3$ ring.

Case (a) showing the pinning mark inside the last formed growth ring was found, as in species *P. macrocarpus*, from Luki (Fig. 3 – 5a) and in *C. procera* from Yangambi (Fig. 3 – 5b). The case (b) showing the pinning mark at the lower limit of the last ring, ring n , was found, for example, in *B. welwitschii* (Fig. 3 – 5c) from Luki, and in *P. oxyphylla* (Fig. 3 – 5d) from

Yangambi. The case C, showing the pinning mark inside the penultimate ring, ring n-1, was found, for example, in *C. griseiflora* from Luki (Fig. 3 – 5e), and in *T. madagascariense* from Yangambi (Fig. 3 – 5f). The case d, showing the pinning mark at the lower limit of the penultimate ring, ring n-1, was found, for example, in *P. angolensis* from Luki (Fig. 3 – 5g) and in *S. kamerunensis* from Yangambi (Fig. 3 – 5h). The case E, showing the pinning mark inside the ring preceding the penultimate ring, ring n-2, was found, for example, in *P. oxyphylla* from Luki (Fig. 3 – 5i) and in *C. mildbraedii* from Yangambi (Fig. 3 – 5j). The case F, showing the pinning mark at the lower limit of the ring preceding the penultimate ring, ring n-2, was found, for example, in *G. suaveolens* from Yangambi (Fig. 3 – 5k). The case G, showing the pinning mark inside the n-3 ring, was found, for example, in *P. oxyphylla* from Yangambi (Fig. 3 – 5l). The case H, showing the pinning mark at the lower limit of the n-3 ring, was found, for example, in *C. africanum* from Yangambi (Fig. 3 – 5m).

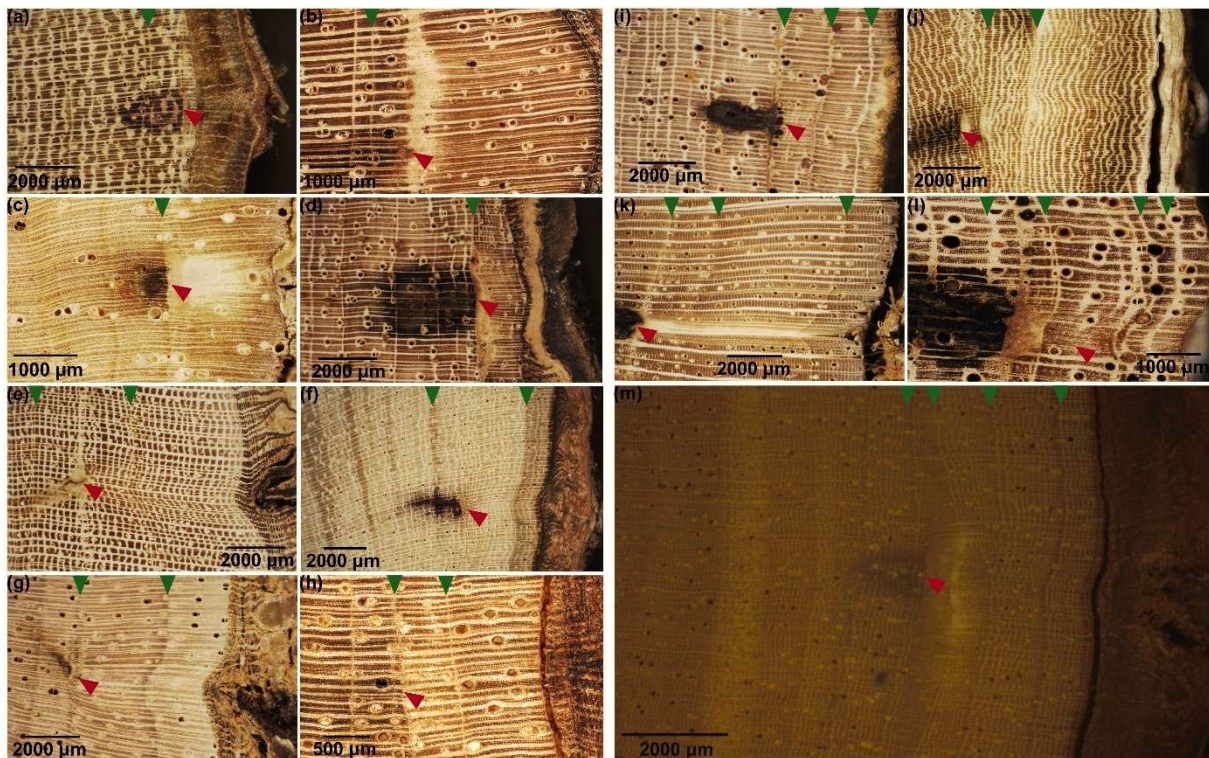


Figure 3-5. Images of wood samples showing the limits of growth rings (green triangles) and the new wood layers containing the scar (red triangle) resulting from cambial marking: (a) *P. macrocarpus*, (b) *C. procera*, (c) *B. welwitschii*, (d) *P. oxyphylla*, (e) *C. griseiflora*, (f) *T. madagascariense*, (g) *P. angolensis*, (h) *S. kamerunensis*, (i) *P. oxyphylla*, (j) *C. mildbraedii*, (k) *G. suaveolens*, (l) *P. oxyphylla*, and (m) *C. africanum*.

3.3.3. Periodicity of growth-ring formation

Nine species in Luki (*B. welwitschii*, *C. griseiflora*, *C. procera*, *G. suaveolens*, *P. angolensis*, *P. oxyphylla*, *S. kamerunensis*, *S. tetrandra*, *T. gilgiana*) and 2 species in Yangambi (*P. angolensis* and *T. gilgiana*) formed growth rings periodically in all their individuals. In Yangambi, 4 species (*C. griseiflora*, *C. procera*, *P. macrophylla* and *P. oxyphylla*) did not form periodical growth rings in any of the studied individuals. In the remaining species, the periodical

formation of growth rings varied from one individual to another. This intra-species variability was observed in 9 species in Luki and 12 species in Yangambi.

The logistic mixed model to predict growth-ring periodicity including parameters DBH, relative mean increment and site as fixed effects and species nested in site as random effects produced the best fit:

periodicity (binary) ~ DBH + Relative mean increment + Site + (1|Site/Species)

The model's explanatory power related to the fixed effects alone (marginal R²) is 0.72. A significant positive effect of DBH (beta = 0.03, 95% CI [6.43e-04, 0.07], p = 0.046; Std. beta = 0.56, 95% CI [0.01, 1.11]) and relative mean increment (beta = 1.91, 95% CI [1.12, 2.69], p < .001; Std. Beta = 2.43, 95% CI [1.43, 3.44]) was found, while a significant negative effect of site [Yangambi] was observed (beta = -3.52, 95% CI [-5.24, -1.79], p < .001; Std. beta = -3.52, 95% CI [-5.24, -1.79]) (Table 3 – 2).

Table 3-2. Model output of quantifying growth-ring periodicity in response to DBH (initial, at start of observation period), relative mean increment, and site as fixed effects, using a generalized linear mixed-effects model. Tree species are nested within site as a random effect.

Predictors	Estimate	SE	z	p	Signif.
Intercept	-1.01079	0.72134	-1.401	0.1611	
DBH (initial)	0.0339	0.01697	1.998	0.0457	*
Relative mean increment	1.90599	0.40122	4.75	< 0.001	***
Site : Yangambi	-3.51591	0.88037	-3.994	< 0.001	***
Random effect	Variance	SD			
Species within site	2.05	1.432			
Species	<0.000	0.00004			

Note: Tree species are nested within site as a random effect (Signif. codes: 0 '***' 0.001 '**' 0.01 '*' 0.05 '.' 0.1 ' ' 1).

The species-level classifications of stratum, phenology or the phenological parameters (phenophase duration or periodicity) did not significantly contribute to the prediction of growth-ring periodicity or improved the model fit.

3.4. Discussion

3.4.1. Distinctness of growth ring

The results of this study indicate that all eighteen species examined can form growth rings, demarcated by the following features, some observed simultaneously within a same species: flattened fibers, one or two layers of marginal parenchyma, tangential band with little or no apotracheal axial parenchyma, or tangential band without vessels or axial parenchyma. These anatomical features are among those used by several authors to formally identify the ring boundary in some tropical trees (Détienne, 1989; Détienne et al., 1998; Worbes, 1999; Robert et al., 2011; Mariaux, 2016). We found that not all growth-ring boundaries were distinct. Ring boundaries of 43.3% of trees showing rings were indistinct. However, the logistic mixed model we fitted revealed that no variables including DBH, mean relative increment, leaf stratum and phenological class, dormancy periodicity, mean dormancy duration, species, and site, predicted the distinctness of growth ring boundaries.

Growth rings are supposed to form when the tree is dormant as a result of an environmental stress factor (Worbes, 2002). The absence or limited seasonality in climatic variables in the tropics has been the basis for the long-held belief that tropical trees exhibit relatively constant growth throughout the year and do not form growth rings (Lieberman & Lieberman, 1985; Brien et al., 2016). It is well known today that many tropical trees form distinct growth rings and that rainfall seasonality (Gourlay, 1995; Worbes, 1995, 1999), temperature (Singh & Kushwaha, 2016) and light (Tarelkin et al., 2019) are by far the most common limiting factors for tropical tree growth. Complex interactions between the tree's organic functions, including transpiration, water uptake and storage, and environmental variables, including precipitation, sunlight, temperature, and soil water reserve, lead to phenological response patterns specific to each species, and even to each tree (Borchert, 1999; Singh & Kushwaha, 2016). Light intensity has been shown to have the greatest influence on the formation of growth-ring boundaries during the dry season. The reduction in daylight length, albeit slight in the tropics, and thick cloud cover during the dry season adversely affect the amount of sunlight in terms of duration and intensity (Tarelkin et al., 2019; Vargas et al., 2022). This can lead to an intensification of leaf fall, which in turn also negatively affects the wall thickness and size of the cells formed in the cambium (Janssen et al., 2021).

Growth-ring distinctness was however not significantly related to any of the investigated variables, including DBH, relative mean increment, tree stratum, leaf phenology, mean leaf phenophase duration, leaf phenophase periodicity and site. Previous studies do however show a relation between growth-ring distinctness and leaf phenological classes (Worbes, 1999). Indeed, Worbes (1999) found, in a study conducted in Venezuela, that ring boundaries, when present, are more pronounced in deciduous than in evergreen species. He postulated that evergreen species tend to show only a short interruption in wood growth during the latter part of the dry season, whereas deciduous species stop growing completely at the end of the rainy season.

In our case, we believe there was a bias due to differences in microclimate that were not considered. Intra-species variability in leaf phenology is high (Kearsley et al., 2023) and will depend on both internal cues and environmental drivers. The phenological observations available for this study did not account for the growing conditions of the individual trees (e.g., location in the canopy, gap effects, neighboring effects) or for the weather during the observation period (how severe was the dry season, what were the light conditions). When repeating this experiment, we recommend the collection of simultaneous phenological observations.

3.4.2. Periodicity of growth-ring formation

We found that site was one of the main predictors of growth-ring periodicity. Only nine species from Luki (*B. welwitschii*, *C. griseiflora*, *C. procera*, *G. suaveolens*, *P. angolensis*, *P. oxyphylla*, *S. kamerunensis*, *S. tetrandra*, *T. gilgiana*) and two species from Yangambi (*P. angolensis* and *T. gilgiana*), had all individuals forming growth rings periodically. Five species, namely *C. griseiflora*, *C. procera*, *G. suaveolens*, *P. oxyphylla* and *S. tetrandra* behaved differently depending on the site: They show exclusively periodic behavior in Luki, but irregular

behavior in Yangambi. Two species, namely *P. angolensis*, and *T. gilgiana* displayed an exclusively periodic behavior in both sites.

The disposition to form growth rings is due to the fluctuation of environmental variables such as precipitation, temperature, soil moisture, air humidity and sunlight. The more marked and seasonal the variations, the more periodic the growth rings (Brienen et al., 2016; Janssen et al., 2021). In contrast to temperate and boreal regions, environmental variables in the tropics are less distinctly seasonal. As a result, temporal morphological markers are either absent, irregular, or unclear (Brienen et al., 2016), depending on the severity and length of arid periods (Worbes, 2002). Accordingly, in Yangambi where the dry season is less pronounced, trees have a lower likelihood for periodical growth-ring formation than trees in Luki. Similar observations were reported in several previous studies (Coster, 1927; Pearson et al., 2011). Nevertheless, even in Luki where a distinct dry season is present, the formation of growth rings is not always periodic. Indeed, Luki's hilly landscape and proximity to the Atlantic Ocean cause frequent fog and dense cloud cover that keeps relative humidity high throughout the year (Sénéchal et al., 1989; Lubini, 1997). Therefore, despite relatively low annual rainfall during the three to four months of the dry season (less than 60 mm of rainfall per month), plants do not experience extreme water stress during this period (Lubini, 1997; Couralet et al., 2013).

The nine remaining species, namely *C. africanum*, *C. mildbraedii*, *E. suaveolens*, *G. punctata*, *G. thompsonii*, *P. macrocarpus*, *P. macrophylla*, *T. madagascariense*, and *T. prieurieana* had an irregular behavior in both sites: some trees formed growth rings periodically and others irregularly, in the same site. This may depend on the microclimate of each individual due to its location in the forest (stratum, soil quality, altitude, etc.), and its own sensitivity. Mariaux (2016) reported that within a species, ring formation can be dependent on the personal life history of individuals (forest fire, damage to the crown, insect attacks, etc.). The periodicity of ring formation may also differ between life stages. Clear, annual rings may be found in the adult stages, but absent, vague, or non-annual rings in the juvenile stages (Dünisch et al., 2002; Brienen & Zuidema, 2005).

We found that relative mean increment was also a main predictor of growth-ring periodicity. Trees with higher relative mean increment have a higher likelihood of having periodical growth rings. In other words, fast-growing trees have a higher chance of periodical growth rings. Previous studies supported that in medium and fast-growing trees it is usually easy to see the annual growth rings (Ogden & West, 1981; Détienne, 1989; Verheyden et al., 2004). Fast-growing trees are often light-demanding (Marra et al., 2014). As such, their growth is more dependent on high light availability. As in the dry season, day length is reduced and there is a cloud cover that reduces the intensity of sunlight in the study sites (Tarelkin et al., 2019), fast-growing species are more prone to a reduction or outright cessation of growth, that induces the formation of a sharp, periodic ring boundaries. Things are different for slow-growing understory species. It has been shown that in western Central Africa, home to light-poor evergreen forests, significant low-level cloud cover during the dry season from June to September results in a sharp reduction in water demand and an improvement in the quality of light available for tree photosynthesis (Philippon et al., 2019). This improvement in light conditions is of particular benefit to evergreen understory species, which find opportunities to

access light when the canopy opens due to the fall of deciduous tree leaves during the dry season (Denslow, 1987).

We found that DBH had a significant positive effect, although a small estimate, on the growth-ring periodicity. Since DBH is related to the height of a tree, DBH can be used as a proxy for a trees' location within the canopy, and as such for light it can receive. So, the signal is potentially larger for trees higher up in the canopy (López et al., 2012). The life history stratum classification of a tree species was, however, not a predictor for growth ring periodicity. Stratum classification at species-level does not represent the growing conditions of an individual tree.

We expected a clear link with phenology, however, the phenological classification and parameters used were not specifically observed for the individual trees under investigation. And indeed, no link was established. Nevertheless, deciduous species, which are more sensitive to water stress than evergreen species, could be more inclined to form growth-ring boundaries not only during the dry season, but also during all periods characterized by a considerable drop in rainfall (such as the period from January to February in Luki and June-July in Yangambi). Previous studies already reported strong differences in species sensitivity to precipitation, due to water storage in the stems, phenology, rooting depth and reserve utilization (Borchert, 1994; Meinzer et al., 1999). In situ observations of leaf phenology of the studied trees might provide more insight. At the site level, the fact that not all trees of deciduous species form the same number of growth rings even though they grow on the same site confirms the individual specificity in the formation of growth rings due to local growing conditions (canopy/understory, gap/no-gap, neighboring trees etc.), as supported by Mariaux (2016).

3.5. Conclusion

In the present study, we examined ring formation in eighteen tree species growing under two different climatic conditions in the semi-deciduous rainforests of the Luki and Yangambi biosphere reserves in the Congo Basin. The study showed that all eighteen species formed growth rings. The periodicity of ring formation varied significantly within and between species, as well as between sites, while ring boundary distinctness was not significantly related to any parameter at either site. The formation of annual growth rings is more likely at Luki than at Yangambi, where climate seasonality is less marked. Inter-species variability in the formation of periodic growth rings is not related to species-level classifications of leaf phenology. Environmental conditions at site and tree level, as well as microclimate, may dictate intra-and-inter-species variability. These results clearly demonstrate that cambial marking can be successfully applied in the Congo Basin. Since the absence of wood anatomically distinct borders between growth rings, a high-resolution assessment of the secondary growth needs to be done with periodic sampling of the cambial zone through microcores. This approach would allow to date the formation of tissue types and production of wood and add to phenological datasets.

Acknowledgments

This study was carried out as part of the PilotMAB and PilotMABplus projects of the Service of Wood Biology of the Royal Museum for Central Africa (RMCA). These projects were funded by the Belgian Directorate-General for Development Cooperation and Humanitarian Aid (DGD). The Hirox HRX-01 3D Digital Microscope, used for some of the images in this

paper, is part of the Laboratory of Wood Technology of Ghent university (UGent-Woodlab) and funded by the Flemish Research Council (Fonds Wetenschappelijk Onderzoek, FWO) through project G014123N (COBARCHIVES: A long-term view of Congo Basin forest resilience from fossil charcoal and living trees). We also thank the Regional Post-Graduate Training School on Integrated Management of Tropical Forests and Lands (ERAIFT), the Institut National pour l'Etude et la Recherche Agronomiques—Luki (INERA-Luki) and the non-profit association NATURE PLUS.

Conflict of interest statement

The authors declare that the research was conducted in the absence of any conflict of interest.

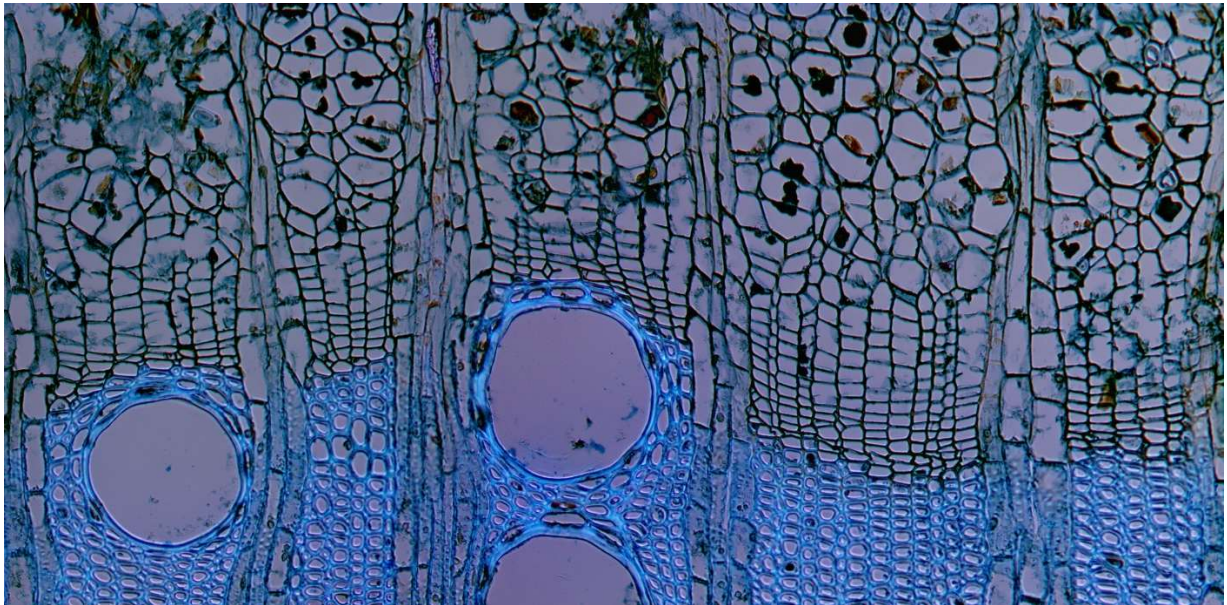
Data availability statement

The data that support the findings of this study are openly available (Belanganayi, 2024) in figshare at <https://doi.org/10.6084/m9.figshare.25167212> and <https://doi.org/10.6084/m9.figshare.25507546>

Supporting information

Additional supporting information can be found online in the Supporting Information section at the end of this article.

Chapter 4: Timing of cambial phenology of rainforest trees as indicator of climate sensitivity of the Congo Basin biome



Trilepissium madagascariense

This chapter is under review in Global Ecology and Conservation under the reference:

Luse Belanganayi B., Mbungu Phaka C., Djiofack B. Y., Laurent F., Liévens K., Luambua N. K., Bolaya T., Bourland N., Hubau W., Beeckman H., & De Mil T. (2024). Timing of Cambial Phenology of Rainforest Trees as Indicator of Climate Sensitivity of the Congo Basin Biome (SSRN Scholarly Paper No. 5076845). Social Science Research Network. <https://doi.org/10.2139/ssrn.5076845>

Abstract

In Congo Basin tropical forests, cambial phenology likely varies widely, with the timing of tree growth still uncertain. With anticipated increases in temperature and changes in precipitation patterns, these forests may face significant threats impacting tree growth and carbon sequestration, highlighting the need for studies on cambial dynamics and their adaptability to climate change.

This study examines cambial phenology in two semi-deciduous rainforests in the Democratic Republic of Congo, each with distinct precipitation patterns. The research focused on the temporal dynamics of cambial cell production and maturation in relation to tree morphological traits, leaf phenology, reproductive traits, and climatic variables. Biweekly microcores were taken from 30 trees across 10 species, and radius dendrometer data from 59 trees in 20 species complemented the study. Microsections were stained and examined to identify cambial activity and dormancy, supported by measured stem diameter variations.

Results revealed complex cambial dynamics without uniform dormancy patterns across or within species. Some species showed irregular cycles of activity and dormancy, while others were continuously active, suggesting high resilience. Trees from the site with a defined dry season (Luki) were more climate-sensitive, potentially heightening their vulnerability to climate change. In contrast, species from the less seasonal site of Yangambi exhibit sensitivity to morphological and reproductive traits, showing resilience to climate variation but a sensitivity to internal growth dynamics.

Keywords: Central Africa forests, secondary growth, carbon storage, cambial dormancy, xylogenesis, lignification, wood anatomy.

4.1. Introduction

Forests are the most effective terrestrial ecosystems in carbon sequestration. By storing approximately 26% of the carbon released by human activities, they play a major role in mitigating global warming (Pan et al., 2011, 2024). Most forest carbon is stored in the woody structures of vascular plants, notably in stems and roots (Malhi et al., 2011). Between the bark and the wood lies a thin layer of meristematic cells called the vascular cambium, or simply cambium. The cambial layer consists of undifferentiated, actively dividing cells, only when active, that are thin-walled and rectangular in shape, when seen on a cross-section. The cells are arranged in radial files, forming vertical columns that facilitate the organized production of new xylem and phloem cells. The cambium is composed of two cell types: fusiform initials, which are long, spindle-shaped cells that form the bulk of the wood and bark, and ray initials, smaller cuboidal cells that generate xylem and phloem rays, allowing lateral transport of nutrients and water (Lachaud et al., 1999; Callado et al., 2013; Fischer et al., 2019). Carbon storage results from several transformations of a portion of the carbon captured through photosynthesis into woody biomass via xylogenesis. Xylogenesis starts in the vascular cambium (Chaffey, 1999). The cells in the cambial zone divide actively to produce new xylem cells toward the inside of the plant and new phloem cells toward the outside. This process is responsible for the radial thickening of stems and roots, and for carbon storage (Lachaud et al., 1999; Callado et al., 2013; D. Wang et al., 2021). Cambial cells differentiate into a variety of xylem cells with a secondary cell wall (Locosselli, 2018) with differing functions. Between 41.9 and 60.7% of the dry mass of these cells consists of pure carbon (Martin & Thomas, 2011;

Thomas & Martin, 2012). The secondary cell walls comprise most terrestrial biomass (Turco et al., 2019) and are consequently the main carbon reservoirs in trees (Locosselli & Buckeridge, 2017). They store carbon for long periods, playing a significant role in the carbon cycle. The three main biopolymers that contribute to carbon storage in wood are cellulose, hemicellulose, and lignin, with cellulose and lignin being the largest contributors (Pettersen & Rowell, 1984).

Xylogenesis proceeds through a succession of five major phases initiated by cambial activity: (1) cell division and differentiation, (2) cell expansion (elongation and radial enlargement), (3) cell wall thickening (involving cellulose, hemicellulose, cell wall proteins, and lignin biosynthesis and deposition), (4) programmed fiber (and/or tracheid) cell death, and (5) heart wood formation (programmed parenchyma death) (Plomion et al., 2001). From the above, carbon storage in the strict sense occurs during phase 3, when the secondary cell wall forms (Verbančič et al., 2018). However, additional depositions may occur as heartwood forms (Lehnebach et al., 2019). Despite the fundamental nature of the xylogenesis process, the onset, duration, and completion of these phases are species-specific and can be influenced by environmental variables (Savidge, 1996).

In temperate climatic regions, the vascular cambium of trees follows a seasonal cycle of activity and dormancy. The dormancy period, which lasts approximately six months and includes the fall and winter months, corresponds to a cessation of meristematic activity (Riding & Little, 1984; Mellerowicz et al., 1992; Lachaud et al., 1999; Guo et al., 2022). In tropical regions, cambial phenology is likely to exhibit various patterns (De Mil et al., 2017; Angoboy Ilondea et al., 2021; Luse Belanganayi, Angoboy Ilondea, et al., 2024), but very little is known about them. The Congo Basin, situated in the Central-African tropical region, hosts the second largest tropical forests-, following the rapidly degrading Amazon Basin forests (Hubau et al., 2020). These forests are a vast carbon sink, holding approximately 9% of the world's forest carbon (FAO & ITTO, 2011).

However, our understanding of the timing of xylogenesis phases in Congo Basin trees remains limited. Meanwhile, climate projections for Central-Africa predict either more frequent and intense droughts (Fauset et al., 2012) or higher temperatures and increased rainfall (WMO, 2023), both of which could affect the various phases of xylogenesis. This underscores the importance of understanding how xylogenesis functions and how the forests can adapt to anticipated climate disruptions.

To assess cambial activity in detail, four approaches are available depending on the timescale: 1) Weekly/biweekly: regular analysis of the cambial zone using thin sections of micro-cores, or simply microsampling (Rossi, Deslauriers, et al., 2006; Noyer et al., 2023). 2) Monthly: decoding information in the cross-sectional planes of wood macro-cores, between two dates, using a wound in the cambial zone of living trees as a reference (De Mil et al., 2017; Luse Belanganayi, Delvaux, et al., 2024). 3) Inter-annual: dendrochronology (Hubau et al., 2019; Luse Belanganayi, Delvaux, et al., 2024) and radiocarbon dating (Pompa-García & Camarero, 2020; Giraldo et al., 2023). 4) both intra- and inter-annual timescales: direct measurement of changes in girth or in stem radius using automatic dendrometers (Drew & Downes, 2009; Luse Belanganayi, Ilondea, et al., 2024). Each approach has its own advantages and limitations.

Microsampling is a highly valuable technique for studying cambial activity and wood formation at the cellular level offering greater precision in understanding the growth dynamics of the tissue (Rossi, Deslauriers, et al., 2006), but it may come with limitations such as tree wounding (Tsen et al., 2016) and a limited representativeness of the sampling area. Additionally, micro-coring is labor-intensive. The process involves regular sample collection, careful preparation of thin sections for microscopic analysis, and the identification of cellular changes. This level of precision requires both time and technical expertise, making it a resource-heavy method (Rossi, Deslauriers, et al., 2006). Therefore, automatic dendrometers can serve as an approximation as well.

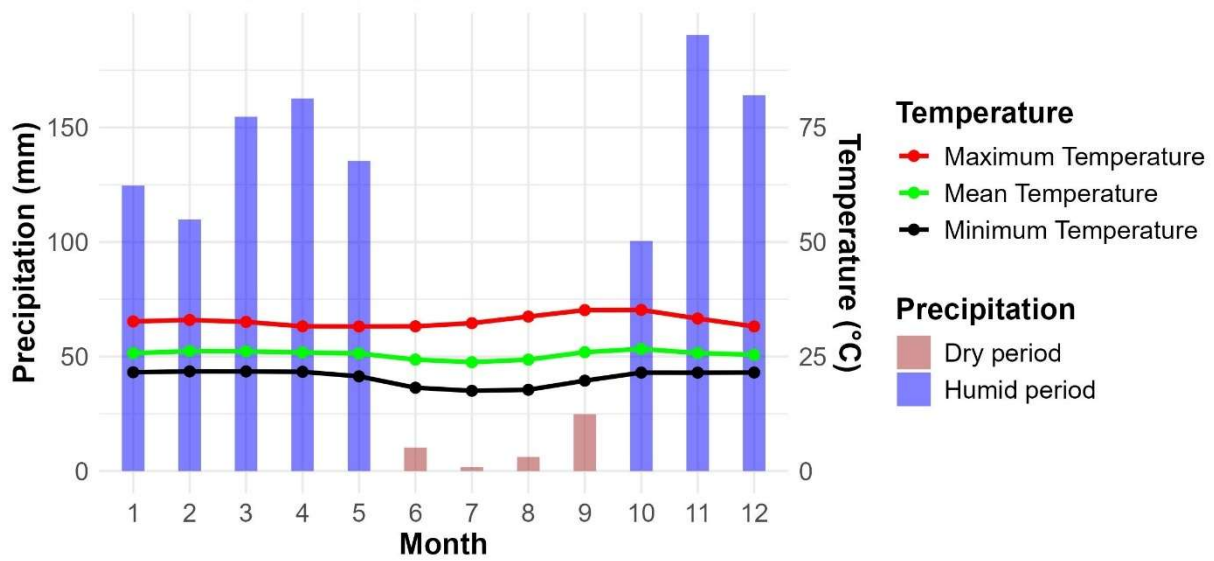
The present study is one of the few that explores cambial activity in tropical trees through regular biweekly microcore sampling over the course of a calendar year (Morel et al., 2015), and is the first of its kind in the Congo Basin. We focused precisely on temporal dynamics of cambial cell production and maturation in relation to tree morphological traits, leaf phenology and reproductive efforts, as well as with the climatic variables and actual stem radius changes by using automated dendrometers. To explore this, micro-core samples were analyzed from the semi-deciduous rainforests of the Luki and Yangambi Biosphere Reserves in the Democratic Republic of Congo, addressing the following research questions: (1) Is there a period of cambial dormancy? If so, how long does it last? (2) When exactly does cambial activity peak during the phenological year? (3) How do climatic factors, along with tree morphological traits, leaf phenology, and reproductive efforts, influence the growth cycle?

4.2. Materials and Methods

4.2.1. Study sites

The study sites are situated in the semi-deciduous rainforests of the Luki (-5.65°S; 13.07°E) and Yangambi (0.78°N; 24.52°E) Biosphere Reserves in the Democratic Republic of Congo. These locations experience distinct climatic conditions: Luki has an Aw climate, while Yangambi is classified as Af according to the Köppen system, as updated by Kottek et al. (2006). Luki experiences a dry season from June to September, with monthly precipitation below 50 mm, while Yangambi has no distinct dry season, though there is a reduction in precipitation to around 60 mm per month between December and February (Luse Belanganayi, Delvaux, et al., 2024). Luki's distinctive climate, shaped by its hilly landscape and proximity to the Atlantic Ocean, sustains relatively high air humidity year-round. This helps protect the trees from severe water stress and extreme temperatures, particularly during the dry season (Couralet et al., 2013; Luse Belanganayi, Angoboy Ilondea, et al., 2024). The climatic diagrams of the study site, from 1981 to 2021, are presented in Figure 1.

(A) Luki (2013-2022) Lat:-5.65° Lon:13.07° Alt:350.00m



(B) Yangambi (2013-2022) Lat:0.78° Lon:24.52° Alt:430.94m

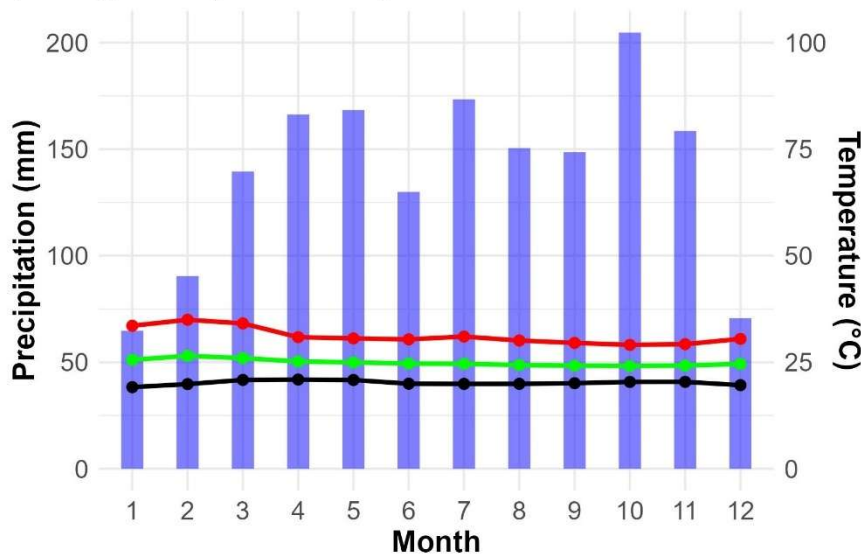


Figure 4-1. Climatic diagrams of the study sites from the Democratic Republic of Congo: (A) for the Luki biosphere reserve, (B) for the Yangambi biosphere reserve. Monthly averages of precipitation (bars) and temperatures (green: average, black: minimum, red: maximum) from 2013–2022. Data were obtained from <https://power.larc.nasa.gov/data-access-viewer/>.

4.2.2. Monitored trees

We selected 10 abundant tree species from 9 different families, including 4 species from Luki and 6 species from Yangambi (Table S4 – 1A), specifically for the purpose of collecting microcores to study cambial activity. For each species, we selected 3 healthy adult individuals that were well-established in the canopy to minimize the potential effects of varying light exposure. The morphological characteristics and geographical locations of each of the 18 trees are provided in Table S4 – 1. Simultaneously, 42 healthy adult trees from 9 species (Table S4 – 1B) at Yangambi, including 3 species that were also micro-cored, were monitored with point dendrometers (Model TOMST, Measurement resolution 0.27μm, temporary resolution 15

minutes). For the Luki site, dendrometer data from a recent study (Luse Belanganayi, Angoboy Ilondea, et al., 2024), were used to discuss the link with the xylogenesis data from this study.

4.2.3. Sample collection

Micro-core sampling was conducted from February 14, 2022, to March 13, 2023, in Luki and from October 1, 2022, to September 23, 2023, in Yangambi. Three microcores were collected from each monitored tree trunk every 14 days, using a Trephor tool (Rossi, Anfodillo, et al., 2006) in a downward spiral pattern around the trunk, starting at 175 cm above ground (J. Vieira et al., 2020). Each 1.5 cm-long microcore included the phloem, the vascular cambium, and a part of recently formed xylem. Microcores were collected at approximately 10 cm apart to avoid getting traumatic tissue (Deslauriers et al., 2003). After sampling, the microcores were placed directly in Eppendorf microtubes with a 50% aqueous ethanol solution (Rossi, Deslauriers, et al., 2006).

For each individual tree, the diameter at breast height (DBH, measured at 130 cm height) and the total height were recorded during the initial collection using a diameter tape and a Nikon Forestry Pro, respectively. At each subsequent micro-core collection, leaf phenological and reproductive traits—including the proportion of leaves lost, flowers present, and fruits borne—were estimated through binocular observation and documented. The descriptions of the wood anatomy for all species are presented in Table S4 – 2 and Fig. S4 – 1, in appendices.

In Yangambi, the dendrometers were installed between May 13 and 14, 2022 and removed on April 13, 2023. The dendrometer data from Luki utilized in this study are those pushed in Luse Belanganayi, Angoboy Ilondea, et al. (2024). They span several seasons.

4.2.4. Sample preparation

In the laboratory, each microcore sample was stripped of excess outer bark and wood and oriented by marking the transverse plane with a pencil under a magnifier at $\times 10$ magnification. The microcores were then placed in histological cassettes, dehydrated, and embedded in paraffin through successive immersions in 50%, 75%, 96%, and 100% ethanol, followed by D-limonene and liquid paraffin at 65°C, using a Thermo Microm STP 120 tissue processor.

Each microcore, with the marked plane positioned horizontally on top, was then embedded in a paraffin matrix cast in a histological cassette using a ‘Leica HistoCore Arcadia’ paraffin dispenser. The microcores fixed in paraffin blocks were then immersed in water at room temperature until they were cut with a rotary microtome. Transverse sections of 12–14 μm thickness were cut with a rotary microtome *HistoCore MULTICUT R*. After some runs, the continuous paraffin strip produced was spread on a water surface at 40°C to stretch the sections and place the films on the microscope slides (Rossi, Deslauriers, et al., 2006). The slides bearing the sections were placed in an oven at 70°C for 10 minutes, then air-dried for 10 minutes to allow the albumin to bind the wood sample. Residual paraffin was removed by immersing the sections in D-limonene and ethanol solutions. Subsequently, the sections were stained using a water-ethanol solution of Alcian Blue (1%) and Safranin O (1%). This staining method allows for clear differentiation between lignified tissues, which are stained pink to red by Safranin, and non-lignified cell walls, which are stained blue by Alcian Blue. Sections were permanently mounted using Euparal (Wolberg et al., 2023).

Histological wood sections were observed under an Olympus BX60 optic microscope with visible and ultraviolet (UV) light at $\times 100$ - 400 magnifications to distinguish each zone of xylem development. Under visible light, the sections displayed colors attributed to the Safranin/Alcian blue staining solution, while under UV light, the lignified regions fluoresced with varying intensities depending on the lignin content (Fig. 4 – 2). In some cases, we combined visible and UV light to enhance image contrast and highlight the degree of lignification more clearly.

4.2.5. Anatomical observation of cambial activity

On a cross-section, the microcores extracted during the growing season are composed of both mature cells, including phloem and xylem cells, and immature cells, including initial cambial cells and those in the elongation and thickening phase (Rossi, Anfodillo, et al., 2006). Mature xylem cells, fully lignified, have a thick secondary wall that appears pink to red under visible light (Fig. 4 – 2A & D) and are fluorescent under UV light (Fig. 4 – 2B & C). Phloem cells have a thinner secondary wall and a larger diameter than xylem fiber cells. Sclerenchyma tissue, composed of sclereids and fibers, can be found scattered throughout the phloem (Fig. S4 – 2, in appendices). Cambial cells are characterized by a small diameter and a thin cell wall that appears blue under visible light and does not exhibit fluorescence under UV light. Enlarging cells have a larger diameter but still only possess a primary cell wall, displaying the same response to light as cambial cells. Cells undergoing wall thickening and lignification begin to show fluorescence under UV light, with an increasingly thick cell wall that shifts from blue to pink/red under visible light (Fig. 4 – 2).

A high number of cells in the enlarging phase adjacent to the cambium indicates a high (Fig. 4 – 2A & B) to moderate (Fig. 4 – 2C) activity. Conversely, the presence of only a few xylem cells undergoing secondary wall formation and lignification suggests that the cambium ceased producing new cells some time ago (Fig. 4 – 2D & Figs. 4 – 3). This is because newly formed xylem cells continue to develop even after cambial cell production has stopped (Gričar et al., 2005; Prislan et al., 2016). A dormant cambium (Figs. 4 – 3) is characterized by the cessation of cell division and a reduction in metabolic activity resulting in no production of new xylem or phloem: no establishing division plates can be observed at this stage (Prislan et al., 2016). The cell walls of dormant cambial cells are often slightly thicker compared to their active state (Figs. 4 – 3). These cells also appear more flattened and compressed compared to their actively dividing counterparts (Chaffey et al., 1998). In preparation for dormancy, the phloem and axial and radial parenchyma may accumulate storage materials, such as starch, which can be utilized when growth resumes under favorable conditions (Guo et al., 2022).

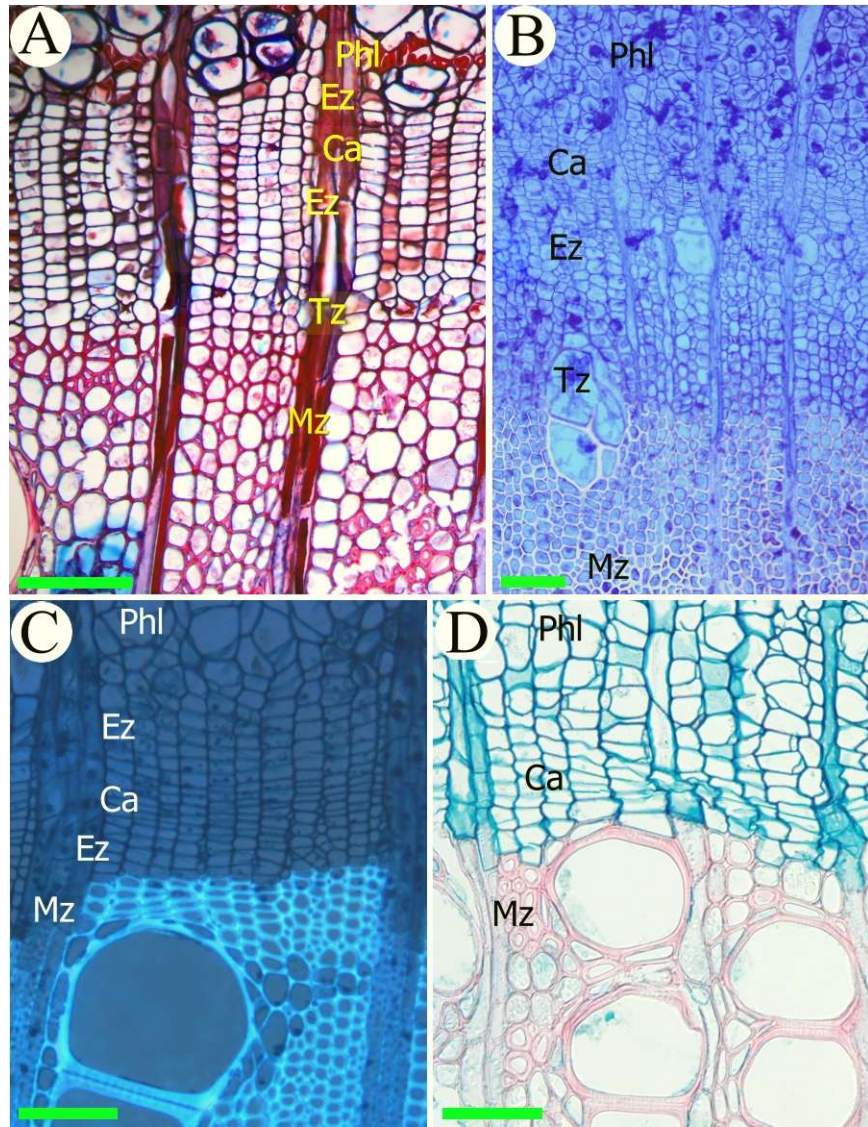


Figure 4-2. Cross sections of stems from four of ten study species showing different intensity of cambial activity. A large number of cells in the enlarging phase near the cambium indicates a highly ((A) and (B)) to moderately (C) productive stage. In contrast, the presence of only a few xylem cells undergoing secondary wall formation and lignification suggests that the cambium stopped producing new cells some time ago (D). (A) *P. balsamifera* in visible light (Luki, May 9, 2022), (B) *F. elastica* in UV light (Luki, July 18, 2022), (C) *T. madagascariense* in UV light (Yangambi, October 15, 2022), (D) *L. thompsonii* in visible light (Yangambi, October 1, 2022). (A) and (B) Periods of strong cambial activity. (C) Period of moderate cambial activity and (D) Period of low cambial activity. (A) and (D). Phl = Phloem, Ca = Cambial zone, Ez = Enlarging zone, Tz = thickening zone, Mz = Mature xylem cells. Scale bars = 100 μ m.

Ideally, the start of micro-coring is recommended at the beginning of the growing season, so that the very last growth-ring boundary is the benchmark for counting cells in all zones of the new growth ring being formed, including lignified zone (Mz), thickening zone (Tz), enlarging zone (Ez) and cambial zone (Cz), (Cuny et al., 2015). However, in our study, ring boundaries were observed only in the *S. zenkeri* species (Fig. 4 – 3G), and in many cases discontinuous or

absent. As a result, it was impossible to determine the total radial number of cells in the rings that may have formed during the study, and to assess the rate of cell lignification over time. We have therefore used the term ‘developing zone’ (DZ) to refer to the entire area comprising the cambial zone, enlarging zone, and thickening zone (Rossi, Deslauriers, et al., 2006). We based our study on anatomical analysis of the developing zone to determine the presence or absence of cambial activity. Key indicators of this activity include the multiplication of meristematic cambium cells, the formation of vascular tissue, the expanding of vessel elements, the presence of enlarging cells, the axial elongation of fibers that interrupt the strict radial pattern of cambial cells and derivatives, and the progression of lignification. A section at the peak of its cambial activity includes all three subzones of the developing zone (Figs. 4 – 2A & B). However, during other phases of activity, we may find (i) only a cambium undergoing strong or weak multiplication, (ii) or a cambial zone and an enlarging zone (Fig. 4 – 2C), or (iii) a cambial zone and a thickening zone. Furthermore, in each collection date, we counted the number of cells in the developing zone along three radial rows of each individual tree sample and averaged them, avoiding enlarging vessels and defects of thin sections. Variations in this number were analyzed to describe cambial dynamics throughout the phenological year.

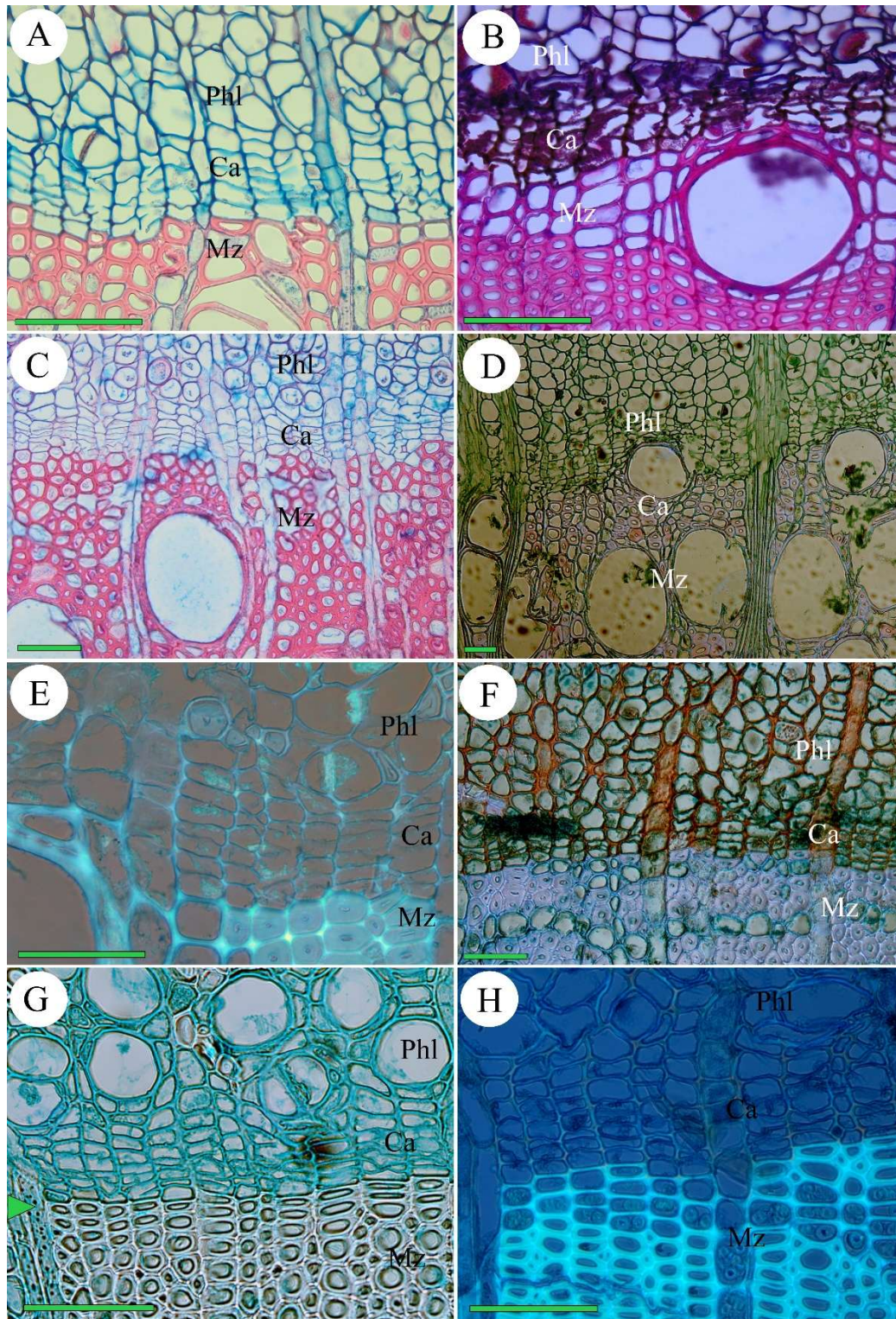


Figure 4-3. Illustration of cambial dormancy in eight of the ten species studied. What persists is a cambial zone composed of a few layers of cells, between the phloem and the xylem. (A) *F. elastica* (Luki, July 4, 2022); (B) *G. giganteum* (Luki, May 23, 2022), (C) *O. gore* (Luki, May 23, 2022); (D) *P. oleosa* (Yangambi, June 6, 2023); (E) *P. macrocarpus* (Yangambi, October 10, 2022); (F) *S. subcordatum* (Yangambi, May 20, 2023); (G) *S. zenkeri* (Yangambi, May 6, 2023), the boundary of the newly formed ring is visible, distinguished by two flattened cell layers with thick secondary walls (Green triangle); (H) *T. madagascariense* (Yangambi, March 11, 2023).

4.2.6. Data processing and analysis

To assess the relationship between environmental variables, tree-morphological traits, and reproductive effort with cambial activity at a biweekly resolution, we fitted a linear mixed-effects model (LMM) with a Gaussian link function using the R package "lme4" (R Core Team, 2023; Bates et al., 2024). Standardized parameters were obtained by fitting the model on a standardized version of the dataset. We computed 95% confidence intervals (CIs) and p-values using a Wald t-distribution approximation. The response variable was the radial number of cells in the developing zone (No. of cells in the developing zone) while the fixed effects included mean biweekly temperature (Temp), mean biweekly air relative humidity (RH), total biweekly precipitation (Precip), mean biweekly vapor pressure deficit (VPD), the proportion of leaves lost (leaves_lost), the proportion of flowers borne (Flowers), the proportion of fruits borne (Fruits), and individual trees (Tree). Species were included as a random effect to account for species-specific effects.

The LMM formulas assessed were:

- 1) No. of cells in the developing zone ~ Temp + RH + Leaves_lost + Flowers + Fruits + DBH + Height + Tree + (1|Species)
- 2) No. of cells in the developing zone ~ Temp * RH + Leaves_lost + Flowers + Fruits + DBH + Height + Tree + (1|Species)
- 3) No. of cells in the developing zone ~ VPD + Precip + Leaves_lost + Flowers + Fruits + DBH + Height + Tree + (1|Species)
- 4) No. of cells in the developing zone ~ Temp + Precip + RH + Leaves_lost + Flowers + Fruits + DBH + Height + Tree + (1|Species)

The best model fit was selected by comparing Akaike Information Criterion (AIC; Burnham & Anderson, 2002) and conditional and marginal coefficients of determination (R^2).

This model, as detailed in the results, demonstrated significant explanatory power, with a high conditional R^2 value. However, the marginal R^2 , representing the contribution of fixed effects alone, was very low. To address this, we explored species-specific models on a species-by-species basis. The LMM was formulated as follows:

No. of cells in the developing zone ~ Temp + RH + Leaves_lost + Flowers + Fruits + DBH + Height + (1|Individual).

The dendrometer data were processed based on Zweifel's zero-growth principle (Zweifel et al., 2016), as applied in Luse Belanganayi, Ilondea, et al., (2024).

4.3. Results

4.3.1. Cambial activity patterns

We observed several distinct patterns of cambial dynamics among the studied species. Cambial activity varied between and within the ten species for both sites.

In Luki (Fig. 4 – 4 & 4 – 5), *F. elastica* exhibits mixed cambial activity, with predominant resting phases from mid-May to early July 2022 and from early January to mid-February 2023. *G. giganteum* displays greater variability, with extended resting periods typically occurring from early June 2022 to early November 2022. *O. gore* demonstrates prolonged resting phases interrupted by brief periods of activity, reflecting pronounced dormancy cycles. This species has the lowest average biweekly radial number of cells in the developing zone among all species

studied (mean = 6.30, SD = 2.77), with a coefficient of variation of 44% (Fig. 4 – 5A). *P. balsamifera* maintained continuous activity with minimal growth reduction and emerged as the most active species across both sites. It has the highest average biweekly radial number of cells in the developing zone (mean = 23.07, SD = 6.48) and the lowest coefficient of variation (CV = 28.07%) (Fig. 4 – 5A).

In Yangambi (Fig. 4 – 4 and 4 – 5), the variability in cambial activity patterns is more pronounced, even within the same species. *L. thompsonii* and *T. madagascariense* exhibit relatively consistent cambial activity throughout the year, with only brief resting phases. *P. oleosa* shows mixed activity characterized by high intraspecific variability. *P. macrocarpus* and *S. zenkeri* tend to have more extended resting periods. *S. subcordatum* is most active from early October to early November 2022 and from late February to mid-March 2023, while remaining from time to time active during other periods.

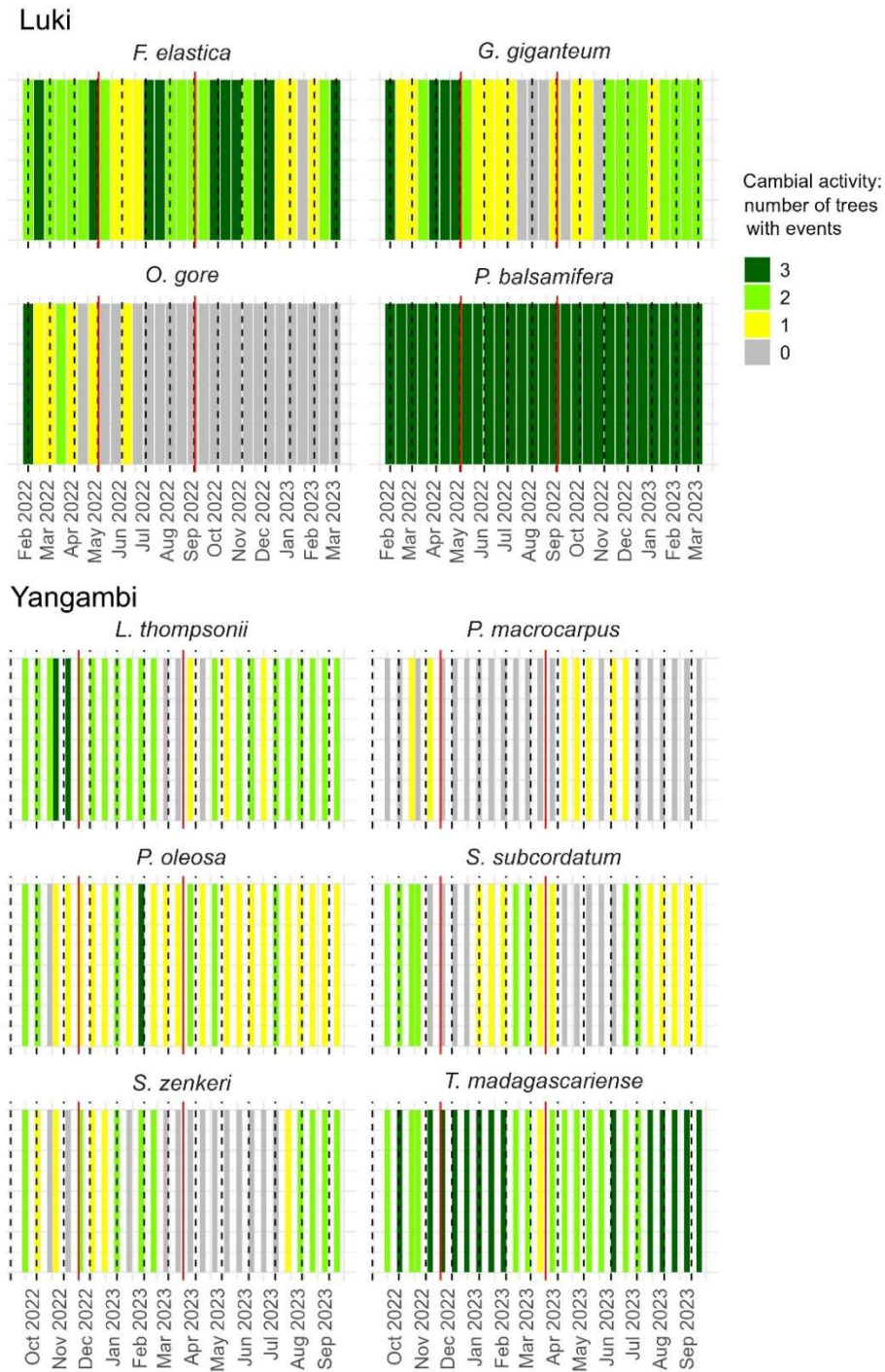


Figure 4-4. Overview of Cambial Activity for Study Species, exhibiting the number of trees with cambial activity event for each species. Vertical dashed lines indicate the beginning and end of each month. Vertical red lines represent the onset and end of the dry season in Luki, as well as the start and end of the period with low monthly rainfall (<150mm) in Yangambi.

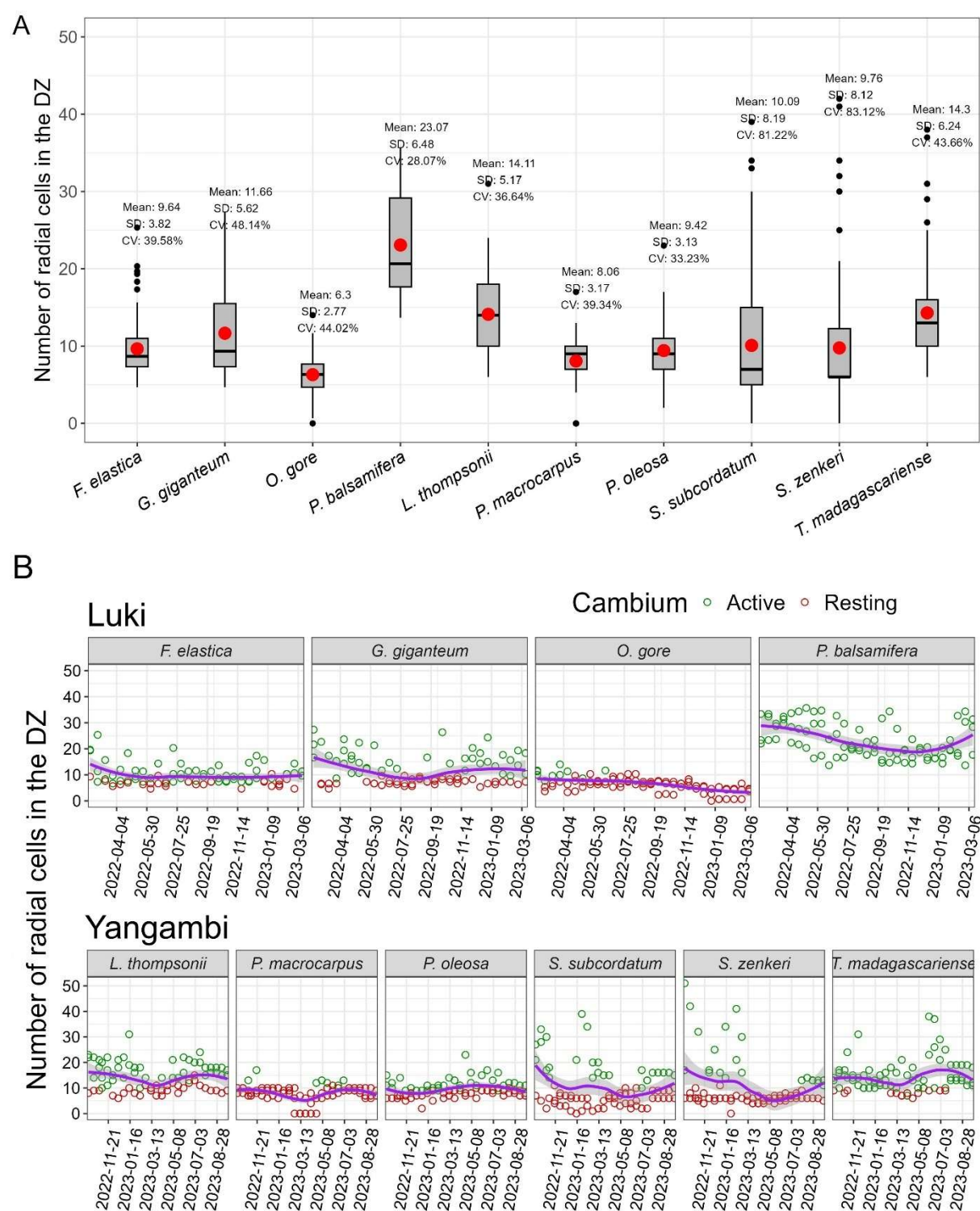


Figure 4-5. Annual variation in the radial number of cells in the developing zone. (A) The box plots display the median (horizontal line within the box), the 25th and 75th percentiles (lower and upper edges of the box), of data grouped by species. The vertical lines extending from the box represent the minimum and maximum values, the red dot indicates the mean value, and the black dots denote outliers. (B) The dots represent raw data, with red dots indicating a dormant cambium and green dots indicating an active cambium. The solid lines represent the fitted LOESS (locally estimated scatterplot smoothing) curve, and the shaded area represents the 95% confidence interval.

The dendrometer data from Yangambi indicate that on an annual basis, there is no clear evidence of an overall seasonal dormancy. However, as revealed through the analysis of cambial zone cross-sections, each individual tree exhibits a period of rest, which can be as short as possible, with the timing varying between individuals, even within the same species (Fig. 4 – 6B & C). For more information, please refer to the supporting information (Figs. S4 – 3, in appendices), where we provide a binary graph for each tree, showing the occurrence of hourly growth throughout the year. On a diel basis, most trees begin increasing their radial increment rate around 4 p.m., with the increment peaking at approximately 6 a.m. After this peak, the increment rate declines sharply, dropping off by 1 p.m., and remains close to zero until 4 p.m (Fig. 4 – 5A).

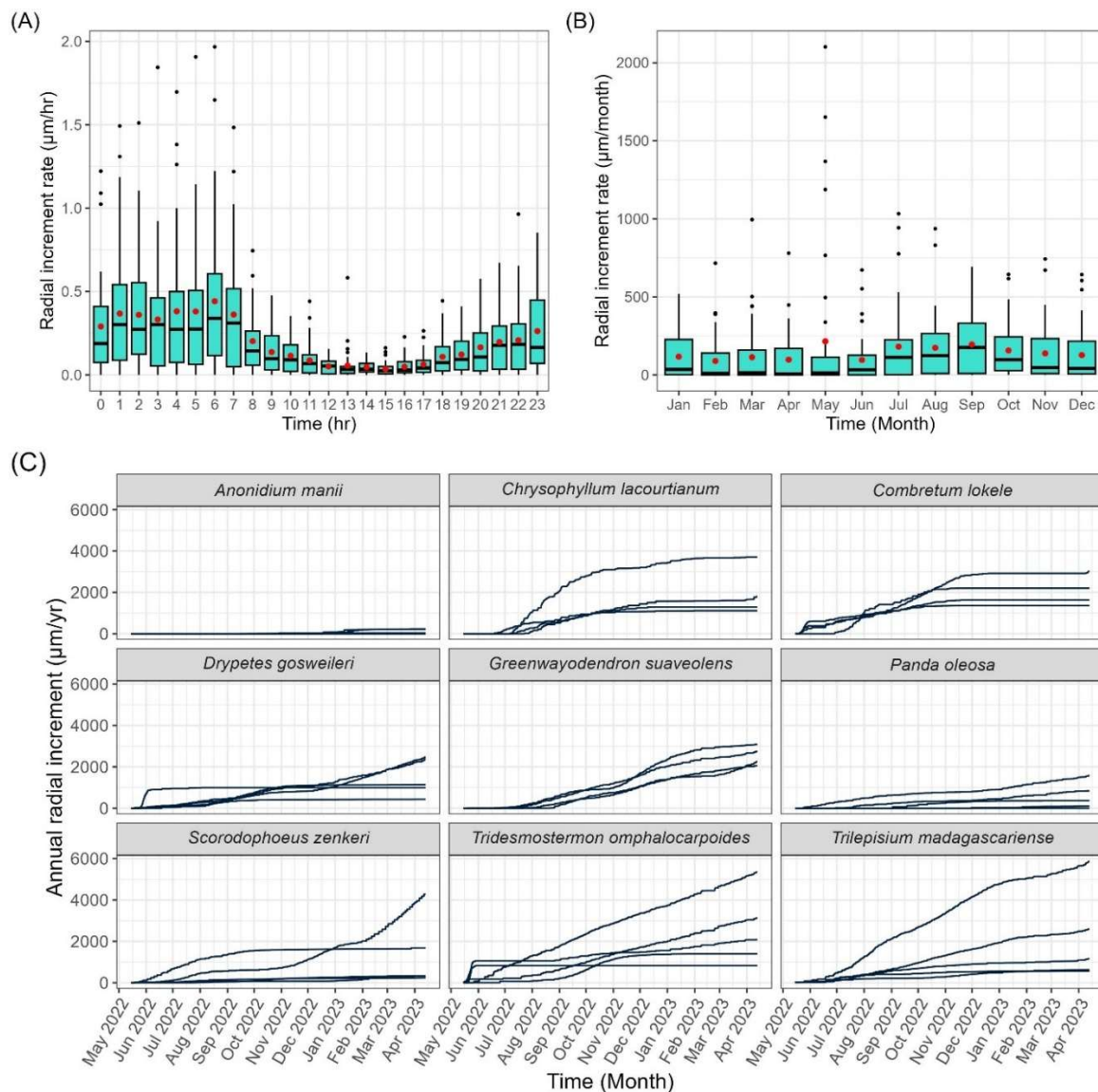


Figure 4-6. Radial Growth dynamics from dendrometer measurements in Yangambi. (A, B) Boxplots show hourly (A) and monthly (B) radial increment rates (μm), with the median (horizontal line), 25th and 75th percentiles (box edges), minimum and maximum values (whiskers), mean (red dot), and outliers (black dots) for all tree individuals. (C) Cumulative annual growth curves represent the daily contributions to total annual radial growth (μm) for each tree.

According to the findings of Luse Belanganayi, Angoboy Ilondea, et al., (2024), trees at Luki exhibit a slightly different diel growth pattern, with radial increment rates beginning to rise around 6 p.m., peaking between 6 and 9 a.m., and then declining sharply until noon, followed by near-zero growth throughout the afternoon. Annually, growth shows pronounced seasonal variation tied to the wet and dry seasons. Growth is generally rapid during the rainy season, which typically extends from mid-September to mid-May. However, a marked decline in growth occurs during the dry season, with many trees either sharply reducing their growth or stopping altogether. Growth commonly resumes in October and fluctuates between October and April, depending on species and annual phenological cycles. The seasonal growth patterns were more pronounced in deciduous species, such as *T. superba* and *H. gabunense*, which displayed longer and clearer dormancy during the dry season. In contrast, evergreen species such as *F. elastica*, *G. giganteum*, and *G. suaveolens* exhibited only a brief slowdown or interruption in growth, rather than complete cessation. Figures S4 – 4 (in appendices) present the binary graph for each tree, depicting the occurrence of hourly growth throughout the phenological year.

4.3.2. Species-specific responses to the predictive variables

The LMM to predict radial number of cells in the developing zone including variables temperature (Temp), relative humidity (RH), the proportion of leaves lost (Leaves lost), the proportion of flowers borne (Flowers), the proportion of fruits borne (Fruits) and individual tree as fixed effects, and tree species as random effects, produced the best fit (Showing the lowest AIC) (table S4 – 3):

No. of cells in the developing zone ~ Temp + RH + Leaves_lost + Flowers + Fruits + DBH + Height + Individual + (1|Species)

The model's overall explanatory power is substantial, with a conditional R^2 of 0.81. The portion attributed to the fixed effects alone (marginal R^2) is 0.16. Within this model, we identified a significant and positive effect of relative humidity (RH) and a significant and negative effect of the proportion of leaves lost.

The model explains 81% of the variance in the response variable, 'number of cells in the developing zone, when both fixed effects and the random effect of species are considered. This high level of explanatory power suggests that the combination of fixed and random effects is effective in modeling the data. However, the fixed effects alone account for only 16% of the variance. The substantial difference between the conditional and marginal R^2 values, combined with the observation that most levels of the 'tree individual' factor show non-significant effects, suggests that the influence of fixed effects on the response variable varies significantly across species. In light of this, we explored species-specific models rather than adopting a one-size-fits-all approach. The LMM assessed on a species-by-species basis was as follows:

No. of cells in the developing zone ~ Temp + RH + Leaves_lost + Flowers + Fruits + DBH + Height + (1|Individual)

The model highlights the diversity in cambial activity responses among the studied species, with some showing strong sensitivities to environmental conditions, morphological traits and reproduction effort, while others maintain more stable growth patterns (Table 4 – 1 and table S4 – 4).

Table 4-1. Significance of predictor variables on the radial number of cells in the developing zone.

Species	Site	Significant negative effect	Significant positive effect
<i>P. balsamifera</i>	Luki	Proportion of flowers borne Proportion of fruits borne DBH	Temperature Tree height
<i>P. macrocarpus</i>	Yangambi	Proportion of flowers borne	DBH Relative humidity Temperature Tree height
<i>G. giganteum</i>	Luki	Proportion of leaves lost DBH	Temperature Tree height
<i>L. thompsonii</i>	Yangambi	DBH	Proportion of fruits borne Tree height
<i>O. gore</i>	Luki	Proportion of fruits borne Relative humidity Temperature	
<i>S. zenkeri</i>	Yangambi	DBH Tree height	Proportion of fruits borne
<i>P. oleosa</i>	Yangambi		Proportion of leaves lost
<i>S. subcordatum</i>	Yangambi		Tree height

The species can be categorized based on the significance of the effects of the predictor variables and the types of these variables (environmental variables, morphological traits, and reproductive effort) in four categories: 1) **Species with mixed response:** *G. giganteum*, *P. balsamifera*, and *P. macrocarpus*. These species show significant responses across all three categories of predictor variables: environmental variables, morphological traits, and reproductive effort. 2) **Species with selective response:** *L. thompsonii*, *O. gore*, and *S. zenkeri*. These species show significant responses to two out of the three categories of predictor variables. 3) **Species with specialized response:** *P. oleosa* and *S. subcordatum*. These species respond significantly to only one category of predictor variables. 4) **Resilient species:** *Funtumia elastica* and *T. madagascariense*. These species show non-significant effects across all factors, suggesting a stable cambial phenology dynamic that is less responsive to the environmental variables and tree traits considered in this study.

4.3.3. Site effects

Based on observations of the species according to their site (Luki and Yangambi), different patterns emerge. Luki species (*F. elastica*, *G. giganteum*, *O. gore* and *P. balsamifera*) appear to be more sensitive to climatic variables than Yangambi species (*L. thompsonii*, *P. macrocarpus*, *P. oleosa*, *S. subcordatum*, *S. zenkeri*, and *Trilepisium madagascariense*), which appear to be less sensitive to climatic variables but more sensitive to reproductive efforts and morphological traits (Table 4 – 1). The species from Luki show a variety of response types, with some being highly sensitive across all predictor categories (*G. giganteum*, *P. balsamifera*) and others being more selective (*O. gore*) or resilient (*F. elastica*). The species from Yangambi tend to show more specialized or selective responses, compared to the Luki species. This could indicate a more stable or uniform environment where species have evolved to respond strongly

to a limited set of conditions or traits, with species *P. macrocarpus* being more adaptable across a range of conditions, while others are more selective (*L. thompsonii* and *S. zenkeri*), specialized (*P. oleosa* and *S. subcordatum*) or resilient (*T. madagascariense*) to specific factors.

4.4. Discussion

4.4.1. Cambial activity patterns

Our results show that there was no synchronicity in cambial dynamics among the species studied, with a higher asynchrony in Yangambi as compared to Luki (Fig. 4 – 4 and Table 4 – 1). Dormancy timing and duration varies widely not only across both Luki and Yangambi sites, but also between species and among individual trees within species. Some individuals, independently of the site, remain active year-round (e.g. *P. balsamifera*) or almost (certain individuals of *F. elastica*, *L. thompsonii*, and *T. madagascariense*), while others experience dormancy during specific periods, which differ from tree to tree. Although asynchronous cambial activity has also been observed in *Parkia velutina* in French Guiana (Morel et al., 2015), a periodic annual cambial activity, strongly influenced by rainfall seasonality, is more commonly reported for tropical forest species of south America (Callado et al., 2013).

4.4.2. Scope of environmental variables, morphological traits and reproductive efforts on cambial activity

The present study reveals complex and varied cases of cambial dynamics, with no uniform pattern of dormancy with seasonal changes. The scope of influence for environmental variables, morphological traits, and reproductive efforts varies across species, reflecting their unique adaptations and ecological strategies (Fig. 4 – 4 & Fig. 4 – 5).

We found that environmental variables such as temperature and RH play a crucial role in determining the overall habitat suitability and stress levels that species experience. Temperature has been shown to have significant effects on cambial activity in several species. The *G. giganteum*, *P. balsamifera*, and *P. macrocarpus* species showed positive responses to temperature, indicating that warmer conditions favor their growth. However, some species like *O. gore* and *S. zenkeri* showed negative responses, suggesting that higher temperatures might be stressful or detrimental to them. The rest of the species showed no significant response to the temperature. This suggest that, like for photosynthesis, whose temperature dependence varies according to growing environment and species (Medlyn et al., 2002), cambial activity has an optimal temperature range for high activity, depending on species.

RH significantly affects the cambial activity of only two species: *P. macrocarpus* from Yangambi and *O. gore* from Luki. High RH levels were beneficial for *P. macrocarpus* (Table 1). In contrast, for *O. gore*, higher relative humidity levels were associated with reduced cambial activity. Both study Luki and Yangambi experience stable RH levels that are generally favorable to tree growth (Couralet et al., 2013). Luki's stability is due to its proximity to the ocean and hilly terrain (Lubini, 1997; Sénéchal et al., 1989), while Yangambi's is a result of the absence of a clearly defined dry season (Luse Belanganayi, Delvaux, et al., 2024). The sensitivity of these two species to RH, although not a limiting factor in the two study sites, suggests that these two species are more demanding with regard to humidity than the others. Precipitation and VPD had non-significant effects across the species (Table 4 – 1). This suggests

that while these variables are important, they may not be the primary drivers of species cambial activity in the analyzed environments. Instead, other factors might buffer or modulate their impact, making them non-limiting.

Morphological traits (DBH and tree height) are often indicative of a species' competitive ability, resource allocation strategies, and overall fitness in their respective environments. A tree's height is a key factor in determining its access to light (Philippon et al., 2019). We found that tree height is a critical factor influencing cambial activity in several species, including *G. giganteum*, *L. thompsonii*, *P. macrocarpus*, *P. balsamifera*, *S. zenkeri*, and *S. subcordatum*, most of which are native to Yangambi. Except for *S. zenkeri*, cambial activity of all the above species showed a significant positive correlation with tree height, meaning that taller trees had more cell production, likely due to advantages in light acquisition and reduced competition (Fransson et al., 2021). Tree height's positive correlation with cambial activity underscores its importance in species survival and competitive strategy. In a recent study, Fernández-de-Uña et al. (2023) showed that taller trees have a more efficient water use, enhanced water transport, and increased water uptake and storage capacity. These adaptations help mitigate the decline in water potential associated with greater height, enabling taller trees to endure periods of water stress. Exception in *S. zenkeri* where shorter trees exhibit better cambial activity, likely results from a combination of resource allocation strategies, environmental conditions, and physiological trade-offs.

The factor DBH resulted in mixed responses on cambial activity across species. Many species, including *G. giganteum*, *L. thompsonii*, *P. balsamifera*, and *S. zenkeri* displayed significant negative responses to DBH, suggesting that while increasing DBH might indicate maturity, it may also come at the cost of growth processes (Speer, 2010). In contrast, *P. macrocarpus* exhibited a positive response to DBH. This may again result from a combination of resource allocation strategies, environmental conditions, and physiological trade-offs. For larger trees, greater access to resources like light and nutrients can be sufficient to enhance cambial activity (Stephenson et al., 2014).

We found that production of flowers and fruits was a key factor for cambial activity of several species (Table 2). *P. balsamifera* species exhibited negative responses to both flower and fruit production, while *O. gore* and *P. macrocarpus* species exhibited negative responses to fruit and flower production respectively. This suggests a trade-off where energy is diverted from reproduction to survival or growth. In general, reproductive efforts encompass the allocation of resources to reproductive activities, such as the production of flowers and fruits. These efforts are crucial for species survival and propagation, influencing both individual fitness and population dynamics (Lovett Doust, 1989). We found, in contrast, that *L. thompsonii* and *S. zenkeri* responded positively to fruit production. This may suggest that these species had adequate access to resources and face minimal competition.

We observed a negative response to leaf shedding in *G. giganteum* and a positive response in *P. oleosa*. Leaf shedding can serve as a resource-saving strategy under unfavorable environmental conditions, such as low temperature or drought (Pineda-García et al., 2013).

Depending on the degree of physiological strain it places on the tree, leaf shedding can result in reduced or even stunted growth (Lohbeck et al., 2015).

F. elastica and *T. madagascariense*, exhibited non-significant responses across all categories, indicating a high degree of resilience or indifference to changes in the environmental conditions, morphological traits, and reproductive effort.

4.4.3. Site-specific observations

The species from Luki show a range of responses, from highly sensitive (*G. giganteum* and *P. balsamifera*) to more selective (*O. gore*) and resilient (*F. elastica*) (Luse Belanganayi, Angoboy Ilondea, et al., 2024). This diversity suggests that the Luki site may be influenced by variable environmental conditions, potentially encouraging species to adapt across multiple conditions or specialize in specific strategies to thrive. The coexistence of both highly adaptive and more resilient species could indicate that Luki trees incorporate a broader range of environmental signals in their lignified tissues compared to Yangambi trees. However, this interpretation remains hypothetical and warrants further investigation to confirm these patterns. The lack of low activity in some trees along the entire growing year (e.g. Ongokea gore), probably suggests the presence of missing rings, frequently observed in Luki (Hubau et al., 2019; Luse Belanganayi, Delvaux, et al., 2024).

The species from Yangambi generally exhibit more specialized or selective responses, with some species focusing on specific morphological traits (*S. subcordatum*) or reproductive efforts (*P. oleosa*). The mixed-response species, *P. macrocarpus*, still show sensitivity across multiple categories, however, the overall trend at Yangambi suggests that each species responds to its own specific ecological variables. The trend toward specialization in Yangambi suggests that this site may provide a more stable environment, allowing species to fine-tune their responses to specific conditions. This specialization might indicate less competitive pressure or less seasonality, enabling species to optimize certain aspects of their growth or reproduction.

4.4.4. Comparing dendrometers measurements and cambial zone analysis

Dendrometers measure tree secondary growth with high temporal resolution, capturing data every few minutes over extended periods. However, they may not always reflect precise cellular growth due to the influence of stem swelling and shrinkage from water uptake, potentially leading to confusion between actual growth and swelling (Mencuccini et al., 2017) and between shrinkage and cambium rest. For instance, at Luki, the decline in growth during the dry season may reflect reduced water availability rather than a true cessation of cambial activity. Studies of cambial activity, although limited by the lower temporal resolution of biweekly sampling, provide detailed insights into the precise physiological phases of growth and dormancy. However, some information is inevitably lost between sampling dates. This is where dendrometers play a crucial role, as they help bridge these gaps as best as possible. In our case, the cambial monitoring offers detailed insights, such as prolonged dormancy in *P. oleosa* and *S. zenkeri*, and extended dormancy in *S. subcordatum* and *O. gore*, which dendrometers may miss. Cambial zone analysis also reveals ring formation and provides more accurate data on growth cessation. For example, *S. zenkeri* shows specific ring boundaries, and *P. balsamifera*, though active year-round, shows consistent cambial cell production. Together, these methods complement each other, with dendrometers offering a broad overview and cambial zone

analysis providing finer physiological detail, giving a fuller understanding of tree secondary growth in different environments.

4.5. Conclusion

This study offers an overview of tree secondary growth in two distinct forest environments of the Congo Basin, showing species-specific and individual specific cambial activity. Our results reveal that cambial dynamics are complex and varied, with no consistent pattern of dormancy across or within species. Some trees exhibit irregular cambial activity, alternating between periods of cell division and rest, while others maintain continuous activity year-round. As a result, there is no uniform period when cambial activity reaches its peak. This unique behavior suggests significant resilience among these trees. Trees in Luki and Yangambi exhibit varied responses to climate fluctuations, driven by species-specific adaptations. In both regions, temperature plays a crucial role in cambial activity, with some species benefiting from warmer conditions, while others experience stress. Humidity, although stable in both areas, significantly affects only a few species. Overall, tree growth is optimized within certain environmental thresholds, with morphological traits like height positively influencing cambial activity. However, reproductive efforts and traits like diameter showed mixed effects, indicating complex trade-offs between growth, resource allocation, and survival strategies. Luki species are more sensitive to climatic factors, while Yangambi species focus on morphological traits and reproductive efforts, demonstrating resilience to climatic variations but sensitivity to internal growth dynamics. Further research is needed to explore the connections between cambial activity and the tree's environment to clarify their interrelationships.

Author contributions

BLB, HB, WH, NB, and TDM designed the study. BLB, FM, TB, and NL collected the data in the field. BLB, FL, and KL processed samples in Laboratory, BLB analyzed the data and wrote the manuscript. TDM, NB, WH, and HB reviewed the manuscript.

Funding

This research was carried out thanks to a grant awarded by the Royal Museum for Central Africa within the framework of the PilotMAB project, which is funded by the Belgian Directorate General for Development Cooperation and Humanitarian Aid (DGD).

Acknowledgements

We are grateful to the management of the Royal Museum for Central Africa, The Regional Post-Graduate Training School on Integrated Management of Tropical Forests and Lands (ERAIFT), and the Institut National pour l'Etude et la Recherche Agronomiques Luki (INERA-Luki). Our heartfelt thanks go to Mr. Maximilien Iyokwa for his invaluable contributions as a forest guide, particularly in micro-core sampling, species identification, and the monitoring of foliar and reproductive phenology.

Chapter 5: Towards a better understanding of secondary growth in the Congo Basin



Yangambi reserve

5.1. Key Findings and possible limitations of the results

This study has provided an integrated examination of secondary growth in tropical tree species of the Congo Basin, encompassing the diel and annual rhythms of stem size changes (Chapter 2), growth periodicity in semi-deciduous tropical forests (Chapter 3), and cambial phenology of woody species (Chapter 4). By synthesizing these distinct but interconnected aspects, we gain a clearer understanding of how environmental variables, tree physiology, and growth patterns interact to shape the dynamics of tree secondary growth in tropical rainforests.

In Chapter 2, the diel stem size changes demonstrated strong correlations with environmental variables, particularly vapor pressure deficit (VPD) and relative humidity (RH). The results indicated that most trees maximized their increment rate during the nighttime when VPD was low and RH was high, with peak growth occurring between 6 pm and 9 am. Annual growth patterns, on the other hand, were characterized by rapid growth during the rainy season, with most trees ceasing growth in the dry season. This diel and annual rhythm highlights the significant influence of climatic conditions on tree growth, suggesting a high sensitivity of secondary growth to water availability and atmospheric demand. The differences in growth rhythms between deciduous and evergreen species underscore a key ecological differentiation: deciduous species exhibited more pronounced growth cessation during the dry season, while evergreen species maintained continuous but reduced growth. These findings align with the hypothesis that evergreen species are better adapted to persist in dry conditions by modulating their water use efficiency and photosynthetic activity (Worbes, 1999). However, these findings are drawn from a relatively small sample size and should be viewed cautiously. Additional research with more extensive datasets would be beneficial to validate these patterns and enhance the robustness of the analysis.

Chapter 3 expanded upon these findings by examining the periodicity of growth ring formation in both deciduous and evergreen species, using the cambial marking technique. This chapter highlighted the variability of growth-ring periodicity across different individuals and sites, with trees in Luki, site with clearly defined dry season, displaying more regular growth-ring formation compared to those in Yangambi, the site without clearly defined dry season. These differences suggest that local environmental conditions, such as rainfall patterns and soil moisture availability, significantly influence the regularity of cambial activity and ring formation. While some species displayed distinct growth rings, others exhibited indistinct boundaries, reflecting variability in tree species' responses to seasonal environmental cues. The presence of clear growth rings in some individuals, such as *Carapa procera* and *Prioria oxyphylla*, points to periodic cambial activity, likely driven by seasonal fluctuations in temperature and precipitation. This periodicity was less pronounced in other species, indicating a more continuous or erratic growth pattern that may be influenced by microenvironmental factors or individual tree physiology. Nonetheless, these results are derived from observations conducted over a relatively brief timeframe (two phenological years). Extended studies over longer periods are necessary to provide deeper insights.

In Chapter 4, the focus shifted to cambial phenology, revealing distinct patterns of cambial activity among the studied species. The temporal variations in cambial dynamics were closely linked to environmental variables, particularly temperature and humidity, as well as tree-

specific traits, such as height, diameter, and reproductive effort. For instance, species like *Funtumia elastica* and *Prioria balsamifera* displayed continuous cambial activity throughout the year, while others, such as *Ganophyllum giganteum*, exhibited extended periods of dormancy. Importantly, the study found that species from different sites (Luki vs. Yangambi) responded differently to environmental factors. Luki species were more sensitive to climatic variables, particularly humidity (chapter 2, (Luse Belanganayi, Angoboy Ilondea, et al., 2024)) and temperature, while Yangambi species appeared more influenced by reproductive effort and morphological traits (Chapiter. 2 and Chapter 4). This highlights the need to account for both regional climatic conditions and species-specific responses when studying secondary growth in tropical forests. We remain convinced that additional research is needed to gain a more comprehensive understanding of the interactions between Congo Basin trees and their environment.

5.2. Strengths, limitations, and issues in applied methodologies

The three methodological approaches used in this thesis—stem size measurements, growth ring analysis, and cambial phenology monitoring—are highly complementary for most species. Each approach provides a unique perspective on secondary growth, allowing for a more comprehensive understanding of tree growth dynamics in the Congo Basin. Among the three approaches, cambial phenology monitoring stands out for its precision. It consistently provides the most accurate and detailed insights, especially in distinguishing between actual growth and water-related swelling.

Unlike the other two methods, cambial marking, as applied in our study with a single marking, mainly allows for the observation of growth ring formation and its periodicity. When applied on a weekly or biweekly basis, it can provide more detailed information. However, this method is often destructive, as it frequently necessitates felling the tree at the end of the study to analyze the discs containing the markings (De Mil et al., 2017).

The use of dendrometers and cambial zone analysis allows for the monitoring of secondary growth at fine scales over extended periods. Both methods come with distinct advantages and limitations. When used in tandem, they offer a comprehensive view of secondary growth.

The comparison between the results obtained from point dendrometers and cambial activity studies provides valuable insights into the dynamics of tree growth at both Luki and Yangambi. Each method brings its own advantages, while also highlighting the complexity of tree growth patterns across different species and sites.

Dendrometers offer the advantage of measuring tree secondary growth with extremely high temporal resolution, capturing data every few minutes and covering extended periods of up to several phenological years. However, this method, which primarily tracks stem swelling and shrinkage, can be influenced by water uptake, particularly during stress periods, potentially leading to confusion between actual growth and temporary swelling, or between dormancy and water stress (Mencuccini et al., 2017). For example, in Luki, the sharp decline in growth during the dry season may not reflect a true cessation of cambial activity but rather reduced stem swelling due to limited water availability.

Cambial activity studies, on the other hand, provide a more detailed understanding of annual growth, though with a lower temporal resolution due to the need to preserve tree health and the complexity of sample processing (Rossi, Deslauriers, et al., 2006). Cambial analysis reveals the exact physiological phases when cellular growth halts, which explains why dendrometers often show more continuous growth periods, while cambial zone analysis indicates more intermittent patterns at the cellular level. However, since the microcores used for the cambial zone analysis were collected biweekly, events occurring between these collection intervals may be missed. Hence this gap can be partially filled by the continuous data provided by the dendrometers (Francon et al., 2024), offering a more complete picture of growth dynamics. Microcores also have the disadvantage of being sampled from different locations, which can lead to circumferential variations and a limited representativeness of the sampling area.

Species monitored with dendrometers at both Luki and Yangambi display distinct, species-specific growth patterns. The cambial zone study adds precision to these observations, especially in revealing dormancy periods that dendrometers may fail to capture accurately. For instance, species such as *P. oleosa* and *S. zenkeri* experience prolonged dormancy not always detected by dendrometers. Similarly, in *S. subcordatum* and *O. gore*, dendrometer data may suggest low growth, whereas cambial analysis reveals extended dormancy. This suggests that dendrometers capture external stem fluctuations, such as swelling from water movement, which may obscure periods of true growth cessation. Cambial zone analysis, therefore, provides a more precise understanding of these critical phases.

The cambial analysis also reveals ring formation patterns that dendrometers cannot detect, providing insight into wood structure and growth history. For instance, *S. zenkeri* displayed ring boundaries at specific times during the year, reflecting periods of cellular growth and rest. *P. balsamifera*, being the most active species in both studies, corroborates the dendrometer findings of continuous growth, but cambial studies provide more granular details about the timing and consistency of cambial cell production.

Together, these two methods complement each other well. Dendrometers provide a broad, continuous overview of tree growth dynamics, while cambial activity studies offer a finer resolution of the cellular processes driving that growth. By combining these two approaches, a more complete understanding of tree growth behavior in response to environmental conditions can be achieved, as demonstrated by the contrasting results from both Luki and Yangambi.

5.3. Responses to the key research questions

The various findings from this study allow us to propose answers to the key research questions outlined in this thesis.

5.3.1. Is there a dormant period in the tree growth cycle?

Yes, a dormant period exists, but its occurrence and duration vary significantly between the two study sites due to their contrasting climates, and within species.

In Luki, where there is a pronounced dry season (May to September), many trees exhibit a well-defined dormancy during this period, particularly deciduous species like *Terminalia superba*. In contrast, in Yangambi, where there is no distinct dry season, most species show continuous

growth or only brief interruptions (Luse Belanganayi, Angoboy Ilondea, et al., 2024). This aligns with the Af climate's more consistent rainfall and higher humidity throughout the year.

Furthermore, the deciduous species in Luki exhibit more pronounced dormancy, whereas evergreen species in both locations maintain low-level growth year-round, although with reduced rates during the drier months in Luki (Luse Belanganayi, Angoboy Ilondea, et al., 2024).

5.3.2. What is the timing and length of both dormancy and growing season?

The timing and duration of dormancy, as well as the growing season, are influenced not only by climatic differences between Luki and Yangambi but also, very likely, by intrinsic factors specific to each tree and/or species. This is further supported by the inter- and intraspecific variability highlighted in Chapters 2, 3, and 4 of this work, though these factors remain to be fully elucidated.

In Luki (Aw climate), southern hemisphere, the growing season typically starts in October with the return of the rains and extends until April or May, depending on the species. For species that experience seasonal dormancy, this period coincides with the dry season from May to September, during which growth sharply reduces or ceases entirely, particularly in deciduous trees (Angoboy Ilondea et al., 2021; Luse Belanganayi, Angoboy Ilondea, et al., 2024).

In Yangambi (Af climate): Given the lack of a distinct dry season, growth tends to be more continuous, with minor fluctuations in response to brief dry periods (December to February). Species in Yangambi generally exhibit less pronounced dormancy or slower growth rates during these months, but complete cessation is uncommon.

As revealed in Chapter 2 and confirmed in Chapter 4, dormancy lacks synchronicity between species. This pattern is also evident at the intraspecific level for certain species. Numerous variations are observed, including trees with dormancy overlapping much of the dry season, trees that remain nearly inactive year-round, trees with alternating periods of rest and activity throughout the year, and trees that are nearly active all year. These variations sometimes occur regardless of the site or climate type. Similar kinds of asynchronicity has been previously observed in some studies conducted in tropical forests across South America (Callado et al., 2013; Morel et al., 2015), Asia (Pumijumnong & Buajan, 2013; Rahman et al., 2019), and the Congo Basin (De Mil et al., 2019; Angoboy Ilondea et al., 2021).

These observations underscore the complexity and variability of cambial phenology in tropical forests, particularly in the Congo Basin, highlighting the significant influence of environmental factors and intrinsic species-specific traits, and indicating that further research is needed.

5.3.3. How is the growth cycle influenced by climatic variables?

Climatic factors such as rainfall, VPD, and temperature have different effects in Luki and Yangambi.

In Luki, the distinct dry season leads to greater stress on trees during the dry months, as evidenced by higher VPD and lower RH. These conditions reduce cambial activity and induce

dormancy, especially in deciduous species. Rainfall during the wet season triggers a resumption of growth, particularly in October, as trees respond to improved moisture conditions.

In Yangambi, more consistent rainfall and humidity throughout the year mean that trees experience fewer environmental stressors that would induce dormancy. This results in more continuous cambial activity, with only slight reductions in growth during the drier months from December to February.

Chapter 4 demonstrated that trees in Luki appeared more responsive to climatic variations, showing stronger correlations between cambial activity and humidity levels. In contrast, trees in Yangambi were less affected by seasonal fluctuations in rainfall and VPD, likely due to differences in the range of environmental conditions studied at the two sites. This confirms the role of rainfall in driving growth dynamics in tropical environments, as highlighted in previous studies (Worbes, 1999; S. Vieira et al., 2004; Brien et al., 2005; Gliniars et al., 2013), while also highlighting that it is not the sole factor influencing these dynamics.

5.3.4. What anatomical marks does the growth cycle leave on the wood?

The secondary growth cycles of trees in Luki and Yangambi differ significantly due to their contrasting climates. In Luki, the relatively stronger seasonality induces a well-defined dormancy period in many species, leaving more periodically clear anatomical marks such as growth rings. In contrast, Yangambi's more stable climate results in less periodic growth-ring formation. The findings from Chapter 3, which provided the most reliable data on cambial phenology, reinforce these differences, with trees in Luki being more sensitive to environmental changes compared to those in Yangambi (Luse Belanganayi, Delvaux, et al., 2024).

However, it is important to emphasize that dormancy does not always manifest as a distinct ring boundary. Nevertheless, it appears to be a crucial resting phase in the tree's developmental cycle. At our study site, although trees may enter dormancy, this does not always result in the formation of a visible growth ring boundary. Visible ring boundaries typically occur when environmental conditions become unfavorable for growth, as is seasonally common in temperate and boreal regions (Rathgeber et al., 2016; Tumajer & Lehejček, 2019). However, in tropical environments like ours, where environmental stress is not strongly marked, trees can experience dormancy without producing distinct ring boundaries. Conversely, they can produce multiple growth rings within a single year when subjected to unexpected stress (Worbes, 1999; Luse Belanganayi, Delvaux, et al., 2024).

5.4. Broader relevance of this research and findings

5.4.1. Complementarity with other research methodologies

Understanding secondary growth dynamics in tropical forests is crucial for refining our knowledge of carbon sequestration, forest productivity, and climate change resilience. The three core chapters of this thesis (Chapters 2, 3 and 4) offer a detailed, mechanistic perspective on tree growth dynamics, which is highly complementary to various large-scale forest monitoring and modeling approaches. Below, is discussed how the findings of this thesis integrate with and enhance other research fields, including carbon sink estimations by traditional long-term forest measurements, flux tower data, and remote sensing technologies.

Permanent inventory plots provide valuable long-term data on tree growth and biomass accumulation, typically measured through diameter at breast height (DBH) increments at annual or multi-year intervals. However, these measurements do not capture the intra-annual variability in stem growth, nor do they distinguish stem swelling due to water storage from true radial growth (Brown, 2002; Gibbs et al., 2007). This thesis, particularly, helps disentangle these effects by linking cambial activity and wood formation to observed stem fluctuations. By incorporating high-frequency dendrometer data and cambial activity timing into carbon sink models, my research enhances the accuracy of biomass increment calculations and aids in interpreting discrepancies in long-term DBH measurements.

Eddy covariance flux towers measure net ecosystem exchange (NEE) by tracking CO₂ fluxes between forests and the atmosphere, providing insights into gross primary productivity (GPP) and respiration (Reco). However, flux tower data primarily estimate carbon uptake at the ecosystem level and do not directly quantify carbon allocation into different tree compartments (leaves, stems, roots, etc.) (Aubinet et al., 2012). The finding of this thesis on cambial phenology and intra-annual growth periodicity adds a crucial missing link by revealing when and how trees allocate carbon to secondary growth. Seasonal shifts in cambial activity can help explain mismatches between carbon uptake (photosynthesis) and stem growth, improving carbon allocation models.

Remote sensing technologies, particularly Airborne LiDAR Scanning (ALS) (Xiang et al., 2024) and Terrestrial LiDAR Scanning (TLS) (Calders et al., 2015; Liang et al., 2016) provide high-resolution, 3D forest structure data, revolutionizing forest biomass estimation and growth monitoring. While ALS is excellent for assessing canopy structure and large-scale forest dynamics (Maltamo et al., 2014), it lacks the temporal resolution to track seasonal and diel stem growth variations. TLS, which offers detailed tree-level structural data (Calders et al., 2015), could greatly benefit from the integration of cambial activity insights to distinguish true growth increments from temporary changes in stem size (e.g., water-related swelling). This thesis provides a physiological basis to interpret LiDAR-derived growth estimates, ensuring that observed changes in tree structure reflect actual wood formation rather than transient fluctuations.

5.4.2. Complementarity with others research findings

Tree growth in tropical forests is driven by a complex interplay of environmental factors, morphological traits, reproductive efforts, and resource allocation strategies. This thesis investigates these dynamics by analyzing the timing of cambial activity and the influence of climatic conditions, particularly temperature, rainfall, vapor pressure deficit (VPD), and relative humidity (RH). By comparing the key findings of this research with previous studies, I aim to position them within the broader framework of tropical forest ecology and identify the primary drivers of growth variability in the Congo Basin.

5.4.2.1. Dormancy and Growth Rhythms

This thesis identifies distinct periods of dormancy in studied trees, which, while not synchronous across all trees, are closely linked to seasonal variations in water availability. This observation is consistent with findings from Worbes, (1999) and Locosselli et al., (2020), who reported that growth cessation in tropical trees often coincides with dry periods and that species

growing in areas with a pronounced dry season exhibit more distinct growth rings. This periodicity suggests that water availability is a primary driver of growth cycles in tropical forests. However, while rainfall is a key determinant, dormancy in some species appears to be influenced by other environmental cues, including temperature and atmospheric conditions. This thesis highlights that trees in relatively aseasonal regions can still experience growth slowdowns, potentially linked to high evaporative demand (VPD) and shifts in carbon allocation strategies.

While seasonal growth patterns exist, they do not show a distinct peak across species at the seasonal level. Instead, stem size variations are primarily driven by daily water balance dynamics, particularly reversible stem contractions and expansions, rather than a clear seasonal growth peak.

Our results indicate that peak growth timing is not fully synchronized across species, especially in less-seasonal forests. In a site like Yangambi, where climatic conditions are more stable, the weaker seasonality may promote greater diversification in growth phenologies, with species occupying different phenological niches. This desynchronization in growth peaks could enhance species coexistence by reducing direct competition for resources and distributing growth activity over time.

If this holds true, species in Yangambi would exhibit a broader range of growth timing than those in Luki, where seasonality is stronger, and growth synchronization is higher. This suggests that in Yangambi, species may be more temporally segregated in their cambial activity, potentially supporting greater species diversity by minimizing competition during peak growth phases.

5.4.2.2. Temperature and rainfall

Temperature influences tree growth through its effects on metabolism, respiration, and carbon assimilation (Feeley et al., 2020). This thesis found a statistically significant negative interaction between temperature and rainfall, suggesting that high temperatures can mitigate the positive effects of precipitation on growth. This aligns with Schippers et al. (2015), who demonstrated that while moderate warming may enhance growth in some tropical species, excessive heat can increase respiration rates, reducing the net carbon gain. In this thesis, it was found that temperature sensitivity varies across species, highlighting the diversity of responses to climate fluctuations in the studied regions. This aligns with the study by Choury et al., (2022), which investigated Australian rainforest seedlings from tropical, subtropical, and warm-temperate climates. The study found that tropical and subtropical species had higher optimal temperatures for photosynthesis compared to temperate species. Furthermore, tropical and subtropical species exhibited a greater rate of acclimation to warmer growing conditions, highlighting variability in temperature sensitivity among species.

However, findings from different studies highlight variations in how temperature metrics—maximum, minimum, and average temperatures—affect forest productivity, biomass accumulation, and growth.

Hubau et al. (2020) reported a significant negative effect of mean annual temperature on carbon gains in tropical forests, suggesting that long-term warming could lead to reduced forest

productivity. This finding aligns with the general expectation that higher temperatures may accelerate respiration rates, increase evapotranspiration, and lead to water stress, ultimately limiting carbon sequestration. In contrast, Sullivan et al. (2020) provided a more detailed analysis of tropical forests' long-term thermal sensitivity, using repeated diameter measurements. Their study found that maximum temperature is the most critical predictor of above-ground biomass loss, primarily through its negative impact on woody productivity. Notably, the negative effect of maximum temperature was strongest in the hottest forests (above 32.2 °C), implying that temperature-induced growth limitations become more pronounced beyond a critical thermal threshold. Interestingly, minimum temperature had no significant effect on biomass or growth, which contrasts with findings from research conducted in a seasonal tropical forest in Thailand, where both maximum and minimum temperatures were negatively correlated with growth in certain tree species (Vlam et al., 2014).

These discrepancies suggest that temperature sensitivity is not uniform across all tropical forests and may be influenced by species composition, climatic conditions, physiological thresholds specific to different ecosystems, analytical approaches, and temporal scales of observation.

Rainfall, by contrast, emerges as a key driver of growth variability. The findings of this thesis indicate that sufficient rainfall promotes growth, while prolonged dry periods can trigger dormancy. This is consistent with Locosselli et al. (2020), who emphasized that changes in rainfall patterns, particularly decreases in precipitation, can lead to reduced growth rates and increased mortality in tropical tree species. The positive relationship between precipitation and tree growth observed in this study also aligns with the findings of Doughty (2011) and Hubau et al. (2020), who demonstrated that fluctuations in precipitation patterns significantly influence forest carbon dynamics. However, this thesis further highlights that the effect of rainfall on growth is not uniform across species, underscoring the importance of species-specific physiological responses.

5.4.2.3. Vapor Pressure Deficit (VPD) and Relative Humidity (RH)

VPD, which quantifies the difference between the amount of moisture in the air and its saturation point, plays a critical role in tree water balance (Lawrence, 2005). Elevated VPD increases transpiration, leading to stomatal closure and reduced carbon assimilation (Grossiord et al., 2020). The findings of this thesis suggest that periods of high VPD correspond to reduced growth rates, as trees prioritize water conservation over biomass production.

This aligns with research demonstrating that increased atmospheric dryness (high VPD) negatively impacts tropical forest productivity (Yuan et al., 2019) and reduces tree growth across multiple biomes (Zweifel et al., 2021; Mirabel et al., 2023). These studies indicate that tropical trees, despite their adaptation to humid conditions, may still experience growth constraints under prolonged atmospheric moisture stress.

RH generally acts in the opposite direction by reducing evaporative demand and alleviating water stress (Couralet et al., 2013). This thesis aligns with previous studies suggesting a synergistic relationship between RH and tree growth, where high RH conditions enhance carbon assimilation and cambial activity. However, research on RH and tree growth in tropical forests presents a more nuanced picture, offering evidence that both supports and complicates the idea that higher RH consistently mitigates water stress and promotes growth.

However, Perez & Feeley. (2018) discussed how future increases in RH might reduce the efficacy of transpiration, potentially pushing leaf temperatures beyond the thermal limits of photosynthesis in tropical plant species. This suggests that while higher RH can alleviate water stress, it may also impair the plant's ability to regulate leaf temperature, leading to negative effects on carbon assimilation.

5.4.2.4. Morphological traits

The effect of diameter at breast height (DBH) on secondary growth in tropical trees reveals a complex interplay of species-specific physiological responses, resource allocation strategies, and environmental conditions. The findings from this thesis indicate mixed responses to DBH among species, with most species exhibiting negative correlations, while one show positive correlations with growth. These results align with existing literature, which highlights that DBH influences growth dynamics in diverse ways across tropical forests.

The observed negative relationship between DBH and cambial activity in several species suggests that, when comparing trees within a species, radial growth slows, in general, as diameter increases. This well-documented trend in tropical trees occurs due to physiological constraints, including hydraulic limitations and shifts in resource allocation, which contribute to the decline in growth rates with increasing age and size within a species (Speer, 2010).

However, total annual wood production increases with size – Larger trees accumulate more absolute biomass per year due to their extensive vascular systems and greater photosynthetic capacity (Stephenson et al., 2014). Slik et al. (2013) demonstrated that large trees disproportionately contribute to aboveground biomass in tropical forests, playing a dominant role in carbon storage. Similarly, Rozendaal & Zuidema (2011) emphasized that growth rates in tropical trees are size-dependent, with larger trees generally accumulating more biomass through cambial activity.

While large trees are crucial for carbon storage, their growth responses vary widely, necessitating interpretations that consider species identity, ecological roles, and physiological constraints. This may explain why *Petersianthus macrocarpus*, in this study, exhibited a positive correlation between DBH and cambial activity, suggesting that some large trees sustain or even enhance radial growth. This finding aligns with Stephenson et al. (2014), who reported that certain species continue to accumulate biomass at substantial rates due to enhanced resource availability. Similarly, (Metcalf et al., 2009) highlight the complex interactions between tree size, light availability, age, and mortality in tropical forests. Their study shows that radial growth rates are closely tied to a tree's size and light environment, shaping its survival and life history trajectory.

This study also found that the relationship between tree height and secondary growth is complex. While most species showed sustained growth in taller individuals, some exhibited the opposite trend. This last trend may be due to hydraulic limitations, as highlighted by Araújo et al. (2024), who reported that taller trees in the Amazon experience greater hydraulic stress, which can restrict secondary growth, particularly during drought conditions.

5.4.2.5. Reproductive efforts

The results of this thesis support the idea that growth-reproduction trade-offs are a key but variable factor in tree carbon dynamics. The findings confirm that reproductive events, such as flowering and fruiting, generally have a negative impact on secondary growth, with significant

reductions in radial increment during peak reproductive periods. This aligns with Couralet et al. (2013), who found that increased reproductive investment in Central African rainforest species diverts resources away from growth. Similarly, Charlesworth & Morgan (1991) reported that fruiting represents a major resource investment for trees and may reduce allocation to growth.

Interestingly, the degree of growth suppression varies across species, indicating species-specific trade-offs. This is consistent with Blumstein et al. (2022), who showed that trees adopt different carbohydrate allocation strategies, with some prioritizing reproduction over growth, while others maintain a balance between the two.

5.4.2.6. Leaf phenology

This study clearly demonstrates the influence of leaf phenology on secondary growth. While some species exhibited reduced cambial activity during leaf loss, others showed the opposite trend, and a third group remained unaffected. The general pattern observed aligns with the notion that leaf shedding limits growth, particularly in deciduous and semi-deciduous species, as reported in numerous studies across tropical regions. For example, Singh & Kushwaha (2016) found that in tropical dry forests, synchronized leaf drop during drought periods conserves water but reduces carbon assimilation, thereby limiting growth. Similarly, Janssen et al. (2021) demonstrated that during drought conditions in the Amazon forest, increased leaf fall led to a decline in stem growth. The reduction in leaf area diminished the trees' capacity for carbon assimilation, thereby limiting growth.

While the prevailing hypothesis suggests that leaf loss reduces stem growth, some studies indicate that leaf shedding can enhance photosynthesis in the remaining canopy, ultimately improving overall growth efficiency. For example, Tanaka et al. (2018) found that the timing of leaf fall is driven by nitrogen utilization, optimizing canopy photosynthesis across a wide range of woody species.

These findings this thesis suggest that the growth response to leaf drop is influenced by multiple factors, including drought effects, tree characteristics (whether a species is fully deciduous, semi-deciduous, or semievergreen), and environmental conditions such as soil moisture (Singh & Kushwaha, 2016; Wu et al., 2017). This is supported by Reich (2014), who emphasize that tree growth is determined by a species' position on the fast-slow plant economics spectrum, which integrates leaf, stem, and root traits. Growth rates depend on how efficiently a species acquires, utilizes, and conserves resources, shaping its ecological strategy and distribution in tropical forests.

5.5. Prospects for future research

The current studies have provided valuable insights into the factors influencing secondary growth in the Congo Basin, while also highlighting several unanswered questions and potential directions for future research. The observed variability in secondary growth across species and individuals underscores the importance of employing a multi-methodological approach to study tree growth. Ideally, a comprehensive analysis would involve applying multiple methods, such as dendrometer measurements, wood anatomy, and phenological observations, to the same tree. However, the logistical challenges and time constraints inherent in research, especially in the context of a thesis, make this approach difficult to implement. Future studies could address this limitation by incorporating advanced imaging techniques, such as X-ray microdensitometry and

isotope analysis on wood samples, which offer enhanced resolution and could provide a more detailed understanding of growth dynamics.

Another critical avenue for future research is the long-term monitoring of growth rhythms and cambial activity in response to changing climatic conditions. Continuous data collection over extended periods would not only shed light on how tropical trees adjust their growth patterns but also enable predictions of how tropical forests might respond to future climate change scenarios. Understanding these patterns is essential, as tropical forests play a vital role in global carbon cycling and biodiversity.

The diverse responses of species to environmental variables, as revealed in this study, point to the need for further investigation into species-specific adaptive strategies, particularly in relation to drought tolerance and water-use efficiency. Identifying species that are more resilient to climatic stressors is crucial for informing conservation strategies and forest management practices in the Congo Basin. A focus on species that exhibit higher resistance to water stress could help guide reforestation efforts and the development of sustainable forest management plans in light of the increasing frequency of extreme climate events.

Moreover, while the present research was conducted at two distant sites—Luki and Yangambi—the geographic scope of future studies should be expanded. Including additional regions of the Congo Basin, as well as comparative studies with other tropical forests, would provide a broader perspective on secondary growth across diverse tropical ecosystems. Such expansion would help refine our understanding of how different environmental conditions shape tree growth and contribute to the resilience of tropical forests as a whole.

Conclusion

This thesis provides a comprehensive and integrated exploration of secondary growth in tropical tree species within the Congo Basin, addressing diel and annual stem size variations, growth periodicity, and cambial phenology across contrasting climatic conditions. By synthesizing these approaches, the research offers valuable insights into how environmental variables, tree physiology, and growth patterns interact to influence secondary growth dynamics in this critical tropical ecosystem.

Key findings underscore the significant role of environmental factors, particularly water availability and atmospheric conditions, in shaping growth rhythms.

In Luki, the pronounced seasonality appeared to highlight growth-dormancy cycles, particularly among deciduous species, while evergreen species exhibited more continuous but reduced growth. However, these observations are based on a limited sample size and should be interpreted with caution. Further studies with larger datasets would help confirm these patterns and strengthen the analysis.

In Yangambi, where rainfall and humidity are more consistent, tree growth exhibited fewer interruptions, although certain species showed sensitivity to brief dry periods. The comparative analysis revealed clear distinctions in cambial activity, with Luki species more responsive to climatic variations, whereas Yangambi species exhibited resilience driven by reproductive and morphological traits.

The study's methodological integration—combining dendrometer data, growth ring analysis, and cambial phenology monitoring—allowed for a multi-faceted understanding of tree growth. Dendrometer measurements captured continuous external stem fluctuations, while cambial studies provided precise insights into cellular growth and dormancy. This complementary approach demonstrated the utility of employing diverse techniques to uncover the complex interplay of environmental and physiological factors influencing secondary growth.

Anatomical marks, such as growth rings, varied significantly across species and sites, reflecting differences in climatic conditions. In Luki, clear growth rings were associated with alternating growth and dormancy phases driven by seasonal rainfall. In Yangambi, growth rings were less periodic due to the more stable climatic conditions, although subtle marks were observed in response to short-term rainfall variations.

The findings also addressed fundamental questions about tree growth cycles, emphasizing the variability of dormant periods and their relationship with environmental stressors. Trees in Luki showed well-defined dormancy during the dry season, while in Yangambi, continuous growth dominated, with minimal interruptions. The study illuminated the intricate interactions between climatic factors and growth cycles, providing a foundation for predicting how tropical forests might respond to future climate changes.

Looking ahead, the study highlights several avenues for future research. Long-term monitoring of cambial activity and growth rhythms is critical for understanding tree responses to changing climatic conditions. Employing advanced imaging and isotope analysis techniques could

enhance the resolution of growth dynamics studies, enabling more detailed insights. Expanding the geographic scope to include additional regions of the Congo Basin and other tropical forests would provide a broader perspective on growth variability and resilience across diverse ecosystems.

Ultimately, this research underscores the importance of species-specific adaptive strategies, particularly in the context of increasing climate variability. Identifying species with higher resilience to water stress will be essential for conservation and sustainable forest management efforts in the Congo Basin. By advancing our understanding of tropical tree growth, this thesis contributes to the broader goal of preserving the vital ecological functions and carbon storage capacity of tropical forests in a changing world.

References

- Abedi, T., Castilleux, R., Nibbering, P., & Niittylä, T. (2020). The spatio-temporal distribution of cell wall-associated glycoproteins during wood formation in *Populus*. *Frontiers in Plant Science*, 11. <https://doi.org/10.3389/fpls.2020.611607>
- Albert, L. P., Restrepo-Coupe, N., Smith, M. N., Wu, J., Chavana-Bryant, C., Prohaska, N., Taylor, T. C., Martins, G. A., Ciais, P., Mao, J., Arain, M. A., Li, W., Shi, X., Ricciuto, D. M., Huxman, T. E., McMahon, S. M., & Saleska, S. R. (2019). Cryptic phenology in plants: Case studies, implications, and recommendations. *Glob. Chang. Biol.*, 25(11), 3591–3608. <https://doi.org/10.1111/gcb.14759>
- Anderegg, W. R. L., Ballantyne, A. P., Smith, W. K., Majkut, J., Rabin, S., Beaulieu, C., Birdsey, R., Dunne, J. P., Houghton, R. A., Myneni, R. B., Pan, Y., Sarmiento, J. L., Serota, N., Shevliakova, E., Tans, P., & Pacala, S. W. (2015). Tropical nighttime warming as a dominant driver of variability in the terrestrial carbon sink. *Proceedings of the National Academy of Sciences*, 112(51), 15591–15596. <https://doi.org/10.1073/pnas.1521479112>
- Anderson, C. T. (2016). We be jammin': An update on pectin biosynthesis, trafficking and dynamics. *Journal of Experimental Botany*, 67(2), 495–502. <https://doi.org/10.1093/jxb/erv501>
- Anderson-Teixeira, K. J., Herrmann, V., Rollinson, C. R., Gonzalez, B., Gonzalez-Akre, E. B., Pederson, N., Alexander, M. R., Allen, C. D., Alfaro-Sánchez, R., Awada, T., Baltzer, J. L., Baker, P. J., Birch, J. D., Bunyavejchewin, S., Cherubini, P., Davies, S. J., Dow, C., Helcoski, R., Kašpar, J., ... Zuidema, P. A. (2022). Joint effects of climate, tree size, and year on annual tree growth derived from tree-ring records of ten globally distributed forests. *Glob. Chang. Biol.*, 28(1), 245–266. <https://doi.org/10.1111/gcb.15934>
- Angoboy Ilondea, B., Beeckman, H., Van Acker, J., Van den Bulcke, J., Fayolle, A., Couralet, C., Hubau, W., Kafuti, C., Rousseau, M., Kaka di-Makwala, A., Bourland, N., Deklerck, V., Kasongo Yakusu, E., Ewango, C., & De Mil, T. (2021). Variation in Onset of Leaf Unfolding and Wood Formation in a Central African Tropical Tree Species. *Frontiers in Forests and Global Change*, 4, 152. <https://doi.org/10.3389/ffgc.2021.673575>
- Araújo, I., Marimon, B. S., Junior, B. H. M., Oliveira, C. H. L., Silva, J. W. S., Beú, R. G., da Silva, I. V., Simioni, P. F., Tavares, J. V., Phillips, O. L., Gloor, M. U., & Galbraith, D. R. (2024). Taller trees exhibit greater hydraulic vulnerability in southern Amazonian forests. *Environmental and Experimental Botany*, 226, 105905. <https://doi.org/10.1016/j.envexpbot.2024.105905>
- Aubinet, M., Vesala, T., & Papale, D. (Eds.). (2012). *Eddy Covariance: A Practical Guide to Measurement and Data Analysis*. Springer Netherlands. <https://doi.org/10.1007/978-94-007-2351-1>
- Aubréville, A. (1957). Accord à Yangambi sur la nomenclature des types africains de végétation. *Bois et Forêts des Tropiques*. <https://agritrop.cirad.fr/443212/>
- Babst, F., Alexander, M. R., Szejner, P., Bouriaud, O., Klesse, S., Roden, J., Ciais, P., Poulter, B., Frank, D., Moore, D. J. P., & Trouet, V. (2014). A tree-ring perspective on the terrestrial carbon cycle. *Oecologia*, 176(2), 307–322. <https://doi.org/10.1007/s00442-014-3031-6>
- Bailey, I. W. (1920). The cambium and its derivative tissues II. Size variations of cambial initials in gymnosperms and angiosperms. *American Journal of Botany*, 7(9), 355–367. <https://doi.org/10.1002/j.1537-2197.1920.tb05590.x>
- Baldocchi, D., Falge, E., Gu, L., Olson, R., Hollinger, D., Running, S., Anthoni, P., Bernhofer, C., Davis, K., Evans, R., Fuentes, J., Goldstein, A., Katul, G., Law, B., Lee, X., Malhi, Y., Meyers, T., Munger, W., Oechel, W., ... Wofsy, S. (2001). *FLUXNET: A New Tool to Study the Temporal and Spatial Variability of Ecosystem-Scale Carbon Dioxide, Water Vapor, and Energy Flux Densities*. https://journals.ametsoc.org/view/journals/bams/82/11/1520-0477_2001_082_2415_fantts_2_3_co_2.xml
- Balzano, A., Čufar, K., & Micco, V. D. (2021). Cell-wall fluorescence highlights the phases of xylogenesis. *IAWA J.*, 43(1–2), 80–91. <https://doi.org/10.1163/22941932-bja10080>
- Bannan, M. W. (1950). The frequency of anticlinal divisions in fusiform cambial cells of *Chamaecyparis*. *American Journal of Botany*, 37(7), 511–519. <https://doi.org/10.2307/2438026>
- Barlow, P. W., Brain, P., & Powers, S. J. (2002). Estimation of directional division frequencies in vascular cambium and in marginal meristematic cells of plants. *Cell Proliferation*, 35(1), 49–68. <https://doi.org/10.1046/j.1365-2184.2002.00225.x>

- Bates, D., Maechler, M., Bolker, B., Walker, S., Singmann, H., Dai, B., Scheipl, F., Grothendieck, G., Green, P., Fox, J., Bauer, A., Krivitsky, P. N., Tanaka, E., & Jagan, M. (2024). *lme4: Linear Mixed-Effects Models using "Eigen" and S4* (Version 1.1-35.3) [Computer software]. <https://cran.r-project.org/web/packages/lme4/index.html>
- Bauman, D., Fortunel, C., Cernusak, L. A., Bentley, L. P., McMahon, S. M., Rifai, S. W., Aguirre-Gutiérrez, J., Oliveras, I., Bradford, M., Laurance, S. G. W., Delhaye, G., Hutchinson, M. F., Dempsey, R., McNellis, B. E., Santos-Andrade, P. E., Ninantay-Rivera, H. R., Chambi Paucar, J. R., Phillips, O. L., & Malhi, Y. (2022). Tropical tree growth sensitivity to climate is driven by species intrinsic growth rate and leaf traits. *Glob. Chang. Biol.*, 28(4), 1414–1432. <https://doi.org/10.1111/gcb.15982>
- Bauters, M., Moonen, P., Summerauer, L., Doetterl, S., Wasner, D., Griepentrog, M., Mumbanza, F. M., Kearsley, E., Ewango, C., Boyemba, F., Six, J., Muys, B., Verbist, B., Boeckx, P., & Verheyen, K. (2021). Soil nutrient depletion and tree functional composition shift following repeated clearing in secondary forests of the Congo Basin. *Ecosystems*, 24(6), 1422–1435. <https://doi.org/10.1007/s10021-020-00593-6>
- Beeckman, H. (2016). Wood Anatomy and Trait-based Ecology. *IAWA J.*, 37(2), 127–151. <https://doi.org/10.1163/22941932-20160127>
- Beckmann, M., Gallois, S., & Rondinini, C. (2024). Uncertain future for Congo Basin biodiversity: A systematic review of climate change impacts. *Biological Conservation*, 297, 110730. <https://doi.org/10.1016/j.biocon.2024.110730>
- Beirne, C., Houslay, T. M., Morkel, P., Clark, C. J., Fay, M., Okouyi, J., White, L. J. T., & Poulsen, J. R. (2021). African forest elephant movements depend on time scale and individual behavior. *Scientific Reports*, 11(1), 12634. <https://doi.org/10.1038/s41598-021-91627-z>
- Bele, M. Y., Sonwa, D. J., & Tiani, A.-M. (2015). Adapting the Congo Basin forests management to climate change: Linkages among biodiversity, forest loss, and human well-being. *Forest Policy and Economics*, 50, 1–10. <https://doi.org/10.1016/j.forpol.2014.05.010>
- Bieniu, S. A., Lubalega, T. K., Khasa, D. P., kaviriri, D. K., Yang, L., Yuhua, L., Eyul'Anki, D. M., Tango, E. K., & Katula, H. B. (2023). Floristic diversity and structural parameters on the forest tree population in the Luki biosphere reserve, Democratic Republic of Congo. *Global Ecology and Conservation*, 44, e02489. <https://doi.org/10.1016/j.gecco.2023.e02489>
- Blumstein, M., Sala, A., Weston, D. J., Holbrook, N. M., & Hopkins, R. (2022). Plant carbohydrate storage: Intra- and inter-specific trade-offs reveal a major life history trait. *New Phytologist*, 235(6), 2211–2222. <https://doi.org/10.1111/nph.18213>
- Bonan, G. B. (2008). Forests and Climate Change: Forcings, Feedbacks, and the Climate Benefits of Forests. *Science*, 320(5882), 1444–1449. <https://doi.org/10.1126/science.1155121>
- Borchert, R. (1999). Climatic Periodicity, Phenology, and Cambium Activity in Tropical Dry Forest Trees. *IAWA J.*, 20(3), 239–247. <https://doi.org/10.1163/22941932-90000687>
- Bourland, N., Kouadio Yao, L., Lejeune, P., Sonké, B., Philippart, J., Dainou, K., Fétéké, F., & Doucet, J. (2012). Ecology of *pericopsis elata* (Fabaceae), an endangered timber species in southeastern Cameroon. *Biotropica*, 44(6), 840–847. <https://doi.org/10.1111/j.1744-7429.2012.00874.x>
- Bowman, D. M. J. S., Brien, R. J. W., Gloor, E., Phillips, O. L., & Prior, L. D. (2013). Detecting Trends in Tree Growth: Not so Simple. *Trends Plant Sci.*, 18(1), 11–17. <https://doi.org/10.1016/j.tplants.2012.08.005>
- Brien, R. J. W., Phillips, O. L., Feldpausch, T. R., Gloor, E., Baker, T. R., Lloyd, J., Lopez-Gonzalez, G., Monteagudo-Mendoza, A., Malhi, Y., Lewis, S. L., Vásquez Martínez, R., Alexiades, M., Álvarez Dávila, E., Alvarez-Loayza, P., Andrade, A., Aragão, L. E. O. C., Araujo-Murakami, A., Arets, E. J. M. M., Arroyo, L., ... Zagt, R. J. (2015). Long-term decline of the Amazon carbon sink. *Nature*, 519(7543), 344–348. <https://doi.org/10.1038/nature14283>
- Brien, R. J. W., Schöngart, J., & Zuidema, P. A. (2016). Tree Rings in the Tropics: Insights into the Ecology and Climate Sensitivity of Tropical Trees. In G. Goldstein & L. S. Santiago (Eds.), *Tropical Tree Physiology: Adaptations and Responses in a Changing Environment* (pp. 439–461). Springer International Publishing. https://doi.org/10.1007/978-3-319-27422-5_20
- Brien, R. J. W., & Zuidema, P. A. (2005). Relating tree growth to rainfall in Bolivian rain forests: A test for six species using tree ring analysis. *Oecologia*, 146(1), 1–12. <https://doi.org/10.1007/s00442-005-0160-y>

- Brown, S. (2002). Measuring carbon in forests: Current status and future challenges. *Environmental Pollution*, 116(3), 363–372. [https://doi.org/10.1016/S0269-7491\(01\)00212-3](https://doi.org/10.1016/S0269-7491(01)00212-3)
- Burnham, K. P., & Anderson, D. R. (2002). *Model Selection and Multimodel Inference* (2nd ed.). Springer. <https://doi.org/10.1007/b97636>
- Cabon, A., Fernández-de-Uña, L., Gea-Izquierdo, G., Meinzer, F. C., Woodruff, D. R., Martínez-Vilalta, J., & De Cáceres, M. (2020). Water potential control of turgor-driven tracheid enlargement in Scots pine at its xeric distribution edge. *New Phytol.*, 225(1), 209–221. <https://doi.org/10.1111/nph.16146>
- Caffall, K. H., & Mohnen, D. (2009). The structure, function, and biosynthesis of plant cell wall pectic polysaccharides. *Carbohydrate Research*, 344(14), 1879–1900. <https://doi.org/10.1016/j.carres.2009.05.021>
- Calders, K., Newnham, G., Burt, A., Murphy, S., Raunonen, P., Herold, M., Culvenor, D., Avitabile, V., Disney, M., Armston, J., & Kaasalainen, M. (2015). Nondestructive estimates of above-ground biomass using terrestrial laser scanning. *Methods in Ecology and Evolution*, 6(2), 198–208. <https://doi.org/10.1111/2041-210X.12301>
- Callado, C. H., Roig, F. A., Tomazello-Filho, M., & Barros, C. F. (2013). Cambial growth periodicity studies of south american woody species – a review. *IAWA Journal*, 34(3), 213–230. <https://doi.org/10.1163/22941932-00000019>
- Campbell, N. A., & Reece, J. B. (2012). *Biologie* (4ème). ERPI Sciences. http://www.renaud-bray.com/Livres_Produit.aspx?id=939441&def=Biologie+4e+%c3%a9d.%2cCAMPBELL%2c+NEIL+A%2cREECE%2c+JANE+B%2c9782761328562&utm_campaign=partage-réseaux-sociaux&utm_medium=réseaux-sociaux&utm_source=facebook-like
- Cardoso, F. C. G., Marques, R., Botosso, P. C., & Marques, M. C. M. (2012). Stem growth and phenology of two tropical trees in contrasting soil conditions. *Plant Soil*, 354(1), 269–281. <https://doi.org/10.1007/s11104-011-1063-9>
- Carlquist, S. (2012). Wood Anatomy of Gnetales in a Functional, Ecological, and Evolutionary Context. *Aliso: A Journal of Systematic and Floristic Botany*, 30(1), 33–47. <https://doi.org/10.5642/aliso.20123001.05>
- Catesson, A.-M. (1994). Cambial ultrastructure and biochemistry: Changes in relation to vascular tissue differentiation and the seasonal cycle. *International Journal of Plant Sciences*, 155(3), 251–261. <https://doi.org/10.1086/297165>
- Cavaleri, M. A., Reed, S. C., Smith, W. K., & Wood, T. E. (2015). Urgent Need for Warming Experiments in Tropical Forests. *Glob. Chang. Biol.*, 21(6), 2111–2121. <https://doi.org/10.1111/gcb.12860>
- Cernusak, L. A., Ubierna, N., Winter, K., Holtum, J. A. M., Marshall, J. D., & Farquhar, G. D. (2013). Environmental and physiological determinants of carbon isotope discrimination in terrestrial plants. *New Phytologist*, 200(4), 950–965. <https://doi.org/10.1111/nph.12423>
- Chaffey, N. (1999). Cambium: Old challenges – new opportunities. *Trees*, 13(3), 138–151. <https://doi.org/10.1007/PL00009745>
- Chaffey, N., Barlow, P. W., & Barnett, J. R. (1998). A seasonal cycle of cell wall structure is accompanied by a cyclical rearrangement of cortical microtubules in fusiform cambial cells within taproots of *Aesculus hippocastanum* (Hippocastanaceae). *New Phytologist*, 139(4), 623–635. <https://doi.org/10.1046/j.1469-8137.1998.00241.x>
- Charlesworth, D., & Morgan, M. T. (1991). Allocation of resources to sex functions in flowering plants. *Philosophical Transactions of the Royal Society of London. Series B: Biological Sciences*, 332(1262), 91–102. <https://doi.org/10.1098/rstb.1991.0036>
- Chebli, Y., Bidhendi, A. J., Kapoor, K., & Geitmann, A. (2021). Cytoskeletal regulation of primary plant cell wall assembly. *Current Biology*, 31(10), R681–R695. <https://doi.org/10.1016/j.cub.2021.03.092>
- Choury, Z., Wujeska-Klaue, A., Bourne, A., Bown, N. P., Tjoelker, M. G., Medlyn, B. E., & Crous, K. Y. (2022). Tropical rainforest species have larger increases in temperature optima with warming than warm-temperate rainforest trees. *The New Phytologist*, 234(4), 1220–1236. <https://doi.org/10.1111/nph.18077>

- Chowdhury, M. Q., Schmitz, N., Verheydens, A., Sass-Klaassen, U., Koedam, N., & Beeckman, H. (2008). Nature and Periodicity of Growth Rings in two Bangladeshi Mangrove Species. *IAWA Journal*, 29(3), 265–276. <https://doi.org/10.1163/22941932-90000185>
- Chowdhury, T., Islam, M., & Rahman, M. (2023). Long-term growth and xylem hydraulic responses of *Albizia procera* (Roxb.) Benth. To climate in a moist tropical forest of Bangladesh. *PPEES*, 61, 125762. <https://doi.org/10.1016/j.ppees.2023.125762>
- Christman, M. A., & Sperry, J. S. (2010). Single-vessel flow measurements indicate scalariform perforation plates confer higher flow resistance than previously estimated. *Plant, Cell & Environment*, 33(3), 431–443. <https://doi.org/10.1111/j.1365-3040.2009.02094.x>
- Cook, K. H., Vizzy, E. K., Andrews, P. C., & Zhao, S. (2024). Temperature Increases Threaten the Congo Basin Rainforest in the Twenty-First Century More than Precipitation Changes. *Journal of Climate*, 38(1), 369–386. <https://doi.org/10.1175/JCLI-D-24-0289.1>
- Couralet, C. (2010). *Community dynamics, phenology and growth of tropical trees in the rain forest reserve of Luki, Democratic Republic of Congo* [Dissertation, Ghent University]. <http://hdl.handle.net/1854/LU-1028918>
- Couralet, C., Sterck, F. J., Sass-Klaassen, U., Van Acker, J., & Beeckman, H. (2010). Species-Specific Growth Responses to Climate Variations in Understory Trees of a Central African Rain Forest. *Biotropica*, 42(4), 503–511. <https://doi.org/10.1111/j.1744-7429.2009.00613.x>
- Couralet, C., Van den Bulcke, J., Ngoma, L., Van Acker, J., & Beeckman, H. (2013). Phenology in functional groups of Central African rainforest trees. *Journal of Tropical Forest Science*, 25(3), 361–374.
- Courtois-Moreau, C. L., Pesquet, E., Sjödin, A., Muñiz, L., Bollhöner, B., Kaneda, M., Samuels, L., Jansson, S., & Tuominen, H. (2009). A unique program for cell death in xylem fibers of *Populus* stem. *The Plant Journal*, 58(2), 260–274. <https://doi.org/10.1111/j.1365-313X.2008.03777.x>
- Crang, R., Lyons-Sobaski, S., & Wise, R. (2018). *Plant anatomy: A concept-based approach to the structure of seed plants*. Springer International Publishing. <https://doi.org/10.1007/978-3-319-77315-5>
- Cresswell, R., Dupree, R., Brown, S. P., Pereira, C. S., Skaf, M. S., Sorieul, M., Dupree, P., & Hill, S. (2021). Importance of Water in Maintaining Softwood Secondary Cell Wall Nanostructure. *Biomacromolecules*, 22(11), 4669–4680. <https://doi.org/10.1021/acs.biomac.1c00937>
- Crosby, A. G., Fishwick, S., & White, N. (2010). Structure and evolution of the intracratonic Congo Basin. *Geochemistry, Geophysics, Geosystems*, 11(6). <https://doi.org/10.1029/2009GC003014>
- Cuny, H. E., Rathgeber, C. B. K., Frank, D., Fonti, P., Mäkinen, H., Prislan, P., Rossi, S., del Castillo, E. M., Campelo, F., Vavřík, H., Camarero, J. J., Bryukhanova, M. V., Jyske, T., Gričar, J., Gryc, V., De Luis, M., Vieira, J., Čufar, K., Kirdyanov, A. V., ... Fournier, M. (2015). Woody biomass production lags stem-girth increase by over one month in coniferous forests. *Nature Plants*, 1(11), 1–6. <https://doi.org/10.1038/nplants.2015.160>
- Dai, Z., Edwards, G. E., & Ku, M. S. B. (1992). Control of Photosynthesis and Stomatal Conductance in *Ricinus communis* L. (Castor Bean) by Leaf to Air Vapor Pressure Deficit. *Plant Physiol.*, 99(4), 1426–1434.
- Dargie, G. C., Lewis, S. L., Lawson, I. T., Mitchard, E. T. A., Page, S. E., Bocko, Y. E., & Ifo, S. A. (2017). Age, extent and carbon storage of the central Congo Basin peatland complex. *Nature*, 542(7639), 86–90. <https://doi.org/10.1038/nature21048>
- Day, M. E. (2000). Influence of temperature and leaf-to-air vapor pressure deficit on net photosynthesis and stomatal conductance in red spruce (*Picea rubens*). *Tree Physiol.*, 20(1), 57–63. <https://doi.org/10.1093/treephys/20.1.57>
- De Frenne, P., Florian, Z., Rodríguez-Sánchez, F., Scheffers, B. R., Kristoffer, H., Miska, L., Vellend, M., Verheyen, K., & Lenoir, J. (2019). *Global buffering of temperatures under forest canopies*. 3(5), 744–749. <https://doi.org/10.1038/s41559-019-0842-1>
- De Micco, V., Carrer, M., Rathgeber, C. B. K., Camarero, J. J., Voltas, J., Cherubini, P., & Battipaglia, G. (2020). From xylogenesis to tree rings: Wood traits to investigate tree response to environmental changes. *IAWA J.*, 40(2), 155–182. <https://doi.org/10.1163/22941932-40190246>
- De Mil, T., Angoboy Ilondela, B., Maginet, S., Duveiller, J., Van Acker, J., Beeckman, H., & Van den Bulcke, J. (2017). Cambial activity in the understory of the Mayombe forest, DR Congo. *Trees*, 31, 49–61. <https://doi.org/10.1007/s00468-016-1454-x>

- De Mil, T., Hubau, W., Angoboy Ilondea, B., Rocha Vargas, M. A., Boeckx, P., Steppe, K., Van Acker, J., Beeckman, H., & Van den Bulcke, J. (2019). Asynchronous leaf and cambial phenology in a tree species of the Congo Basin requires space–time conversion of wood traits. *Annals of Botany*, 124(2), 245–253. <https://doi.org/10.1093/aob/mcz069>
- De Wasseige, C., de Marcken, P., Bayol, N., Hiol Hiol, F., Mayaux, P., Desclée, B., Nasi, R., Billand, A., Defourny, P., & Eba’a Atyi, R. (Eds.). (2010). *The Forests of the Congo Basin—State of the Forest 2010*. Publications Office of the European Union. <https://pfbc-cbfp.org/app.php/forests-2010.html>
- Delmer, D. P., & Amor, Y. (1995). Cellulose biosynthesis. *The Plant Cell*, 7(7), 987–1000. <https://doi.org/10.1105/tpc.7.7.987>
- Deslauriers, A., Morin, H., & Begin, Y. (2003). Cellular phenology of annual ring formation of *Abies balsamea* in the Quebec boreal forest (Canada). *Canadian Journal of Forest Research*, 33(2), 190–200. <https://doi.org/10.1139/x02-178>
- Deslauriers, A., Rossi, S., Anfodillo, T., & Saracino, A. (2008). Cambial phenology, wood formation and temperature thresholds in two contrasting years at high altitude in southern Italy. *Tree Physiology*, 28(6), 863–871. <https://doi.org/10.1093/treephys/28.6.863>
- Deslauriers, A., Rossi, S., Turcotte, A., Morin, H., & Krause, C. (2011). A three-step procedure in SAS to analyze the time series from automatic dendrometers. *Dendrochronologia*, 29(3), 151–161. <https://doi.org/10.1016/j.dendro.2011.01.008>
- D’Orangeville, L., Itter, M., Kneeshaw, D., Munger, J. W., Richardson, A. D., Dyer, J. M., Orwig, D. A., Pan, Y., & Pederson, N. (2022). Peak radial growth of diffuse-porous species occurs during periods of lower water availability than for ring-porous and coniferous trees. *Tree Physiology*, 42(2), 304–316. <https://doi.org/10.1093/treephys/tpab101>
- Drew, D. M., & Downes, G. M. (2009). The Use of Precision Dendrometers in Research on Daily Stem Size and Wood Property Variation: A Review. *Dendrochronologia*, 27(2), 159–172. <https://doi.org/10.1016/j.dendro.2009.06.008>
- Duchesne, L. C., & Larson, D. W. (1989). Cellulose and the evolution of plant life. *BioScience*, 39(4), 238–241. <https://doi.org/10.2307/1311160>
- Eba’a Atyi, R., Hiol Hiol, F., Lescuyer, G., Mayaux, P., Defourny, P., Bayol, N., Saracco, F., Pokem, D., Sufo Kankeu, R., & Nasi, R. (Eds.). (2022). *The forests of the Congo Basin: State of the forests 2021*. CIFOR. <https://doi.org/10.17528/cifor/008700>
- Eberhard, S., Finazzi, G., & Wollman, F.-A. (2008). The Dynamics of Photosynthesis. *Annu. Rev. Genet.*, 42, 463–515. <https://doi.org/10.1146/annurev.genet.42.110807.091452>
- Egbe, O. D. J. (2022). “let them eat their declarations”: Interrogating natural resource-rich states’ inertia towards biodiversity conservation treaties in sub-saharan africa. In S. Chibueze Izah (Ed.), *Biodiversity in Africa: Potentials, Threats and Conservation* (pp. 505–523). Springer Nature. https://doi.org/10.1007/978-981-19-3326-4_19
- Evert, R. F. (2006). *Esau’s plant anatomy: Meristems, cells, and tissues of the plant body: Their structure, function, and development* (Third, Vol. 99). John Wiley & Sons, Inc.
- FAO, & ITTO. (2011). *The State of Forests in the Amazon Basin, Congo Basin and Southeast Asia*. FAO.
- Fastré, C., Igwili, B., Van de Perre, F., & van der Hoek, Y. (2024). Visitation patterns of endangered grey parrots (*Psittacus erithacus*) in a forest clearing in the Democratic Republic of the Congo. *Ecology and Evolution*, 14(8), e70039. <https://doi.org/10.1002/ece3.70039>
- Fatichi, S., Pappas, C., Zscheischler, J., & Leuzinger, S. (2019). Modelling carbon sources and sinks in terrestrial vegetation. *New Phytologist*, 221(2), 652–668. <https://doi.org/10.1111/nph.15451>
- Fauset, S., Baker, T. R., Lewis, S. L., Feldpausch, T. R., Affum-Baffoe, K., Foli, E. G., Hamer, K. C., & Swaine, M. D. (2012). Drought-Induced Shifts in the Floristic and Functional Composition of Tropical Forests in Ghana. *Ecology Letters*, 15(10), 1120–1129. <https://doi.org/10.1111/j.1461-0248.2012.01834.x>
- Fay, J. M., & Agnagna, M. (1991). A population survey of forest elephants (*Loxodonta africana cyclotis*) in northern Congo. *African Journal of Ecology*, 29(3), 177–187. <https://doi.org/10.1111/j.1365-2028.1991.tb01000.x>

- Fay, J. M., Agnagna, M., Moore, J., & Oko, R. (1989). Gorillas (*Gorilla gorilla gorilla*) in the Likouala swamp forests of north central Congo: Preliminary data on populations and ecology. *International Journal of Primatology*, 10(5), 477–486. <https://doi.org/10.1007/BF02736372>
- Feeley, K., Martinez-Villa, J., Perez, T., Silva Duque, A., Triviño Gonzalez, D., & Duque, A. (2020). The Thermal Tolerances, Distributions, and Performances of Tropical Montane Tree Species. *Front. for. Glob. Change*, 3(25). <https://doi.org/doi:10.3389/ffgc.2020.00025>
- Fernández-de-Uña, L., Martínez-Vilalta, J., Poyatos, R., Mencuccini, M., & McDowell, N. G. (2023). The role of height-driven constraints and compensations on tree vulnerability to drought. *New Phytologist*, 239(6), 2083–2098. <https://doi.org/10.1111/nph.19130>
- Ferster, C. J., Trofymow, J. (Tony), Coops, N. C., Chen, B., & Black, T. A. (2015). Comparison of carbon-stock changes, eddy-covariance carbon fluxes and model estimates in coastal Douglas-fir stands in British Columbia. *Forest Ecosystems*, 2(1), 13. <https://doi.org/10.1186/s40663-015-0038-3>
- Fétéké, F., Fayolle, A., Dainou, K., Bourland, N., Dié, A., Lejeune, P., Doucet, J.-L., & Beeckman, H. (2017). Variations saisonnières de la croissance diamétrique et des phénologies foliaire et reproductive de trois espèces ligneuses commerciales d’Afrique centrale. *Bois For. Trop.*, 330(330), 3. <https://doi.org/10.19182/bft2016.330.a31315>
- Fischer, U., Kucukoglu, M., Helariutta, Y., & Bhalerao, R. P. (2019). The Dynamics of Cambial Stem Cell Activity. *Annual Review of Plant Biology*, 70(1), 293–319. <https://doi.org/10.1146/annurev-arplant-050718-100402>
- Forni, E., Rossi, V., Gillet, J.-F., Bénédet, F., Cornu, G., Freycon, V., Zombo, I., Alberny, E., Mayinga, M., Istace, V., & Gourlet-Fleury, S. (2019). Dispositifs permanents de nouvelle génération pour le suivi de la dynamique forestière en Afrique centrale: Bilan en République du Congo. *Bois For. Trop.*, 341, 55–70. <https://doi.org/10.19182/bft2019.341.a31760>
- Francon, L., Edvardsson, J., Corona, C., & Stoffel, M. (2024). The timing of wood formation in peatland trees as obtained with different approaches. *Dendrochronologia*, 85, 126210. <https://doi.org/10.1016/j.dendro.2024.126210>
- Fransson, P., Brännström, Å., & Franklin, O. (2021). A tree’s quest for light—Optimal height and diameter growth under a shading canopy. *Tree Physiology*, 41(1), 1–11. <https://doi.org/10.1093/treephys/tpaa110>
- Fredriksson, M., Rüggeberg, M., Nord-Larsen, T., Beck, G., & Thybring, E. E. (2023). Water sorption in wood cell walls—data exploration of the influential physicochemical characteristics. *Cellulose*, 30(3), 1857–1871. <https://doi.org/10.1007/s10570-022-04973-0>
- Friedlingstein, P., Allen, M., Canadell, J. G., Peters, G. P., & Seneviratne, S. I. (2019). Comment on “The global tree restoration potential.” *Science*, 366(6463), eaay8060. <https://doi.org/10.1126/science.aay8060>
- Friend, A. D., Eckes-Shephard, A. H., Fonti, P., Rademacher, T. T., Rathgeber, C. B. K., Richardson, A. D., & Turton, R. H. (2019). On the need to consider wood formation processes in global vegetation models and a suggested approach. *Ann. For. Sci.*, 76(2), 49. <https://doi.org/10.1007/s13595-019-0819-x>
- Funada, R., Yamagishi, Y., Begum, S., Kudo, K., Nabeshima, E., Nugroho, W. D., Hasnat, R., Oribe, Y., & Nakaba, S. (2016). Xylogenesis in trees: From cambial cell division to cell death. In Y. S. Kim, R. Funada, & A. P. Singh (Eds.), *Secondary xylem biology* (pp. 25–43). Academic Press. <https://doi.org/10.1016/B978-0-12-802185-9.00002-4>
- Gibbs, H. K., Brown, S., Niles, J. O., & Foley, J. A. (2007). Monitoring and estimating tropical forest carbon stocks: Making REDD a reality. *Environmental Research Letters*, 2(4), 045023. <https://doi.org/10.1088/1748-9326/2/4/045023>
- Gilliam, F. S. (2007). The Ecological Significance of the Herbaceous Layer in Temperate Forest Ecosystems. *BioScience*, 57(10), 845–858. <https://doi.org/10.1641/B571007>
- Giraldo, J. A., del Valle, J. I., González-Caro, S., David, D. A., Taylor, T., Tobón, C., & Sierra, C. A. (2023). Tree growth periodicity in the ever-wet tropical forest of the Americas. *Journal of Ecology*, 111(4), 889–902. <https://doi.org/10.1111/1365-2745.14069>
- Giraldo, J. A., del Valle, J. I., González-Caro, S., & Sierra, C. A. (2022). Intra-annual isotope variations in tree rings reveal growth rhythms within the least rainy season of an ever-wet tropical forest. *Trees*, 36(3), 1039–1052. <https://doi.org/10.1007/s00468-022-02271-7>

- Glimn-Lacy, J., & Kaufman, P. B. (2006). *Botany Illustrated*. Springer US. <https://doi.org/10.1007/0-387-28875-9>
- Gliniars, R., Becker, G. S., Braun, D., & Dalitz, H. (2013). Monthly stem increment in relation to climatic variables during 7 years in an East African rainforest. *Trees*, 27(4), 1129–1138. <https://doi.org/10.1007/s00468-013-0863-3>
- Gond, V., Fayolle, A., Pennec, A., Cornu, G., Mayaux, P., Camberlin, P., Doumenge, C., Fauvet, N., & Gourlet-Fleury, S. (2013). Vegetation structure and greenness in Central Africa from Modis multi-temporal data. *Philos. Trans. R. Soc. Lond., B, Biol. Sci.*, 368(1625), 20120309. <https://doi.org/10.1098/rstb.2012.0309>
- Gričar, J., Čufar, K., Oven, P., & Schmitt, U. (2005). Differentiation of Terminal Latewood Tracheids in Silver Fir Trees During Autumn. *Annals of Botany*, 95(6), 959–965. <https://doi.org/10.1093/aob/mci112>
- Groenendijk, P., Sass-Klaassen, U., Bongers, F., & Zuidema, P. A. (2014). Potential of tree-ring analysis in a wet tropical forest: A case study on 22 commercial tree species in Central Africa. *Forest Ecology and Management*, 323, 65–78. <https://doi.org/10.1016/j.foreco.2014.03.037>
- Grossiord, C., Buckley, T. N., Cernusak, L. A., Novick, K. A., Poulter, B., Siegwolf, R. T. W., Sperry, J. S., & McDowell, N. G. (2020). Plant responses to rising vapor pressure deficit. *New Phytol.*, 226(6), 1550–1566. <https://doi.org/10.1111/nph.16485>
- Guidosse, Q., Biwolé, A., De Clerck, C., Ekome, S. N., Lassois, L., & Doucet, J.-L. (2024). Seedling ecology of *Aucoumea klaineana* Pierre, the most important timber species in Central Africa. *Forest Ecology and Management*, 569, 122221. <https://doi.org/10.1016/j.foreco.2024.122221>
- Güney, A., Kerr, D., Sökücü, A., Zimmermann, R., & Küppers, M. (2015). Cambial activity and xylogenesis in stems of *Cedrus libani* A. Rich at different altitudes. *Botanical Studies*, 56(1), 20. <https://doi.org/10.1186/s40529-015-0100-z>
- Guo, Y., Xu, H., Wu, H., Shen, W., Lin, J., & Zhao, Y. (2022). Seasonal changes in cambium activity from active to dormant stage affect the formation of secondary xylem in *Pinus tabulaeformis* Carr. *Tree Physiology*, 42(3), 585–599. <https://doi.org/10.1093/treephys/tpab115>
- Hacke, U. G., Lachenbruch, B., Pittermann, J., Mayr, S., Domec, J.-C., & Schulte, P. J. (2015). The hydraulic architecture of conifers. In U. G. Hacke (Ed.), *Functional and Ecological Xylem Anatomy* (pp. 39–75). Springer International Publishing. https://doi.org/10.1007/978-3-319-15783-2_2
- Hacke, U. G., Sperry, J. S., & Pittermann, J. (2005). Efficiency versus safety tradeoffs for water conduction in angiosperm vessels versus gymnosperm tracheids. In N. M. Holbrook & M. A. Zwieniecki (Eds.), *Vascular transport in plants* (pp. 333–353). Academic Press. <https://doi.org/10.1016/B978-012088457-5/50018-6>
- Hajdas, I., Ascough, P., Garnett, M. H., Fallon, S. J., Pearson, C. L., Quarta, G., Spalding, K. L., Yamaguchi, H., & Yoneda, M. (2021). Radiocarbon dating. *Nature Reviews Methods Primers*, 1(1), 1–26. <https://doi.org/10.1038/s43586-021-00058-7>
- Hallé, F., Hallé, F., & Martin, R. (1968). Étude de la croissance rythmique chez l’Hévéa (*Hevea brasiliensis* Müll-Arg.-Euphorbiacées-Crotonoïdées). *Adansonia*, 8(4), 475–503. <https://doi.org/10.5962/p.296542>
- Hallé, F., & Oldeman, R. (1970). *Essai sur l’architecture et la dynamique de croissance des arbres tropicaux*. Masson & Cie.
- Harholt, J., Suttangkakul, A., & Vibe Scheller, H. (2010). Biosynthesis of pectin. *Plant Physiology*, 153(2), 384–395. <https://doi.org/10.1104/pp.110.156588>
- Harrison, I. J., Brummett, R., & Stiassny, M. L. J. (2016). Congo River Basin. In C. M. Finlayson, G. R. Milton, R. C. Prentice, & N. C. Davidson (Eds.), *The Wetland Book: II: Distribution, Description and Conservation* (pp. 1–18). Springer Netherlands. https://doi.org/10.1007/978-94-007-6173-5_92-2
- Hart, J. W. (2012). *Light and Plant Growth*. Springer Science & Business Media.
- Hart, T. B., Hart, J. A., & Murphy, P. G. (1989). Monodominant and Species-Rich Forests of the Humid Tropics: Causes for Their Co-Occurrence. *The American Naturalist*, 133(5), 613–633.
- Hastie, A., Lauerwald, R., Ciais, P., Papa, F., & Regnier, P. (2021). Historical and future contributions of inland waters to the Congo Basin carbon balance. *Earth System Dynamics*, 12(1), 37–62. <https://doi.org/10.5194/esd-12-37-2021>

- Helbig, M., Gerken, T., Beamesderfer, E. R., Baldocchi, D. D., Banerjee, T., Biraud, S. C., Brown, W. O. J., Brunsell, N. A., Burakowski, E. A., Burns, S. P., Butterworth, B. J., Chan, W. S., Davis, K. J., Desai, A. R., Fuentes, J. D., Hollinger, D. Y., Kljun, N., Mauder, M., Novick, K. A., ... Richardson, A. D. (2021). Integrating continuous atmospheric boundary layer and tower-based flux measurements to advance understanding of land-atmosphere interactions. *Agricultural and Forest Meteorology*, 307, 108509. <https://doi.org/10.1016/j.agrformet.2021.108509>
- Hladik, A., & Blanc, P. (1987). Croissance des plantes en sous-bois de forêt dense humide (Makokou, Gabon). *Rev. Ecol. (Terre Vie)*, 42(3), 209–234. <https://doi.org/10.3406/revec.1987.5404>
- Hoare, A. L. (2007). *Clouds on the horizon: The Congo Basin's forests and climate change*. <https://www.semanticscholar.org/paper/CLOUDS-ON-THE-HORIZON%3A-The-Congo-Basin%E2%80%99s-Forests-Hoare/3f3de5e4fbc563cd0a41cca09fe4ccc4dd5c6081>
- Holm, J. A., Kueppers, L. M., & Chambers, J. Q. (2017). Novel Tropical Forests: Response to Global Change. *New Phytol*, 213(3), 988–992. <https://doi.org/10.1111/nph.14407>
- Huang, R., Xu, C., Griesinger, J., Feng, X., Zhu, H., & Bräuning, A. (2023). Rising utilization of stable isotopes in tree rings for climate change and forest ecology. *Journal of Forestry Research*, 35(1), 13. <https://doi.org/10.1007/s11676-023-01668-5>
- Hubau, W., De Mil, T., Van den Bulcke, J., Phillips, O. L., Angoboy Ilondea, B., Van Acker, J., Sullivan, M. J. P., Nsenga, L., Toirambe, B., Couralet, C., Banin, L. F., Begne, S. K., Baker, T. R., Bourland, N., Chezeaux, E., Clark, C. J., Collins, M., Comiskey, J. A., Cuni-Sanchez, A., ... Beeckman, H. (2019). The persistence of carbon in the African forest understory. *Nat. Plants*, 5(2), Article 2. <https://doi.org/10.1038/s41477-018-0316-5>
- Hubau, W., Lewis, S. L., Phillips, O. L., Affum-Baffoe, K., Beeckman, H., Cuní-Sanchez, A., Daniels, A. K., Ewango, C. E. N., Fauset, S., Mukinzi, J. M., Sheil, D., Sonké, B., Sullivan, M. J. P., Sunderland, T. C. H., Taedoumg, H., Thomas, S. C., White, L. J. T., Abernethy, K. A., Adu-Bredu, S., ... Zemagho, L. (2020). Asynchronous carbon sink saturation in African and Amazonian tropical forests. *Nature*, 579(7797), Article 7797. <https://doi.org/10.1038/s41586-020-2035-0>
- Hufkens, K., & Kearsley, E. (2023). *bluegreen-labs/junglerhythms: The Jungle Rhythms workflow: recovering historical tropical tree phenology data* [Computer software]. Zenodo. <https://doi.org/10.5281/zenodo.7650295>
- Huntley, B. J. (2019). Angola in Outline: Physiography, Climate and Patterns of Biodiversity. In B. J. Huntley, V. Russo, F. Lages, & N. Ferrand (Eds.), *Biodiversity of Angola: Science & Conservation: A Modern Synthesis* (pp. 15–42). Springer International Publishing. https://doi.org/10.1007/978-3-030-03083-4_2
- IAWA Committee. (1989). IAWA list of microscopic features for hardwood identification. *IAWA Bull n. s.*, 10(3), 219–332.
- Imarhiagbe, O., Onyeukwu, I. I., Egboduku, W. O., Mukah, F. E., & Ogwu, M. C. (2022). Forest conservation strategies in Africa: Historical perspective, status and sustainable avenues for progress. In S. Chibueze Izah (Ed.), *Biodiversity in Africa: Potentials, Threats and Conservation* (pp. 547–572). Springer Nature. https://doi.org/10.1007/978-981-19-3326-4_21
- Jamet, E., Canut, H., Boudart, G., & Pont-Lezica, R. F. (2006). Cell wall proteins: A new insight through proteomics. *Trends in Plant Science*, 11(1), 33–39. <https://doi.org/10.1016/j.tplants.2005.11.006>
- Jamet, E., & Dunand, C. (2020). Plant cell wall proteins and development. *International Journal of Molecular Sciences*, 21(8), 2731. <https://doi.org/10.3390/ijms21082731>
- Janssen, T., van der Velde, Y., Hofhansl, F., Luyssaert, S., Naudts, K., Driessen, B., Fleischer, K., & Dolman, H. (2021). Drought effects on leaf fall, leaf flushing and stem growth in the Amazon forest: Reconciling remote sensing data and field observations. *Biogeosciences*, 18(14), 4445–4472. <https://doi.org/10.5194/bg-18-4445-2021>
- Jiang, H., Wu, Y., Wang, H., Ferguson, D. K., & Li, C.-S. (2013). Ancient plant use at the site of Yuergou, Xinjiang, China: Implications from desiccated and charred plant remains. *Vegetation History and Archaeobotany*, 22(2), 129–140. <https://doi.org/10.1007/s00334-012-0365-z>
- Johnson, L. K., Mahoney, M. J., Desrochers, M. L., & Beier, C. M. (2023). Mapping historical forest biomass for stock-change assessments at parcel to landscape scales. *Forest Ecology and Management*, 546, 121348. <https://doi.org/10.1016/j.foreco.2023.121348>

- Kafuti, C., Van den Bulcke, J., Beeckman, H., Van Acker, J., Hubau, W., De Mil, T., Hatakiwe, H., Djiofack, B., Fayolle, A., Loubota Panzou, G. J., & Bourland, N. (2022). Height-diameter allometric equations of an emergent tree species from the Congo Basin. *Forest Ecology and Management*, 504, 119822. <https://doi.org/10.1016/j.foreco.2021.119822>
- Kampe, A., & Magel, E. (2013). New insights into heartwood and heartwood formation. In J. Fromm (Ed.), *Cellular Aspects of Wood Formation* (pp. 71–95). Springer. https://doi.org/10.1007/978-3-642-36491-4_3
- Kasongo Yakusu, E., Monthe, F. S., Bourland, N., Hardy, O. J., Louppe, D., Bola Mbele Lokanda, F., Hubau, W., Kahindo Muhongya, J.-M., Acker, J. V., & Beeckman, H. (2018). Le genre Entandrophragma (Meliaceae): Taxonomie et écologie d'arbres africains d'intérêt économique (synthèse bibliographique). *Biotechnologie, Agronomie, Société et Environnement*, 22(2), 113–127. <https://doi.org/10.25518/1780-4507.16353>
- Kasongo Yakusu, E., Van Acker, J., Van de Vyver, H., Bourland, N., Mbifo Ndiapo, J., Besango Likwela, T., Lokonda Wa Kipifo, M., Mbuya Kankolongo, A., Van den Bulcke, J., Beeckman, H., Bauters, M., Boeckx, P., Verbeeck, H., Jacobsen, K., Demarée, G., Gellens-Meulenberghs, F., & Hubau, W. (2023). Ground-based climate data show evidence of warming and intensification of the seasonal rainfall cycle during the 1960–2020 period in Yangambi, central Congo Basin. *Climatic Change*, 176(10), 142. <https://doi.org/10.1007/s10584-023-03606-0>
- Kearsley, E., Moonen, P. C., Hufkens, K., Doetterl, S., Lisingo, J., Boyemba Bosela, F., Boeckx, P., Beeckman, H., & Verbeeck, H. (2017). Model performance of tree height-diameter relationships in the central Congo Basin. *Annals of Forest Science*, 74(1), Article 1. <https://doi.org/10.1007/s13595-016-0611-0>
- Kearsley, E., Verbeeck, H., Stoffelen, P., Janssens, S. B., Yakusu, E. K., Kosmala, M., De Mil, T., Bauters, M., Kitima, E. R., Ndiapo, J. M., Chuda, A. L., Richardson, A. D., Wingate, L., Ilondea, B. A., Beeckman, H., van den Bulcke, J., Boeckx, P., & Hufkens, K. (2024). Historical tree phenology data reveal the seasonal rhythms of the Congo Basin rainforest. *Plant-Environment Interactions*, 5(2), e10136. <https://doi.org/10.1002/pei3.10136>
- Knüsel, S., Peters, R. L., Haeni, M., Wilhelm, M., & Zweifel, R. (2021). Processing and Extraction of Seasonal Tree Physiological Parameters from Stem Radius Time Series. *Forests*, 12(6), Article 6. <https://doi.org/10.3390/f12060765>
- Kottek, M., Grieser, J., Beck, C., Rudolf, B., & Rubel, F. (2006). World Map of the Köppen-Geiger climate classification updated. *Meteorologische Zeitschrift*, 15(3), 259–263. <https://doi.org/10.1127/0941-2948/2006/0130>
- Lachaud, S., Catesson, A.-M., & Bonnemain, J.-L. (1999). Structure and functions of the vascular cambium. *Comptes Rendus de l'Académie Des Sciences - Series III - Sciences de La Vie*, 322(8), 633–650. [https://doi.org/10.1016/S0764-4469\(99\)80103-6](https://doi.org/10.1016/S0764-4469(99)80103-6)
- Lack, A., & Evans, D. E. (2001). *Instant notes Plant Biology*. BIOS Scientific Publishers. <https://www.semanticscholar.org/paper/Instant-notes-plant-biology-Lack-Evans/cf6677662f6a3788f4626325392b70a1083aa798>
- Larson, P. R. (1994). *The Vascular Cambium*. Springer. <https://doi.org/10.1007/978-3-642-78466-8>
- Lawrence, M., G. (2005). The relationship between relative humidity and the dewpoint temperature in moist air: A simple conversion and applications. *Bulletin of the American Meteorological Society*, 86, 225–234.
- Leavitt, S. W. (2010). Tree-ring C–H–O isotope variability and sampling. *Science of The Total Environment*, 408(22), 5244–5253. <https://doi.org/10.1016/j.scitotenv.2010.07.057>
- Lehnebach, R., Bossu, J., Va, S., Morel, H., Amusant, N., Nicolini, E., & Beauchêne, J. (2019). Wood density variations of legume trees in French Guiana along the shade tolerance continuum: Heartwood effects on radial patterns and gradients. *Forests*, 10(2), Article 2. <https://doi.org/10.3390/f10020080>
- Leroux, O. (2012). Collenchyma: A versatile mechanical tissue with dynamic cell walls. *Annals of Botany*, 110(6), 1083–1098. <https://doi.org/10.1093/aob/mcs186>
- Leszczuk, A., Kalaitzis, P., Kulik, J., & Zdunek, A. (2023). Review: Structure and modifications of arabinogalactan proteins (AGPs). *BMC Plant Biology*, 23(1), 45. <https://doi.org/10.1186/s12870-023-04066-5>

- Lewis, S. L., Edwards, D. P., & Galbraith, D. (2015). Increasing human dominance of tropical forests. *Science*, 349(6250), 827–832. <https://doi.org/10.1126/science.aaa9932>
- Li, W., Lin, Y.-C. J., Chen, Y.-L., Zhou, C., Li, S., De Ridder, N., Oliveira, D. M., Zhang, L., Zhang, B., Wang, J. P., Xu, C., Fu, X., Luo, K., Wu, A.-M., Demura, T., Lu, M.-Z., Zhou, Y., Li, L., Umezawa, T., ... Chiang, V. L. (2024). Woody plant cell walls: Fundamentals and utilization. *Molecular Plant*, 17(1), 112–140. <https://doi.org/10.1016/j.molp.2023.12.008>
- Liang, X., Kankare, V., Hyypää, J., Wang, Y., Kukko, A., Haggrén, H., Yu, X., Kaartinen, H., Jaakkola, A., Guan, F., Holopainen, M., & Vastaranta, M. (2016). Terrestrial laser scanning in forest inventories. *ISPRS Journal of Photogrammetry and Remote Sensing*, 115, 63–77. <https://doi.org/10.1016/j.isprsjprs.2016.01.006>
- Liu, Q., Luo, L., & Zheng, L. (2018). Lignins: Biosynthesis and biological functions in plants. *International Journal of Molecular Sciences*, 19(2), Article 2. <https://doi.org/10.3390/ijms19020335>
- Locosselli, G. M. (2018). The cambium activity in a changing world. *Trees*, 32(1), 1–2. <https://doi.org/10.1007/s00468-017-1616-5>
- Locosselli, G. M., Brien, R. J. W., Leite, M. de S., Gloor, M., Krottenthaler, S., Oliveira, A. A. de, Barichivich, J., Anhu, D., Ceccantini, G., Schöngart, J., & Buckeridge, M. (2020). Global tree-ring analysis reveals rapid decrease in tropical tree longevity with temperature. *Proc. Natl. Acad. Sci*, 117(52), 33358–33364. <https://doi.org/10.1073/pnas.2003873117>
- Locosselli, G. M., & Buckeridge, M. S. (2017). Dendrochemistry, a missing link to further understand carbon allocation during growth and decline of trees. *Trees*, 31(6), 1745–1758. <https://doi.org/10.1007/s00468-017-1599-2>
- Lohbeck, M., Lebrija-Trejos, E., Martínez-Ramos, M., Meave, J. A., Poorter, L., & Bongers, F. (2015). Functional Trait Strategies of Trees in Dry and Wet Tropical Forests Are Similar but Differ in Their Consequences for Succession. *PLOS ONE*, 10(4), e0123741. <https://doi.org/10.1371/journal.pone.0123741>
- López, L., Villalba, R., & Peña-Claros, M. (2012). Determining the annual periodicity of growth rings in seven tree species of a tropical moist forest in Santa Cruz, Bolivia. *Forest Systems*, 21(3), Article 3. <https://doi.org/10.5424/fs/2012213-02966>
- Lovett Doust, J. (1989). Plant reproductive strategies and resource allocation. *Trends in Ecology & Evolution*, 4(8), 230–234. [https://doi.org/10.1016/0169-5347\(89\)90166-3](https://doi.org/10.1016/0169-5347(89)90166-3)
- Lowman, M. D., & Moffett, M. (1993). The ecology of tropical rain forest canopies. *Trends Ecol. Evol.*, 8(3), 104–107. [https://doi.org/10.1016/0169-5347\(93\)90061-S](https://doi.org/10.1016/0169-5347(93)90061-S)
- Lubini, A. (1997). *La végétation de la Réserve de biosphère de Luki au Mayombe (Zaire)* (Vol. 10). Jardin botanique national de Belgique.
- Luo, J., Lian, C., Liu, R., Zhang, S., Yang, F., & Fei, B. (2019). Comparison of metaxylem vessels and pits in four sympodial bamboo species. *Scientific Reports*, 9(1), 10876. <https://doi.org/10.1038/s41598-019-47419-7>
- Luse Belanganayi, B. (2016). Causes de la monodominance de l'essence *Cynometra alexandri* C.H. Wright (Eggeling 1947; Hamilton 1981), dans la forêt de Banana (Mambasa/Ituri/R.D. Congo). *Bulletin de la Société Royale des Sciences de Liège*. <https://doi.org/10.25518/0037-9565.5910>
- Luse Belanganayi, B., Angoboy Ilondea, B., Mbungu Phaka, C., Laurent, F., Djiofack, B. Y., Kafuti, C., Peters, R. L., Bourland, N., Beeckman, H., & De Mil, T. (2024). Diel and annual rhythms of tropical stem size changes in the Mayombe forest, Congo Basin. *Frontiers in Forests and Global Change*, 7. <https://doi.org/10.3389/ffgc.2024.1185225>
- Luse Belanganayi, B., Delvaux, C., Kearsley, E., Lievens, K., Rousseau, M., Mbungu Phaka, C., Djiofack, B. Y., Laurent, F., Bourland, N., Hubau, W., De Mil, T., & Beeckman, H. (2024). Growth periodicity in semi-deciduous tropical tree species from the Congo Basin. *Plant-Environment Interactions*, 5(3), e10144. <https://doi.org/10.1002/pei3.10144>
- Mabrouk, E. H., Moursy, F. I., & Morsy, M. (2022). Assessment of climate characteristics and long-term trends of rainfall and drought in the Congo River Basin. *Journal of Water and Climate Change*, 13(11), 3906–3933. <https://doi.org/10.2166/wcc.2022.241>
- Malhi, Y., Doughty, C., & Galbraith, D. (2011). The allocation of ecosystem net primary productivity in tropical forests. *Philosophical Transactions of the Royal Society B: Biological Sciences*, 366(1582), 3225–3245. <https://doi.org/10.1098/rstb.2011.0062>

- Maltamo, M., Næsset, E., & Vauhkonen, J. (Eds.). (2014). *Forestry Applications of Airborne Laser Scanning: Concepts and Case Studies* (Vol. 27). Springer Netherlands. <https://doi.org/10.1007/978-94-017-8663-8>
- Mariaux, A. (1967). Les cernes dans les bois tropicaux africains. _ Nature et Périodicité. Peuvent-ils révéler l'âge des arbres? *Bois et Forêts des Tropiques*, 113, 3–14. <https://doi.org/10.19182/bft1967.113.a19012>
- Mariaux, A. (1969). La périodicité des cernes dans le bois de Limba. *Bois et Forêts des Tropiques*, 128, 39–54. <https://doi.org/10.19182/bft1969.128.a19059>
- Martin, A. R., & Thomas, S. C. (2011). A reassessment of carbon content in tropical trees. *PLoS ONE*, 6(8), e23533. <https://doi.org/10.1371/journal.pone.0023533>
- Mayaux, P., Pekel, J.-F., Desclée, B., Donnay, F., Lupi, A., Achard, F., Clerici, M., Bodart, C., Brink, A., Nasi, R., & Belward, A. (2013). State and evolution of the African rainforests between 1990 and 2010. *Philosophical Transactions of the Royal Society B: Biological Sciences*, 368(1625), 20120300. <https://doi.org/10.1098/rstb.2012.0300>
- Medlyn, B. E., Dreyer, E., Ellsworth, D., Forstreuter, M., Harley, P. C., Kirschbaum, M. U. F., Le Roux, X., Montpied, P., Strassmeyer, J., Walcroft, A., Wang, K., & Loustau, D. (2002). Temperature response of parameters of a biochemically based model of photosynthesis. II. A review of experimental data. *Plant, Cell & Environment*, 25(9), 1167–1179. <https://doi.org/10.1046/j.1365-3040.2002.00891.x>
- Megevand, C., Mosnier, A., Hourticq, J., Sanders, K., Doetinchem, N., & Streck, C. (2013). *Deforestation trends in the Congo Basin: Reconciling economic growth and forest protection*. The World Bank. <https://documents.worldbank.org/en/publication/documents-reports/documentdetail/175211468257358269/Deforestation-trends-in-the-Congo-Basin-reconciling-economic-growth-and-forest-protection>
- Mellerowicz, E. J., Riding, R. T., & Little, C. H. A. (1992). Periodicity of cambial activity in *Abies balsamea*. II. Effects of temperature and photoperiod on the size of the nuclear genome in fusiform cambial cells. *Physiologia Plantarum*, 85(3), 526–530. <https://doi.org/10.1111/j.1399-3054.1992.tb05821.x>
- Mencuccini, M., Salmon, Y., Mitchell, P., Hölttä, T., Choat, B., Meir, P., O'Grady, A., Tissue, D., Zweifel, R., Sevanto, S., & Pfautsch, S. (2017). An empirical method that separates irreversible stem radial growth from bark water content changes in trees: Theory and case studies. *Plant Cell Environ.*, 40(2), 290–303. <https://doi.org/10.1111/pce.12863>
- Metcalf, C. J. E., Horvitz, C. C., Tuljapurkar, S., & Clark, D. A. (2009). A time to grow and a time to die: A new way to analyze the dynamics of size, light, age, and death of tropical trees. *Ecology*, 90(10), 2766–2778. <https://doi.org/10.1890/08-1645.1>
- Mirabel, A., Girardin, M. P., Metsaranta, J., Way, D., & Reich, P. B. (2023). Increasing atmospheric dryness reduces boreal forest tree growth. *Nature Communications*, 14, 6901. <https://doi.org/10.1038/s41467-023-42466-1>
- Mohnen, D. (2008). Pectin structure and biosynthesis. *Current Opinion in Plant Biology*, 11(3), 266–277. <https://doi.org/10.1016/j.pbi.2008.03.006>
- Mokea, D. A., Basia, A. A., & Nkongolo, N. V. (2023). Predicting the Distribution of Tree Species and Their Biomass in Yangambi Biosphere Using Spatial Interpolation. *Trends in Agricultural Sciences*, 2(3), 221–231. <https://doi.org/10.17311/tas.2023.221.231>
- Monteiro, R. F. R. (1962). Le massif forestier du Mayumbe Angolais. *Bois et Forêts des Tropiques*, 82, 3–17. <https://doi.org/10.19182/bft1962.82.a18862>
- Morel, H., Mangenet, T., Beauchêne, J., Ruelle, J., Nicolini, E., Heuret, P., & Thibaut, B. (2015). Seasonal variations in phenological traits: Leaf shedding and cambial activity in *Parkia nitida* Miq. and *Parkia velutina* Benoist (Fabaceae) in tropical rainforest. *Trees*, 29(4), 973–984. <https://doi.org/10.1007/s00468-015-1177-4>
- Morin-Rivat, J., Fayolle, A., Favier, C., Bremond, L., Gourlet-Fleury, S., Bayol, N., Lejeune, P., Beeckman, H., & Doucet, J.-L. (2017). Present-day central African forest is a legacy of the 19th century human history. *eLife*, 6, e20343. <https://doi.org/10.7554/eLife.20343>
- Munzimi, Y. A., Hansen, M. C., Adusei, B., & Senay, G. B. (2015). *Characterizing Congo Basin Rainfall and Climate Using Tropical Rainfall Measuring Mission (TRMM) Satellite Data and Limited Rain Gauge Ground Observations*. <https://doi.org/10.1175/JAMC-D-14-0052.1>

- Nackoney, J., & Terada, S. (2023). The Importance of Monitoring Bonobos and Their Habitats for Informing Bonobo-Specific Conservation Prioritization and Planning. In T. Furuichi, G. Idani, D. Kimura, H. Ihobe, & C. Hashimoto (Eds.), *Bonobos and People at Wamba: 50 Years of Research* (pp. 443–461). Springer Nature. https://doi.org/10.1007/978-981-99-4788-1_32
- Nkem, J., Idinoba, M., & Sendashonga, C. (2008). *Forests for climate change adaptation in the congo basin: Responding to an urgent need with sustainable practices*. Center for International Forestry Research. <https://www.jstor.org/stable/resrep01868>
- Noyer, E., Stojanović, M., Horáček, P., & Pérez-de-Lis, G. (2023). Toward a better understanding of angiosperm xylogenesis: A new method for a cellular approach. *New Phytologist*, 239(2), 792–805. <https://doi.org/10.1111/nph.18959>
- Ortega, J. K. E. (2017). Dimensionless number is central to stress relaxation and expansive growth of the cell wall. *Scientific Reports*, 7(1), 3016. <https://doi.org/10.1038/s41598-017-03002-6>
- Orwig, D. A., Boucher, P., Paynter, I., Saenz, E., Li, Z., & Schaaf, C. (2018). The potential to characterize ecological data with terrestrial laser scanning in Harvard Forest, MA. *Interface Focus*, 8(2), 20170044. <https://doi.org/10.1098/rsfs.2017.0044>
- Oskolski, A. A., & Jansen, S. (2009). Distribution of scalariform and simple perforation plates within the vessel network in secondary xylem of Araliaceae and its implications for wood evolution. *Plant Systematics and Evolution*, 278(1), 43–51. <https://doi.org/10.1007/s00606-008-0130-z>
- Ouédraogo, D.-Y., Mortier, F., Gourlet-Fleury, S., Freycon, V., & Picard, N. (2013). Slow-growing species cope best with drought: Evidence from long-term measurements in a tropical semi-deciduous moist forest of Central Africa. *J. Ecol.*, 101(6), 1459–1470. <https://doi.org/10.1111/1365-2745.12165>
- Pan, Y., Birdsey, R. A., Fang, J., Houghton, R., Kauppi, P. E., Kurz, W. A., Phillips, O. L., Shvidenko, A., Lewis, S. L., Canadell, J. G., Ciais, P., Jackson, R. B., Pacala, S. W., McGuire, A. D., Piao, S., Rautiainen, A., Sitch, S., & Hayes, D. (2011). A Large and Persistent Carbon Sink in the World's Forests. *Science*, 333(6045), 988–993. <https://doi.org/10.1126/science.1201609>
- Pan, Y., Birdsey, R. A., Phillips, O. L., Houghton, R. A., Fang, J., Kauppi, P. E., Keith, H., Kurz, W. A., Ito, A., Lewis, S. L., Nabuurs, G.-J., Shvidenko, A., Hashimoto, S., Lerink, B., Schepaschenko, D., Castanho, A., & Murdiyarso, D. (2024). The enduring world forest carbon sink. *Nature*, 631(8021), 563–569. <https://doi.org/10.1038/s41586-024-07602-x>
- Pauly, M., Gille, S., Liu, L., Mansoori, N., de Souza, A., Schultink, A., & Xiong, G. (2013). Hemicellulose biosynthesis. *Planta*, 238(4), 627–642. <https://doi.org/10.1007/s00425-013-1921-1>
- Peh, K. S.-H., Lewis, S. L., & Lloyd, J. (2011). Mechanisms of monodominance in diverse tropical tree-dominated systems. *Journal of Ecology*, 99(4), 891–898. <https://doi.org/10.1111/j.1365-2745.2011.01827.x>
- Pérez, M. R., Ezzine de Blas, D., Nasi, R., Sayer, J. A., Sassen, M., Angoué, C., Gami, N., Ndoeye, O., Ngono, G., Nguingiri, J.-C., Nzala, D., Toirambe, B., & Yalibanda, Y. (2005). Logging in the Congo Basin: A multi-country characterization of timber companies. *Forest Ecology and Management*, 214(1), 221–236. <https://doi.org/10.1016/j.foreco.2005.04.020>
- Perez, T. M., & Feeley, K. J. (2018). Increasing humidity threatens tropical rainforests. *Frontiers in Ecology and Evolution*, 6. <https://doi.org/10.3389/fevo.2018.00068>
- Perez, T. M., & Feeley, K. J. (2020). Photosynthetic heat tolerances and extreme leaf temperatures. *Funct. Ecol.*, 34(11), 2236–2245. <https://doi.org/10.1111/1365-2435.13658>
- Peters, R. L., Steppe, K., Cuny, H. E., De Pauw, D. J. W., Frank, D. C., Schaub, M., Rathgeber, C. B. K., Cabon, A., & Fonti, P. (2021). Turgor – a limiting factor for radial growth in mature conifers along an elevational gradient. *New Phytol.*, 229(1), 213–229. <https://doi.org/10.1111/nph.16872>
- Pettersen, R. C., & Rowell, R. M. (1984). The chemical composition of wood. In *The Chemistry of Solid Wood* (world; Vol. 207, p. 614). American Chemical Society. <https://doi.org/10.1021/ba-1984-0207.ch002>
- Philippon, N., Cornu, G., Monteil, L., Gond, V., Moron, V., Pergaud, J., Sèze, G., Bigot, S., Camberlin, P., Doumenge, C., Fayolle, A., & Ngomanda, A. (2019). The light-deficient climates of western Central African evergreen forests. *Environmental Research Letters*, 14(3), 034007. <https://doi.org/10.1088/1748-9326/aaf5d8>

- Piabuo, S. M., Minang, P. A., Tieguhong, C. J., Foundjem-Tita, D., & Nghobuoche, F. (2021). Illegal logging, governance effectiveness and carbon dioxide emission in the timber-producing countries of Congo Basin and Asia. *Environment, Development and Sustainability*, 23(10), 14176–14196. <https://doi.org/10.1007/s10668-021-01257-8>
- Pineda-García, F., Paz, H., & Meinzer, F. C. (2013). Drought resistance in early and late secondary successional species from a tropical dry forest: The interplay between xylem resistance to embolism, sapwood water storage and leaf shedding. *Plant, Cell & Environment*, 36(2), 405–418. <https://doi.org/10.1111/j.1365-3040.2012.02582.x>
- Plomion, C., Leprovost, G., & Stokes, A. (2001). Wood formation in trees. *Plant Physiology*, 127(4), 1513–1523. <https://doi.org/10.1104/pp.010816>
- Pompa-García, M., & Camarero, J. J. (Eds.). (2020). *Latin American Dendroecology: Combining Tree-Ring Sciences and Ecology in a Megadiverse Territory*. Springer. <https://doi.org/10.1007/978-3-030-36930-9>
- Prislan, P., Gričar, J., de Luis, M., Novak, K., Martinez del Castillo, E., Schmitt, U., Koch, G., Štrus, J., Mrak, P., Žnidarič, M. T., & Čufar, K. (2016). Annual Cambial Rhythm in *Pinus halepensis* and *Pinus sylvestris* as Indicator for Climate Adaptation. *Frontiers in Plant Science*, 7. <https://doi.org/10.3389/fpls.2016.01923>
- Pumijumnong, N., & Buajan, S. (2013). Seasonal cambial activity of five tropical tree species in central Thailand. *Trees*, 27(2), 409–417. <https://doi.org/10.1007/s00468-012-0794-4>
- Pumijumnong, N., Muangsong, C., Buajan, S., Songtrirat, P., Chatwatthana, R., & Chareonwong, U. (2023). Factors Affecting Cambial Growth Periodicity and Wood Formation in Tropical Forest Trees: A Review. *Forests*, 14(5), Article 5. <https://doi.org/10.3390/f14051025>
- Quarta, G., D’Elia, M., Valzano, D., & Calcagnile, L. (2005). New bomb pulse radiocarbon records from annual tree rings in the northern hemisphere temperate region. *Radiocarbon*, 47(1), 27–30. <https://doi.org/10.1017/S0033822200052164>
- R Core Team. (2023). *R: A Language and Environment for Statistical Computing*. R Foundation for Statistical Computing.
- Rahman, M. H., Nugroho, W. D., Nakaba, S., Kitin, P., Kudo, K., Yamagishi, Y., Begum, S., Marsoem, S. N., & Funada, R. (2019). Changes in cambial activity are related to precipitation patterns in four tropical hardwood species grown in Indonesia. *American Journal of Botany*, 106(6), 760–771.
- Ralph, J., Lundquist, K., Brunow, G., Lu, F., Kim, H., Schatz, P. F., Marita, J. M., Hatfield, R. D., Ralph, S. A., Christensen, J. H., & Boerjan, W. (2004). Lignins: Natural polymers from oxidative coupling of 4-hydroxyphenyl- propanoids. *Phytochemistry Reviews*, 3(1), 29–60. <https://doi.org/10.1023/B:PHYT.0000047809.65444.a4>
- Rathgeber, C. B. K., Cuny, H. E., & Fonti, P. (2016). Biological basis of tree-ring formation: A crash course. *Frontiers in Plant Science*, 7. <https://doi.org/10.3389/fpls.2016.00734>
- Ray, D. M., & Savage, J. A. (2021). Seasonal changes in temperate woody plant phloem anatomy and physiology: Implications for long-distance transport. *AoB PLANTS*, 13(4). <https://doi.org/10.1093/aobpla/plab028>
- Reich, P. B. (2014). The world-wide ‘fast–slow’ plant economics spectrum: A traits manifesto. *Journal of Ecology*, 102(2), 275–301. <https://doi.org/10.1111/1365-2745.12211>
- Réjou-Méchain, M., Mortier, F., Bastin, J.-F., Cornu, G., Barbier, N., Bayol, N., Bénédet, F., Bry, X., Dauby, G., Deblauwe, V., Doucet, J.-L., Doumenge, C., Fayolle, A., Garcia, C., Kibamba Lubamba, J.-P., Loumeto, J.-J., Ngomanda, A., Ploton, P., Sonké, B., ... Gourlet-Fleury, S. (2021). Unveiling African rainforest composition and vulnerability to global change. *Nature*, 593(7857), 90–94. <https://doi.org/10.1038/s41586-021-03483-6>
- Riding, R. T., & Little, C. H. A. (1984). Anatomy and histochemistry of *Abies balsamea* cambial zone cells during the onset and breaking of dormancy. *Canadian Journal of Botany*, 62(12), 2570–2579. <https://doi.org/10.1139/b84-349>
- Rittner, D., & McCabe, T. L. (2004). *Encyclopedia of biology*. Facts On File.
- Rossi, S., Anfodillo, T., & Menardi, R. (2006). Trephor: A new tool for sampling microcores from tree stems. *IAWA Journal*, 27(1), 89–97. <https://doi.org/10.1163/22941932-90000139>

- Rossi, S., Deslauriers, A., & Anfodillo, T. (2006). Assessment of Cambial Activity and Xylogenesis by Microsampling Tree Species: An Example at the Alpine Timberline. *IAWA Journal*, 27(4), 383–394. <https://doi.org/10.1163/22941932-90000161>
- Rozendaal, D. M. A., & Zuidema, P. A. (2011). Dendroecology in the tropics: A review. *Trees*, 25(1), 3–16. <https://doi.org/10.1007/s00468-010-0480-3>
- Rudall, P. J. (2007). *Anatomy of flowering plants: An introduction to structure and development* (Third). Cambridge University Press.
- Salmén, L. (2018). Wood cell wall structure and organisation in relation to mechanics. In A. Geitmann & J. Gril (Eds.), *Plant Biomechanics: From Structure to Function at Multiple Scales* (pp. 3–19). Springer International Publishing. https://doi.org/10.1007/978-3-319-79099-2_1
- Savard, M. M., & Siegwolf, R. T. W. (2022). Nitrogen isotopes in tree rings—Challenges and prospects. In R. T. W. Siegwolf, J. R. Brooks, J. Roden, & M. Saurer (Eds.), *Stable Isotopes in Tree Rings: Inferring Physiological, Climatic and Environmental Responses* (pp. 361–380). Springer International Publishing. https://doi.org/10.1007/978-3-030-92698-4_12
- Savidge, R. A. (1996). Xylogenesis, Genetic and Environmental Regulation—A Review-. *IAWA Journal*, 17(3), 269–310. <https://doi.org/10.1163/22941932-90001580>
- Schöngart, J., Piedade, M. T. F., Ludwigshausen, S., Horna, V., & Worbes, M. (2002). Phenology and stem-growth periodicity of tree species in Amazonian floodplain forests. *Journal of Tropical Ecology*, 18(4), 581–597. <https://doi.org/10.1017/S0266467402002389>
- Schuetz, M., Smith, R., & Ellis, B. (2013). Xylem tissue specification, patterning, and differentiation mechanisms. *Journal of Experimental Botany*, 64(1), 11–31. <https://doi.org/10.1093/jxb/ers287>
- Sénéchal, J., Matuka Kabala, & Fournier, F. (1989). *Revue des Connaissances sur le Mayombe*. UNESCO-PNUD. <https://library.wur.nl/WebQuery/isric/2254166>
- Seo, J.-W., Eckstein, D., & Schmitt, U. (2007). The pinning method: From pinning to data preparation. *Dendrochronologia*, 25(2), 79–86. <https://doi.org/10.1016/j.dendro.2007.04.001>
- Singh, K. P., & Kushwaha, C. P. (2016). Deciduousness in tropical trees and its potential as indicator of climate change: A review. *Ecological Indicators*, 69, 699–706. <https://doi.org/10.1016/j.ecolind.2016.04.011>
- Slik, J. W. F., Paoli, G., McGuire, K., Amaral, I., Barroso, J., Bastian, M., Blanc, L., Bongers, F., Boundja, P., Clark, C., Collins, M., Dauby, G., Ding, Y., Doucet, J.-L., Eler, E., Ferreira, L., Forshed, O., Fredriksson, G., Gillet, J.-F., ... Zweifel, N. (2013). Large trees drive forest aboveground biomass variation in moist lowland forests across the tropics. *Global Ecology and Biogeography*, 22(12), 1261–1271. <https://doi.org/10.1111/geb.12092>
- Somorin, O. A., Brown, H. C. P., Visseren-Hamakers, I. J., Sonwa, D. J., Arts, B., & Nkem, J. (2012). The Congo Basin forests in a changing climate: Policy discourses on adaptation and mitigation (REDD+). *Global Environmental Change*, 22(1), 288–298. <https://doi.org/10.1016/j.gloenvcha.2011.08.001>
- Speer, J. H. (2010). *Fundamentals of Tree-Ring Research*. University of Arizona Press. <https://doi.org/10.1002/gea.20357>
- Sperry, J. S., Hacke, U. G., & Pittermann, J. (2006). Size and function in conifer tracheids and angiosperm vessels. *American Journal of Botany*, 93(10), 1490–1500. <https://doi.org/10.3732/ajb.93.10.1490>
- Stanton, D. W. G., Hart, J., Galbusera, P., Helsen, P., Shephard, J., Kümpel, N. F., Wang, J., Ewen, J. G., & Bruford, M. W. (2014). Distinct and Diverse: Range-Wide Phylogeography Reveals Ancient Lineages and High Genetic Variation in the Endangered Okapi (*Okapia johnstoni*). *PLoS ONE*, 9(7), e101081. <https://doi.org/10.1371/journal.pone.0101081>
- Stanton, D. W. G., Hart, J., Kümpel, N. F., Vosper, A., Nixon, S., Bruford, M. W., Ewen, J. G., & Wang, J. (2015). Enhancing knowledge of an endangered and elusive species, the okapi, using non-invasive genetic techniques. *Journal of Zoology*, 295(4), 233–242. <https://doi.org/10.1111/jzo.12205>
- Stephenson, N. L., Das, A. J., Condit, R., Russo, S. E., Baker, P. J., Beckman, N. G., Coomes, D. A., Lines, E. R., Morris, W. K., Rüger, N., Alvarez, E., Blundo, C., Bunyavejchewin, S., Chuyong, G., Davies, S. J., Duque, Á., Ewango, C. N., Flores, O., Franklin, J. F., ... Zavala, M. A. (2014). Rate of tree carbon accumulation increases continuously with tree size. *Nature*, 507(7490), 90–93. <https://doi.org/10.1038/nature12914>

- Steppe, K., Sterck, F., & Deslauriers, A. (2015). Diel growth dynamics in tree stems: Linking anatomy and ecophysiology. *Trends Plant Sci.*, 20(6), 335–343. <https://doi.org/10.1016/j.tplants.2015.03.015>
- Strindberg, S., Maisels, F., Williamson, E. A., Blake, S., Stokes, E. J., Aba'a, R., Abitsi, G., Agbor, A., Ambahe, R. D., Bakabana, P. C., Bechem, M., Berlemont, A., Bokoto de Semboli, B., Boundja, P. R., Bout, N., Breuer, T., Campbell, G., De Wachter, P., Ella Akou, M., ... Wilkie, D. S. (2018). Guns, germs, and trees determine density and distribution of gorillas and chimpanzees in Western Equatorial Africa. *Science Advances*, 4(4), eaar2964. <https://doi.org/10.1126/sciadv.aar2964>
- Sullivan, M. J. P., Lewis, S. L., Affum-Baffoe, K., Castilho, C., Costa, F., Sanchez, A. C., Ewango, C. E. N., Hubau, W., Marimon, B., Monteagudo-Mendoza, A., Qie, L., Sonké, B., Martinez, R. V., Baker, T. R., Brien, R. J. W., Feldpausch, T. R., Galbraith, D., Gloor, M., Malhi, Y., ... Phillips, O. L. (2020). Long-term thermal sensitivity of Earth's tropical forests. *Science*, 368(6493), 869–874. <https://doi.org/10.1126/science.aaw7578>
- Sullivan, M. J. P., Talbot, J., Lewis, S. L., Phillips, O. L., Qie, L., Begne, S. K., Chave, J., Cuni-Sanchez, A., Hubau, W., Lopez-Gonzalez, G., Miles, L., Monteagudo-Mendoza, A., Sonké, B., Sunderland, T., ter Steege, H., White, L. J. T., Affum-Baffoe, K., Aiba, S., de Almeida, E. C., ... Zeng, L. (2017). Diversity and carbon storage across the tropical forest biome. *Scientific Reports*, 7(1), 39102. <https://doi.org/10.1038/srep39102>
- Taiz, L., & Zeiger, E. (2010). *Plant Physiology* (5th edition). Sinauer Associates Inc.
- Tan, L., Eberhard, S., Pattathil, S., Warder, C., Glushka, J., Yuan, C., Hao, Z., Zhu, X., Avci, U., Miller, J. S., Baldwin, D., Pham, C., Orlando, R., Darvill, A., Hahn, M. G., Kieliszewski, M. J., & Mohnen, D. (2013). An arabidopsis cell wall proteoglycan consists of pectin and arabinoxylan covalently linked to an arabinogalactan protein. *The Plant Cell*, 25(1), 270–287. <https://doi.org/10.1105/tpc.112.107334>
- Tanaka, T., Kurokawa, C., & Oikawa, S. (2018). Leaf shedding increases the photosynthetic rate of the canopy in N₂-fixing and non-N₂-fixing woody species. *Tree Physiology*, 38(12), 1903–1911. <https://doi.org/10.1093/treephys/tpy104>
- Tarelkin, Y., Delvaux, C., Ridder, M. D., Berkani, T. E., Cannière, C. D., & Beeckman, H. (2016). Growth-Ring Distinctness and Boundary Anatomy Variability in Tropical Trees. *IAWA Journal*, 37(2), 275–S7. <https://doi.org/10.1163/22941932-20160134>
- Tarelkin, Y., Hufkens, K., Hahn, S., Van den Bulcke, J., Bastin, J.-F., Ilondea, B. A., Debeir, O., Van Acker, J., Beeckman, H., & De Cannière, C. (2019). Wood anatomy variability under contrasted environmental conditions of common deciduous and evergreen species from central African forests. *Trees*, 33(3), 893–909. <https://doi.org/10.1007/s00468-019-01826-5>
- Thomas, S. C., & Martin, A. R. (2012). Carbon content of tree tissues: A synthesis. *Forests*, 3(2), Article 2. <https://doi.org/10.3390/f3020332>
- Timell, T. E. (1967). Recent progress in the chemistry of wood hemicelluloses. *Wood Science and Technology*, 1(1), 45–70. <https://doi.org/10.1007/BF00592255>
- Torti, S. D., Coley, P. D., & Kursar, T. A. (2001). Causes and consequences of monodominance in tropical lowland forests. *Am. Nat.*, 157(2), 141–153. <https://doi.org/10.1086/318629>
- Torti, S. D., Coley, P. D., Kursar, T. A., & Wedin, A. E. D. A. (2001). Causes and Consequences of Monodominance in Tropical Lowland Forests. *The American Naturalist*, 157(2), 141–153. <https://doi.org/10.1086/318629>
- Trenberth, K. E. (2011). Changes in precipitation with climate change. *Clim. Res.*, 47(1–2), 123–138. <https://doi.org/10.3354/cr00953>
- Trouet, V., Coppin, P., & Beeckman, H. (2006). Annual Growth Ring Patterns in Brachystegia spiciformis Reveal Influence of Precipitation on Tree Growth. *Biotropica*, 38(3), 375–382.
- Tsen, E. W. J., Sitzia, T., & Webber, B. L. (2016). To core, or not to core: The impact of coring on tree health and a best-practice framework for collecting dendrochronological information from living trees. *Biological Reviews*, 91(4), 899–924. <https://doi.org/10.1111/brv.12200>
- Tumajer, J., & Leheček, J. (2019). Boreal tree-rings are influenced by temperature up to two years prior to their formation: A trade-off between growth and reproduction? *Environmental Research Letters*, 14(12), 124024. <https://doi.org/10.1088/1748-9326/ab5134>

- Turco, G. M., Rodriguez-Medina, J., Siebert, S., Han, D., Valderrama-Gómez, M. Á., Vahldick, H., Shulse, C. N., Cole, B. J., Juliano, C. E., Dickel, D. E., Savageau, M. A., & Brady, S. M. (2019). Molecular mechanisms driving switch behavior in xylem cell differentiation. *Cell Reports*, 28(2), 342–351.e4. <https://doi.org/10.1016/j.celrep.2019.06.041>
- UNEP. (2023, February 27). *Critical ecosystems: Congo Basin peatlands*. <https://www.unep.org/news-and-stories/story/critical-ecosystems-congo-basin-peatlands>
- van den Berg, E., Chazdon, R., & Corrêa, B. S. (2012). Tree growth and death in a tropical gallery forest in Brazil: Understanding the relationships among size, growth, and survivorship for understory and canopy dominant species. *Plant Ecol.*, 213(7), 1081–1092. <https://doi.org/10.1007/s11258-012-0067-8>
- Verbančič, J., Lunn, J. E., Stitt, M., & Persson, S. (2018). Carbon supply and the regulation of cell wall synthesis. *Molecular Plant*, 11(1), 75–94. <https://doi.org/10.1016/j.molp.2017.10.004>
- Verdu, P. (2016). African Pygmies. *Current Biology*, 26(1), R12–R14. <https://doi.org/10.1016/j.cub.2015.10.023>
- Vieira, J., Carvalho, A., & Campelo, F. (2020). Tree growth under climate change: Evidence from xylogenesis timings and kinetics. *Frontiers in Plant Science*, 11, 90. <https://doi.org/10.3389/fpls.2020.00090>
- Vieira, J., Rossi, S., Campelo, F., Freitas, H., & Nabais, C. (2014). Xylogenesis of *Pinus pinaster* under a Mediterranean climate. *Annals of Forest Science*, 71(1), Article 1. <https://doi.org/10.1007/s13595-013-0341-5>
- Vieira, S., de Camargo, P. B., Selhorst, D., da Silva, R., Huttyra, L., Chambers, J. Q., Brown, I. F., Higuchi, N., dos Santos, J., Wofsy, S. C., Trumbore, S. E., & Martinelli, L. A. (2004). Forest structure and carbon dynamics in Amazonian tropical rain forests. *Oecologia*, 140(3), 468–479. <https://doi.org/10.1007/s00442-004-1598-z>
- Vlam, M., Baker, P. J., Bunyavejchewin, S., & Zuidema, P. A. (2014). Temperature and rainfall strongly drive temporal growth variation in Asian tropical forest trees. *Oecologia*, 174(4), 1449–1461. <https://doi.org/10.1007/s00442-013-2846-x>
- Wagner, F., Rossi, V., Aubry-Kientz, M., Bonal, D., Dalitz, H., Gliniars, R., Stahl, C., Trabucco, A., & Hérault, B. (2014). Pan-Tropical Analysis of Climate Effects on Seasonal Tree Growth. *PLOS ONE*, 9(3), e92337. <https://doi.org/10.1371/journal.pone.0092337>
- Wang, D., Chen, Y., Li, W., Li, Q., Lu, M., Zhou, G., & Chai, G. (2021). Vascular cambium: The source of wood formation. *Frontiers in Plant Science*, 12. <https://doi.org/10.3389/fpls.2021.700928>
- Wang, S., Zhang, X., Hou, L., Sun, J., & Xu, M. (2024). Estimating Global Gross Primary Production Using an Improved MODIS Leaf Area Index Dataset. *Remote Sensing*, 16(19), Article 19. <https://doi.org/10.3390/rs16193731>
- White, L. J. T., Bazaiba Masudi, E., Ndongo, J. D., Matondo, R., Soudan-Nonault, A., Ngomanda, A., Averti, I. S., Ewango, C. E. N., Sonké, B., & Lewis, S. L. (2021). Congo Basin rainforest—Invest US\$150 million in science. *Nature*, 598(7881), 411–414. <https://doi.org/10.1038/d41586-021-02818-7>
- WMO. (2023). *WMO Global Annual to Decadal Climate Update (Target years: 2023-2027)*. World Meteorological Organization. https://library.wmo.int/index.php?lvl=notice_display&id=22272
- Wolberg, S., Haim, M., & Shtein, I. (2023). Simple differential staining method of paraffin-embedded plant sections with safranin-alcian blue. *IAWA Journal*, 44(2), 170–175. <https://doi.org/10.1163/22941932-bja10124>
- Worbes, M. (1999). Annual growth rings, rainfall-dependent growth and long-term growth patterns of tropical trees from the Caparo Forest Reserve in Venezuela. *J. Ecol.*, 87(3), 391–403. <https://doi.org/10.1046/j.1365-2745.1999.00361.x>
- Worbes, M. (2002). One Hundred Years of Tree-Ring Research in the Tropics – a Brief History and an Outlook to Future Challenges. *Dendrochronologia*, 20(1), 217–231. <https://doi.org/10.1078/1125-7865-00018>
- Worbes, M. (2011). Wood Anatomy and Tree-Ring Structure and Their Importance for Tropical Dendrochronology. In W. J. Junk, M. T. F. Piedade, F. Wittmann, J. Schöngart, & P. Parolin (Eds.), *Amazonian Floodplain Forests: Ecophysiology, Biodiversity and Sustainable Management* (pp. 329–346). Springer Netherlands. https://doi.org/10.1007/978-90-481-8725-6_17

- Wróblewska, M. M. (2015). The progressive and ancestral traits of the secondary xylem within Magnolia clad – the early diverging lineage of flowering plants. *Acta Societatis Botanicorum Poloniae*, 84(1), Article 1. <https://doi.org/10.5586/asbp.2014.028>
- Wu, J., Serbin, S. P., Xu, X., Albert, L. P., Chen, M., Meng, R., Saleska, S. R., & Rogers, A. (2017). The phenology of leaf quality and its within-canopy variation is essential for accurate modeling of photosynthesis in tropical evergreen forests. *Global Change Biology*, 23(11), 4814–4827. <https://doi.org/10.1111/gcb.13725>
- Xiang, B., Wielgosz, M., Kontogianni, T., Peters, T., Puliti, S., Astrup, R., & Schindler, K. (2024). Automated forest inventory: Analysis of high-density airborne LiDAR point clouds with 3D deep learning. *Remote Sensing of Environment*, 305, 114078. <https://doi.org/10.1016/j.rse.2024.114078>
- Xu, H., Giannetti, A., Sugiyama, Y., Zheng, W., Schneider, R., Watanabe, Y., Oda, Y., & Persson, S. (2022). Secondary cell wall patterning—Connecting the dots, pits and helices. *Open Biology*, 12(5), 210208. <https://doi.org/10.1098/rsob.210208>
- Xu, T., Zhi, S., Su, Y., Li, Z., & Zheng, E. (2022). Water transport characteristics of multiple structures of xylem vessels in magnolia. *Forests*, 13(10), Article 10. <https://doi.org/10.3390/f13101617>
- Yuan, W., Zheng, Y., Piao, S., Ciais, P., Lombardozzi, D., Wang, Y., Ryu, Y., Chen, G., Dong, W., Hu, Z., Jain, A. K., Jiang, C., Kato, E., Li, S., Lienert, S., Liu, S., Nabel, J. E. M. S., Qin, Z., Quine, T., ... Yang, S. (2019). Increased atmospheric vapor pressure deficit reduces global vegetation growth. *Science Advances*, 5(8), eaax1396. <https://doi.org/10.1126/sciadv.aax1396>
- Yuh, Y. G., N’Goran, K. P., Kross, A., Heurich, M., Matthews, H. D., & Turner, S. E. (2024). Monitoring forest cover and land use change in the Congo Basin under IPCC climate change scenarios. *PLOS ONE*, 19(12), e0311816. <https://doi.org/10.1371/journal.pone.0311816>
- Zarra, I., Revilla, G., Sampedro, J., & Valdivia, E. R. (2020). Biosynthesis and Regulation of Secondary Cell Wall. In F. M. Cánovas, U. Lüttge, C. Leuschner, & M.-C. Risueño (Eds.), *Progress in Botany Vol. 81* (pp. 189–226). Springer International Publishing. https://doi.org/10.1007/124_2019_27
- Zuidema, P. A., Babst, F., Groenendijk, P., Trouet, V., Abiyu, A., Acuña-Soto, R., Adenesky-Filho, E., Alfaro-Sánchez, R., Aragão, J. R. V., Assis-Pereira, G., Bai, X., Barbosa, A. C., Battipaglia, G., Beeckman, H., Botosso, P. C., Bradley, T., Bräuning, A., Brien, R., Buckley, B. M., ... Zhou, Z.-K. (2022). Tropical tree growth driven by dry-season climate variability. *Nature Geoscience*, 15(4), Article 4. <https://doi.org/10.1038/s41561-022-00911-8>
- Zuidema, P. A., Brien, R. J. W., & Schöngart, J. (2012). Tropical forest warming: Looking backwards for more insights. *Trends in Ecology & Evolution*, 27(4), 193–194. <https://doi.org/10.1016/j.tree.2011.12.007>
- Zweifel, R. (2016). Radial stem variations – a source of tree physiological information not fully exploited yet. *Plant Cell Environ.*, 39(2), 231–232. <https://doi.org/10.1111/pce.12613>
- Zweifel, R., Haeni, M., Buchmann, N., & Eugster, W. (2016). Are trees able to grow in periods of stem shrinkage? *New Phytologist*, 211(3), 839–849. <https://doi.org/10.1111/nph.13995>
- Zweifel, R., Sterck, F., Braun, S., Buchmann, N., Eugster, W., Gessler, A., Häni, M., Peters, R. L., Walthert, L., Wilhelm, M., Ziemińska, K., & Etzold, S. (2021). Why Trees Grow at Night. *New Phytologist*, 231(6), 2174–2185. <https://doi.org/10.1111/nph.17552>

Appendices

Chapter 2: Diel and annual rhythms of tropical stem size changes in the Mayombe forest, Congo Basin.

Table S2 – 1. Annual growth rate of tree individuals by phenological year.

Phenological year	Species	Tree id.	Annual GR ($\mu\text{m}/\text{yr}$)
2013-2014	<i>T. superba</i>	TermA	7287.68
2013-2014	<i>T. superba</i>	TermB	3693.54
2013-2014	<i>T. superba</i>	TermC	1891.08
2013-2014	<i>T. superba</i>	TermD	1257.12
2014-2015	<i>T. superba</i>	TermA	4378.53
2014-2015	<i>T. superba</i>	TermB	6860.61
2014-2015	<i>T. superba</i>	TermC	2796.33
2014-2015	<i>T. superba</i>	TermD	4966.81
2018-2019	<i>C.mildbraedii</i>	C.mildbraedii	3502.00
2018-2019	<i>C.bruneelii</i>	C.bruneelii	676.70
2018-2019	<i>C.paniculata</i>	C.paniculata	1324.66
2018-2019	<i>F.elastica</i>	F.elastica	1224.21
2018-2019	<i>G.giganteum</i>	G.giganteum	2039.36
2018-2019	<i>G.suaveolens</i>	G.suaveolens	1201.82
2018-2019	<i>H.gabunense</i>	H.gabunense	319.92
2018-2019	<i>I.dewevrei</i>	I.dewevrei	1245.46
2018-2019	<i>M.puberula</i>	M.puberula	31.24
2018-2019	<i>O.gore</i>	O.gore	4176.04
2021-2022	<i>F.elastica</i>	Fe1039	1188.29
2021-2022	<i>F.elastica</i>	Fe1040	2678.33
2021-2022	<i>F.elastica</i>	Fe1046	2218.73

Table S2 – 2. Output parameters of Gaussian RBF kernel models applied to our data set.

Variables	Sigma (σ)	Number of Support Vectors	Objective Function Value	Training Error	proportion of classified data points (%)
Precipitation (mm) - VPD (kPa)	2.2893	440	-238.4164	0.9462	5.38
RH (%) - Temperature ($^{\circ}\text{C}$)	3.4258	423	-224.4136	0.8778	12.22
Precipitation (mm) - Temperature ($^{\circ}\text{C}$)	2.4410	430	-229.9569	0.8677	13.23

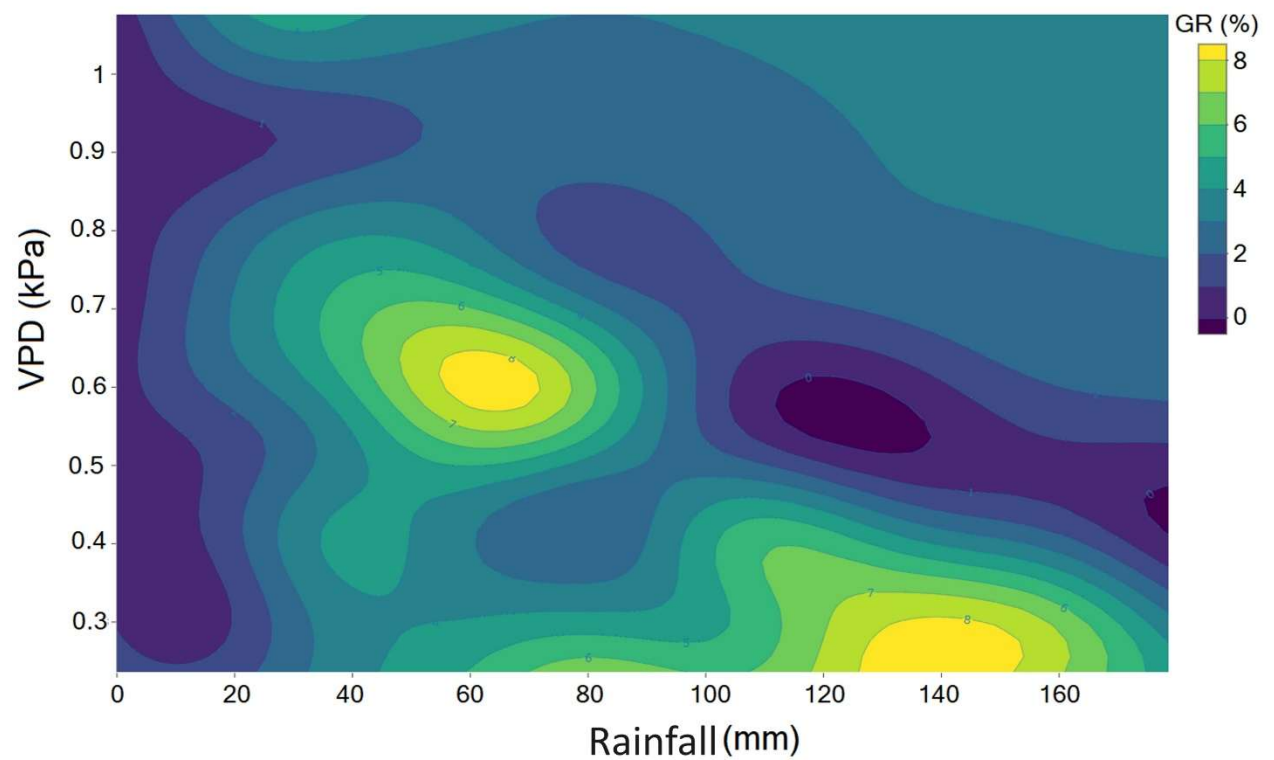


Figure S2 – 1. Biweekly-resolved, radial annual GR in the measured space of VPD and rainfall across all individual trees. GR was quantified as the relative annual contribution to the total annual growth for each tree and ranged from dark purple (no growth, 0%), over yellow (marginal growth, $\geq 8\%$).

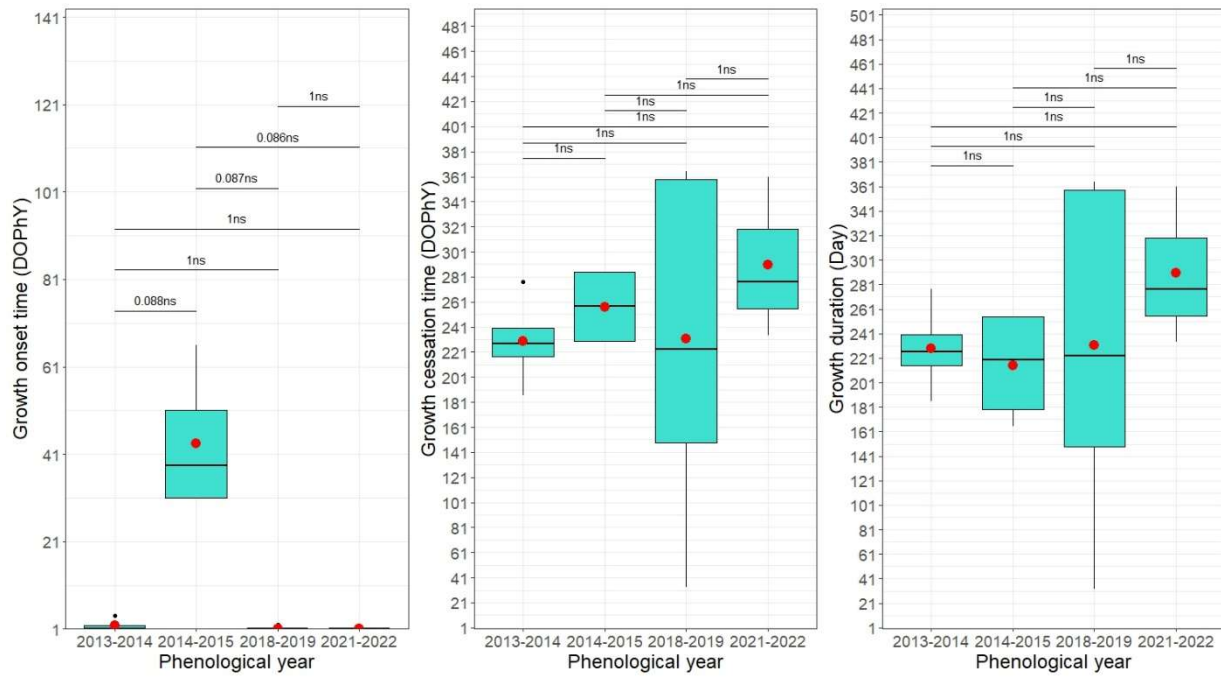


Figure S2 – 2. Growth onset and cessation times and growth duration (in Day of the Phenological Year (DOPhY)) for the 2013-2014, 2014-2015, 2018-2019 and 2021-2022 phenological year. The horizontal bases of the box indicate the 25th and 75th percentiles, the horizontal line inside the box represent the median, the vertical lines attached to the box represent the minimum and maximum values, the red dot inside the box represents the mean value. The black dots are outliers. The numbers above the boxes indicate the p-values of the student test (i.e., the probability that an observed difference between two means is significant), ns means not significant.

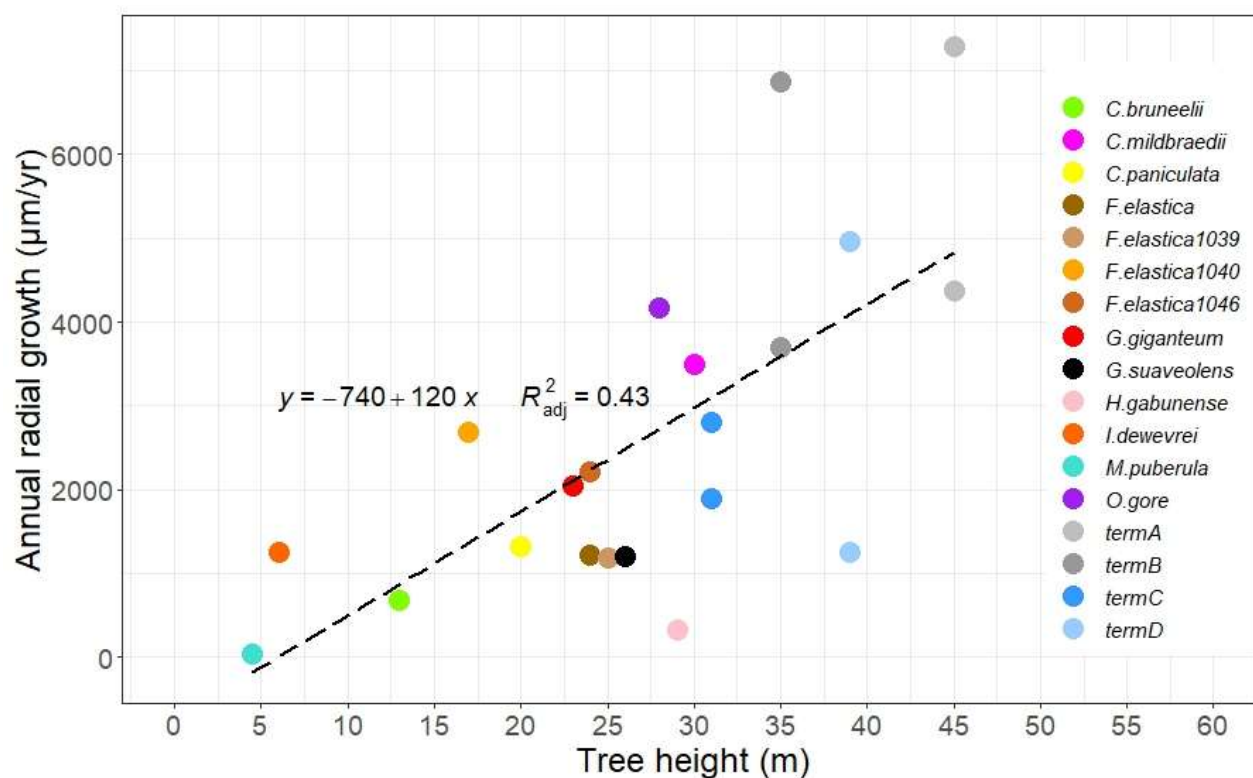


Figure S2 – 3. Correlation between tree height and annual growth. Tree height is significantly correlated with seasonal growth. This means that growth is lower in the understory than in the canopy.

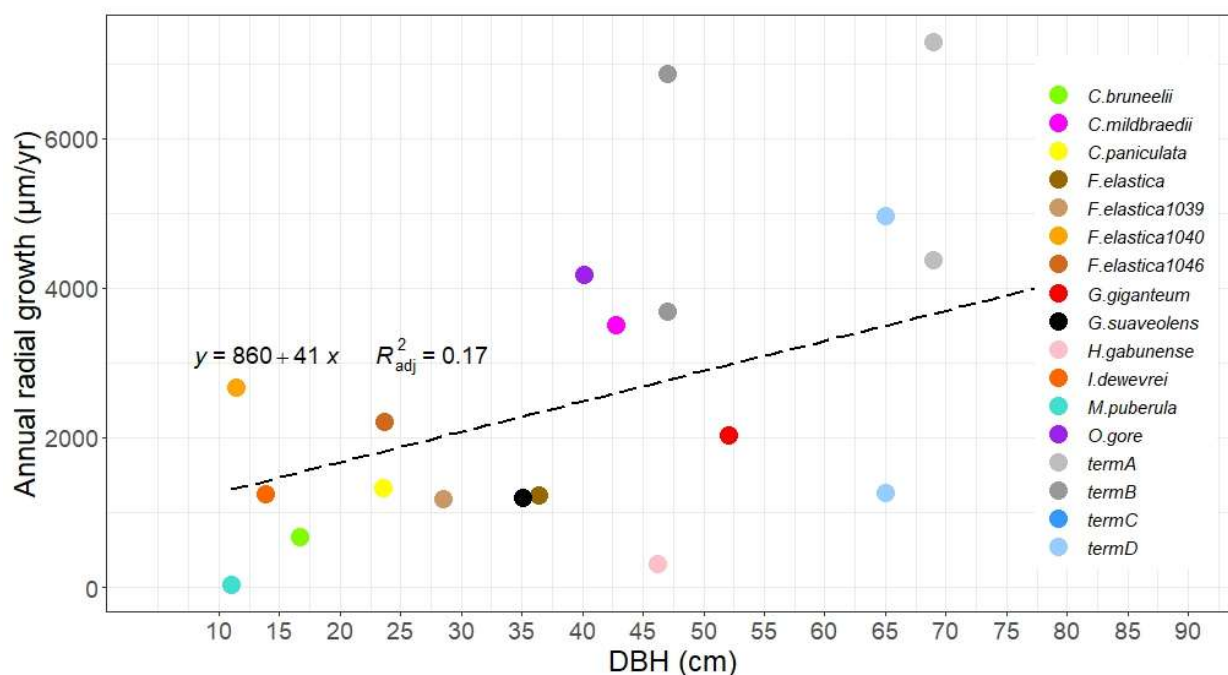


Figure S2 – 4. Correlation between tree DBH and annual radial growth. Tree DBH is significantly but weakly correlated with seasonal growth, suggesting that growth is higher for large-diameter trees than for small-diameter trees.

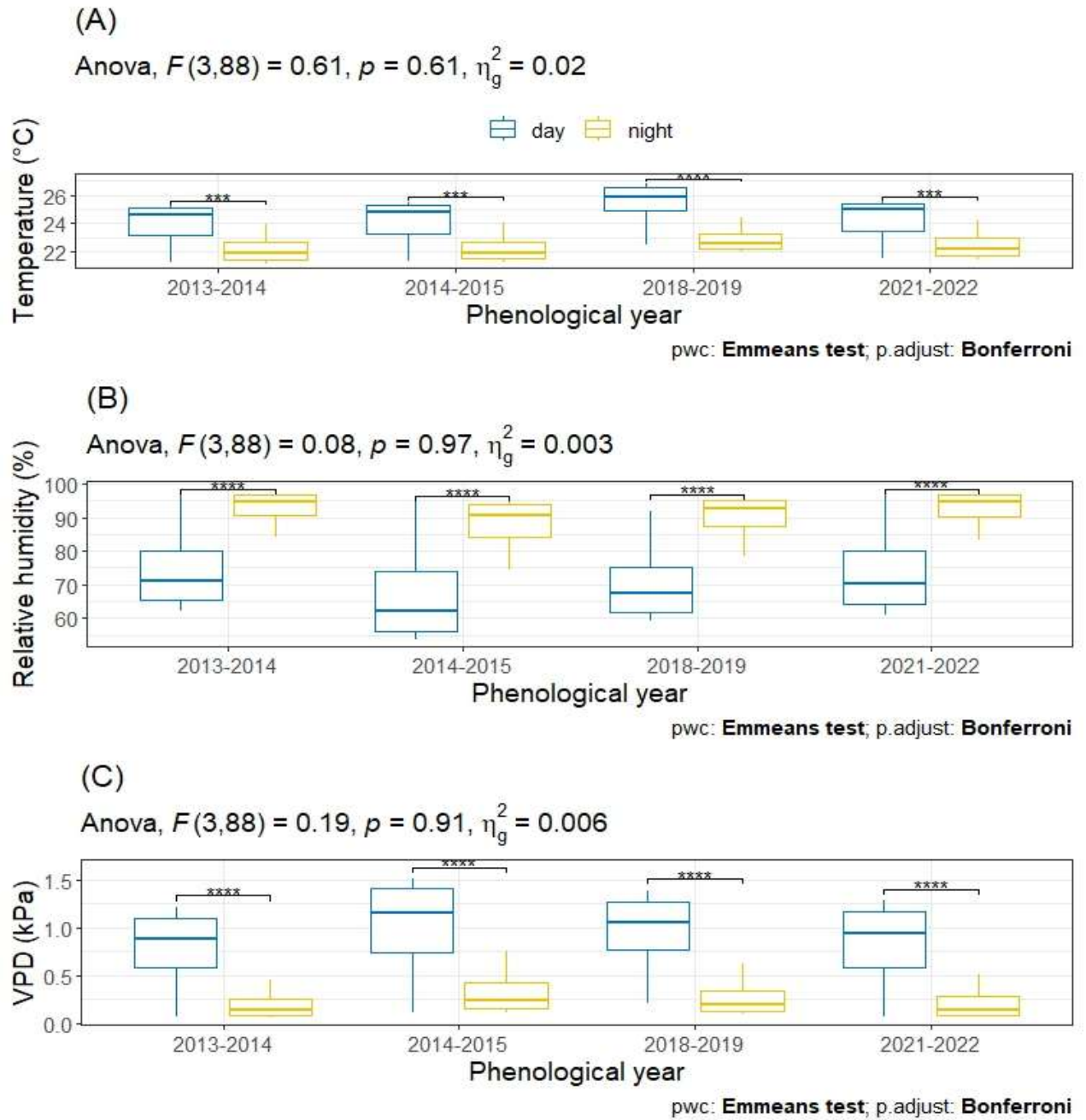


Figure S2 – 5. Daytime and nighttime climatic variables for the 2013-2014, 2014-2015, 2018-2019, and 2021-2022 phenological year. The horizontal bases of the box indicate the 25th and 75th percentiles, the horizontal line inside the box represents the median, the vertical lines attached to the box represent the minimum and maximum values. The dots are outliers. Asterisks indicate that differences are significant between daytime and nighttime values. Hourly mean temperature is shown in (A), hourly mean relative humidity in (B), and hourly mean vapor pressure deficit in (C).

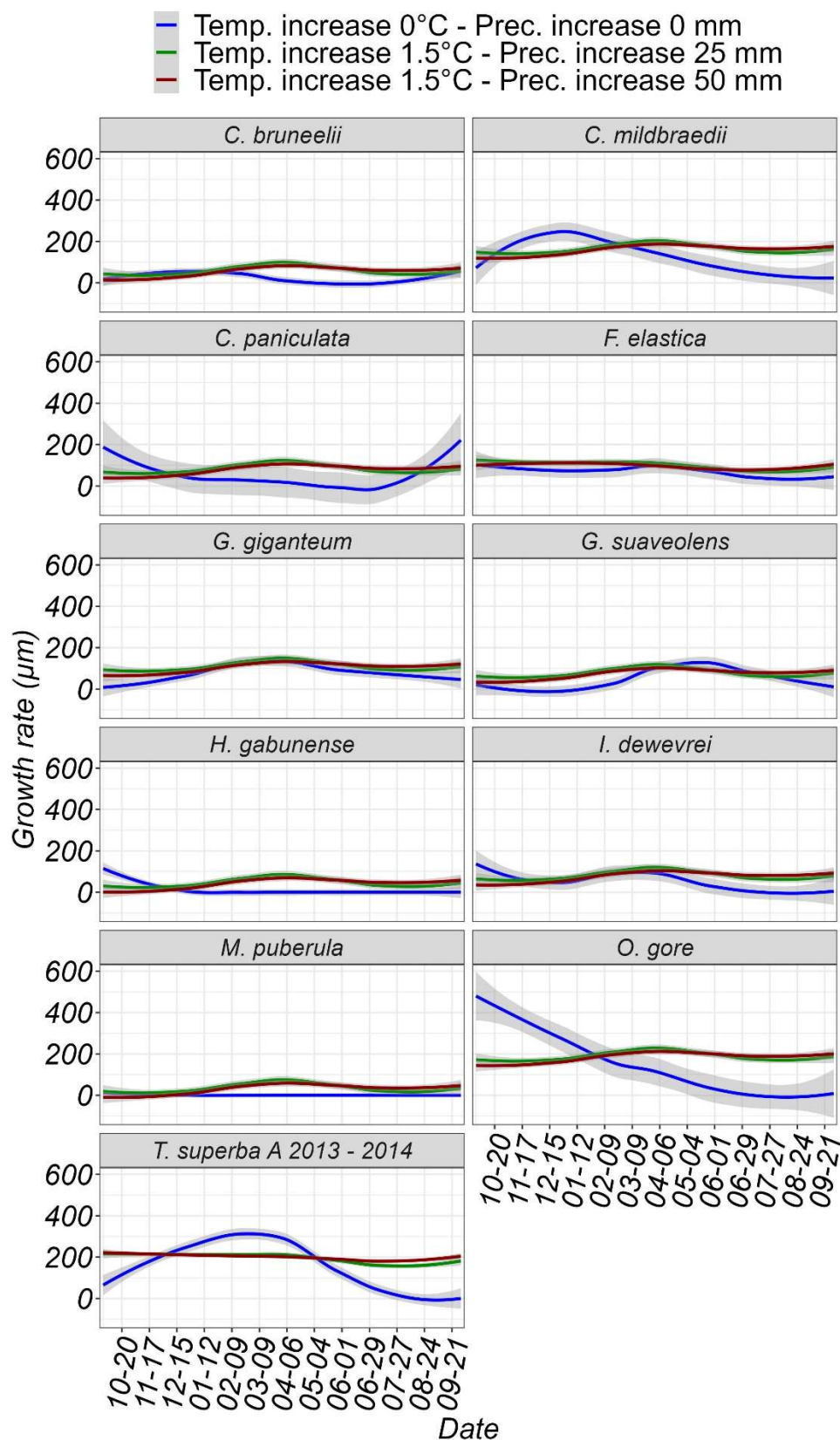


Figure S2 – 6. Comparison of growth rate variation between observed scenario (bleu curve) and the two predicted scenarios of a 1.5°C temperature increase coupled with a biweekly rainfall increase of 25mm (green curve) and 50mm (red curve), respectively. The line is a fitted LOESS (locally estimated scatterplot smoothing) curve. Shadow represents 95 % confidence interval.

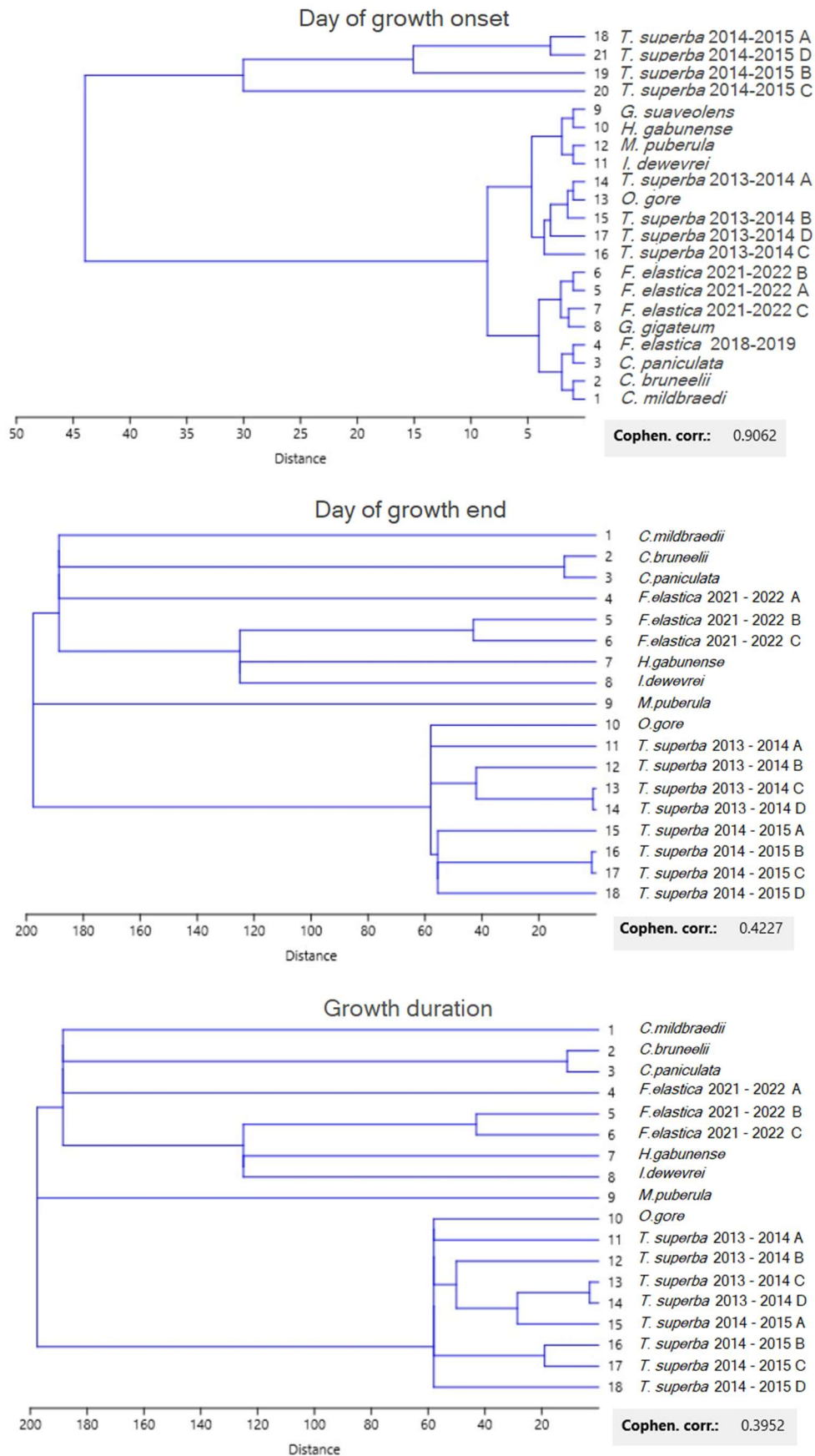


Figure S2 – 7. Classical clustering of the days on which trees start and end their growth, as well as the length of the growing season.

Results of the lmer to predict GR variation throughout the year including the variables temperature, rainfall, RH, and tree as fixed effects and the variable species as random effect

We fitted a linear mixed model (estimated using REML and nlptwrap optimizer) to predict GR_{μm} with Temp, Prec_mm, RH and Tree (formula: GR_{μm} ~ Temp * Prec_mm + Temp * RH + Tree). The model included Species as random effect (formula: ~1 |Species). The model's total explanatory power is substantial (conditional R² = 0.32) and the part related to the fixed effects alone (marginal R²) is of 0.31. The model's intercept, corresponding to Temp = 0, Prec_mm = 0, RH = 0 and Tree = Celtis, is at 578.23 (95% CI [-2114.49, 3270.96], t(543) = 0.42, p = 0.673). Within this model:

- The effect of Temp is statistically non-significant and negative (beta = -16.39, 95% CI [-133.20, 100.41], t(543) = -0.28, p = 0.783; Std. beta = 0.23, 95% CI [0.09, 0.37])
- The effect of Prec mm is statistically significant and positive (beta = 12.78, 95% CI [5.47, 20.09], t(543) = 3.44, p < .001; Std. beta = 0.21, 95% CI [0.08, 0.33])
- The effect of RH is statistically non-significant and negative (beta = -18.35, 95% CI [-53.17, 16.46], t(543) = -1.04, p = 0.301; Std. beta = -0.06, 95% CI [-0.18, 0.05])
- The effect of Tree [Cola] is statistically significant and negative (beta = -104.64, 95% CI [-181.39, -27.89], t(543) = -2.68, p = 0.008; Std. beta = -0.68, 95% CI [-1.54, 0.17])
- The effect of Tree [Corynanthe] is statistically significant and negative (beta = -80.64, 95% CI [-157.39, -3.89], t(543) = -2.06, p = 0.039; Std. beta = -0.53, 95% CI [-1.38, 0.33])
- The effect of Tree [FuntA] is statistically non-significant and negative (beta = -66.00, 95% CI [-146.81, 14.80], t(543) = -1.60, p = 0.109; Std. beta = -0.43, 95% CI [-1.30, 0.44])
- The effect of Tree [FuntB] is statistically non-significant and negative (beta = -10.82, 95% CI [-91.62, 69.99], t(543) = -0.26, p = 0.793; Std. beta = -0.07, 95% CI [-0.94, 0.80])
- The effect of Tree [FuntC] is statistically non-significant and negative (beta = -27.84, 95% CI [-108.64, 52.96], t(543) = -0.68, p = 0.499; Std. beta = -0.18, 95% CI [-1.05, 0.69])
- The effect of Tree [Funtumia] is statistically significant and negative (beta = -84.36, 95% CI [-161.11, -7.61], t(543) = -2.16, p = 0.031; Std. beta = -0.55, 95% CI [-1.41, 0.30])
- The effect of Tree [Ganophyllum] is statistically non-significant and negative (beta = -54.17, 95% CI [-130.92, 22.58], t(543) = -1.39, p = 0.166; Std. beta = -0.35, 95% CI [-1.21, 0.50])
- The effect of Tree [Greenwayodendron] is statistically significant and negative (beta = -85.19, 95% CI [-161.94, -8.44], t(543) = -2.18, p = 0.030; Std. beta = -0.56, 95% CI [-1.41, 0.30])
- The effect of Tree [Hylodendron] is statistically significant and negative (beta = -117.85, 95% CI [-194.60, -41.11], t(543) = -3.02, p = 0.003; Std. beta = -0.77, 95% CI [-1.63, 0.08])
- The effect of Tree [Isolona] is statistically significant and negative (beta = -83.58, 95% CI [-160.32, -6.83], t(543) = -2.14, p = 0.033; Std. beta = -0.55, 95% CI [-1.40, 0.31])
- The effect of Tree [Microdesmis] is statistically significant and negative (beta = -128.55, 95% CI [-205.30, -51.80], t(543) = -3.29, p = 0.001; Std. beta = -0.84, 95% CI [-1.70, 0.01])
- The effect of Tree [Ongokea] is statistically non-significant and positive (beta = 24.96, 95% CI [-51.78, 101.71], t(543) = 0.64, p = 0.523; Std. beta = 0.16, 95% CI [-0.69, 1.02])
- The effect of Tree [TermA] is statistically significant and positive (beta = 109.17, 95% CI [38.21, 180.13], t(543) = 3.02, p = 0.003; Std. beta = 0.71, 95% CI [-0.12, 1.55])

- The effect of Tree [TermB] is statistically significant and positive (beta = 88.58, 95% CI [17.62, 159.54], $t(543) =$

2.45, $p = 0.015$; Std. beta = 0.58, 95% CI [-0.25, 1.41])

- The effect of Tree [TermC] is statistically non-significant and negative (beta = -20.06, 95% CI [-91.02, 50.90], $t(543) = -0.56$, $p = 0.579$; Std. beta = -0.13, 95% CI [-0.96, 0.70])

- The effect of Tree [TermD] is statistically non-significant and positive (beta = 8.39, 95% CI [-62.57, 79.35], $t(543) = 0.23$, $p = 0.816$; Std. beta = 0.05, 95% CI [-0.78, 0.89])

- The effect of Temp \times Prec mm is statistically significant and negative (beta = -0.51, 95% CI [-0.81, -0.21], $t(543) = -3.37$, $p < .001$; Std. beta = -0.24, 95% CI [-0.37, -0.10])

- The effect of Temp \times RH is statistically non-significant and positive (beta = 0.73, 95% CI [-0.77, 2.23], $t(543) = 0.96$, $p = 0.338$; Std. beta = 0.07, 95% CI [-0.07, 0.21])

Standardized parameters were obtained by fitting the model on a standardized version of the dataset. 95% Confidence Intervals (CIs) and p -values were computed using a Wald t -distribution approximation.

Chapter 3: Growth periodicity in semi-deciduous tropical tree species from the Congo Basin.



Figure S3 – 1. Wood samples marked, sanded, and mounted on a numbered support from the Tervuren wood (Tw) xylotheque.

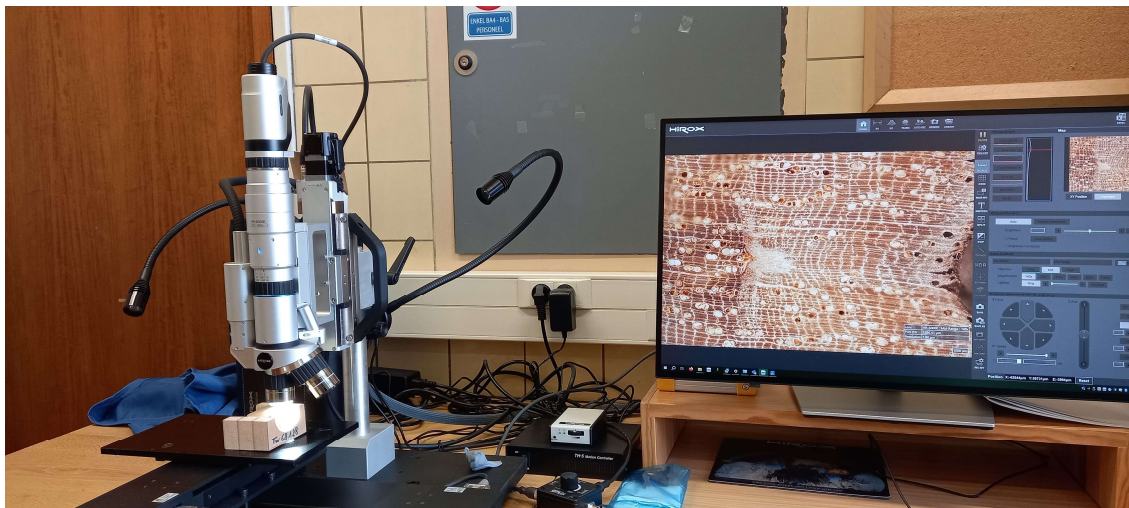
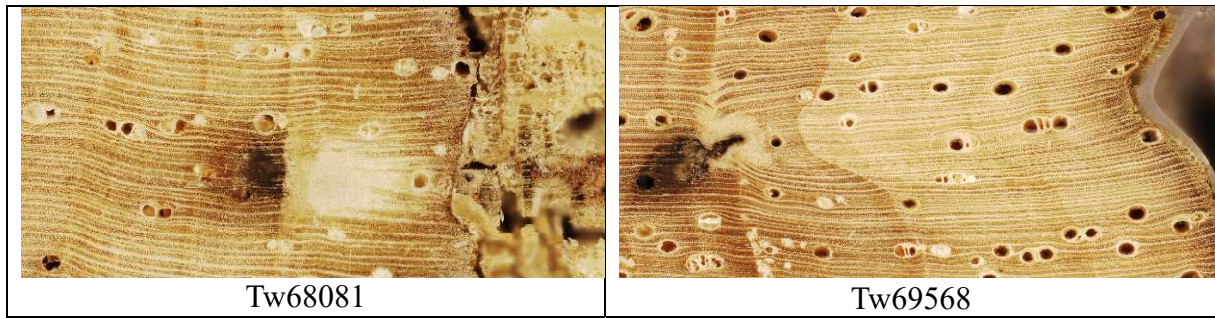


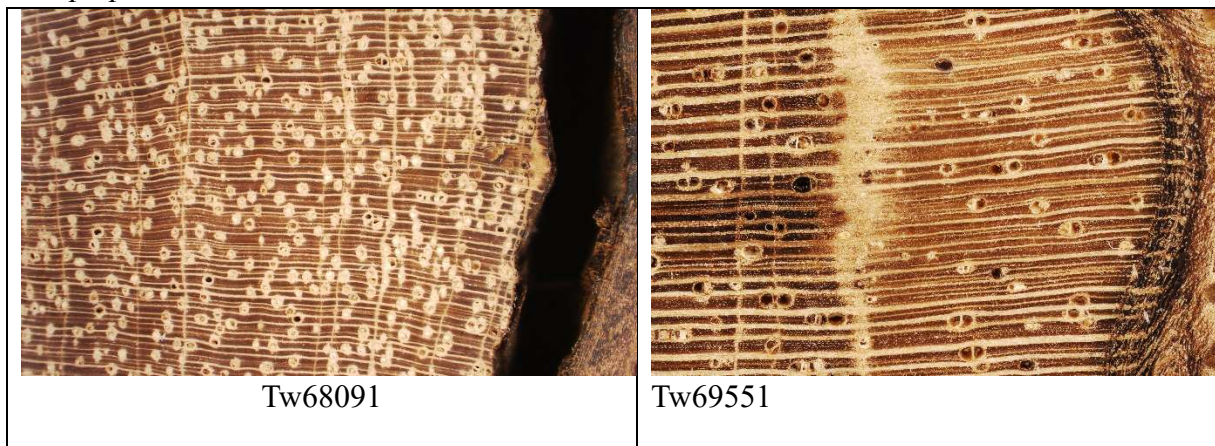
Figure S3 – 2. Capturing an image of a marked wood sample using an HRX-01 3D Digital Microscope.

Table S3 – 1. Species-by-species comparison of wood samples from Luki and Yangambi.

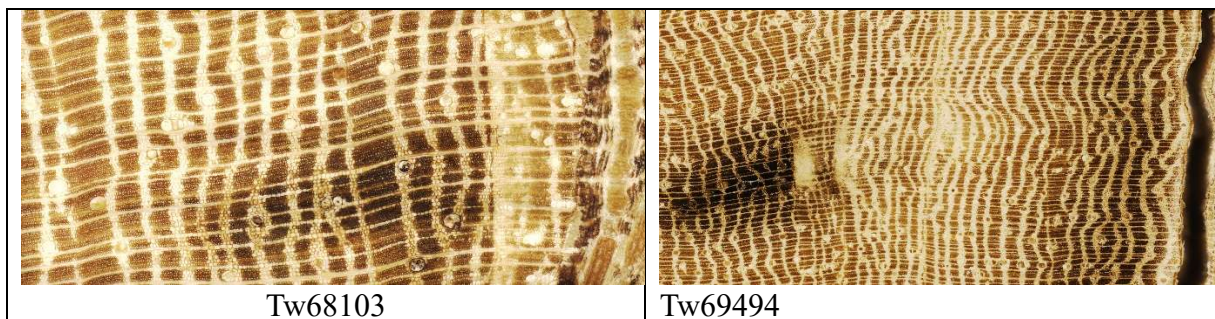
Blighia welwitschii



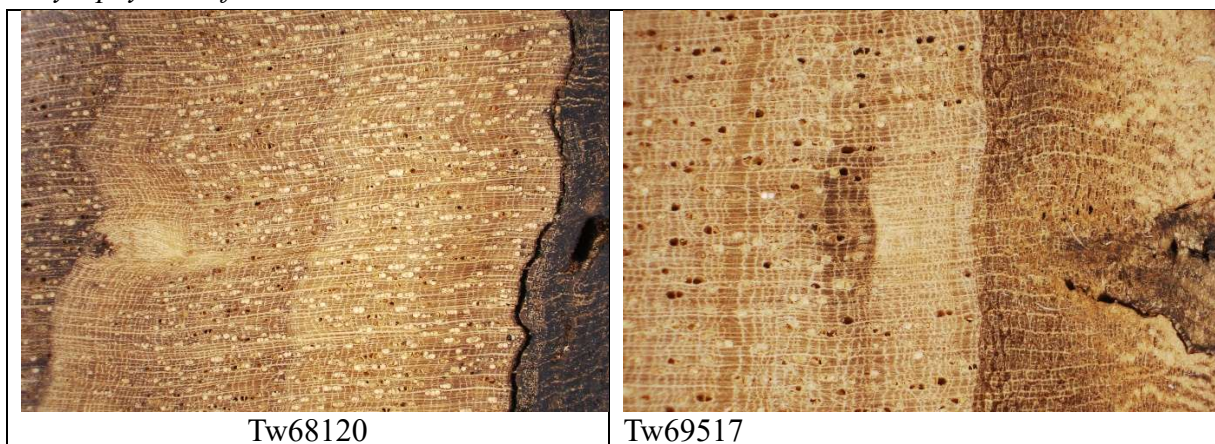
Carapa procera



Celtis mildbraedii



Chrysophyllum africanum



Cola griseiflora



Tw68134

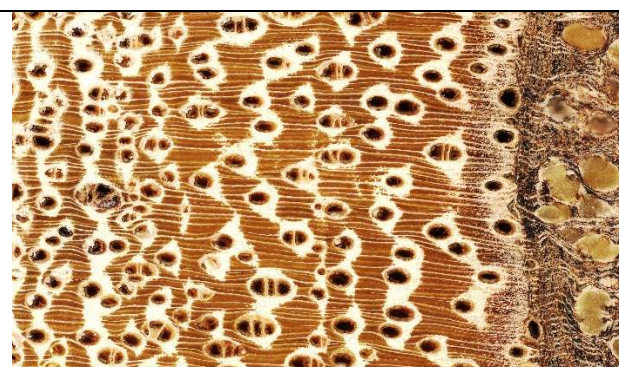


Tw69597

Erythrophleum suaveolens



Tw68145



Tw69544

Garcinia punctata



Tw68155

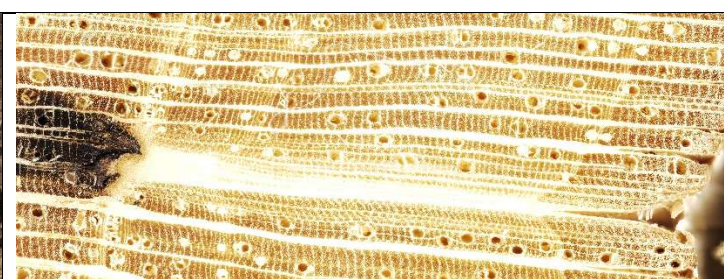


Tw69542

Greenwayodendron suaveolens

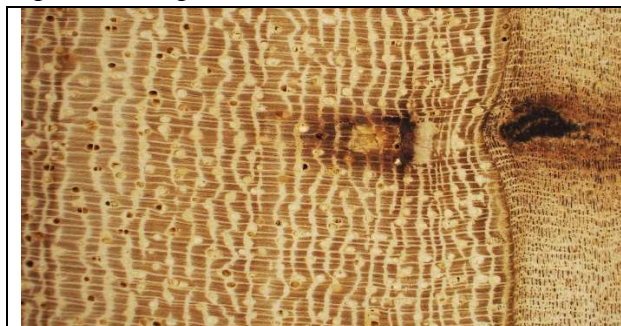


Tw68175



Tw69480

Leplaea thompsonii



Tw68184



Tw69534

Pentaclethra macrophylla

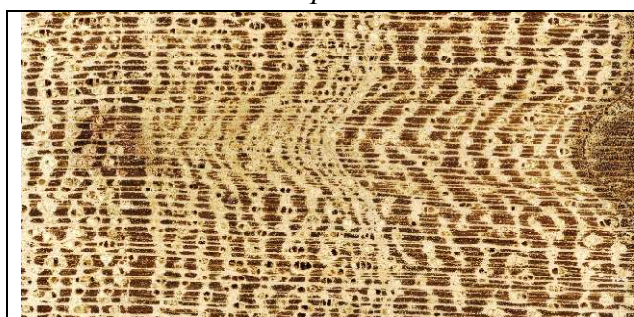


Tw68189

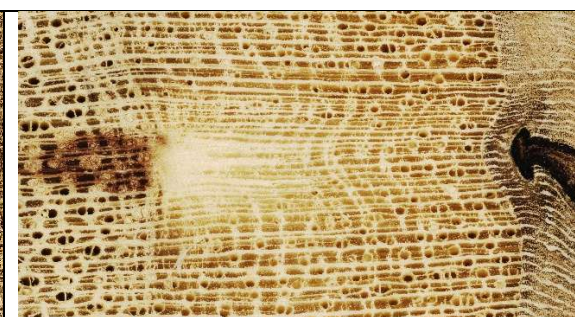


Tw69541

Petersianthus macrocarpus



Tw68204



Tw69578

Prioria oxyphylla



Tw68219



Tw6925

Pycnanthus angolensis



Tw68230



Tw69565

Staudtia kamerunensis var *gabonensis*

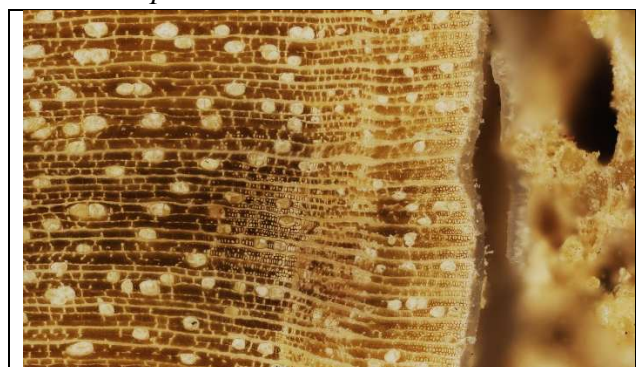


Tw68244



Tw69511

Strombosiopsis tetrandra



Tw68249

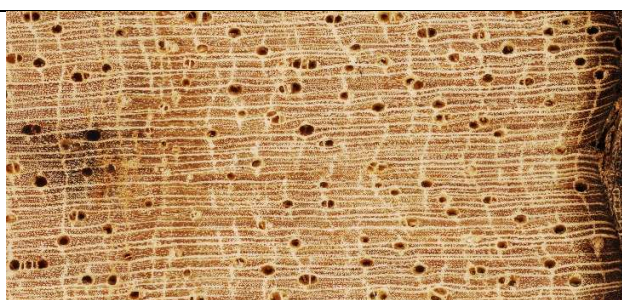


Tw69490

Trichilia gilgiana



Tw68259



Tw69594

Trichilia prieuriana



Tw68275

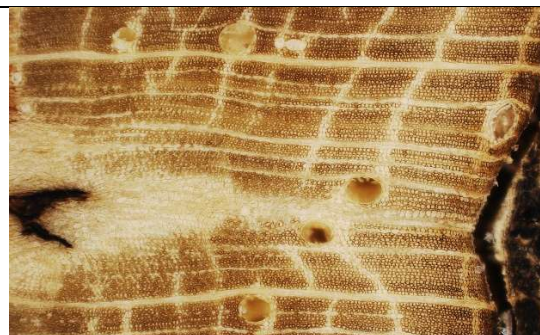


Tw69513

Trilepisium madagascariense



Tw68318



Tw69475

Chapter 4: Timing of cambial phenology of rainforest trees as indicator of climate sensitivity of the Congo Basin biome

Meaning of column headers in tables.

Cambium status	: State of the cambium at the sampling date.
Date	: the date of micro-core sampling.
DBH	: The Diameter at Breast Height. It refers to the diameter of a tree's trunk measured at 1.30 meters above the ground (in centimeters).
Dendrometer number	: Serial number of the dendrometer.
Family	: The tree botanical family.
Flowers	: The proportion of flowers on the tree, expressed as a percentage of the total volume of the tree's crown, including leaves, fruits, and flowers.
Fruits	: The proportion of fruits present on the tree, expressed as a percentage of the total volume of the tree's crown, including leaves, fruits, and flowers.
Height	: The tree total height (in meters).
Leaves_lost	: The proportion of leaves lost by the tree, expressed as a percentage of the total volume of the tree's crown, including leaves, fruits, and flowers.
nb_cell	: The number of cells in the developing zone
No	: Order number.
Precip	: Sum of biweekly precipitation, in millimeters.
RH	: Averaged biweekly air relative humidity, in %.
Season	: The weather season.
Site	: The study site
Species	: The tree botanical species.
Temp	: Averaged biweekly air temperature, in °C.
Tree identity	: An arbitrary name assigned to each tree to differentiate it from others of the same species.
Tree number	: The tree number on the site, assigned during official site inventory.
VPD	: Vapor Pressur Deficit

Table S4 – 1A. Botanical family, morphological traits and location of study trees from which micro-core samples were collected.

No	Tree identity	Tree number	Species	Family	Longitude (°)	Latitude (°)	DBH (cm)	Height (m)
1	<i>F. elastica</i> - 1	1025	<i>Funtumia elastica</i>	Apocynaceae	13.103	-5.621	35.9	31.0
2	<i>F. elastica</i> - 2	1027	<i>Funtumia elastica</i>	Apocynaceae	13.103	-5.621	49.5	33.0
3	<i>F. elastica</i> - 3	1039	<i>Funtumia elastica</i>	Apocynaceae	13.103	-5.621	28.7	26.0
4	<i>G. giganteum</i> - 1	1019	<i>Ganophyllum giganteum</i>	Sapindaceae	13.103	-5.621	47.0	25.0
5	<i>G. giganteum</i> - 2	1021	<i>Ganophyllum giganteum</i>	Sapindaceae	13.103	-5.621	53.9	38.0
6	<i>G. giganteum</i> - 3	1429	<i>Ganophyllum giganteum</i>	Sapindaceae	13.103	-5.622	42.1	20.0
7	<i>O. gore</i> - 1	407	<i>Ongokea gore</i>	Lacaceae	13.099	-5.620	68.4	29.0
8	<i>O. gore</i> - 2	408	<i>Ongokea gore</i>	Lacaceae	13.099	-5.620	79.5	32.0
9	<i>O. gore</i> - 3	409	<i>Ongokea gore</i>	Lacaceae	13.099	-5.620	74.7	36.0
10	<i>P. balsamifera</i> - 1	401	<i>Prioria balsamifera</i>	Fabaceae Detarioideae	13.103	-5.621	98.5	40.0
11	<i>P. balsamifera</i> - 2	402	<i>Prioria balsamifera</i>	Fabaceae Detarioideae	13.103	-5.621	74.2	32.0
12	<i>P. balsamifera</i> - 3	403	<i>Prioria balsamifera</i>	Fabaceae Detarioideae	13.103	-5.621	78.6	34.0
1	<i>L. thompsonii</i> - 1	12	<i>Leplaea thompsonii</i>	Meliaceae	24.523	0.787	30.4	21.2
2	<i>L. thompsonii</i> - 2	1	<i>Leplaea thompsonii</i>	Meliaceae	24.521	0.781	40.0	23.0
3	<i>L. thompsonii</i> - 3	321	<i>Leplaea thompsonii</i>	Meliaceae	24.521	0.781	30.9	19.0
4	<i>P. oleosa</i> - 1	50	<i>Panda oleosa</i>	Pandaceae	24.524	0.787	47.2	26.0
5	<i>P. oleosa</i> - 2	177	<i>Panda oleosa</i>	Pandaceae	24.523	0.787	59.0	23.0
6	<i>P. oleosa</i> - 3	182	<i>Panda oleosa</i>	Pandaceae	24.521	0.781	32.8	28.3
7	<i>P. macrocarpus</i> - 1	130	<i>Petersianthus macrocarpus</i>	Lecythidaceae	24.524	0.786	37.6	28.7
8	<i>P. macrocarpus</i> - 2	387	<i>Petersianthus macrocarpus</i>	Lecythidaceae	24.523	0.787	50.1	21.0
9	<i>P. macrocarpus</i> - 3	210	<i>Petersianthus macrocarpus</i>	Lecythidaceae	24.524	0.786	40.4	28.6
10	<i>S. zenkeri</i> - 1	103	<i>Scorodophloeus zenkeri</i>	Fabaceae Detarioideae	24.524	0.787	33.7	23.4
11	<i>S. zenkeri</i> - 2	67	<i>Scorodophloeus zenkeri</i>	Fabaceae Detarioideae	24.524	0.787	50.1	22.5
12	<i>S. zenkeri</i> - 3	57	<i>Scorodophloeus zenkeri</i>	Fabaceae Detarioideae	24.524	0.787	33.3	23.6
13	<i>S. sucordatum</i> - 1	211	<i>Synsepalum subcordatum</i>	Sapotaceae	24.524	0.786	34.2	24.4
14	<i>S. sucordatum</i> - 2	170	<i>Synsepalum subcordatum</i>	Sapotaceae	24.521	0.781	58.2	22.2
15	<i>S. sucordatum</i> - 3	365	<i>Synsepalum subcordatum</i>	Sapotaceae	24.522	0.781	25.0	21.6
16	<i>T. madagascariense</i> - 1	324	<i>Trilepisium madagascariense</i>	Moraceae	24.521	0.781	51.4	37.8
17	<i>T. madagascariense</i> - 2	35	<i>Trilepisium madagascariense</i>	Moraceae	24.521	0.780	44.8	41.4
18	<i>T. madagascariense</i> - 3	304	<i>Trilepisium madagascariense</i>	Moraceae	24.521	0.781	46.3	34.6

Table S4 – 1B. Botanical family, morphological traits and location of study trees on which dendrometers were installed.

No.	Tree identity	Tree number	Species	Family	Longitude (°)	Latitude (°)	Dendrometer number	DBH (cm)	Height (m)
1	<i>A. manii1</i>	214/191	<i>Anonidium mannii</i>	Annonaceae	24.520884	0.780242	92210002	50.4	21.00
2	<i>A. manii2</i>	393	<i>Anonidium mannii</i>	Annonaceae	24.521268	0.780358	92221463	32.6	22.50
3	<i>A. manii3</i>	314	<i>Anonidium mannii</i>	Annonaceae	24.521096	0.780574	92221454	45.7	17.00
4	<i>A. manii4</i>	144	<i>Anonidium mannii</i>	Annonaceae	24.520869	0.780460	92221455	37.5	24.30
5	<i>A. manii5</i>	376	<i>Anonidium mannii</i>	Annonaceae	24.521350	0.780519	92221462	33.3	15.50
6	<i>C. lacourtianum1</i>	153	<i>Chrysophyllum lacourtianum</i>	Sapotaceae	24.520846	0.780616	92221456	48.9	31.00
7	<i>C. lacourtianum2</i>	292	<i>Chrysophyllum lacourtianum</i>	Sapotaceae	24.521164	0.780402	92221461	40.9	26.20
8	<i>C. lacourtianum3</i>	209	<i>Chrysophyllum lacourtianum</i>	Sapotaceae	24.521118	0.780469	92221478	62.0	35.70
9	<i>C. lacourtianum4</i>	135	<i>Chrysophyllum lacourtianum</i>	Sapotaceae	24.520814	0.780364	92221489	22.7	23.00
10	<i>C. lokele1</i>	336	<i>Combretum lokele</i>	Combretaceae	24.521414	0.780809	92221474	52.3	39.40
11	<i>C. lokele2</i>	203	<i>Combretum lokele</i>	Combretaceae	24.520954	0.780488	92221479	29.3	25.20
12	<i>C. lokele3</i>	202	<i>Combretum lokele</i>	Combretaceae	24.520982	0.780503	92221480	21.0	22.80
13	<i>C. lokele4</i>	298/292	<i>Combretum lokele</i>	Combretaceae	24.520819	0.780200	92221490	33.9	28.30
14	<i>D. gossweileri1</i>	50	<i>Drypetes gossweileri</i>	Putranjivaceae	24.520641	0.780307	92221484	25.0	27.60
15	<i>D. gossweileri2</i>	43	<i>Drypetes gossweileri</i>	Putranjivaceae	24.520665	0.780248	92221486	19.8	20.30
16	<i>D. gossweileri3</i>	163	<i>Drypetes gossweileri</i>	Putranjivaceae	24.520794	0.780558	92221487	34.7	26.40
17	<i>D. gossweileri4</i>	165	<i>Drypetes gossweileri</i>	Putranjivaceae	24.520843	0.780656	92221488	22.7	18.70
18	<i>D. gossweileri5</i>	383	<i>Drypetes gossweileri</i>	Putranjivaceae	24.521390	0.780447	92221494	66.0	40.30
19	<i>G. suaveolens1</i>	183	<i>Greenwayodendron suaveolens</i>	Annonaceae	24.521045	0.780701	92221452	40.1	32.00
20	<i>G. suaveolens2</i>	332	<i>Greenwayodendron suaveolens</i>	Annonaceae	24.521209	0.780819	92221453	46.2	34.00
21	<i>G. suaveolens3</i>	228	<i>Greenwayodendron suaveolens</i>	Annonaceae	24.521126	0.780105	92221492	26.1	24.30
22	<i>G. suaveolens4</i>	276	<i>Greenwayodendron suaveolens</i>	Annonaceae	24.521092	0.780139	92221493	42.0	38.80
23	<i>P. oleosa1</i>	38	<i>Panda oleosa</i>	Pandaceae	24.520693	0.780522	92221457	53.3	26.90
24	<i>P. oleosa2</i>	22	<i>Panda oleosa</i>	Pandaceae	24.520517	0.780556	92221458	37.0	24.30
25	<i>P. oleosa3</i>	217	<i>Panda oleosa</i>	Pandaceae	24.520947	0.780405	92221460	67.5	28.60
26	<i>P. oleosa4</i>	392	<i>Panda oleosa</i>	Pandaceae	24.521334	0.780359	92221464	49.7	27.30
27	<i>P. oleosa5</i>	216	<i>Panda oleosa</i>	Pandaceae	24.521054	0.780316	92221459	63.2	33.50
28	<i>S. zenkeri1</i>	328	<i>Scorodophloeus zenkeri</i>	Fabaceae Detarioideae	24.521270	0.780770	92221473	40.1	32.60
29	<i>S. zenkeri2</i>	379	<i>Scorodophloeus zenkeri</i>	Fabaceae Detarioideae	24.521491	0.780440	92221476	29.5	28.70
30	<i>S. zenkeri3</i>	154	<i>Scorodophloeus zenkeri</i>	Fabaceae Detarioideae	24.520902	0.780530	92221481	55.7	31.40
31	<i>S. zenkeri4</i>	145	<i>Scorodophloeus zenkeri</i>	Fabaceae Detarioideae	24.521087	0.780487	92221482	54.2	38.60
32	<i>S. zenkeri5</i>	17	<i>Scorodophloeus zenkeri</i>	Fabaceae Detarioideae	24.520739	0.780573	92221483	36.4	28.40
33	<i>T. omphalocarpoides1</i>	307	<i>Tridesmostemon omphalocarpoides</i>	Sapotaceae	24.521210	0.780565	92221466	48.1	30.20
34	<i>T. omphalocarpoides2</i>	184	<i>Tridesmostemon omphalocarpoides</i>	Sapotaceae	24.521076	0.780739	92221467	55.3	30.50
35	<i>T. omphalocarpoides3</i>	12	<i>Tridesmostemon omphalocarpoides</i>	Sapotaceae	24.520578	0.780796	92221468	72.8	33.90
36	<i>T. omphalocarpoides4</i>	325	<i>Tridesmostemon omphalocarpoides</i>	Sapotaceae	24.521250	0.780784	92221472	28.1	27.60
37	<i>T. omphalocarpoides5</i>	72	<i>Tridesmostemon omphalocarpoides</i>	Sapotaceae	24.520617	0.780096	92221485	25.8	18.30
38	<i>T. madagascariense1</i>	296	<i>Trilepisium madagascariense</i>	Moraceae	24.521278	0.780337	92221469	51.6	44.70
39	<i>T. madagascariense2</i>	208	<i>Trilepisium madagascariense</i>	Moraceae	24.521092	0.780426	92221470	39.4	34.40
40	<i>T. madagascariense3</i>	56	<i>Trilepisium madagascariense</i>	Moraceae	24.520699	0.780143	92221471	32.3	34.90
41	<i>T. madagascariense4</i>	368	<i>Trilepisium madagascariense</i>	Moraceae	24.521490	0.780571	92221475	34.0	29.20
42	<i>T. madagascariense5</i>	290/288	<i>Trilepisium madagascariense</i>	Moraceae	24.520905	0.780218	92221491	35.0	36.80

Table S4 – 2. Main anatomical characteristics of the wood of species from which microcores were collected.

No	Species	Wood porosity	Resin canals	Vessels	Axial parenchyma	Leaf persistence	Family	Growth-ring boundary distinctness	Site
1	<i>Funtumia elastica</i> (P. Preuss) Stapf	Diffuse-porous	Absent	In diagonal to radial pattern. In radial multiples of 2 - 4.	Apotracheal diffuse. Apotracheal diffuse in aggregates. paratracheal scanty	Evergreen	Apocynaceae	Absent	Luki
2	<i>Ganophyllum giganteum</i> (A. Chev.) Hauman	Diffuse-porous	Absent	In diagonal to radial pattern. Partly solitary, partly in radial multiples of 2 - 4.	Diffuse. Vasicentric. Aliform. Lozenge-aliform. Winged-aliform. Confluent. Paratracheal unilateral. Paratracheal in bands	Evergreen	Sapindaceae	Absent	Luki
3	<i>Ongokea gore</i> (Hua) Pierre	Diffuse-porous	Absent	In diagonal to radial pattern. Exclusively solitary. Partly solitary, partly in radial multiples of 2 - 4.	Diffuse. Diffuse in aggregates. Paratracheal Scanty. In narrow bands up to 3 cells wide.	Evergreen	Olacaceae	Absent	Luki
4	<i>Prioria balsamifera</i> (Vermoesen) Breteler	Diffuse-porous	Present	In diagonal to radial pattern. Exclusively solitary. Partly solitary, partly in radial multiples of 2 - 4.	Paratracheal in bands. Vasicentric. Aliform Lozenge-aliforme.	Deciduous	Fabaceae Detarioideae	Absent	Luki
5	<i>Lepalea thompsonii</i> (Sprague & Hutch.) E.J.M.Koenen & J.J.de Wilde	Diffuse-porous	Absent	In diagonal to radial pattern. Partly solitary, partly in radial multiples of 2 - 4.	Confluent. In line or narrow bands up to 3 cells wide. In bands of more than 3 cells wide.	Evergreen	Meliaceae	Absent	Yangambi
6	<i>Panda oleosa</i> Pierre	Diffuse-porous	Absent	In radial to diagonal pattern. Partly solitary, partly in radial multiples of 2 - 4.	Diffuse in aggregates. Paratracheal scanty. In line or narrow bands up to 3 cells wide. Scaliform	Evergreen	Pandaceae	Absent	Yangambi
7	<i>Petersianthus macrocarpus</i> (P.Beauv.) Liben	Diffuse-porous	Absent	In diagonal to radial pattern. Partly solitary, partly in radial multiples of 2 - 4.	Diffuse. Aliform. Lozenge-aliform. Winged-aliform. Confluent.	Evergreen	Lecythidaceae	Absent	Yangambi
8	<i>Synsepalum subcordatum</i> De Wild.	Diffuse-porous	Absent	In diagonal to radial pattern. Partly solitary, partly in radial multiples of 2 - 4.	In line or narrow bands up to 3 cells wide. Reticulate. In bands of more than 3 cells wide.	Evergreen	Sapotaceae	Absent	Yangambi
9	<i>Scorodophloeus zenkeri</i> Harms	Diffuse-porous	Absent	In diagonal to radial pattern. Partly solitary, partly in radial multiples of 2 - 4.	Diffuse. Paratracheal scanty. Vasicentric. Confluent. In line or narrow bands up to 3 cells wide. In bands of more than 3 cells wide.	Evergreen	Fabaceae Detarioideae	Distinct or absent	Yangambi
10	<i>Trilepisium madagascariense</i> DC.	Diffuse-porous	Absent	In diagonal to radial pattern. Partly solitary, partly in radial multiples of 2 - 4.	Paratracheal scanty. Vasicentric. In line or narrow bands up to 3 cells wide. In bands of more than 3 cells wide.	Evergreen	Moraceae	Absent	Yangambi

Table S4 – 3. Model output, for all species combined, of quantifying number of cells in the DZ in response to temperature, relative humidity, amount of leaves lost, amount of flowers borne, amount of fruits borne, DBH and tree height as fixed effects, using a linear mixed-effects model. Tree species variable was included as a random effect.

Predicted variable	Fixed effect	Sign.	Statistics	Cond. R2	Marg. R2	AIC
number of cells in the DZ	Temperature	ns	beta = 0.29, 95% CI [-0.08, 0.67], t(797) = 1.53, p = 0.126; Std. beta = 0.05, 95% CI [-0.01, 0.12]	0.81	0.16	5061.854
number of cells in the DZ	Relative humidity	s	beta = 0.08, 95% CI [9.18e-03, 0.14], t(797) = 2.24, p = 0.026; Std. beta = 0.08, 95% CI [9.46e-03, 0.15]			
number of cells in the DZ	Amount of leaves lost	s	beta = -0.19, 95% CI [-0.31, -0.07], t(797) = -3.16, p = 0.002; Std. beta = -0.12, 95% CI [-0.19, -0.04]			
number of cells in the DZ	Amount of flowers borne	ns	beta = 8.39e-03, 95% CI [-0.05, 0.07], t(797) = 0.26, p = 0.794; Std. beta = 7.29e-03, 95% CI [-0.05, 0.06]			
number of cells in the DZ	Amount of fruits borne	ns	beta = -0.02, 95% CI [-0.06, 0.02], t(797) = -1.00, p = 0.315; Std. beta = -0.03, 95% CI [-0.10, 0.03]			
number of cells in the DZ	DBH	ns	beta = -0.19, 95% CI [-2.73, 2.35], t(797) = -0.14, p = 0.885; Std. beta = -0.45, 95% CI [-1.33, 0.43]			
number of cells in the DZ	Tree height	ns	beta = 0.17, 95% CI [-0.51, 0.85], t(797) = 0.50, p = 0.617; Std. beta = 0.15, 95% CI [-0.18, 0.48]			

Table S4 – 4. Species-specific models output of quantifying number of cells in the DZ in response to temperature, relative humidity, amount of leaves lost, amount of flowers borne, amount of fruits borne, DBH and tree height as fixed effects, using a linear mixed-effects model. Tree individual variable was included as a random effect.

Site	Species	Predicted variable	Fixed effect	Significance	Signe	Statistics	Cond. R2	Marg. R2
Luki	<i>Funtumia elastica</i>	number of cells in the DZ	Temperature	ns	Positive	beta = 0.13, 95% CI [-0.82, 1.09], t(77) = 0.27, p = 0.784; Std. beta = 0.04, 95% CI [-0.25, 0.33]	0.24	0.14
Luki	<i>Funtumia elastica</i>	number of cells in the DZ	Relative humidity	ns	Negative	beta = -0.04, 95% CI [-0.16, 0.08], t(77) = -0.65, p = 0.516; Std. beta = -0.07, 95% CI [-0.29, 0.15]		
Luki	<i>Funtumia elastica</i>	number of cells in the DZ	Amount of leaves lost	ns	Negative	beta = -0.07, 95% CI [-0.46, 0.33], t(77) = -0.33, p = 0.741; Std. beta = -0.05, 95% CI [-0.36, 0.26]		
Luki	<i>Funtumia elastica</i>	number of cells in the DZ	Amount of flowers borne	ns	Negative	beta = -6.35e-04, 95% CI [-0.10, 0.10], t(77) = -0.01, p = 0.990; Std. beta = -1.66e-03, 95% CI [-0.26, 0.26]		
Luki	<i>Funtumia elastica</i>	number of cells in the DZ	Amount of fruits borne	ns	Positive	beta = 0.04, 95% CI [-0.10, 0.18], t(77) = 0.54, p = 0.589; Std. beta = 0.11, 95% CI [-0.31, 0.54]		
Luki	<i>Funtumia elastica</i>	number of cells in the DZ	DBH	ns	Negative	beta = -0.08, 95% CI [-0.57, 0.42], t(77) = -0.30, p = 0.763; Std. beta = -0.17, 95% CI [-1.33, 0.99]		
Luki	<i>Funtumia elastica</i>	number of cells in the DZ	Tree height	ns	Positive	beta = 0.65, 95% CI [-0.82, 2.12], t(77) = 0.88, p = 0.382; Std. beta = 0.50, 95% CI [-0.67, 1.68]		
Luki	<i>Ganophyllum giganteum</i>	number of cells in the DZ	Temperature	s	Positive	beta = 0.97, 95% CI [0.12, 1.81], t(79) = 2.29, p = 0.025; Std. beta = 0.20, 95% CI [0.03, 0.38]	0.40	0.40
Luki	<i>Ganophyllum giganteum</i>	number of cells in the DZ	Relative humidity	ns	Positive	beta = 0.13, 95% CI [-0.02, 0.28], t(79) = 1.69, p = 0.095; Std. beta = 0.15, 95% CI [-0.03, 0.33]		
Luki	<i>Ganophyllum giganteum</i>	number of cells in the DZ	Amount of leaves lost	s	Negative	beta = -0.47, 95% CI [-0.91, -0.04], t(79) = -2.17, p = 0.033; Std. beta = -0.20, 95% CI [-0.39, -0.02]		
Luki	<i>Ganophyllum giganteum</i>	number of cells in the DZ	DBH	s	Negative	beta = -2.35, 95% CI [-3.63, -1.07], t(79) = -3.65, p < .001; Std. beta = -2.04, 95% CI [-11.02, 6.94]		
Luki	<i>Ganophyllum giganteum</i>	number of cells in the DZ	Tree height	s	Positive	beta = 1.77, 95% CI [0.96, 2.59], t(79) = 4.32, p < .001; Std. beta = 2.41, 95% CI [-6.57, 11.39]		
Luki	<i>Ongokea gore</i>	number of cells in the DZ	Temperature	s	Negative	beta = -0.54, 95% CI [-1.05, -0.02], t(78) = -2.09, p = 0.040; Std. beta = -0.23, 95% CI [-0.44, -0.01]	0.17	0.17
Luki	<i>Ongokea gore</i>	number of cells in the DZ	Relative humidity	s	Negative	beta = -0.16, 95% CI [-0.26, -0.06], t(78) = -3.23, p = 0.002; Std. beta = -0.40, 95% CI [-0.64, -0.15]		
Luki	<i>Ongokea gore</i>	number of cells in the DZ	Amount of leaves lost	ns	Negative	beta = -0.20, 95% CI [-0.51, 0.11], t(78) = -1.30, p = 0.197; Std. beta = -0.15, 95% CI [-0.37, 0.08]		
Luki	<i>Ongokea gore</i>	number of cells in the DZ	Amount of fruits borne	s	Negative	beta = -0.06, 95% CI [-0.10, -0.02], t(78) = -2.97, p = 0.004; Std. beta = -0.39, 95% CI [-0.66, -0.13]		
Luki	<i>Ongokea gore</i>	number of cells in the DZ	DBH	ns	Positive	beta = 0.13, 95% CI [-0.01, 0.28], t(78) = 1.79, p = 0.077; Std. beta = 0.22, 95% CI [-0.12, 0.56]		
Luki	<i>Ongokea gore</i>	number of cells in the DZ	Tree height	ns	Negative	beta = -0.16, 95% CI [-0.41, 0.09], t(78) = -1.29, p = 0.202; Std. beta = -0.17, 95% CI [-0.52, 0.18]		
Luki	<i>Prioria balsamifera</i>	number of cells in the DZ	Temperature	s	Positive	beta = 1.46, 95% CI [0.51, 2.40], t(77) = 3.08, p = 0.003; Std. beta = 0.26, 95% CI [0.09, 0.43]	0.44	0.44
Luki	<i>Prioria balsamifera</i>	number of cells in the DZ	Relative humidity	ns	Positive	beta = 0.17, 95% CI [-3.48e-03, 0.34], t(77) = 1.95, p = 0.055; Std. beta = 0.18, 95% CI [-3.64e-03, 0.36]		
Luki	<i>Prioria balsamifera</i>	number of cells in the DZ	Amount of leaves lost	ns	Negative	beta = -0.21, 95% CI [-0.45, 0.03], t(77) = -1.74, p = 0.086; Std. beta = -0.19, 95% CI [-0.41, 0.03]		
Luki	<i>Prioria balsamifera</i>	number of cells in the DZ	Amount of flowers borne	s	Negative	beta = -0.29, 95% CI [-0.42, -0.15], t(77) = -4.19, p < .001; Std. beta = -0.39, 95% CI [-0.57, -0.20]		
Luki	<i>Prioria balsamifera</i>	number of cells in the DZ	Amount of fruits borne	s	Negative	beta = -0.10, 95% CI [-0.19, -0.01], t(77) = -2.33, p = 0.022; Std. beta = -0.23, 95% CI [-0.44, -0.03]		
Luki	<i>Prioria balsamifera</i>	number of cells in the DZ	DBH	s	Negative	beta = -2.66, 95% CI [-4.18, -1.14], t(77) = -3.49, p < .001; Std. beta = -4.37, 95% CI [-20.06, 11.33]		
Luki	<i>Prioria balsamifera</i>	number of cells in the DZ	Tree height	s	Positive	beta = 8.78, 95% CI [4.07, 13.49], t(77) = 3.71, p < .001; Std. beta = 4.64, 95% CI [-11.06, 20.33]		

Unraveling the periodicity of secondary growth in the Congo Basin

Yangambi	<i>Leplaea thompsonii</i>	number of cells in the DZ	Temperature	ns	Positive	beta = 0.51, 95% CI [-1.94, 2.97], t(71) = 0.42, p = 0.679; Std. beta = 0.14, 95% CI [-0.53, 0.82]	0.59	0.58
Yangambi	<i>Leplaea thompsonii</i>	number of cells in the DZ	Relative humidity	ns	Positive	beta = 0.35, 95% CI [-0.08, 0.78], t(71) = 1.61, p = 0.111; Std. beta = 0.55, 95% CI [-0.13, 1.24]		
Yangambi	<i>Leplaea thompsonii</i>	number of cells in the DZ	Amount of leaves lost	ns	Positive	beta = 0.14, 95% CI [-0.32, 0.61], t(71) = 0.61, p = 0.542; Std. beta = 0.05, 95% CI [-0.12, 0.22]		
Yangambi	<i>Leplaea thompsonii</i>	number of cells in the DZ	Amount of flowers borne	ns	Positive	beta = 0.02, 95% CI [-0.19, 0.24], t(71) = 0.23, p = 0.820; Std. beta = 0.02, 95% CI [-0.14, 0.17]		
Yangambi	<i>Leplaea thompsonii</i>	number of cells in the DZ	Amount of fruits borne	s	Positive	beta = 0.21, 95% CI [0.06, 0.36], t(71) = 2.72, p = 0.008; Std. beta = 0.28, 95% CI [0.07, 0.49]		
Yangambi	<i>Leplaea thompsonii</i>	number of cells in the DZ	DBH	s	Negative	beta = -1.08, 95% CI [-1.41, -0.75], t(71) = -6.46, p < .001; Std. beta = -0.93, 95% CI [-1.55, -0.30]		
Yangambi	<i>Leplaea thompsonii</i>	number of cells in the DZ	Tree height	s	Positive	beta = 4.41, 95% CI [3.41, 5.41], t(71) = 8.81, p < .001; Std. beta = 1.40, 95% CI [0.77, 2.04]		
Yangambi	<i>Petersianthus macrocarpus</i>	number of cells in the DZ	Temperature	s	Positive	beta = 2.26, 95% CI [0.30, 4.21], t(71) = 2.30, p = 0.024; Std. beta = 1.01, 95% CI [0.14, 1.89]	0.35	0.35
Yangambi	<i>Petersianthus macrocarpus</i>	number of cells in the DZ	Relative humidity	s	Positive	beta = 0.53, 95% CI [0.19, 0.86], t(71) = 3.15, p = 0.002; Std. beta = 1.38, 95% CI [0.51, 2.25]		
Yangambi	<i>Petersianthus macrocarpus</i>	number of cells in the DZ	Amount of leaves lost	ns	Positive	beta = 0.04, 95% CI [-0.07, 0.14], t(71) = 0.70, p = 0.485; Std. beta = 0.07, 95% CI [-0.14, 0.29]		
Yangambi	<i>Petersianthus macrocarpus</i>	number of cells in the DZ	Amount of flowers borne	s	Negative	beta = -0.08, 95% CI [-0.14, -0.03], t(71) = -3.05, p = 0.003; Std. beta = -0.29, 95% CI [-0.48, -0.10]		
Yangambi	<i>Petersianthus macrocarpus</i>	number of cells in the DZ	Amount of fruits borne	ns	Positive	beta = 0.01, 95% CI [-0.04, 0.07], t(71) = 0.46, p = 0.648; Std. beta = 0.05, 95% CI [-0.16, 0.25]		
Yangambi	<i>Petersianthus macrocarpus</i>	number of cells in the DZ	DBH	s	Positive	beta = 0.72, 95% CI [0.13, 1.31], t(71) = 2.44, p = 0.017; Std. beta = 1.23, 95% CI [-2.02, 4.47]		
Yangambi	<i>Petersianthus macrocarpus</i>	number of cells in the DZ	Tree height	s	Positive	beta = 1.15, 95% CI [0.28, 2.02], t(71) = 2.64, p = 0.010; Std. beta = 1.32, 95% CI [-1.92, 4.56]		
Yangambi	<i>Panda oleosa</i>	number of cells in the DZ	Temperature	ns	Negative	beta = -0.35, 95% CI [-2.13, 1.42], t(71) = -0.40, p = 0.692; Std. beta = -0.16, 95% CI [-0.97, 0.65]	0.82	0.12
Yangambi	<i>Panda oleosa</i>	number of cells in the DZ	Relative humidity	ns	Negative	beta = -0.13, 95% CI [-0.44, 0.18], t(71) = -0.84, p = 0.401; Std. beta = -0.35, 95% CI [-1.17, 0.47]		
Yangambi	<i>Panda oleosa</i>	number of cells in the DZ	Amount of leaves lost	s	Positive	beta = 0.46, 95% CI [0.19, 0.73], t(71) = 3.35, p = 0.001; Std. beta = 0.33, 95% CI [0.13, 0.53]		
Yangambi	<i>Panda oleosa</i>	number of cells in the DZ	Amount of flowers borne	ns	Negative	beta = -0.08, 95% CI [-0.30, 0.14], t(71) = -0.71, p = 0.479; Std. beta = -0.07, 95% CI [-0.26, 0.12]		
Yangambi	<i>Panda oleosa</i>	number of cells in the DZ	Amount of fruits borne	ns	Negative	beta = -0.09, 95% CI [-0.30, 0.12], t(71) = -0.84, p = 0.406; Std. beta = -0.09, 95% CI [-0.30, 0.12]		
Yangambi	<i>Panda oleosa</i>	number of cells in the DZ	DBH	ns	Positive	beta = 0.80, 95% CI [-3.20, 4.80], t(71) = 0.40, p = 0.690; Std. beta = 2.76, 95% CI [-8.07, 13.59]		
Yangambi	<i>Panda oleosa</i>	number of cells in the DZ	Tree height	ns	Positive	beta = 4.31, 95% CI [-15.43, 24.04], t(71) = 0.43, p = 0.665; Std. beta = 3.00, 95% CI [-7.82, 13.83]		
Yangambi	<i>Synsepalum subcordatum</i>	number of cells in the DZ	Temperature	ns	Positive	beta = 0.69, 95% CI [-4.18, 5.56], t(72) = 0.28, p = 0.778; Std. beta = 0.12, 95% CI [-0.73, 0.97]	0.35	0.33
Yangambi	<i>Synsepalum subcordatum</i>	number of cells in the DZ	Relative humidity	ns	Positive	beta = 0.34, 95% CI [-0.50, 1.18], t(72) = 0.81, p = 0.423; Std. beta = 0.34, 95% CI [-0.51, 1.19]		
Yangambi	<i>Synsepalum subcordatum</i>	number of cells in the DZ	Amount of leaves lost	ns	Positive	beta = 0.36, 95% CI [-0.39, 1.10], t(72) = 0.95, p = 0.345; Std. beta = 0.11, 95% CI [-0.12, 0.34]		
Yangambi	<i>Synsepalum subcordatum</i>	number of cells in the DZ	Amount of fruits borne	ns	Positive	beta = 0.03, 95% CI [-0.18, 0.25], t(72) = 0.31, p = 0.756; Std. beta = 0.05, 95% CI [-0.25, 0.34]		
Yangambi	<i>Synsepalum subcordatum</i>	number of cells in the DZ	DBH	ns	Positive	beta = 0.07, 95% CI [-0.10, 0.24], t(72) = 0.84, p = 0.403; Std. beta = 0.12, 95% CI [-0.54, 0.78]		
Yangambi	<i>Synsepalum subcordatum</i>	number of cells in the DZ	Tree height	s	Positive	beta = 3.88, 95% CI [1.93, 5.83], t(72) = 3.96, p < .001; Std. beta = 0.57, 95% CI [-0.09, 1.23]		
Yangambi	<i>Scorodophloeus zenkeri</i>	number of cells in the DZ	Temperature	ns	Negative	beta = -2.43, 95% CI [-8.04, 3.17], t(72) = -0.87, p = 0.390; Std. beta = -0.37, 95% CI [-1.23, 0.49]	0.32	0.32
Yangambi	<i>Scorodophloeus zenkeri</i>	number of cells in the DZ	Relative humidity	ns	Negative	beta = -0.26, 95% CI [-1.23, 0.71], t(72) = -0.53, p = 0.599; Std. beta = -0.23, 95% CI [-1.09, 0.63]		
Yangambi	<i>Scorodophloeus zenkeri</i>	number of cells in the DZ	Amount of leaves lost	ns	Negative	beta = -0.48, 95% CI [-1.25, 0.28], t(72) = -1.26, p = 0.211; Std. beta = -0.16, 95% CI [-0.41, 0.09]		
Yangambi	<i>Scorodophloeus zenkeri</i>	number of cells in the DZ	Amount of fruits borne	s	Positive	beta = 0.29, 95% CI [0.11, 0.48], t(72) = 3.12, p = 0.003; Std. beta = 0.35, 95% CI [0.13, 0.58]		
Yangambi	<i>Scorodophloeus zenkeri</i>	number of cells in the DZ	DBH	s	Negative	beta = -2.30, 95% CI [-4.16, -0.43], t(72) = -2.46, p = 0.016; Std. beta = -1.95, 95% CI [-3.57, -0.34]		
Yangambi	<i>Scorodophloeus zenkeri</i>	number of cells in the DZ	Tree height	s	Negative	beta = -36.41, 95% CI [-65.81, -7.01], t(72) = -2.47, p = 0.016; Std. beta = -1.89, 95% CI [-3.45, -0.33]		
Yangambi	<i>Trilepisium madagascariense</i>	number of cells in the DZ	Temperature	ns	Negative	beta = -0.78, 95% CI [-4.70, 3.14], t(71) = -0.40, p = 0.693; Std. beta = -0.18, 95% CI [-1.07, 0.72]	0.75	0.11
Yangambi	<i>Trilepisium madagascariense</i>	number of cells in the DZ	Relative humidity	ns	Negative	beta = -0.03, 95% CI [-0.70, 0.64], t(71) = -0.10, p = 0.922; Std. beta = -0.04, 95% CI [-0.93, 0.85]		
Yangambi	<i>Trilepisium madagascariense</i>	number of cells in the DZ	Amount of leaves lost	ns	Negative	beta = -0.14, 95% CI [-0.67, 0.39], t(71) = -0.54, p = 0.594; Std. beta = -0.06, 95% CI [-0.30, 0.17]		
Yangambi	<i>Trilepisium madagascariense</i>	number of cells in the DZ	Amount of flowers borne	ns	Negative	beta = -0.03, 95% CI [-0.20, 0.14], t(71) = -0.32, p = 0.747; Std. beta = -0.03, 95% CI [-0.24, 0.17]		
Yangambi	<i>Trilepisium madagascariense</i>	number of cells in the DZ	Amount of fruits borne	ns	Positive	beta = 0.03, 95% CI [-0.13, 0.19], t(71) = 0.33, p = 0.745; Std. beta = 0.04, 95% CI [-0.22, 0.31]		
Yangambi	<i>Trilepisium madagascariense</i>	number of cells in the DZ	DBH	ns	Positive	beta = 1.20, 95% CI [-2.49, 4.89], t(71) = 0.65, p = 0.519; Std. beta = 0.55, 95% CI [-0.64, 1.73]		
Yangambi	<i>Trilepisium madagascariense</i>	number of cells in the DZ	Tree height	ns	Positive	beta = 0.49, 95% CI [-3.28, 4.27], t(71) = 0.26, p = 0.796; Std. beta = 0.22, 95% CI [-0.98, 1.42]		

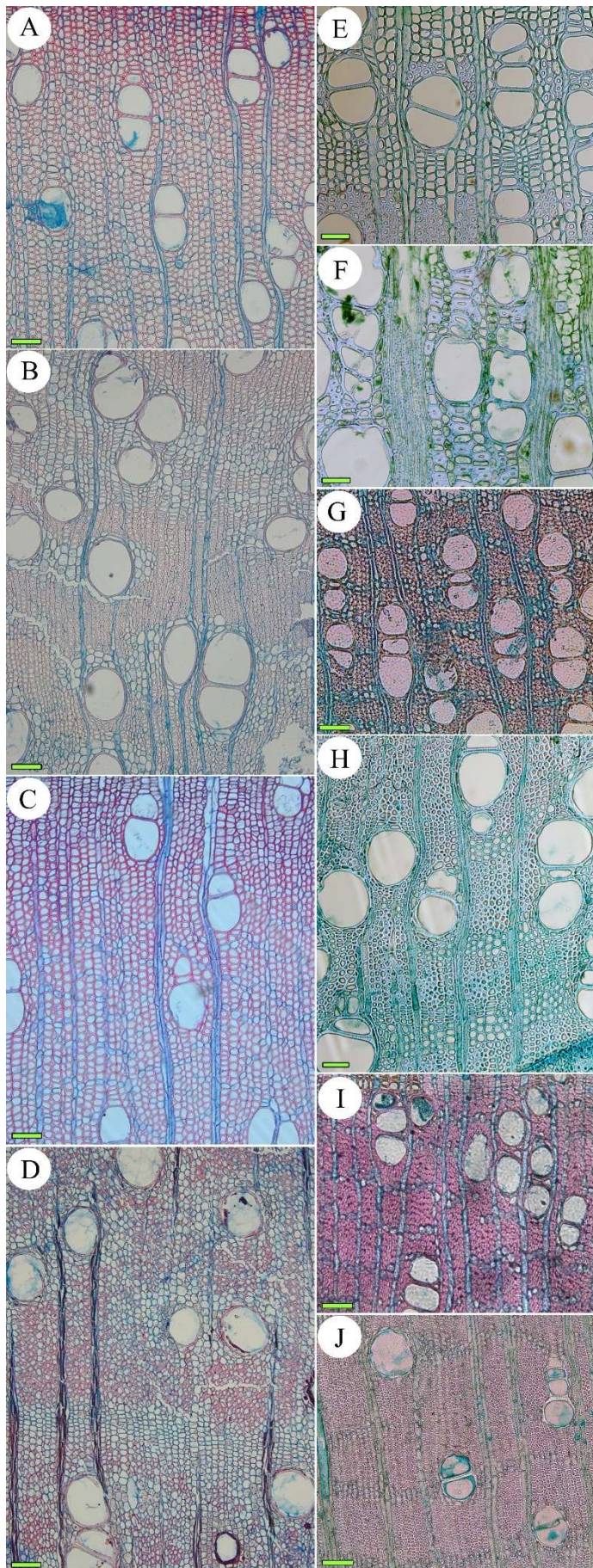


Figure. S4-1. Cross section of the ten study species.

Species from Luki:

(A) *F. elastica*

(B) *G. giganteum*

(C) *O. gore*

(D) *P. balsamifera*

Species from Yangambi:

(E) *L. thompsonii*

(F) *P. Oleosa*

(G) *P. macrocarpus*

(H) *S. zenkeri*

(I) *S. subcordatum*

(J) *T. madagascariense*

Scale bar = 100 μm.

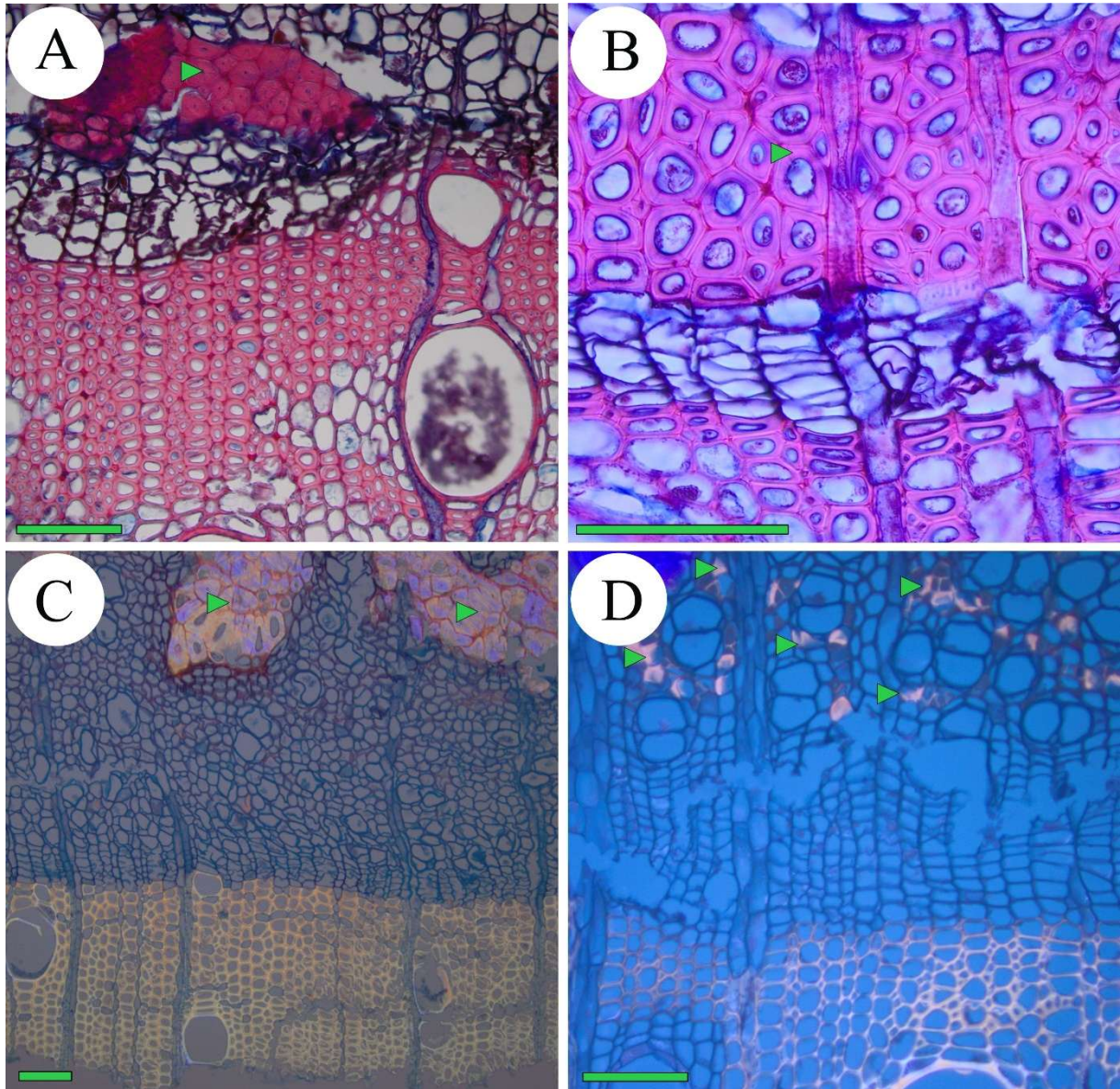


Figure S4 - 2. Illustration of the presence of sclerenchyma in the phloem of 3 of the 10 species studied (green triangle). (A) and (B) *G. giganteum*, (C) *F. elastica*, (D) *P. balsamifera*. Scale bar = 100 μm .

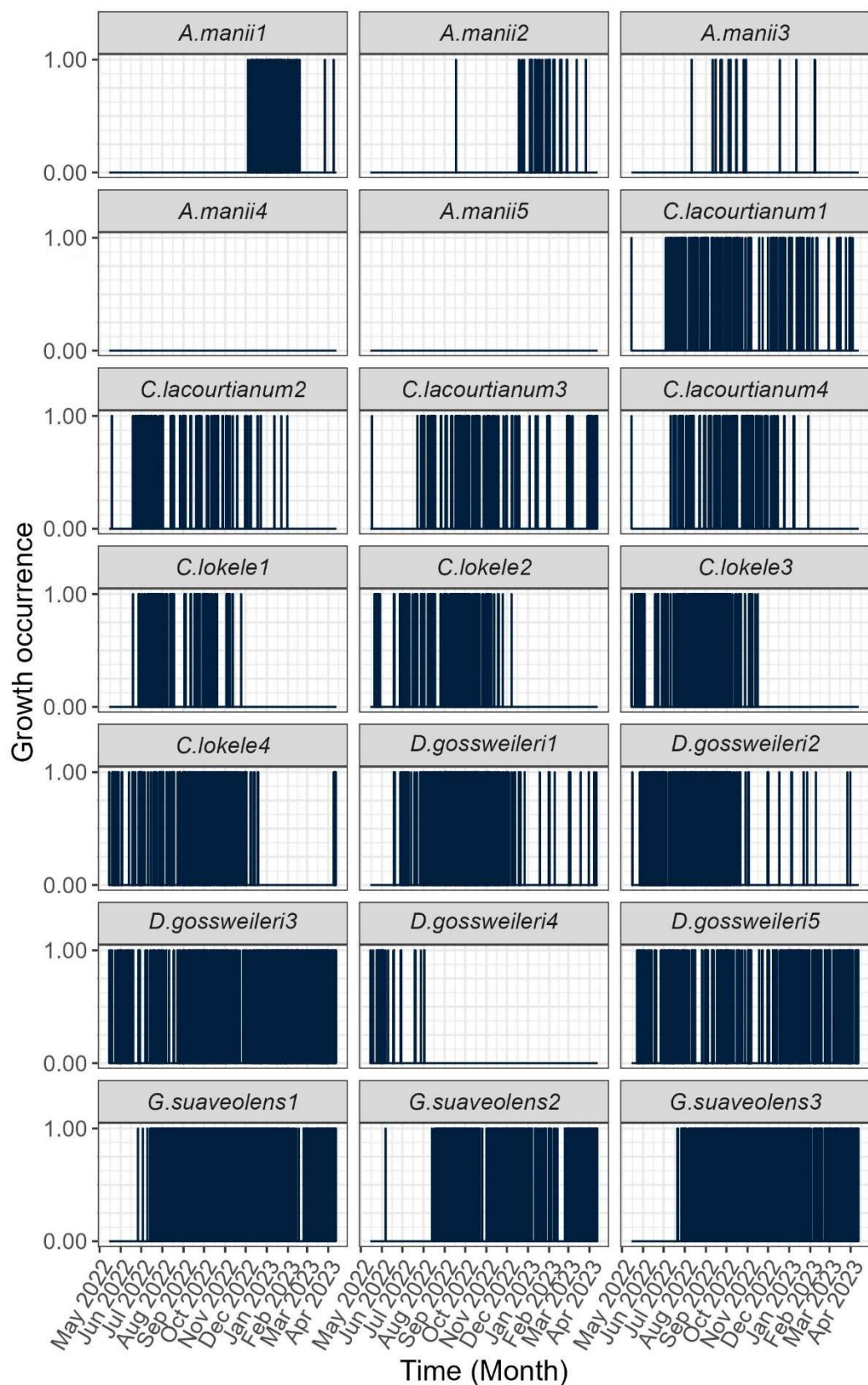


Figure S4 - 3A. The occurrence of hourly growth for the Yangambi studied trees over a one-year period, presented in binary format: 1 indicating growth and 0 indicating no growth (Part 1).

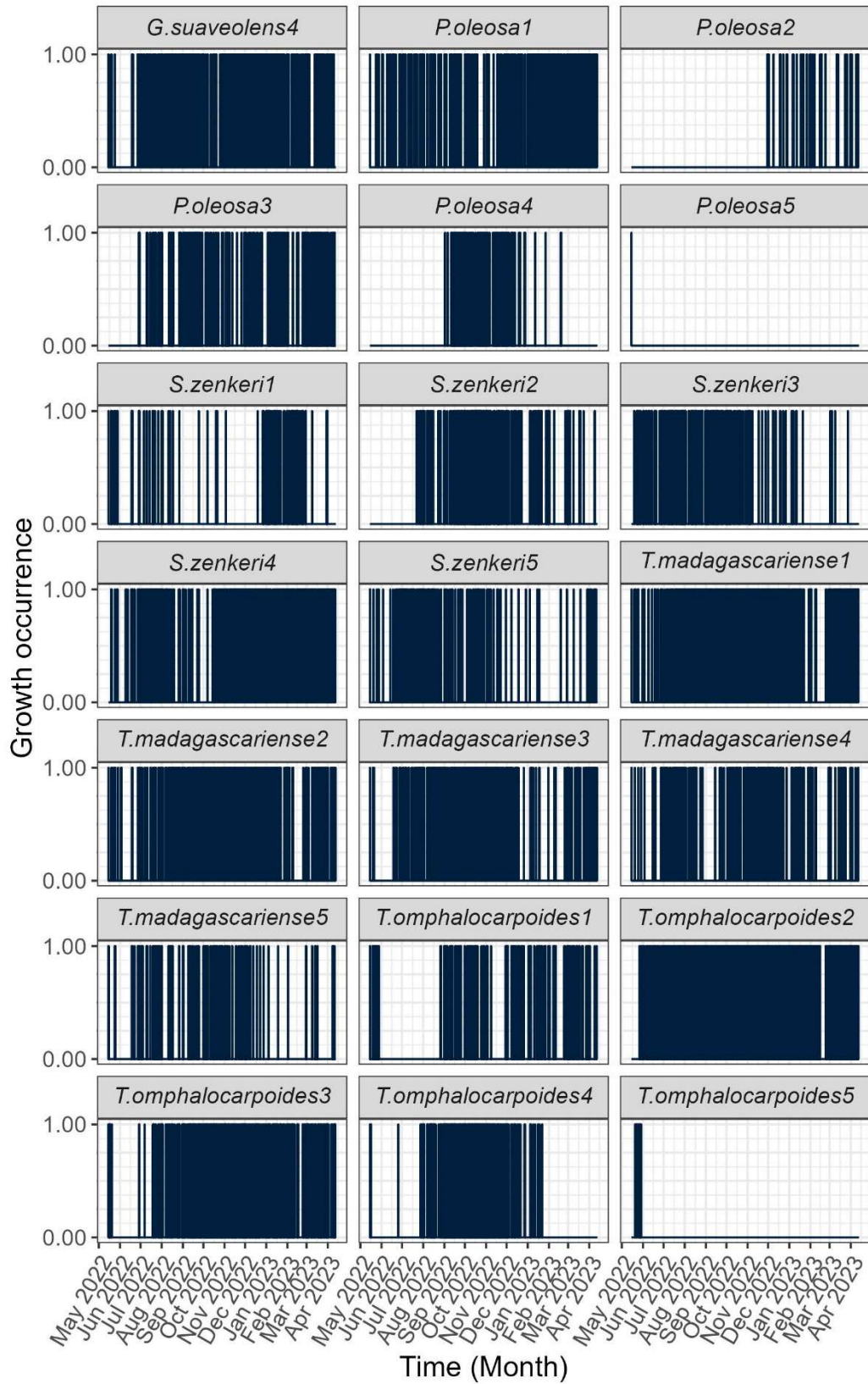


Figure S4 - 3B. The occurrence of hourly growth for the Yangambi studied trees over a one-year period, presented in binary format: 1 indicating growth and 0 indicating no growth (Part 2).

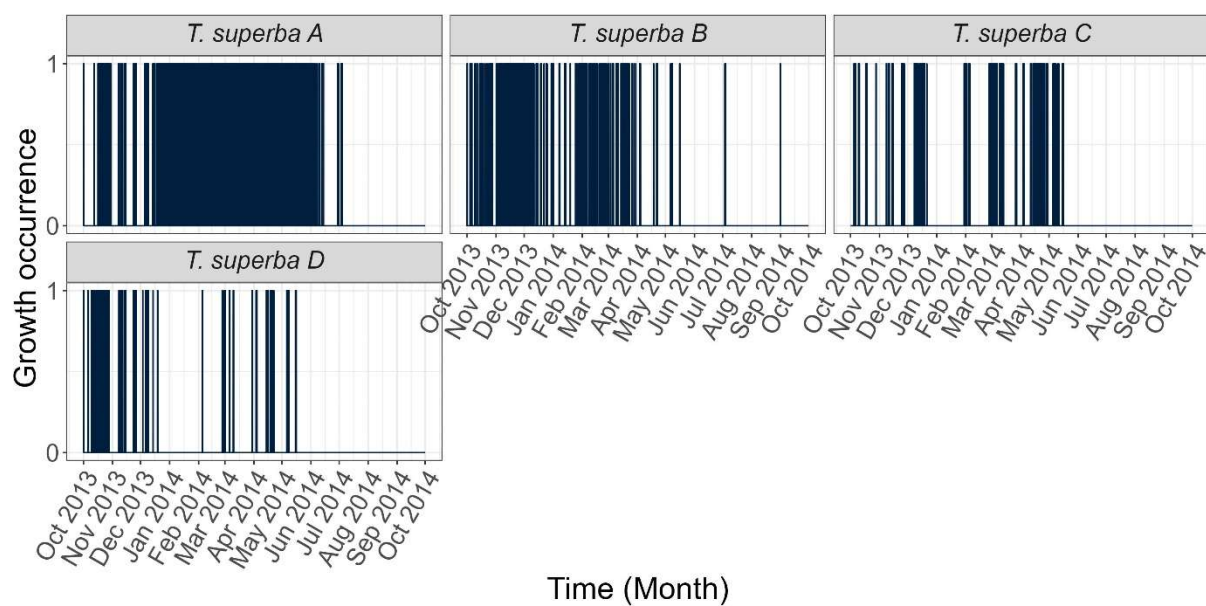


Figure S4 - 4A. The occurrence of hourly growth for the Luki studied trees over the phenological year 2013-2014, presented in binary format: 1 indicating growth and 0 indicating no growth.

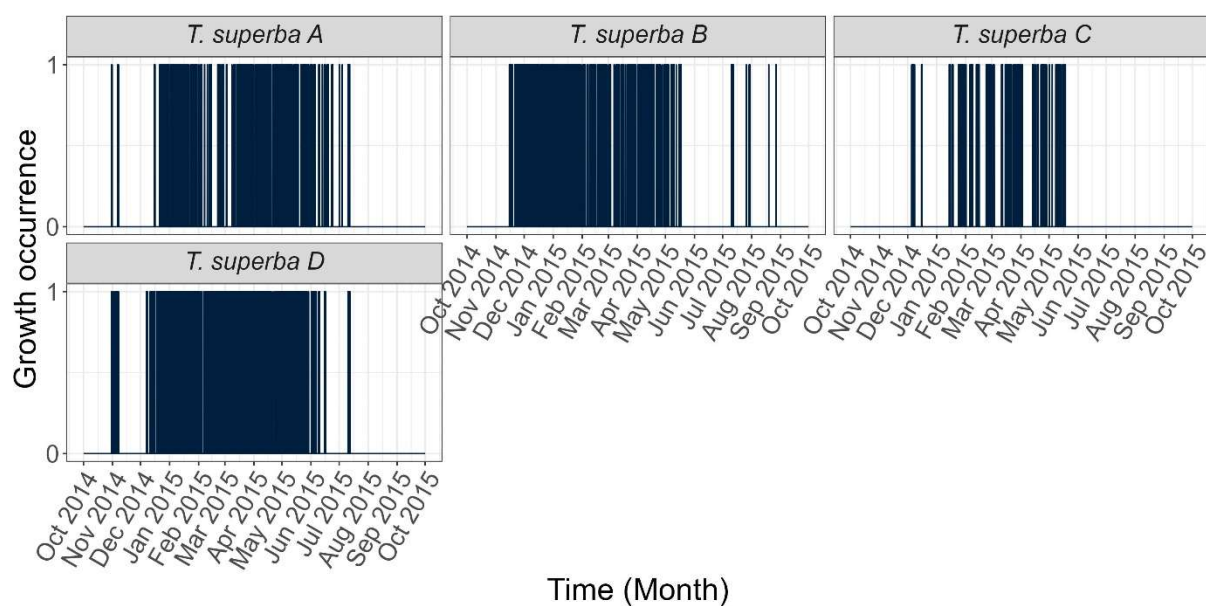


Figure S4 - 4B. The occurrence of hourly growth for the Luki studied trees over the phenological year 2014-2015, presented in binary format: 1 indicating growth and 0 indicating no growth.

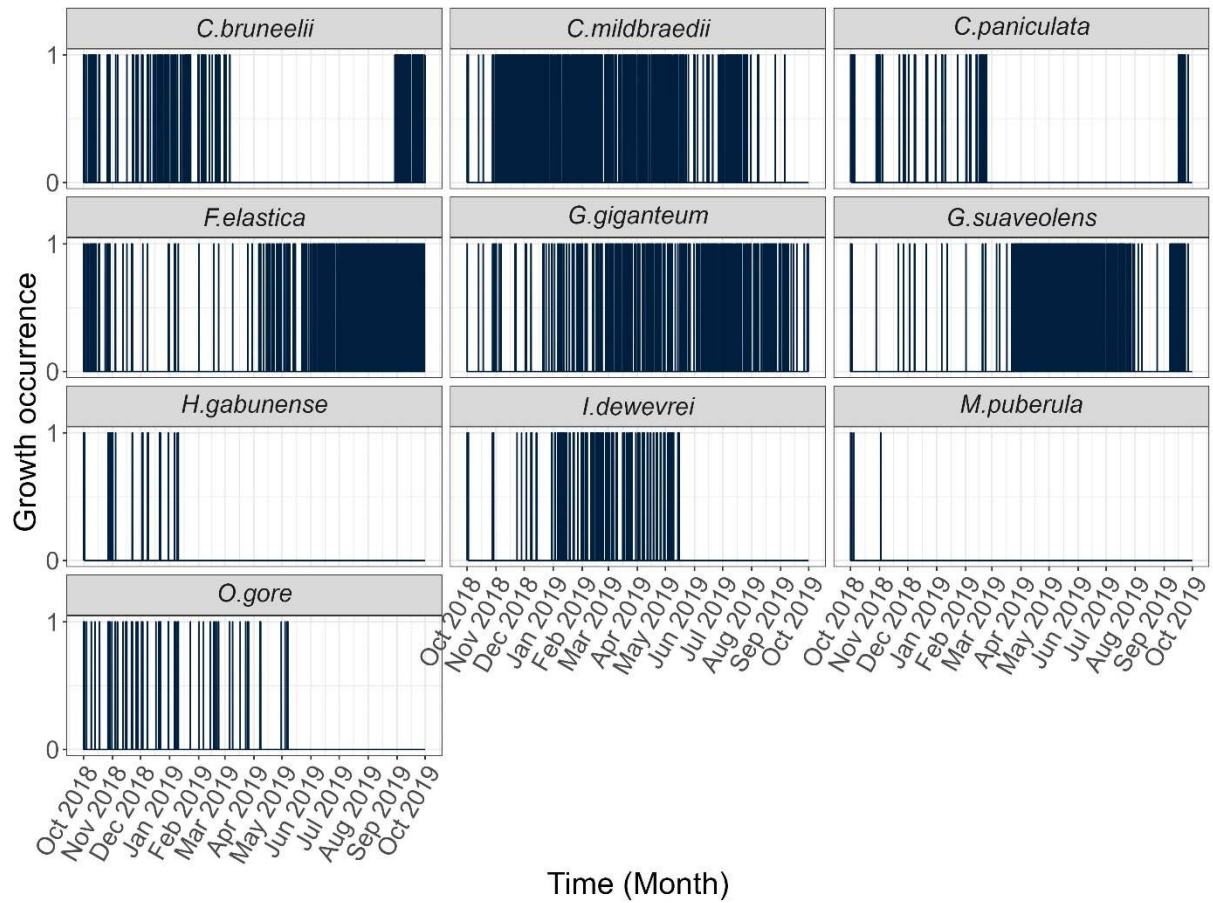


Figure S4 - 4C. The occurrence of hourly growth for the Luki studied trees over the phenological year 2018-2019, presented in binary format: 1 indicating growth and 0 indicating no growth.

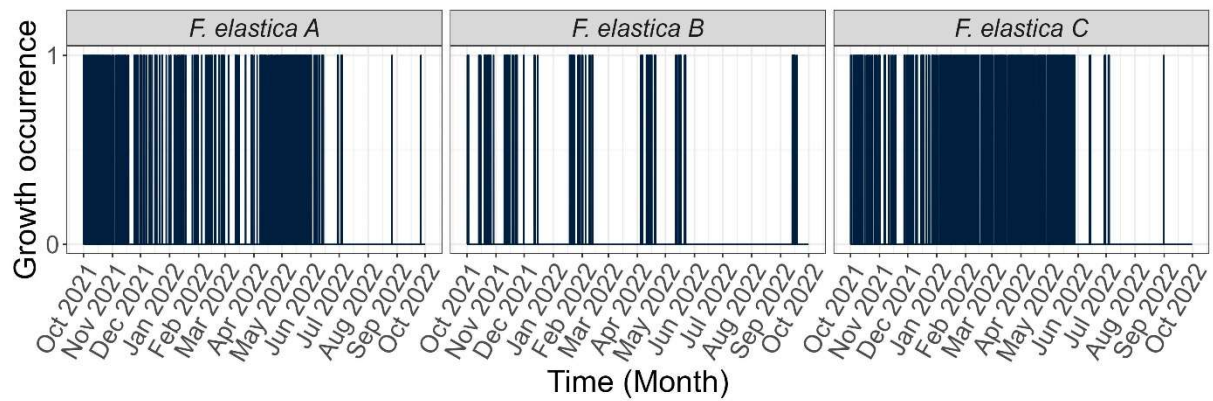


Figure S4 - 4D. The occurrence of hourly growth for the Luki studied trees over the phenological year 2021-2022, presented in binary format: 1 indicating growth and 0 indicating no growth.